# CD40 Stimulation Activates ‘Post-Activated’ B Cells which are Hyporesponsive to B Cell Receptor and Toll-like Receptor 9 Stimulation in Autoimmunity

vorgelegt von

**M. Sc.**

**Sarah Yasmin Weißenberg**

an der Fakultät III – Prozesswissenschaften

der Technischen Universität Berlin

zur Erlangung des akademischen Grades

**Doctor rerum naturalium**

**- Dr. rer. nat. -**

genehmigte Dissertation

Promotionsausschuss:

Vorsitzender: Prof. Dr. Juri Rappsilber

Gutachter: Prof. Dr. Roland Lauster

Gutachter: Prof. Dr. Thomas Dörner

Tag der wissenschaftlichen Aussprache: 20.11.2020

Berlin 2021

# Content

# Abbreviations

| | |
|---|---|
| (ds)DNA | (Double stranded) deoxyribonucleic acid |
| (ds)RNA | (Double stranded) ribonucleic acid |
| (p)DC | (Peripheral) dendritic cell |
| A | Area |
| Abata | Abatacept |
| ACPA | Antibodies against citrullinated antigens |
| ACR | American College of Rheumatology |
| AECG | American-European Consensus Group |
| AF | Alexa flour |
| AhR | Aryl hydrocarbon receptor |
| AID | Autoimmune disease |
| Akt(1) | Protein kinase B |
| ANA | Anti-nuclear antibodies |
| ANOVA | Analysis of variance |
| APC | Antigen presenting cell |
| APC | Allophycocyanin |
| applic. | Application |
| APRIL | A proliferation-inducing ligand |
| ASC | Antibody secreting cell |
| Aza | Azathioprine |
| BAFF | B cell-activating factor |
| BANK1 | B cell scaffold protein with ankyrin repeats |
| BCAP | B cell receptor-associated protein |
| BCL6 | B cell lymphoma 6 protein |
| BCR | B cell receptor |
| Bemab | Belimumab |
| BLK | B lymphocyte kinase |
| BLNK | B cell linker protein |
| BLyS | B lymphocyte stimulator |
| BMCT | Bonferroni test for multiple comparisons |
| Btk | Bruton’s tyrosine kinase |
| BTLA | B- and T-lymphocyte attenuator |
| BV | Brilliant violet |
| C | Constant (region) |
| C1q | Complement component 1q |
| $Ca^{2+}$ | Calcium(II)-ion |
| CCL3 | Chemokine (C-C motif) ligand 3 |
| CFSE | Carboxyfluorescein succinimidyl ester |
| CI | Confidence interval |
| c-Myc | Myc proto-oncogene protein |
| CpG | Cytosine-phosphodiester-guanine |
| CSR | Class switch recombination |
| CTLA-4 | Cytotoxic T-lymphocyte-associated protein 4 |
| CXCL | C-X-C chemokine ligand |
| CXCR | C-X-C chemokine receptor type |
| Cy | Cyanine |

| | |
|---|---|
| CyA | Cyclosporine A |
| Cyclo | Cyclophosphamide |
| D | Diversity (region) |
| DAPI | 4',6-diamidino-2-phenylindole, dihydrochloride |
| DAS28 | Disease activity score 28 |
| DMARD | Disease-modifying antirheumatic drug |
| DMCT | Dunnett's test for multiple comparisons |
| DMR | Differentially methylated regions |
| DMSO | Dimethyl sulfoxide ($C_2H_6O_6$) |
| DOCK8 | Dedicator of cytokinesis protein 8 |
| DRFZ | Deutsches Rheumaforschungszentrum (German Rheumatology Research Center) |
| EBI2 | Epstein-Barr virus-induced G-protein coupled receptor 2 |
| EBV | Epstein-Barr virus |
| EDTA | Ethylenediaminetetraacetic acid |
| egl | Extraglandular |
| EIF2AK2 | Eukaryotic translation initiation factor 2 alpha kinase 2 |
| ERK | Extracellular-signal regulated kinase |
| ESSDAI | EULAR Sjögren's syndrome disease activity index |
| Eterna | Eternacept |
| EULAR | European league against rheumatism |
| EWAS | Epigenome-wide association studies |
| f | Female |
| Fas | Tumor necrosis factor receptor superfamily member 6 |
| FBS | Fetal bovine serum |
| FC | Flow cytometry |
| $F_C$ | Fragment, crystallizable |
| $F_C$R | $F_C$ binding receptors |
| FcγRIIb | $F_C$ fragment of IgG receptor IIb |
| FDC | Follicular dendritic cell |
| FDR | False discovery rate |
| FGF basic | Fibroblast growth factor 2 |
| FITC | Fluorescein isothiocyanate |
| FO | Follicular |
| FOXO | Forkhead box protein O |
| FSC | Forward scatter |
| GC | Germinal center |
| GCRMA | Guanine cytosine robust multi-array analysis |
| G-CSF | Granulocyte colony-stimulating factor |
| gl | Glandular |
| GM-CSF | Granulocyte-macrophage colony-stimulating factor |
| GWAS | Genome wide association studies |
| H | Height |
| $H_2O_2$ | Peroxide |
| HCQ | Hydroxychloroquine |
| HD | Healthy donor |
| HRP | Heterophilic |
| HSC | Hematopoietic stem cell |
| ICOS(-L) | Inducible T cell co-stimulator (ligand) |
| IFI44L | Interferon induced protein 44 like |
| IFITM1 | Interferon-induced transmembrane protein 1 |

| | |
|---|---|
| IFNα/γ | Interferon α/γ |
| IgG/M/A/E/D | Immunoglobulin G/M/A/E/D |
| IgH/L | Ig heavy/light chain |
| IL | Interleukin |
| ILC | Innate lymphoid cells |
| iNKT | Invariant NKT cells |
| IFNAR | Interferon alpha/beta receptor |
| IFNGR | Interferon gamma receptor |
| IP-10 | C-X-C motif chemokine 10 |
| IRAK-4 | Interleukin-1 receptor-associated kinase 4 |
| IRF3 | Interferon regulatory factor 3 |
| ITAM | Immunoreceptor tyrosine-based activation motif |
| ITIM | Immunoreceptor tyrosine-based inhibitory motif |
| ITP | Immune thrombocytopenia |
| J | Joining (region) |
| JAK | Janus kinase |
| LAT | Linker for activation of T cells |
| LFC | Linear fold change |
| LPS | Lipopolysaccharide |
| LTA | Lipoteichoic acid |
| Lyn | Tyrosine-protein kinase Lyn |
| m | Male |
| MAIT | Mucosal-associated invariant T cell |
| MALT | Mucosa-associated lymphoid tissue |
| MAPK | Mitogen-activated protein kinase |
| M-CLL | Mutated chronic lymphatic leukemia |
| MCP-1/MCAF | C-C motif chemokine 2 |
| MFI | Median fluorescence intensity |
| MHC | Major histocompatibility complex |
| MIP-1a/b | Macrophage inflammatory protein 1-alpha/beta |
| MMF | Mycophenolatmofetil |
| MNC | Mononuclear cells |
| MS | Multiple sclerosis |
| mTOR | Mechanistic target of rapamycin |
| MTX | Methotrexate |
| MX1 | Myxoma resistance protein 1 |
| MyD88 | Myeloid differentiation primary response 88 |
| MZ | Marginal zone |
| n | Number of donors |
| NAb | Natural antibody |
| NF-AT | Nuclear factor of activated T cells |
| NFκB | Nuclear factor 'kappa-light-chain-enhancer' of activated B cells |
| NK | Natural killer |
| NOTCH2 | Neurogenic locus notch homolog protein 2 |
| NRPTP | Non-receptor-type protein tyrosine phosphatase |
| NSG | Non-obese diabetic scid gamma |
| P/S | Penicillin-Streptomycin |
| PALS | Periarteriolar lymphoid sheath |
| PAMP | Pathogen associated molecular pattern |
| PB | Pacific blue |

| | |
|---|---|
| PBMC | Peripheral blood mononuclear cells |
| PBS | Phosphate buffered saline |
| PCA | Principal component analysis |
| PD-1 | Programmed cell death protein |
| PDGF bb | Platelet-derived growth factor subunit B |
| PE | Phycoerythrin |
| PerCP | Peridinin-chlorophyll-protein |
| PI3K | Phosphoinositide 3-kinase |
| PIP3 | Phosphatidylinositol-3,4,5-triphosphate |
| PLCγ2 | 1-Phosphatidylinositol-4,5-bisphosphate phosphodiesterase gamma-2 |
| PO | Pacific orange |
| PP2 | Serine/threonine-protein phosphatase 2 |
| PP2A | Serine/threonine-protein phosphatase 2A |
| PPP2R3B | PP2A subunit B isoform PR48 |
| PPP2R5D | PP2A B subunit isoform PR61-delta |
| Pred | Prednisolone |
| PRR | Pattern recognition receptors |
| PSP | Protein serine phosphatase |
| pSS | Primary Sjögren's syndrome |
| PTEN | Phosphatase and tensin homolog |
| PTK | Protein tyrosine kinase |
| PTP | Protein tyrosine phosphatase |
| PTPN | Tyrosine-protein phosphatase non-receptor type |
| PTPRC | PTP receptor type C |
| PTPRN2 | PTP receptor type N 2 |
| PTPRO | PTP receptor type O |
| PYK2 | Protein tyrosine kinase 2 beta |
| R | Pearson's correlation coefficients |
| $R^2$ | Coefficients of determination |
| RA | Rheumatoid arthritis |
| RAG1/2 | Recombination activating gene 1 or 2 |
| RANTES | C-C motif chemokine 5 |
| react. | Reactivity |
| rec | Recombinant |
| RF | Rheumatoid factor |
| RKI | Robert Koch Institute |
| RPTP | Receptor-type protein tyrosine phosphatase |
| RRX | Rhodamine red-X |
| RSS | Recombination signal sequences |
| RT | Room temperature |
| S or Ser | Serine |
| S1PR4 | Sphingosine-1-phosphate receptor 4 |
| SA | Stimulation assay |
| SD | Standard deviation |
| SH2 | Src homology region 2 |
| SHIP1 | SH2 domain containing inositol polyphosphate 5-phosphatase 1 |
| SHM | Somatic hyper mutation |
| SHP-1 | SH2 domain-containing phosphatase-1 |
| Siglec-1 | Sialic acid-binding Ig-like lectin 1 |
| SLAMF7 | Signaling lymphocytic activation molecule family member 7 |

| | |
|---|---|
| SLE | Systemic lupus erythematosus |
| SLEDAI | Systemic lupus erythematosus disease activity index |
| SLICC | Systemic lupus international collaborating clinics |
| SNP | Single nucleotide polymorphism |
| SS-A/B | Sjögren's-syndrome-related antigen A/B |
| SSC | Sideward scatter |
| STAT5 | Signal transducer and activator of transcription |
| Sulfa | Sulfasalazine |
| Syk | Spleen tyrosine kinase |
| T or Thr | Threonine |
| T-1, 2 or 3 | Transitional-1, 2 or 3 |
| TACI | Tumor necrosis factor receptor superfamily member 13B |
| TAK1 | Nuclear receptor subfamily 2 group C member 2 |
| $T_C$ | Cytotoxic T cell |
| TCR | T cell receptor |
| TD | T cell-dependent |
| $T_{FH}$ | T follicular helper cell |
| $T_H$ | T helper cell |
| TI | T cell independent |
| TLR | Toll-like receptor |
| TNF | Tumor necrosis factor |
| TNFR | Tumor necrosis factor receptor |
| Toci | Tocilizumab |
| $T_{PH}$ | 'Peripheral helper' T cells |
| TRAF | TNF receptor-associated factor |
| TRIP6 | Thyroid hormone receptor interactor 6 |
| TT | Tetanus toxin |
| V | Variable (region) |
| VEGF | Vascular endothelial growth factor A |
| WT | Wild type |
| Y or Tyr | Tyrosine |
| ZAP-70 | CD3ζ–zeta chain of TCR associated protein kinase 70 |

# 1 Zusammenfassung

Autoimmunität entsteht, wenn das Immunsystem körpereigene Strukturen (Autoantigene) erkennt. Dies führt zur Zerstörung von Zellen und Geweben. Chronische Autoimmunerkrankungen wie z. B. der Systemischer Lupus Erythematosus (SLE), Rheumatoide Arthritis (RA) und das primäre Sjögren Syndrom (pSS), schränken zum einen die Lebensqualität der Patienten stark ein und zum anderen können sie lebensbedrohliche Krankheitsverläufe wie z. B. eine Lupus-Nephritis entwickeln [1]. Die Erkennung von Autoantigenen mittels des B-Zellrezeptors (*B cell receptor*, BCR), die Bildung eines Autoimmungedächtnisses und die Wirksamkeit von B-Zell-gerichteten Therapiestrategien unterstreichen die pathogene Rolle von B-Zellen bei der Entstehung und Progression von Autoimmunerkrankungen [2-10]. Durch Genotypisierungs- und genomweite Assoziationsstudien (GWAS) von B-Zellen aus Autoimmunpatienten, sowie durch funktionelle Untersuchungen von B-Zellen in Menschen und Mäusen, konnten Zusammenhänge von veränderten BCR-Signalen und Autoimmunität aufgezeigt werden [11-16].

Die Stärke des BCR-Signals zusammen mit Co-Signalen, wie z. B. *toll-like* Rezeptor (TLR)-Signalen und Interaktionen mit T-Zellen, sind entscheidend für die Entwicklung von B-Zellen [17-21]. Bezüglich der Qualität des BCR-Signals in Autoimmunerkrankungen, ob erhöht oder erniedrigt, gibt es unterschiedliche Hinweise in der Literatur [14-16]. Kürzlich berichtete unserer Gruppe von einer BCR-Dysbalance in B-Zellen von SLE Patienten, welche sich durch reduzierte Phosphorylierung der Protein Tyrosinkinase (PTK) *spleen tyrosine kinase* (Syk) und folglich reduzierter Freisetzung von intrazellulärem $Ca^{2+}$ auszeichnet [14]. Des Weiteren gibt es Berichte über eine reduzierte Reaktivität von SLE B-Zellen gegenüber TLR9-Signalen. Der TLR9 ist für die Erkennung von nukleären Antigenen verantwortlich und bildet vermutlich zusammen mit dem BCR ein Schlüsselsignal für den Bruch der Selbsttoleranz gegenüber nukleären Antigenen [22-25]. T-Zellhilfe via CD40/CD40-Ligand (CD40L) Interaktion ist ein entscheidendes Signal für die Keimzellreaktion (*germinal center* (GC) *reaction*). Dadurch wird die Entwicklung eines langzeitigen B-Zell-(Auto-)Immungedächtnisses initiiert und verstärkt das BCR-Signal via Syk [26, 27].

Ziel dieser Studie war es, ein übergeordnetes Bild über die molekularen Prozesse während der B-Zellaktivierung in der Autoimmunität zu erhalten. Zu diesem Zweck wurde eine vergleichende Analyse von peripheren B-Zellen aus verschiedenen Autoimmunerkrankungen, insbesondere SLE, RA und pSS, mit besonderem Schwerpunkt auf die BCR, TLR9 und CD40-Aktivierung durchgeführt. *Ex vivo* Analysen der tonischen und anti-IgG/IgM-induzierten Tyrosin- (Y oder Tyr) oder Serin- (S oder Ser) Phosphorylierung der Kinasen Syk, *Bruton's tyrosine kinase* (Btk) und Protein Kinase B (Akt) in konventionellen $CD27^-$ B-Zellen und $CD27^+$ B-Gedächtniszellen lieferten eine Aussage über die Qualität des BCR-Signals. Ergänzt wurden diese Untersuchungen mit Daten zur Protein-Tyrosin-Phosphatase (PTP) und Protein-Serin/Threonin-Phosphatase- (PSP) Aktivität, sowie der Rekrutierung von PTP *Src homology region 2* (SH2) *domain-containing phosphatase-1* (SHP-1). Die Relevanz von Zytokinen, epigenetische Methylierung und chronische Stimulation von TRL9 und dem BCR wurde ebenfalls analysiert. Des Weiteren wurde das Potenzial von TRL9 und gemeinsamer TLR9 und BCR-

Aktivierung hinsichtlich Proliferation und Differenzierung in Antikörper-sezernierende Zellen (*antibody secreting cell*, ASC) untersucht. Abschließend wurde der Einfluss von CD40 mit und ohne Interleukin (IL)-4 oder IL-21 Co-Stimulation auf die BCR-vermittelte Syk($Y^{352}$) Phosphorylierung und *in vitro* Proliferation und Differenzierung von B-Zellen untersucht. Dies wurde ergänzt durch Expressionsdaten von ausgesuchten PTPs und PSPs nach CD40/IL-4Co-Stimulation.

Es zeigte sich, dass periphere SLE, RA und pSS $CD27^+$ B-Gedächtniszellen eine reduzierte Phosphorylierung der PTKs Syk($Y^{352}$) und Btk($Y^{223}$) im Vergleich zu gesunden Spendern (*healthy donors*, HD) aufwiesen. Bemerkenswerterweise war die Syk($Y^{352}$)-Phosphorylierung in peripheren $CD27^-$ B-Zellen von SLE Patienten und in gewebeansässigen $CD27^+$ B-Zellen von Patienten mit Immunthrombozytopenie (ITP) und pSS, im Vergleich zu nicht-autoimmunen Patienten, ebenfalls reduziert. Im Gegensatz dazu wurden erhöhte Akt($S^{473}$)-Phosphorylierungskinetiken in SLE $CD27^-$ B-Zellen und $CD27^+$ B-Gedächtniszellen gegenüber HDs gemessen. In pSS und RA $CD27^-$ B-Zellen waren diese Kinetiken vergleichbar zu HDs.

Die PTP/PSP Aktivität in SLE, sowie die Rekrutierung von SHP-1 zum negativ Co-Rezeptor CD22 von nicht stimulierten peripheren SLE, RA und pSS $CD19^+$ B-Zellen war im Vergleich mit HDs erhöht. Diese Veränderungen des BCR-Signals von SLE, RA und pSS B-Zellen standen nicht im Zusammenhang mit der tonischen Phosphorylierung oder der Expression von Signalmolekülen (Syk, Btk, *1-Phosphatidylinositol-4,5-bisphosphate phosphodiesterase gamma-2* (PLCγ2) und Akt), Zytokinexpression/-stimulation und epigenetischer Programmierung. Jedoch führte die chronische *in vitro* Stimulation des BCR von gesunden Kontrollen unter Re-Stimulation nach 24, 46 und 72 h, zu einer reduzierten Syk($Y^{352}$)-Phosphorylierung. Die TLR9-induzierte Proliferation und Differenzierung zu $CD27^+CD38^+$ ASCs von peripheren SLE, RA und pSS $CD19^+$ B-Zellen war im Vergleich zu HDs reduziert. Die kombinierte BCR und TLR9 Aktivierung erhöhte die Proliferation und Differenzierung von SLE, RA und pSS $CD19^+$ B-Zellen nur zu einem bestimmten Maße. *In vitro* Co-Stimulation von CD40 mit und ohne IL-4 oder IL-21 erhöhte die anti-IgG/IgM induzierte Syk($Y^{352}$)-Phosphorylierung in peripheren SLE, RA, pSS und HD B-Zellen. Bemerkenswerterweise konnte die Syk($Y^{352}$)-Phosphorylierung in SLE $CD27^-$ B-Zellen auf das Niveau von HDs erhöht werden. Des Weiteren führte CD40-Co-Stimulation zu einer hohen Proliferation von SLE, RA, pSS und HD $CD19^+$ B-Zellen. Die Verbesserung der BCR Antwort durch CD40 Co-Stimulation steht dabei im Einklang zu der reduzierten Expression von *non-receptor-type* PTPs (NRPTPs) wie z. B. *tyrosine-protein phosphatase non-receptor type 2* (*PTPN2*) und *PTPN22,* sowie weitere *receptor-type* PTPs (RPTPs) in HD und SLE $CD19^+$ B-Zellen nach CD40L/IL-4 Co-Stimulation.

Im Gegensatz zur generellen Annahme von hyperreaktiven B-Zellen in Autoimmunerkrankungen konnte diese Arbeit zeigen, dass periphere und gewebeansässige B-Zellen von Autoimmunpatienten funktionell beeinträchtigt sind. Dies zeigt sich unter anderem in einer reduzierten BCR- und TLR9-Stimulierbarkeit aufgrund von erhöhter Negativregulation durch PTPs wie z. B. SHP-1. Der ausgeprägteste Phänotyp wurde dabei in SLE B-Zellen beobachtet. Die beobachtete, reduzierte Reaktionsfähigkeit könnte funktionell der Anergie entsprechen und spiegelt wahrscheinlich einen ‚post-Aktivierungsstatus' auf Grund von chronischer B-Zellaktivierung und keine generelle Signalabnormität

wider. Diese Ergebnisse unterstreichen die Wichtigkeit der Kommunikation von B- und T-Zellen mittels CD40/CD40L Interaktion. Zudem scheint diese Interaktion der Schlüssel für die Reaktivierung von ‚post-aktivierten' B-Zellen in Autoimmunerkrankungen via Modulation der PTPs zu sein. Folglich könnten sich aus der Negativregulation von PTPs und B-Zellaktivierung via CD40 neue Perspektiven für Therapiestrategien ergeben.

# 2 Summary

Autoimmunity arise when the immune system attacks self-antigens and destroys body's own cells and tissues. Chronic autoimmune diseases such as systemic lupus erythematosus (SLE), rheumatoid arthritis (RA) and the primary Sjögren's syndrome (pSS) decrease life quality of patients and can lead to life threatening events such as lupus nephritis [1]. Recognition of self-antigens by the B cell receptor (BCR), development of autoimmune memory and beneficial therapeutic approaches by targeting B cells highlight the pathogenic role of B cells in development and maintenance of autoimmunity [2-10]. Genotyping and genome wide association studies (GWAS) of B cells from autoimmune patients and functional studies in human and mice underline the role of altered BCR signaling and its contribution to autoimmunity [11-16]. Strength of the BCR signal together with co-signals such as cytokines, toll-like receptor (TLR) signaling and interaction with T cells determines cell fate [17-21]. However, the literature is conflicting on whether BCR signaling is reduced or increased [14-16]. Recently, our group reported unbalanced BCR signaling with significantly reduced phosphorylation of the protein tyrosine kinase (PTK) spleen tyrosine kinase (Syk) and reduced intracellular $Ca^{2+}$ release in SLE B cells [14]. Further studies reported reduced responsiveness of SLE B cells to TLR9 stimulation which recognizes nuclear antigens and is considered key in self-tolerance brake to nuclear antigens together with the BCR [22-25]. T cell help by CD40-CD40L binding drives germinal center (GC) reaction and the development of long term (auto)-immune B cell memory and is further known to augment BCR signaling via Syk [26, 27]. To draw a more general picture of B cell activation in autoimmunity, this study aimed at comparatively analyzing the nature of peripheral B cell activation in different autoimmune diseases, mainly SLE, RA and pSS, with emphasis on BCR, TLR9 and CD40 signaling. To do so, BCR signaling quality was assessed in peripheral and tissue resident $CD27^-$ B cells and $CD27^+$ memory B cells by *ex vivo* analysis of tonic and anti-IgG/IgM induced tyrosine (Y or Tyr) or serine (S or Ser) phosphorylation of the kinases Syk, Bruton's tyrosine kinase (Btk) and protein kinase B (Akt). This was supplemented by data on protein tyrosine phosphatase (PTP) and protein serine/threonine phosphatase (PSP) activities and recruitment of the PTP Src homology region 2 (SH2) domain-containing phosphatase-1 (SHP-1). The relevance of cytokines, epigenetic methylation and chronic stimulation of TLR9 and the BCR was assessed. The potential of TLR9 and TLR9 together with BCR activation to induce proliferation and differentiation into antibody secreting cells (ASCs) was comparatively analyzed and finally, the impact of CD40/CD40L with and without interleukin (IL)-4 or IL-21 interaction on BCR-induced Syk($Y^{352}$) phosphorylation and *in vitro* proliferation and differentiation of B cells was determined. This was completed by expression data of selected PTPs and PSPs upon CD40/IL-4 co-stimulation.

As a commonality, phosphorylation of the PTKs Syk($Y^{352}$) and Btk($Y^{223}$) was reduced in peripheral $CD27^+$ memory B cells from SLE, RA and pSS patients in comparison to healthy donor (HD) controls. Notably, Syk($Y^{352}$) phosphorylation was diminished in peripheral SLE $CD27^-$ B cells compared to HD controls and in tissue resident $CD27^+$ B cells from patients with immune thrombocytopenia (ITP) and pSS compared to non-autoimmune patients, too. However, Akt($S^{473}$) phosphorylation kinetics were

increased in SLE CD27$^-$ and CD27$^+$ B cells and comparable to HDs in pSS and RA B cells. PTP/PSP activities in SLE and overall baseline recruitment of SHP-1 to the negative co-receptor CD22 in SLE, RA and pSS peripheral CD19$^+$ B cells were increased compared to HDs. Signaling abnormalities of SLE, RA and pSS B cells did not correlate to differences in tonic phosphorylation or baseline expression of signaling molecules (Syk, Btk, 1-Phosphatidylinositol-4,5-bisphosphate phosphodiesterase gamma-2 (PLCγ2) and Akt), cytokine expression/stimulation and epigenetic programming. However, chronic *in vitro* stimulation of the BCR led to reduced Syk(Y$^{352}$) phosphorylation upon re-stimulation after 24 h, 48 h and 72 h. Proliferation and differentiation into CD27$^+$CD38$^+$ ASCs of SLE, RA and pSS peripheral CD19$^+$ B cells was reduced upon *in vitro* TLR9 stimulation compared to HD controls. Combined BCR and TLR9 activation enhanced proliferation and differentiation of SLE, RA and pSS CD19$^+$ B cells only to a certain degree. CD40 *in vitro* co-stimulation with and without IL-4 or IL-21 increased anti-IgG/IgM induced Syk(Y$^{352}$) phosphorylation in SLE, RA, pSS and HD peripheral B cells. Interestingly, SLE CD27$^-$ B cells increased their Syk(Y$^{352}$) phosphorylation to HD values. Furthermore, CD40 co-stimulation led to high proliferation of SLE, RA, pSS and HD CD19$^+$ B cells. Improvements of CD40 co-stimulation correspond to reduced gene expression of non-receptor-type PTPs (NRPTPs) such as *tyrosine-protein phosphatase non-receptor type 2* (*PTPN2*) and *PTPN22*, and several receptor-type PTPs (RPTPs) in HD as well as SLE CD19$^+$ B cells upon CD40L/IL-4 co-stimulation.

Contrary to the general understanding of B cell hyperreactivity in autoimmune diseases, this study found peripheral and tissue resident B cell from autoimmune patients being functionally impaired towards BCR and TLR9 stimulation due to increased negative regulation by PTPs such as SHP-1. However, the strongest phenotype was observed in SLE B cells. This reduced responsiveness may be functionally related to B cell anergy and likely reflects a ‘post-activation’ status due to chronic B cell activation rather than a general signaling abnormality. The results underline that communication of B and T cells via CD40/CD40L interaction might be key for activating ‘post-activated’ B cells in autoimmune diseases via downmodulation of PTPs. Therefore, new therapeutic approaches may target B cell activation via CD40 or negative regulation of PTPs via the BCR.

# 3 Introduction

## 3.1 The Immune System

The immune system is a complex network of physical barriers, lymphoid organs, specialized immune cells, humoral factors and cytokines protecting from pathogens such as bacteria, viruses, parasites and fungi, but also from toxins and cancer cells [28, 29]. As a first line of protection, epithelial cells restrain pathogens from entering the body. Furthermore, physiologic mechanisms such as temperature, acidic pH values, mucus secretion and movement of ciliated epithelium in respiratory and gastro intestinal organs assist with the elimination of pathogens [28, 29]. Microbiota on the skin, in the gut and the lung influences the quality of such barrier functions [30-32]. Lymphoid tissues are sites of lymphoid cell development, maturation and homing. These lymphoid cells include B and T cells which originate from primary lymphoid organs, namely thymus, bone marrow and the fetal liver. In secondary lymphoid organs such as the spleen, lymph nodes and mucosa-associated lymphoid tissue (MALT), cells of the immune system get activated upon pathogen recognition. Blood and lymphatic vessels connect lymphoid tissues and transport cells and soluble immune factors through the body [28, 29].

The immune system can be subdivided into innate and adaptive immunity. Innate immunity is unspecific and recognizes conserved pathogen associated molecular patterns (PAMPs) such as lipopolysaccharides (LPS), lipoteichoic acid (LTA), mannans and double stranded ribonucleic acid (dsRNA) among bacteria, viruses and other pathogens. Fast recognition of PAMPs by pattern recognition receptors (PRRs) provokes an immune reaction within minutes to hours. Soluble factors such as the complement system and germline encoded natural antibodies (NAb) assist with lysis, opsonization and clearance of pathogens, immune complexes and dead cells by phagocytes (macrophages and neutrophils). Mast cells, basophil, eosinophils, dendritic cells (DCs), natural killer (NK) cells and innate lymphoid cells (ILCs) are further cells of innate immunity expressing their own specific functions [28, 29].

The highly variable adaptive immune system identifies a possibly endless number of antigens and forms an individual and specific memory allowing rapid and efficient secondary responses. Antigens are recognized by the BCR and T cell receptor (TCR) expressed by B and T cells, respectively. The BCR directly binds antigens by a 3-dimensional recognition. However, the TCR requires antigen presentation by the expression of major histocompatibility complex (MHC) class I and class II on antigen presenting cells (APC) and is restricted to linear recognition of amino acid sequences. $CD8^+$ cytotoxic T ($T_C$) cells mediated cellular immunity whereas $CD4^+$ T helper ($T_H$) cells promote the development and maturation of activated B cells into memory B cells, antibody secreting plasmablasts and plasma cells [28, 29]. Close interaction between B and $T_H$ cell takes place in GCs located in follicles of lymphatic tissues [33].

However, innate and adaptive immunity share certain features such as APC function, expression of Ig crystallizable fragment ($F_C$) binding receptors ($F_CR$) or the expression of PRRs such as TLRs by B cells [28]. Furthermore, B and T cell subsets such as invariant NKT (iNKT), γδ T, mucosal-associated

invariant T (MAIT), B-1 and marginal zone (MZ) B cells possessing innate functions [33-35]. The latter two of them have overlapping functions by producing NAbs.

The immune system is crucial for pathogen defense and survival. However, if the anti-pathogenic system accidently recognizes self-antigens, autoimmunity can arise, and the own immune system combats self-targets. The spectrum of autoimmune diseases is diverse and depends on the specific target organ. SLE patients are typically self-reactive against nuclear antigens such as double stranded deoxyribonucleic acid (dsDNA) and ribonucleoproteins resulting in multiple organ damage [36, 37]. Inflammation of the skin and nephritis are often found among those patients. RA and pSS patients suffer mainly from synovitis and dry eyes and mouth due to destruction of excretory glands, respectively [38-43]. Breach of B cell self-tolerance induces the development of autoreactive ASCs producing high titers of autoreactive antibodies targeting self-antigens [38-40, 44-47]. Chronic maintenance of self-reactivity is thought to be related to a positive feed-forward loop resulting in chronic inflammation and tissue damage [48]. Beneficial B cell directed therapeutic approaches underscore the pathogenic and clinical relevance of B cells in the development, maintenance and treatment of autoimmunity [3-10].

## 3.2 The B Cell Lineage – Development, Subsets and Tolerance Checkpoints

### *3.2.1 The Course of T Cell-Dependent and T Cell-Independent B Cell Responses*

During an immunologic challenge, different B cell subsets become active at different and partly overlapping time points. Circulating NAbs, continuously produced by B-1 and MZ, detect the pathogen within minutes or hours. This is followed by a T cell-independent (TI) response of B-1 and MZ B cells within hours to days. At the same time follicular (FO) B cells develop into IgM secreting extrafollicular plasma cells. Those antibodies form immune complexes with the pathogens to be phagocytized and presented by APCs fueling T cell-dependent (TD) B cell responses by FO B cells which can take days or weeks. The development of a constitutive humoral memory represented by antibody secreting plasma cells and reactive humoral memory by memory B cells enables a fast secondary response with greater magnitude, switched antibody isotypes and higher affinity compared to primary responses [33, 35]. Besides, the development and maintenance of humoral immunity, B cells fulfill further functions. For example as professional APCs and effector cells producing cytokines such as tumor necrosis factor (TNF), chemokine (C-C motif) ligand 3 (CCL3), interferon γ (IFNγ), granulocyte-macrophage colony-stimulating factor (GM-CSF), IL-6, IL-17, IL-2 and expressing regulatory functions due to the secretion of IL-10 and IL-35 [33, 49-51].

### *3.2.2 Early Ontogeny of B-1 and B-2 B Cells*

B cell subsets differ in their function, localization and developmental state determined by the interplay of subset-specific developmental programs, environmental factors and activation state. B-1, MZ and FO B cells are the major B cell subsets, whereas MZ and FO B cells are summarized into B-2 B cells as they share ontogeny which is distinct from B-1 B cells. All B cells develop from bone marrow and fetal liver resident hematopoietic stem cells (HSC). Lymphoid-primed multipotent progenitors develop

from HSC daughter cells and generate common lymphoid progenitors which further develop into B cell as well as T cells, NK cells and DCs [33]. The ‘induced differentiation’ model of B-1 and B-2 B cell development describes a signal-dependent differentiation from common precursor cells, whereas the ‘dual linage model’ describes distinct progenitor cell for B-1 and B-2 B cells. Both models are not mutually exclusive. However, the description of a specific B-1 progenitor cell in fetal liver supports linage specific hypothesis. Accordingly, B-1 B cells arise mainly from fetal liver and are self-renewing, whereas B-2 B cells are continuously produced from bone marrow during the whole life [52, 53].

### *3.2.3 B-1 B Cells Mainly Undergo T Cell-Independent B Cell Responses*

B-1 B cells mainly reside in pleural and peritoneal cavities. Furthermore, they populate the spleen, secondary lymphoid and mucosal tissues, the omentum, the blood and the bone marrow. B-1 B cells are the main producer of NAbs. The repertoire of those germline encoded IgM antibodies is generated in the absence of antigen exposure. NAbs are polyreactive and bind to antigens expressed by various bacteria, viruses and parasites enabling an innate-like quick first line of defense response. Moreover, binding of self-antigens and antigens expressed by apoptotic cells assists with tissue homeostasis and clearance of apoptotic material. Expression of PRRs such as TLR3, 4, 7 and 9 facilitates the activation of B-1 B cells. Activated B-1 B cells start producing high levels of NAbs. In addition, they can accumulate locally in the regional lymph nodes, migrate to spleen or mucus tissue where they differentiate into ASCs. B-1 B cells can undergo class switch recombination (CSR) into all Ig isotypes *in vitro* with IgA as preferred Ig class. Poly-specific IgA produced by B-1 B cells is the major pool of commensal-specific antibodies and plays a role in the homeostasis of the gastro-intestinal microflora. Furthermore, it represents a first layer of defense in the gut mucosa and respiratory tract. B-1 B cells further subdivide into B-1a and B-1b B cells with distinct roles in immunity. B-1a B cells spontaneously produce NAbs upon activation whereas B-1b B cells produce antibodies after exposure to antigen and develop into memory cells which accumulate in the peritoneal cavity. In mice CD5 is a typical marker expressed by B-1a, but not by B-1b B cells [53]. The existence of B-1 B cells in humans has been controversially discussed. However, human B cell populations functionally similar to B-1 B cells were described with spontaneous IgM secretion, limited somatic hyper mutation (SHM) and germline Ig repertoire [52].

### *3.2.4 B-2 B Cells Subdivide into MZ and FO B Cells in the Spleen*

IgM expressing immature B-2 B cells leave the bone marrow after they passed through the pro- and pre-B cell stages. Next, they pass through two sequential transitional stages called transitional-1 (T-1) and T-2 and finalize their development in the spleen where they become IgM- or IgD-expressing mature naive B cells [33]. MZ and FO B cells descend from those transitional B cells [33, 35]. The spleen histologically divides into red and white pulp. The blood slowly passes through the red pulp where red blood cell components are filtered and recycled [33, 54]. The white pulp contains lymphocytes and functions as secondary lymphoid organ containing B cell follicles and T cell zones [33, 35]. T-1 B cells reside in T cell rich areas known as periarteriolar lymphoid sheath (PALS) where they undergo negative

selection upon self-reactivity. T-2 B cells colonize the follicles where they require survival signals transduced by the BCR and B cell-activating factor (BAFF) receptor. BCR signal strength may guide the developmental fate into MZ or FO B cells. In contrast, B cell differentiation into MZ B cells depends on neurogenic locus notch homolog protein 2 (NOTCH2) signaling which is independent of the BCR [35].

### *3.2.5 MZ B Cells Screen the Blood for Antigens*

The MZ is a specialized micro-anatomic structure providing an interface between red and white pulp. Cells leaving the blood stream transit through the MZ before they enter the white pulp which enables MZ B cells to interact with circulating antigens for the clearance of blood-borne microorganisms and apoptotic cells [35, 54]. The microscopic anatomy of humans and mice MZs differs. In mice, the marginal sinus forms an inner border between the white pulps and surrounding MZ. Marginal metallophilic macrophages populate the marginal sinus and expose native antigens to MZ B cells [35, 54, 55]. Humans completely lack the marginal sinus and marginal metallophilic macrophages [35, 55]. Here, MZ B cells are exposed to antigens within the perifollicular zone which contains neutrophils with strong B cell helper function. Human MZ B cells can circulate and populate MZ-like zones in lymph nodes, epithelium of tonsillar crypts and intestinal Peyer's patches, whereas murine MZ B cells are restricted to the MZ [35, 55]. Circulating human MZ B cells are characterized by IgM, IgD, and CD27 expression [56].

Like B-1 B cells, MZ B cells express innate-like functions with NAb production, recognition of blood-borne type 1 TI antigens, such as LPS and type 2 TI antigens, such as polysaccharides. Furthermore, they can bind self-antigens with low affinity [33, 35]. Activated MZ B cells develop into polyreactive low-affinity IgM producing plasmablasts and APCs [33, 35, 54]. In contrast, TD-activated MZ B cells differentiate into high-affinity antibody secreting long-lived plasma cells. Moreover, human and murine MZ B cells can undergo CSR to IgA and IgG, but SHM is unique for human MZ B cells [33, 35]. Additionally, naïve $CD4^+$ T follicular helper ($T_{FH}$) cells activated by MZ B cells can stimulate FO B cells in the white pulp [54].

### *3.2.6 FO B Cells Undergo TD Activation and Raise Antigen-Specific Immune Responses*

Protein antigens are primarily recognized by FO B cells which represent the most prevalent B cell subset within secondary lymphoid organs such as the white pulp of the spleen. Prior to activation, resting naive FO B cells circulate or populate primary B cell follicles [33, 57]. Once pathogens entering the lymph, proximal draining lymph nodes or the spleen via the blood stream they can be directly sensed by BCRs on FO B cells, or the antigen is delivered by lymphoid organ homing DCs or activated MZ B cells. B cell follicles are surrounded by a T cell zone, which enables close interaction of activated B and T cells [57]. For TD activation, $T_H$ cells are activated by MHCII-antigen complexes on APCs [54, 58]. Meanwhile, activated FO B cells migrate to the T/B border guided by C-X-C chemokine receptor type 4 (CXCR4), sphingosine-1-phosphate receptor 4 (S1PR4) and Epstein-Barr virus-induced G-protein coupled receptor 2 (EBI2) expression, where they present antigen and receive cognate helper

signals by $T_H$ cells [58, 59]. Only B cell clones with appropriate or high antigen affinity are selected to undergo the GC reaction. The more T cell help a B cell receives at the T/B border the more likely it is that a B cell enters the GC and becomes a GC B cell. If there is a rather short contact of B and T cells then a B cell is more likely to become a GC-independent memory B cell [26, 33, 57, 58]. However, further signals by the infectious milieu, such as non-cognate bystander T cell help or TLR activation, can affect B cell fate [58].

In the pre-GC phase, high affinity B cells directly differentiate into GC-independent extrafollicular short-lived plasmablasts or memory B cells at the T/B border, whereas moderate affinity B cells seed GC within the follicle [26, 58, 60]. In this phase CSR can occur, but not SHM. Therefore, many of those short-lived plasmablasts secrete non-mutated low affinity IgM antibodies, but also IgG and IgA. Also, GC-independent $IgG^+$ and $IgA^+$ memory B cells exist. These GC independent memory B cells display a broad spectrum of antigen affinities and are able to rejoin the immune reaction at later time points during primary infection [26, 58]. FO B cells within GC undergo proliferation, affinity maturation and class switching into $IgG^+$, $IgA^+$ or $IgE^+$ B cells. Upon this process FO B cells can differentiate into memory B cells or long lived plasma cells expressing high affinity BCR or secrete high affinity antibodies, respectively [26, 33, 54, 57, 58]. After antigen-specific differentiation of B cells into plasmablasts, they migrate to the red pulp to provide rapid entry of antibodies to the blood stream [54].

### *3.2.7 The Germinal Center Response of B Cells after TD Activation*

The GC is a specialized microenvironment within secondary follicles mainly populated by B cells, but also FDCs, $T_{FH}$ cells and macrophages [57]. The GC can be subdivided into the dark and the light zone. The dark zone is populated by B cells called centroblasts, undergoing rapid proliferation and SHM, while the light zone harbors a class of B cells called centrocytes which compete for antigen to undergo affinity selection [33, 57, 58]. FDCs present antigen to B cells and support the interaction of $T_{FH}$ cells and centrocytes [58]. In addition to the important B cell stimulant CD40L, $T_{FH}$ cells also characteristically express the inducible T cell co-stimulator (ICOS) and CXCR5 [61]. The interaction of centrocytes and $T_{FH}$ cells determines whether B cells undergo another round of SHM and proliferation or leave the GC reaction as memory B or plasma cell [57]. T/B cell interaction via CD40/CD40L ligation is of great importance for the activation of naive FO B cells, promoting survival of GC B cells and priming for $T_{FH}$ cytokine responsiveness [59]. CD40 together with cytokines such as IL-21 and IL-4 are required for GC B cell differentiation [26, 62]. In this process, IL-21 is a key inducer of B cell lymphoma 6 protein (BCL6) transcription factor for GC formation, maintenance, induction of SHM and CSR and plasma cell differentiation, whereas CD40 ligation alone induced CSR, but not SHM in naive B cells [33, 59, 63, 64].

After entering the GC, B cells follow different fates depending on their BCR affinity [58]. They can exit the GC as memory B cell or plasma cell, recycle or undergo apoptosis [58]. B cells with high affinity BCRs exit the GC as plasma cells, whereas memory B cells preferentially originate from low affinity GC B cell. Intermediate affinity B cells are prone to recycle and participate to another round of affinity maturation by SHM [58]. In case of no affinity, GC B cells would not receive T cell help and undergo

tumor necrosis factor receptor superfamily member 6 (Fas) mediated apoptosis [60]. However, it is published that memory B and plasma cells develop from GC in a temporal order. Memory B cells appear rather early, whereas long-lived plasma cells develop rather late during GC reaction [65]. These hypotheses are not mutually exclusive as developmental fate depends on B cell affinity and affinity develops over time. Antigen affinity of the BCR is indirectly sensed by $T_{FH}$ cells via the quantity of peptide-MHCII expression on the B cell surface. The higher the BCR affinity, the more antigen is endocytosed and the more peptide-MHCII is presented to $T_{FH}$ cells inducing long lasting $T_{FH}$ cell help to the B cell [26, 33, 58].

The expression of CD27 marks human post-GC memory B cells, which accumulate at the follicular periphery outside the $CD27^-$ naive B cell region or circulate in the periphery [55, 66-68]. After CSR, memory B cells can express IgG, IgA or IgE isotypes on the cell surface. However, $CD27^+IgM^+$, $CD27^+IgM^+IgD^+$ and $CD27^-IgG^+$ memory B cells are described [69-73], and B cell classification upon CD27 and IgD expression distinguishes between $CD27^-IgD^+$ naive, $CD27^-IgD^-$ double negative, $CD27^+IgD^-$ switched memory and CD27+IgD+ un-switched memory B cells as well as $CD27^{++}IgD^-$ plasmablasts [74-78]. Further surface markers such as CD38, CD21, CD24, CD19, B220, $F_CRH4$ and CD25 indicate additional heterogeneity among human memory B cells with individual subset-specific functions [74].

### *3.2.8 Memory B and Long-Lived Plasma Cells Provide Long-Term Protection in Case of a Secondary Immune Reaction*

Memory B cells recirculate, populate at immunologically strategic sites of pathogen entry, such as $IgA^+$ memory B cells on mucocutaneous surfaces, and can be secreted such as in breast milk [33, 58, 79]. Upon a secondary challenge, memory B cells form follicular and extrafollicular aggregates in lymphoid tissues and differentiate into plasmablasts or re-enter the GC reaction for a diversified secondary antibody response [26, 33, 80]. Furthermore, $CXCR5^+$ and programmed cell death protein 1 $(PD\text{-}1)^+$ memory $T_{FH}$ cells localize at the follicular T/B border to reactivate memory B cells [59]. Memory B cells provide some cross-reactivity to related targets, which assist with the elimination of similar pathogens upon their primary attack. This was recently demonstrated in a human vaccination study. In this study, primary vaccination led to the activation of cross-reactive memory B cells, whereas the secondary vaccination exclusively recruited specific memory B cells [81]. Long-lived plasma cells migrate into the bone marrow where they find their specific niches provided by stroma cell secreting C-X-C chemokine ligand 12 (CXCL12), IL-6 and a proliferation-inducing ligand (APRIL). Within the bone marrow, plasma cells maintain the serological memory by continuous antigen-specific antibody production [33]. A subset of bone marrow plasma cells lacking the expression of the B cell lineage marker CD19 has been discovered indicating further or alternative developmental steps or functions [82]. Noteworthy, alterations of B cell expression and subset distribution such as increased expression of circulating $CD20^{lo}CD27^{hi}$ plasma cells/plasmablasts in SLE patients are associated with autoimmune diseases [76, 77, 83-86]. This is further discussed in **Section 3.4.2** “B Cell Abnormalities in SLE, RA and pSS”.

## 3.3 The B Cell Receptor Signaling Pathway During Development, Tolerance Induction and Receptor Crosstalk

### *3.3.1 The BCR and Immunoglobulin Subclasses*

The BCR is a surface-bound Ig with approximately $10^5$ molecules being expressed on one B cell, whereas soluble Igs (antibodies) are secreted by plasmablasts and plasma cells [33, 87]. Igs are composed of two identical heavy (IgH) and two identical light (IgL) chains containing an N-terminal variable (*V*) region, characterized by high sequence diversity, and a C-terminal constant (*C*) region, respectively. The C-terminal regions of IgH are connected by disulfide bonds anchoring to the plasma membrane and each IgH chains is connected to one IgL chain. The variable N-terminal sides of IgH and IgL represent the antibody-specific antigen-binding side [33, 87]. Gene recombination of *V*, diversity (*D*) and joining (*J*) genes (*V*(*D*)*J* recombination) upon recombination activating gene (RAG) 1 and RAG2 binding to recombination signal sequences (RSS), next to *V*, *D*, and *J* gene segments, during B cell development generates combinatorial diversity of IgH and IgL [87-89].

IgL genes are located within two separate gene loci, the κ and the λ locus, whereas IgH genes localize within one single gene locus [87, 89]. Arrangement and expression of BCR genes together with BCR-binding characteristics determine B cell development in the bone marrow. Functional IgM expressing Immature B cells leave the bone marrow for further maturation [33, 87, 90]. Activated peripheral B cells further diversify their *V* regions by SHM and can undergo CSR within GCs [87].

The C-terminal constant ($F_C$) region of IgH determines the isotype: IgM (μ-chain), IgD (δ-chain), IgG (γ-chain), IgA (α-chain) and IgE (ε-chain). Antibodies of those isotypes express specific effector functions such as antigen neutralization, binding inhibitory or activating $F_C$R on immune cells and activation of the complement system by binding complement component 1q (C1q) [33, 87]. Furthermore, valency and avidity are increased for multimer-forming antibodies by linking their $F_C$ portions via *J* chains. IgG and IgE are monomeric, IgA is monomeric in serum, but forms dimers when secreted such as in in tears, mucus and saliva, and IgM exists as a pentamer [33, 87]. IgD is mainly expressed as cell surface receptor. IgG and IgA further subdivided into IgG1, IgG2, IgG3 and IgG4 and IgA1 and IgA2 subclasses [33].

The half-life time of single antibody molecules depends on the isotype and ranges within hours and days [33]. Murine IgM molecules survive two days, whereas IgG ranges between four and eight days. IgE and polymeric IgA exhibit a half-life time of about 12 hours and 17 – 22 hours, respectively [91]. However, antibody titers against specific antigens can be detected over years ranging between 11 and 11,552 years half-life time for tetanus toxin (TT) and Epstein-Barr virus (EBV), respectively [92]. Continuous persistence of antibody titers, and therefore, humoral immunity are maintained by long-lived plasma cell residing in the bone marrow [93, 94].

### 3.3.2 Proximal Regulation of the BCR Signaling Pathway

B cell fate is tightly regulated by intracellular BCR signaling strength transduced by post-transcriptional changes to signaling proteins such as tyrosine, serine or threonine phosphorylation resulting in the release of intracellular $Ca^{2+}$ storages [17-20]. According to the dissociation activation model of BCRs, antigen binding to the BCR opens auto-inhibited BCR oligomers to form clustered BCR monomers, which makes the intracellular immunoreceptor tyrosine-based activation motifs (ITAMs) of the BCR associated Igα (CD79a) and Igβ (CD79b) chains accessible for binding and phosphorylation of Syk [95-98]. Upon binding to the ITAM region, Syk gets allosterically activated and further phosphorylates downstream targets such as PLCγ2, Btk and Akt [95, 99]. Depending on the signaling strength, developmental and environmental factors as well as further co-signals, $Ca^{2+}$- and Akt-dependent transcription factors get activated [100, 101].

Positive and negative BCR co-receptors such as CD19, CD21 and CD81 as well as CD22, CD72 and $F_C$ fragment of IgG receptor IIb (FcγRIIb), respectively, regulate BCR signaling strength and shape BCR-dependent $Ca^{2+}$ flux [101-111]. As a negative feedback mechanism, immunoreceptor tyrosine-based inhibitory motif (ITIM) containing co-receptors, such as CD22, CD72 and FcγRIIb recruit phosphatases such as SHP-1 and SH2 domain containing inositol polyphosphate 5-phosphatase 1 (SHIP1) to the proximal signalosome [101, 105-111]. Upon BCR activation, the intracellular ITIM gets phosphorylated by tyrosine-protein kinase Lyn (Lyn) leading to the recruitment of SHP-1 which dephosphorylates PTKs such as Syk [105, 106]. The BCR-dependent balance of Syk and SHP-1 activities is essential for normal B cell development and function. [95, 112].

### 3.3.3 BCR Signaling Strength During B Cell Development and Tolerance Induction

BCR signaling amplitude, frequency and duration in dependence of the developmental B cell state, co-signals and physical properties of the antigen determines cell fate by $Ca^{2+}$-dependent gene expression changes [101, 113-115]. Approximately 70 to 75 % of immature B cells display self-reactivity, and therefore, need to undergo negative selection processes for tolerance maintenance before they leave the bone marrow [87, 116, 117]. Mechanisms like receptor editing and clonal deletion are thought to prevent the development of autoimmunity [118-123]. Immature B cells are most sensitive to BCR signals [124-127]. A small induction of $Ca^{2+}$ signaling can induce RAG1- and RAG2-dependent receptor editing [121, 128, 129]. Upon deficient RAG expression or impaired BCR signaling, autoreactive B cells accumulate and autoimmunity develops [130-132]. Low-avidity autoreactive cells can exit the bone marrow and enter secondary lymphoid organs [87, 133]. In immature transitional stages, B cells are sensitive to BCR-induced apoptosis at lower antigen concentrations than mature B cells [121, 134-137]. Highly self-reactive T-1 B cells undergo negative selection. However, less self-reactive cells can proceed to the T-2 B cell stage and may cause autoimmunity [87, 138].

BCR affinity determines B cell fate within a GC reaction [20]. Besides the indirectly sensed BCR affinity by $T_{FH}$ cells upon peptide-MHCII expression, differential activation of key transcription factors such as nuclear factor of activated T cells (NF-AT) and nuclear factor 'kappa-light-chain-enhancer' of activated

B cells (NFκB) may alter GC outcome. Interestingly, both nuclear factors can be regulated via $Ca^{2+}$ signaling. NF-AT is sensitive to $Ca^{2+}$ signaling frequency and low $Ca^{2+}$ elevation, whereas the peak amplitude of the $Ca^{2+}$ signal is relevant for NFκB regulation [139, 140]. As another potential mechanism of tolerance induction, autoreactive B cells may acquire mutations that decrease BCR affinity away from self-reactivity within a GC [58, 141, 142].

B cell anergy is a functionally non-reactive state of persisting autoreactive cells which escaped receptor editing and clonal deletion [143-145]. Elevated basal $Ca^{2+}$ concentrations, low BCR induced $Ca^{2+}$ mobilization and phosphorylation, constitutive phosphorylation of extracellular-signal regulated kinase (ERK), impaired proliferation, upregulation of activation marker and BCR induced Ig secretion are characteristic for anergic B cells [125, 139, 146-148]. Human anergic B cells are mainly observed among naive B cells such as mature naive $IgD^{+}/IgM^{-}$ B cells which represent 2.5 % of total peripheral B cells [149]. Furthermore, human T-3 peripheral B cells in lymph nodes and peripheral blood, characterized as $R123^{+}CD38^{+}CD24^{+}IgD^{+}CD27^{-}$ B cells, are mainly anergic B cells that exited from T-2 or mature FO B cell subsets [150-152]. Additionally, anergy has been studied in a row of mouse models and does not necessarily affect a distinct B cell population [153]. However, BCR hyperreactivity may overcome B cell anergy and induce autoimmunity which has been studied in mice [13]. This is discussed in more detail in **Section 3.4.4** “Altered BCR Signaling in Autoimmunity”.

### *3.3.4 BCR Crosstalk with TLR9 and CD40 in B Cells*

The interplay of the BCR with other receptors influences intracellular signals and shapes B cell activity and fate. Aberrant activation or defective signaling by one or the other receptor may cause autoimmunity by delivering wrong signals to auto-reactive cells, and therefore, let them pass through tolerance mechanisms. In this context, BCR interactions with CD40 and TLRs such as TLR9 are of great importance as they mediate peripheral B cell tolerance and development of TD and TI plasma cells [13, 154-156]

Membrane-bound and soluble CD40 belongs to the tumor necrosis factor receptor (TNFR) superfamily and is expressed by B cells, professional APCs, as well as non-immune cells and tumor cells [60]. GC formation, CSR, SHM and the development of long-lived memory B and plasma cells requires CD40-CD40L interaction after antigen binding to the BCR [60, 157]. Binding of CD40L to CD40 induces clustering and conformational changes to CD40 exposing the intracellular docking side for TNF receptor-associated factors (TRAFs) [60]. Differential recruitment of signaling molecules, such as TRAF1, TRAF2, TRAF3, TRAF5 and TRAF6 can activate distinct downstream pathways such as canonical and non-canonical NFκB signaling, mitogen-activated protein kinase (MAPK), phosphoinositide 3-kinase (PI3K)/Akt, PLCγ2 and TRAF-independent Janus kinase 3 (JAK3)/signal transducer and activator of transcription 5 (STAT5) pathway [60]. Besides CD40 activation, other accessory signals such as cytokines may modify the responses [60]. Combined BCR and CD40 signaling via Syk induces optimal Myc proto-oncogene protein (c-Myc) expression, which is essential for GC B cell recruitment and maintenance [27, 157].

Spontaneous TLR9 activation by the detection of dsDNA-containing antigens drives B cell activation to become antibody secreting plasma cells by extrafollicular pathways, and therefore, plays an important role in B cell responses against invading pathogens [156, 158-160]. Upon ligand binding, TLR9 monomers dimerize and recruit myeloid differentiation primary response 88 (MyD88) which binds interleukin-1 receptor-associated kinase 4 (IRAK-4). Next, IRAK-4 auto-phosphorylates, associate with IRAK1 and recruit ubiquitin ligase TRAF6. This complex translocates to the cytosol, where it activates nuclear receptor subfamily 2 group C member 2 (TAK1). In a next step, TAK1 activates MAPK and NFκB pathways, which in turn activates downstream transcription factors such as interferon regulatory factor 3 (IRF3), IRF5 and IRF7 [25]. Furthermore, BCR and TLR9 signaling affects TLR9 expression, subcellular localization, proliferation, as well as cytokine and (auto)-antibody production [25].

Patients with defective CD19 alleles have impaired upregulation of CD86, tumor necrosis factor receptor superfamily member 13B (TACI) and CD23 after *in vitro* TLR9 activation which normally induces CD19 phosphorylation through the MyD88/protein tyrosine kinase 2 beta (PYK2)/LYN complex leading to the recruitment of PI3K, Btk and Akt [161]. Subsequently, inhibition of PI3K, Akt or Btk and Btk deficiency results in TRL9 activation defects [161]. Furthermore, signaling molecules such as Lyn, Syk, B cell receptor-associated protein (BCAP), B cell scaffold protein with ankyrin repeats (BANK1) and dedicator of cytokinesis protein 8 (DOCK8) provide a link between the BCR and TLR9 pathways [25, 162, 163].

## 3.4 Autoimmunity

### *3.4.1 Autoimmune Diseases (SLE, RA and pSS)*

Development of autoimmunity is a multifactorial process including genetic factors, environmental and stochastic events that involve innate and adaptive immunity and hormonal mechanisms [43, 133, 164]. Prevalence and incidence of autoimmune diseases depends on ethnicity, age and sex [43, 165, 166]. Disease pathology of B cell-dependent autoimmunity depends on the nature of secreted autoantibodies such as activation or blocking of receptors, induction of altered signaling, thrombosis, cell death and induction of inflammation [167]. The target organ of a specific disease and the associated autoantibody profile, which are often used to classify and diagnose the diseases, differs.

Patients with SLE characteristically produce anti-nuclear antibodies (ANA) including anti-dsDNA autoantibodies [44, 45]. The reduced clearance of immune complexes causes multiple and severe organ damage such as vasculitis or glomerulonephritis [36, 37]. Whereas patients with RA suffer mainly from synovitis which is accompanied by the production of rheumatoid factor (RF) and/or antibodies against citrullinated antigens (ACPA) leading to cartilage and bone destruction [38-40]. In pSS, patients show self-reactivity against excretory glands resulting into dry eyes and mouth and other mucosal surfaces; in a substantial proportion of patients extraglandular manifestations occur [41-43]. Here, autoantibodies against the ANA specificities Ro/ Sjögren's-syndrome-related antigen A (SS-A) and La/SS-B together with RF are typical findings [46, 47, 168]. Autoantibodies typically appear many years before SLE disease onset while patients are still asymptomatic [45]. $ANA^+$ healthy individuals differ

from ANA$^+$ SLE patients in their cytokine expression by lacking the characteristically increased expression of IFNs, B lymphocyte stimulator (BLyS), IL-12p40 and stem cell factor/c-Kit ligand indicating that the cytokines may also play a role in the onset of the autoimmune diseases [169].

### *3.4.2 B cell Abnormalities in SLE, RA and pSS*

B cell hyperreactivity and chronic activation of the B cell compartment is a hallmark of autoimmune diseases such as SLE, RA and pSS. Typical findings in SLE are high frequencies of circulating CD20$^{lo}$CD27$^{hi}$ plasma cells/plasmablasts and CD27$^-$IgD$^-$CD95$^+$IgG$^+$, IgA$^+$ or IgM$^+$ memory-like “double negative” B cells in the peripheral blood [76, 77, 83-86]. This was found to correlate with disease activity [83]. In RA patients circulating FcRL4 tissue-resident B cells have been reported [170]. Notably, CD19$^-$ plasma cells were found in the synovium of RA patients [82]. Patients with pSS appear to have reduced CD27$^+$ memory B cells and increased soluble CD27 in peripheral blood which may correlate with CXCR4 depended accumulation of memory B cells in salivatory glands of pSS patients [171-175]. Several studies concluded that defective tolerance checkpoints before and after antigen activation and defects in peripheral and central selection permit the emergence and maintenance of autoreactive B cells [2, 87, 176-183].

Negative and positive selection during B cell development is mainly driven by the BCR. However, signals by other receptors such as TLRs and CD40 synergize with the BCR signal and may modulate repertoire selection towards autoreactivity along TD and TI pathways [183-185]. In this line, TLR9 activation may govern the development of autoantibodies against dsDNA and ribonucleoproteins [186, 187]. Furthermore, immune complex containing DNA and ribonucleoproteins can activate autoreactive B cells by dual-recognition via the BCR and TLR9 receptor resulting in tolerance break against nuclear antigens [160, 188-190]. Those TRL9-driven B cell responses may be amplified by high activity of peripheral DCs (pDCs) and high IFNα expression, which is a hallmark in SLE and is also described for pSS [191-194]. Furthermore, autoreactive anergic cells can be reactivated by strong T cell help provided by CD40L and IL-4 [183].

In this context, phenotypic and genetic studies of BCR gene rearrangements found abnormalities in the memory B cell repertoire together with autoantibodies almost exclusively being encoded by SHM BCR rearrangements [180, 195, 196]. In SLE patients selection of autoreactive B cells occurs upon ongoing polyclonal activation and recruitment of naive B cells by extrafollicular and early GC pathways [197]. Recent studies of SLE B cells found that ANA$^+$ plasma cells originate from extrafollicular as well as GC pathways [198].

### *3.4.3 Mutations in BCR Signaling and Functional Consequences*

Mutations of BCR-associated signaling molecules or co-receptors can have fatal impact on B cell development, immunologic functions and health of affected individual. For example, patients with X-linked agammaglobulinemia lack the expression of functional Btk which is an important mediator of the BCR signaling cascade. B cell development is abrogated in these patients leading to a lack of

peripheral B cells and reduced antibody titers of all classes, making those patients highly susceptible to infections [199].

Genotyping and GWAS indicated that defects in BCR signaling might be key for disturbed self-recognition and hyperreactivity of B cells in autoimmune diseases such as SLE [11, 200]. Those studies identified certain mutations of downstream scaffold proteins, PTKs or abnormal PTPs, such as Lyn, B lymphocyte kinase (BLK), BANK1 and PTPN22, suggesting intrinsic BCR hyperactivity [11, 201-206]. Indeed, results of these GWAS suggested that certain risk genes might be connected to aberrant BCR signaling in autoimmunity with overlapping ethnicities [11, 201-204, 207-210]. It is reported that RA, SLE and pSS share some common genetic risk genes such as PTPN22 1858C/T risk mutation, whereas BANK1 risk mutation appears to be specific for SLE and RA [207-209, 211-216]. However, another study reported that BANK1 risk mutation is not shared between SLE and RA [217].

The functional impact of those mutations and the global interactions are largely unknown and not fully delineated. A growing body of literature indicates that the PTPN22 1858C/T polymorphism is a gain-of-function mutation reducing TCR as well as BCR responses [218-220]. However, in mice PTPN22 risk mutation is reported to increase BCR signaling [221]. It is also reported that the PTPN22 risk allele is associated with higher IFNα activity and lower TNF expression [222]. The risk mutation of the adapter molecule BANK1, which is mainly expressed in $CD19^+$ B cells, leads to a dysbalanced expression of BANK1 splicing variants, which in turn reduces BCR signaling [204, 223].

### *3.4.4 Altered BCR Signaling in Autoimmunity*

Alterations in the intrinsic BCR signal are thought to promote autoimmunity by affecting the selection of the naive repertoire and promotion of autoreactive clones during extrafollicular and GC responses [184]. Furthermore, abnormal BCR signaling in anergic cells may cause activation of silenced autoreactive B cells [224]. Hyperreactivity in rheumatic diseases is considered to be reflected by alterations in BCR-associated kinase expression and phosphorylation [225, 226]. However, the major understanding of BCR signaling in autoimmunity is based on studies in mice, in which increased BCR signal is a driver of autoimmunity [13]. This is often caused by a lack of negative regulators such as CD22 and FcγRIIb as well as SHP-1, but also PLCγ2 gain-of-function mice are reported to develop autoimmunity [227-230]. The role of Lyn is more complex as both, $Lyn^{-/-}$ and $Lyn^{up/up}$ mice, produce ANAs upon B cell hyper-responsiveness [13]. Furthermore, murine B cells overexpressing Btk were hyperresponsive to BCR stimulation with increased $Ca^{2+}$ influx, resistance to Fas-mediated apoptosis, spontaneous GC formations and defective elimination of self-reactive B cells *in vivo* [231].

Human studies are contradictory in this regard. Some studies reported increased BCR signaling measured by $Ca^{2+}$ release and downstream tyrosine phosphorylation caused by a lack of negative regulation, such as FcγRIIb, phosphatase and tensin homolog (PTEN) and Lyn, in B cells from SLE patients [15, 16, 232-237]. However, more recent studies reported evidence that the BCR signal in autoimmunity is impaired, at least in some B cell subsets, with reduced tyrosine phosphorylation, $Ca^{2+}$

release and recruitment of signaling kinases to lipid rafts upon BCR stimulation [14, 218, 223, 237, 238].

### *3.4.5 B Cell Directed Therapies in Autoimmune Diseases*

The beneficial therapy of SLE, RA and pSS patients with Rituximab underlines the important role of B cells in the pathogenesis of these autoimmune diseases [3-10, 239]. Rituximab targets the B cell lineage marker CD20, which mediates $Ca^{2+}$ influx, and successfully depletes peripheral B cells except mature ASCs which lack CD20 expression [10]. Targeting B cell lineage survival factors by the humanized anti-BAFF antibody belimumab is approved in the EU and the USA for the treatment of SLE. This therapeutic antibody reduces disease activity as well as flare severity and incidence when provided in combination with standard therapy [10, 196]. However, none of those treatment strategies targets all B cell subset at once. Anti-CD20 treatment using Rituximab does not deplete long-lived plasma cells which are responsible for the long-term production of autoantibodies in autoimmune diseases [240]. Also, the anti-BAFF antibody Belimumab does not deplete memory B cells or inhibit IgG autoantibody production [10, 196]. Therefore, a combination therapy targeting precursors of long-lived plasma cells and plasma cells using a plasma cell depleting agent, such as the small molecule proteasome inhibitor bortezomib, might be of therapeutic value and are under research [10, 196, 241].

Besides depletion therapy, another approach is targeting B cell activation by interfering with the BCR signaling pathway via anti-CD22 antibodies. This approach might be useful, because the quality of the BCR signal plays an important role in cell fate decision making, B cell activation and maintenance of self-tolerance [17, 125, 129]. The anti-CD22 therapy aims at reducing BCR hyper-activation by reducing the BCR signaling strength. CD22 helps in maintain the balance between Syk and SHP-1 activity, and interfering with this pathway decreases the BCR signal and enhancing the activation threshold [110, 242]. Furthermore, approaches by targeting the IFNα pathway in SLE may have beneficial effects on B cells by lowering TLR-dependent responses [243].

# 4 Hypothesis and Aim

B cells are the major source of autoantibodies in diseases such as SLE, RA and pSS, and therefore, a key element of disease pathology [38-40, 44-47]. Abnormal BCR signaling events in autoimmune diseases might be responsible for pathologic recognition of autoantigens by B cells. Previous research implicate reduced responsiveness of SLE B cells towards BCR signals due to abnormal negative regulation via CD22 feedback loop and increased tyrosine phosphatase activity [14]. Results from our working group implicate an increased negative regulation by CD22 and SHP-1 as a commonality in SLE, RA and pSS peripheral B cells (**Section 6.1, Figure 5**) [244]. To explore potential underlying molecular or functional abnormalities, this thesis aimed at further characterizing B cell responsiveness in autoimmunity by addressing the following questions:

a) Is the phenotype of recently observed low responsiveness towards BCR and TLR9 stimulation specific for SLE or a commonality among peripheral B cell related autoimmune diseases such as RA and pSS?
    i. Are there specific phenotypic properties among peripheral SLE, RA and pSS B cells with regard on the expression and phosphorylation of BCR signaling molecules and surface markers related to BCR signaling?
    ii. Are there common BCR related functional abnormalities among B cells from SLE, RA and pSS patients?
    iii. Is this phenotype restricted to B cells from the peripheral blood or does this also apply for tissue resident B cells?
b) Are there potential inducers of abnormal signaling events such chronic stimulation with cytokines and TLR9 or BCR?
c) Which impact has T cell-dependent co-stimulation on abnormal signaling events in SLE, RA and pSS?
d) How does T cell-dependent co-stimulation affect proliferation and differentiation of SLE, RA and pSS B cell?

Question a) was addressed by analyzing phenotypic and functional properties of the BCR signaling cascade in peripheral B cells from SLE, RA and pSS patients in comparison to HDs. This was done by analyzing the expression and phosphorylation of BCR signaling molecules with and without BCR stimulation. This thesis also includes data from our group on PTP/PSP activities and CD22/SHP-1 co-localization in B cells from SLE, RA and pSS patients compared to HD controls. Additionally, tissue resident B cells from tonsils, autoimmune ITP and non-autoimmune spleens as well as one pSS parotid were analyzed for functional BCR signaling.

To address question b), pSyk($Y^{352}$) after BCR stimulation in HD, SLE, RA and pSS peripheral B cells was correlated with a panel of 28 different cytokines and sialic acid-binding Ig-like lectin 1 (Siglec-1) expression as a surrogate marker for INFα activity. Furthermore, pERK1/2($T^{202}/Y^{204}$) was tested as a potential marker for anergy in autoimmune disease patients. It was tested whether low B cell

responsiveness could be induced by pre-incubation of HD B cells with IFNα, IFNγ, IL-21, IL-2, IL-6, IL-10 or chronic stimulation of TLR9 and the BCR. In addition, epigenetic abnormalities of SLE, RA and pSS B cells were analyzed in a meta-analysis from publicly available data together with cooperation partners.

To answer question c), different CD40 co-stimulating systems were tested. Moreover, the impact of CD40 co-stimulation together with IL-4 or IL-21 on BCR induced Syk($Y^{352}$) phosphorylation was analyzed in B cells from SLE, RA and pSS patients compared to HDs.

Finally, question d) was addressed analyzing B cell proliferation and differentiation after *in vitro* activation of TLR9 and the BCR with and without CD40 co-stimulation. Furthermore, expression of phosphatases was analyzed from publicly available RNA sequencing data at baseline and upon CD40L/IL-4 stimulation (by cooperation partners).

# 5 Donors, Materials and Methods

## 5.1 Blood and Tissue Donors

This study was approved by the ethic committee of the Charité – Universitätsmedizin Berlin. Written informed consent was obtained from all donors. Patients with RA fulfilling the American College of Rheumatology (ACR)/ European League Against Rheumatism (EULAR) criteria [245], SLE according the Systemic Lupus International Collaborating Clinics (SLICC) criteria [246] and pSS fulfilling the American-European Consensus Group (AECG) criteria [247] were included in this study. Ethylenediaminetetraacetic acid (EDTA) anti-coagulated peripheral and/or serum blood samples from 87 SLE, 51 pSS and 44 RA patients and 129 HDs were collected. Ethnicity, gender, mean age, disease activity and medication of donors are summarized in **Table 1**. Specimens of human spleens and tonsils were collected from surgeries with medical implications (**Table 2**).

**Table 1:** Gender, mean age, ethnicity, disease activity score and medication of blood donors.

| **HD** | **n = 129** |
|---|---|
| Gender | 102 females, 27 males |
| Ethnicity | 128 Caucasians, 1 Indian |
| Mean age [range] | 33 [21 – 65] |
| **SLE** | **n = 87** |
| Gender | 79 females, 7 males |
| Ethnicity | 85 Caucasians, 1 African, 1 Asian |
| Mean age [range] | 40 [19 – 73] |
| SLEDAI | 70 low (< 6), 13 high (> 6) |
| Treatment | 7 none, 12 Pred, 5 MTX, 8 HCQ, 1 Aza, 1 Cyclo, 13 Pred/HCQ, 9 Pred/Aza, 2 Aza/HCQ, 1 MTX/HCQ, 4 Pred/MMF, 1 HCQ/MMF. 2 Pred/Cyclo, 2 Pred/CyA, 2 MTX/Pred/HCQ, 3 Pred/Aza/HCQ, 3 Pred/MMF/HCQ, 1 Pred/HCQ/Bemab, 1 HCQ/MMF/Bemab, 3 Pred/HCQ/Cyclo, 1 Pred/MTX/HCQ, 1 Pred/HCQ/MMF/Bemab |
| **RA** | **n = 44** |
| Gender | 34 females, 9 males |
| Ethnicity | 44 Caucasians |
| Mean age [range] | 55 [26 – 79] |
| DAS28 | 27 low (< 3.2), 7 moderate (3.2 – 5.1), 7 high (> 5.1) |
| Treatment | 1 none, 6 Pred, 6 MTX, 2 Eterna, 1 Toci, 9 MTX/Pred, 1 MTX/Abata, 5 Pred/Toci, 2 Pred/Eterna, 1 MTX/Simponi, 3 MTX/Eterna, 1 MTX/Pred/Sulfa, 1 Pred/Toci/Sulfa, 2 MTX/Pred/Eterna, 1 MTX/Pred/Abata |

| pSS | n = 51 |
|---|---|
| Gender | 50 females, 1 male |
| Ethnicity | 51 Caucasians |
| Mean age [range] | 56 [34 – 80] |
| ESSDAI | 41 low (< 4), 10 high (> 4) |
| Manifestation | 14 gl, 37 egl |
| Treatment | 18 none, 6 Pred, 17 HCQ, 1 Cyclo, 1 CyA, 6 Pred/HCQ, 1 Pred/Aza, 1 Aza/HCQ |

Abatacept (Abata), azathioprine (Aza), belimumab (Bemab), cyclophosphamide (Cyclo), cyclosporine A (CyA), Disease Activity Score 28 (DAS28), eternacept (Eterna), EULAR Sjögren's syndrome (SS) disease activity index (ESSDAI), extraglandular (egl), glandular (gl), hydroxychloroquine (HCQ), methotrexate (MTX), mycophenolatmofetil (MMF), number of donors (n), prednisolone (Pred), sulfasalazine (Sulfa), Systemic Lupus Erythematosus Disease Activity Index (SLEDAI), tocilizumab (Toci)

**Table 2:** Age, disease and gender of spleen, tonsil and parotid donors.

| Tissue | Age at date of surgery | Sex | Disease |
|---|---|---|---|
| Spleen 1 | 66 | m | ITP |
| Spleen 2 | 29 | m | ITP |
| Spleen 3 | 23 | f | ITP |
| Spleen 4 | 49 | f | ITP |
| Spleen 5 | 62 | f | Pancreatitis |
| Spleen 6 | 75 | m | Cancer |
| Spleen 7 | 42 | m | Splenomegaly |
| Spleen 8 | 29 | f | Cysts |
| Spleen 9 | 62 | f | Cancer |
| Spleen 10 | 52 | m | Pancreatitis |
| Spleen 11 | 62 | f | Cancer |
| Tonsil 1 | - | - | - |
| Tonsil 2 | - | - | - |
| Tonsil 3 | - | - | - |
| Tonsil 4 | - | - | - |
| Parotid | - | m | pSS |

Female (f), male (m), no information (-)

## 5.2 Materials

Relevant information on consumables (**Table 3**), chemicals and commercially available buffer (**Table 4**), commercial kits (**Table 5**), buffer, media and preparations (**Table 6Table 7**), antibodies (**Table 7**), stimulation reagents, inhibitors and cytokines (**Table 8**), cell lines (**Table 9**), electronic devices (**Table 10**) and analysis software (**Table 11**) are provided below. Supplier information is listed in the appendix (**Supplementary Table 1**).

**Table 3:** Consumables with supplier.

| Product | Supplier |
|---|---|
| Anti-Mouse Ig, κ/Negative Control Compensation Particles Set | BD Bioscience |
| Calibration Kit BioPlex | BioRad |

| Product | Supplier |
|---|---|
| CELLSTAR cell culture flask, 250 ml, 75 $cm^2$, PS, red cap | Greiner Bio-One International GmbH |
| CELLSTAR cell culture micro plate, 96 well, PS, U–bottom | Greiner Bio-One International GmbH |
| CELLSTAR cell culture multiwell plate, 24 well, PS, F–bottom | Greiner Bio-One International GmbH |
| Combitips (various) | Eppendorf |
| CountBright™ Absolute Counting Beads | Invitrogen/Thermo Fisher |
| CS&T Research Beads (BD FACSDiva™ software v7 or later) | BD Bioscience |
| CS&T Beads Kit (BD FACSDiva™ software v6.x) | BD Bioscience |
| Falcon 70 µm Cell Strainer | Corning |
| Falcon 15 ml Conical Centrifuge Tubes | Fisher scientific/Thermo Fisher |
| Falcon 50 ml Conical Centrifuge Tubes | Fisher scientific/Thermo Fisher |
| Falcon Round-Bottom Polystyrene Tubes | Fisher scientific/Thermo Fisher |
| FcR Blocking Reagent, human | Miltenyi Biotec GmbH |
| Heterophilic (HRP) Blocking Tubes | Scantibodies Laboratory |
| Micrewtube | VWR International GmbH |
| Microcentrifuge tubes, Safe-Lock PCR clean (0.5 µl) | Eppendorf |
| Microplate, 96 Well, PS, U-Bottom | Greiner Bio-One International GmbH |
| $MultiScreen_{HTS}$-BV, 1.2 µm, filter plate | Merck KGaA |
| Pre-Separation Filters (30 µm) | Miltenyi Biotec GmbH |
| Rainbow Calibration Particles (8 peaks), 3.0 - 3.4 µm | BD Bioscience |
| SafeSeal SurPhob filter tips (various) | Biozym Scientific GmbH |
| Serological pipettes (various) | SARSTEDT AG & Co. KG |
| Tube 5 ml, 75x12 mm, PS | SARSTEDT AG & Co. KG |
| VACUETTE EDTA Tubes | Greiner Bio-One International GmbH |
| VACUETTE Serum collection tubes | Greiner Bio-One International GmbH |
| Vacutainer Plastic Plus EDTA Blood Collection Tubes | BD Bioscience |
| Vacutainer Plus Plastic SST Blood Collection Tubes with Polymer Gel for Serum Separation | BD Bioscience |

**Table 4:** Chemicals and commercially available buffers.

| Chemical | Supplier |
|---|---|
| 4',6-diamidino-2-phenylindole, dihydrochloride (DAPI) | Invitrogen/Thermo Fisher |
| AF488 succinimidylester | Molecular Probes/Thermo Fisher |
| autoMACS Rinsing Solution | Miltenyi Biotec GmbH |
| BD Pharm Lyse (10x) | BD Bioscience |
| BD Phosflow Perm Buffer II | BD Bioscience |
| BD Phosflow Perm Buffer III | BD Bioscience |
| Brilliant Stain Buffer | BD Bioscience |
| Buffer EL | Qiagen |
| Dimethyl sulfoxide ($C_2H_6O_6$; DMSO) | Invitrogen/Thermo Fisher |
| Fetal Bovine Serum (FBS), heat inactivated | gibco by life technologies/Thermo Fisher |

| Chemical | Supplier |
|---|---|
| Ficoll Paque Plus | GE Healthcare |
| Lyse/Fix Buffer (5X) | BD Bioscience |
| MACS BSA Stock Solution | Miltenyi Biotec GmbH |
| Dihydrogen peroxide ($H_2O_2$) | Merck KGaA |
| Penicillin-Streptomycin (P/S) (10,000 U/ml) | gibco by life technologies/Thermo Fisher |
| Phosphate Buffered Saline (PBS), without $Ca^{2+}$, $Mg^{2+}$ | Merck KGaA |
| RPMI 1640 Medium, GlutaMAX Supplement | gibco by life technologies/Thermo Fisher |
| Ultra-pure water | Merck KGaA |

**Table 5:** Commercial kits.

| Kit | Supplier |
|---|---|
| Bio-Plex Pro Human Cytokine 27-plex Assay | Bio-Rad Laboratories |
| Bio-Plex Pro Human Th17 Cytokine IL-21 | Bio-Rad Laboratories |
| CellTrace Carboxyfluorescein succinimidyl ester (CFSE) | Invitrogen/Thermo Fisher |

**Table 6:** Buffer, media and preparations.

| Buffer | Reagent | Concentration/dilution |
|---|---|---|
| Complete medium<br>(RPMI, 10 % FBS, 1 % P/S) | FBS<br>P/S (10,000 U/ml) | 10 %<br>1 %<br>in RPMI 1640 with GlutaMAX™ |
| CFSE | CellTrace CFSE<br>(kit component A) | 5 mM (stock)<br><br>in DMSO (kit component B) |
| Erythrocytes lysis buffer | Buffer EL | 4:1<br>in MACS buffer |
| Freezing medium | DMSO | 1:10<br>in FBS |
| Lyse/Fix Buffer | Lyse/Fix Buffer (5X) | 1:5<br>in $H_2O$ |
| MACS Buffer<br>(PBS, 0.5 % BSA, 2 mM EDTA) | MACS BSA Stock Solution | 1:10<br>in autoMACS Rinsing Solution |
| PBS/BSA<br>(PBS, 0.1 % BSA) | MACS BSA Stock Solution | 1:50<br>in PBS |
| Pharm Lyse | BD Pharm Lyse (10x) | 1:10<br>in $H_2O$ |

**Table 7:** Antigens, conjugates, clones and supplier of the applied antibodies.

| Antigen | Conjugate | Clone | Species | React. | Supplier | Applic. |
|---|---|---|---|---|---|---|
| CD3 | PB | UCHT1 | mouse | human | BD Bioscience | FC |
| CD14 | APC-Cy7 | M5E2 | mouse | human | BioLegend | FC |
| CD14 | PB | M5E2 | mouse | human | BD Bioscience | FC |
| CD19 | PE-Cy7 | SJ25C1 | mouse | human | BD Bioscience | FC |

| Antigen | Conjugate | Clone | Species | React. | Supplier | Applic. |
|---|---|---|---|---|---|---|
| CD20 | BV510 | 2H7 | mouse | human | BioLegend | FC |
| CD20 | PO | HI47 | mouse | human | Invitrogene | FC |
| CD20 | PerCp-Cy5.5 | H1(FB1) | mouse | human | BD Bioscience | FC |
| CD22 | PE | S-HCL-1 | mouse | human | BD Bioscience | FC |
| CD27 | APC | L128 | mouse | human | BD Bioscience | FC |
| CD38 | APC-Cy7 | HIT2 | mouse | human | BioLegend | FC |
| CD40 | None | G28-5 | mouse | human | Andreas Hutloff [1)] | SA |
| Akt1 | PerCp-Vio700 | REA134 | rec human | human | Miltenyi Biotec | FC |
| pAkt($S^{473}$) | PE | M89-61 | mouse | human | BD Bioscience | FC |
| Btk | PE | 53/BTK | mouse | human | BD Bioscience | FC |
| pBtk($Y^{223}$) | FITC | N35-86 | mouse | human | BD Bioscience | FC |
| pERK1/2($T^{202}/Y^{204}$) | AF488 | 20A | mouse | human | BD Bioscience | FC |
| IgG/IgM ($F(ab')_2$) | None | Poly | goat | human | Jackson ImmunoResearch | SA |
| Isotype control | AF488 | MOPC-21 | mouse | mouse | BD Bioscience | FC |
| pPI3K p85($Y^{467}$)/ p55($Y^{199}$) | AF488 [2)] | Poly | mouse | human | Invitrogene /Thermo Fisher | FC |
| pPI3CD($Y^{524}$) | AF488 | Poly | rabbit | human | Bioss Antibodies | FC |
| REA Control (I) | PerCp-Vio700 | REA293 | rec human | human | Miltenyi Biotec | FC |
| pSHP-1($Y^{564}$) | AF488 [2)] | Poly | rabbit | human | Thermo Fisher | FC |
| Siglec-1 | AF647 | 7-239 | mouse | human | BD Bioscience | FC |
| Syk | FITC | 4D10 | mouse | human | BD Bioscience | FC |
| pSyk($Y^{352}$) | PE | 17A/P-ZAP70 | mouse | human | BD Bioscience | FC |
| PLCγ2 | PE | K86-1161 | mouse | human | BD Bioscience | FC |
| pPLCγ2($Y^{759}$) | AF488 | K86-689.37 | mouse | human | BD Bioscience | FC |

Alexa flour (AF), allophycocyanin (APC), application (applic.), brilliant violet (BV), Bruton's tyrosine kinase (Btk), cyanine (Cy), flow cytometry (FC), fluorescein isothiocyanate (FITC), Mitogen-activated protein kinase 3 (ERK1), pacific blue (PB), pacific orange (PO), peridinin-chlorophyll-protein (PerCP), 1-phosphatidylinositol-4,5-bisphosphate phosphodiesterase gamma-2 (PLCγ2), phosphoinositide 3-kinase (PI3K), phycoerythrin (PE), protein kinase B (Akt1), reactivity (react.), recombinant (rec), sialic acid-binding immunoglobulin-type lectin 1 (Siglec-1), spleen tyrosine kinase (Syk), src homology region 2 domain-containing phosphatase-1 (SHP-1), stimulation assay (SA)

1) Provided by Andreas Hutloff, German Rheumatology Research Center (DRFZ) and Robert Koch Institute (RKI), Berlin, Germany
2) Labeling at the DRFZ by the lab manager core facility

**Table 8:** Stimulation reagents, inhibitors and cytokines.

| Target | Reagent | Supplier | $c_{final}$ |
|---|---|---|---|
| CD40 | anti-CD40 antibody | Andreas Hutloff (DRFZ/RKI) | 0.1, 1, 5, 10, 100 µg/ml |
| CD40 | CD40L cross-linking Kit | Miltenyi Biotec GmbH | 0.5 µg/ml |
| CD40 | sCD40L | PeproTech | 0.5 µg/ml |
| IgG/IgM [1) 2)] | anti-IgG/IgM $F(ab')_2$ | Jackson ImmunoResearch | 13 µg/ml (LOT 121170)<br>9 µg/ml (LOT 125959)<br>9 µg/ml (LOT 135690) |

| Target | Reagent | Supplier | $c_{final}$ |
|---|---|---|---|
| IgG/IgM [3]) | anti-IgG/IgM F(ab')$_2$ | Jackson ImmunoResearch | 2 µg/ml (LOT 125959) |
| IL-2R | rec. human IL-2 | Miltenyi Biotec GmbH | 0.02 µg/ml |
| IL-4R | rec. human IL-4 | PeproTech | 0.02 µg/ml |
| IL-6R | rec. human IL-6 | PeproTech | 0.02 µg/ml |
| IL-10R | rec. human IL-10 | Miltenyi Biotec GmbH | 0.02 µg/ml |
| IL-21R | rec. human IL-21 | PeproTech | 0.02 µg/ml |
| IFNAR | rec. human IFNα | PeproTech | 100 ng/ml |
| IFNGR | rec. human IFNγ | PeproTech | 100 ng/ml |
| Syk | Entospletenib | Selleck Chemicals | 0.1, 1, 10 µM |
| TLR9 | CpG (ODN2006) | Miltenyi Biotec GmbH | 0.5 µg/ml |

Cytosine-phosphodiester-guanine (CpG), interferon alpha/beta receptor (IFNAR), interferon gamma receptor (IFNGR), recombinant (rec), soluble CD40L (sCD40L), spleen tyrosine kinase (Syk), toll-like receptor 9 (TLR9)

[1] Phospho-kinetics
[2] Reagents with different LOT numbers were titrated to the same biological activity
[3] Cell culture experiments

**Table 9:** Cell lines.

| Cell line | Organism | Cell type | Modifications |
|---|---|---|---|
| L cells [1] | mouse | fibroblasts, adherent | none |
| hCD40L L cells [1] | mouse | fibroblasts, adherent | transfected with hCD40L |

human CD40L (hCD40L)

[1] Provided by Andreas Hutloff, DRFZ and RKI, Berlin, Germany

**Table 10:** Electronic devices.

| Device | Supplier |
|---|---|
| BioPlex System reader | Bio-Rad Laboratories |
| FACSCanto II flow cytometer | BD Bioscience |
| Gammacell® 40 Exactor radiation source | MDS Nordion |
| LSRFortessa flow cytometer | BD Bioscience |

**Table 11:** Applied software

| Software | Supplier |
|---|---|
| FACS Diva v6.1.3 (FACSCanto II) | BD Bioscience |
| FACS Diva v8.0.2 (LSR Fortessa) | BD Bioscience |
| FlowJo 10.4.2 | TreeStar |
| GraphPad Prism v5.04 | GraphPad Software |
| BioPlex Manager v4.1.1 | Bio-Rad Laboratories |

## 5.3 Quality Control of Flow Cytometry Staining

Quality control of flow cytometry staining was performed using SPHERO Rainbow Calibration Particles for stable median fluorescence intensity (MFI) over time and Cytometer Setup and Tracking beads [248].

## 5.4 Siglec-1 Expression as Surrogate Marker for *In Vivo* IFNα Activity

IFNα activity was assessed upon flow cytometric analysis of Siglec-1 (CD169) expression on CD14⁺ monocytes from fresh peripheral whole blood. Sample preparation and analysis described in this section was done in cooperation with Karin Reiter (technical assistant, laboratory of Prof. Dr. Dörner, Charité – Universitätsmedizin Berlin, Berlin, Germany). Siglec-1 analysis was performed as described earlier [194]. Briefly, whole blood (200 µl) was lysed with 2 ml Pharm Lyse (15 min, room temperature (RT)). The cells were centrifuged (310 xg, RT) and washed two times with 3 ml MACS buffer (310 xg, 4 °C). Fifty µl cell suspension were incubated with 2.5 µl human FcR blocking reagent (5 min, RT), stained with CD14-APC-Cy7 and Siglec-1-AF647 (15 min, 4 °C), centrifuged (310 xg, 5 min, 4 °C) and suspended in 100 µl MACS buffer. DAPI (900 nM) was added before measurement for dead cell exclusion. Siglec-1 expression was analyzed as MFI on CD14⁺ monocytes using FACS Canto II and FACS Diva Software (gating strategy in **Figure 1**).

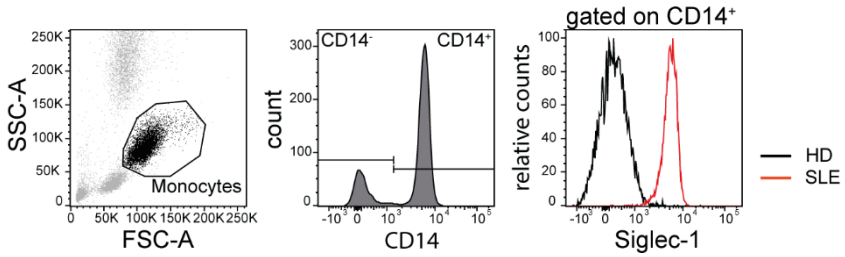


**Figure 1: Analysis of Siglec-1 expression on CD14⁺ monocytes (gating strategy).** Monocytes were gated according to their properties in forward (FSC) and sideward (SSC) scatter (left panel) and their CD14 expression (mid panel). An example of Siglec-1 expression on SLE (red) and HD (black) CD14⁺ monocytes is given in the right panel.

## 5.5 Intracellular B Cell Phenotyping for BCR Downstream Kinase Expression and Phosphorylation at Baseline

Baseline expression and phosphorylation of intracellular kinases were analyzed using intracellular flow cytometry based on formaldehyde and methanol fixation and permeabilization. For this, fresh peripheral whole blood (100 µl) was lysed and fixed in 1 ml pre-warmed Lyse/Fix Buffer (10 min, 37 °C). Next, cells were washed twice with 3 ml ice cold PBS (8 min, 500 xg) and permeabilized with 200 µl Perm buffer II or III (-20 °C, 12 h). Perm buffer II was used for analysis of the combinations Syk/pSyk($Y^{352}$) and PLCγ2/pPLCγ2($Y^{759}$) and Perm buffer III was used for the analysis of Akt/pAkt($S^{473}$) and Btk/pBtk($Y^{223}$). Finally, cells were washed two times with 3 ml MACS buffer (8 min, 500 xg, 4 °C) and stained with the following marker-fluorochrome combination: CD3-PB, CD14-PB, CD19-PE-Cy7, CD20-PO, CD27-APC and one of the combinations of Syk-FITC/pSyk($Y^{352}$)-PE, PLCγ2-PE/pPLCγ2($Y^{759}$)-FITC, Akt1-PerCp-Vio700/pAkt($S^{473}$)-PE or Btk-PE/pBtk($Y^{223}$)-FITC.

Washed cells were analyzed using FACS Canto II flow cytometer and FACS Diva Software. Akt, pAkt($S^{473}$), Btk, pBtk($Y^{223}$), PLCγ2, pPLCγ2($Y^{759}$), Syk, pSyk($Y^{352}$) MFIs were analyzed from CD27⁻ B cells and CD27⁺ memory B cells (gating strategy in **Figure 2**). CD3⁺ lymphocytes served as internal negative control, except for the staining of Akt1. Here an isotype control using REA Control (I)-PerCp-Vio700 in the same concentration as the antibody was used.

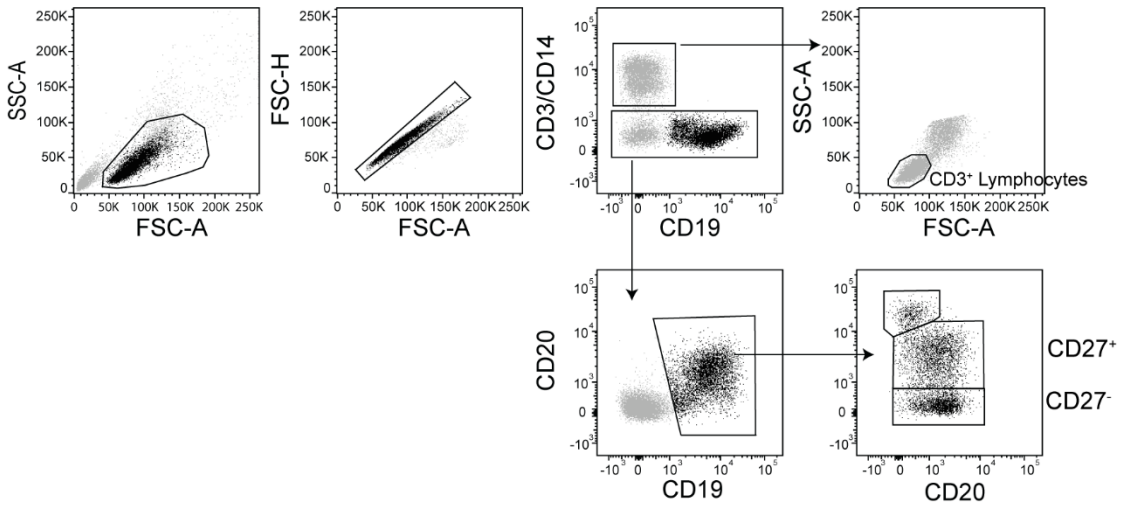


**Figure 2: Analysis of intracellular kinases within CD27$^-$ B cells and CD27$^+$ memory B cells.** Lymphocytes were identified based on their FSC and SSC characteristics (left panel). Doublets, CD3$^+$ and CD14$^+$ cells were excluded using height (H) and area (A) of FSC (second left panel). B cells were defined as CD3$^-$/CD14$^-$ and CD19$^+$ cells (third panels from left). The CD27$^-$ B cells and CD27$^+$ memory B cell subsets were gated upon their expression of CD20 and CD27 (lower right panel). CD3$^+$/CD14$^+$ cells were back gated on lymphocytes (upper right panel). CD3$^+$ lymphocytes served as unstimulated negative control.

## 5.6 Analysis of pERK1/2(T$^{202}$/Y$^{204}$) Expression as a Surrogate Marker for B Cell Anergy

Cells from fresh peripheral whole blood were prepared as described in **Section 5.5**. Phospho-(p)ERK1/2(T$^{202}$/Y$^{204}$) was analyzed using Perm III and the antibodies anti-CD3-PB, anti-CD14-APC-Cy7, anti-CD19-PE-Cy7, anti-CD20-BV510, anti-CD27-APC and anti-pERK1/2(T$^{202}$/Y$^{204}$)-AF488. An isotype control labeled with AF488 (clone MOPC-21) was used to verify the staining. Washed cells were analyzed using LSR Fortessa flow cytometer and FACS Diva Software. Phospho-(p)ERK1/2(T$^{202}$/Y$^{204}$) MFIs were analyzed in CD27$^-$ B cells and CD27$^+$ memory B cells (gating strategy in **Figure 3**).

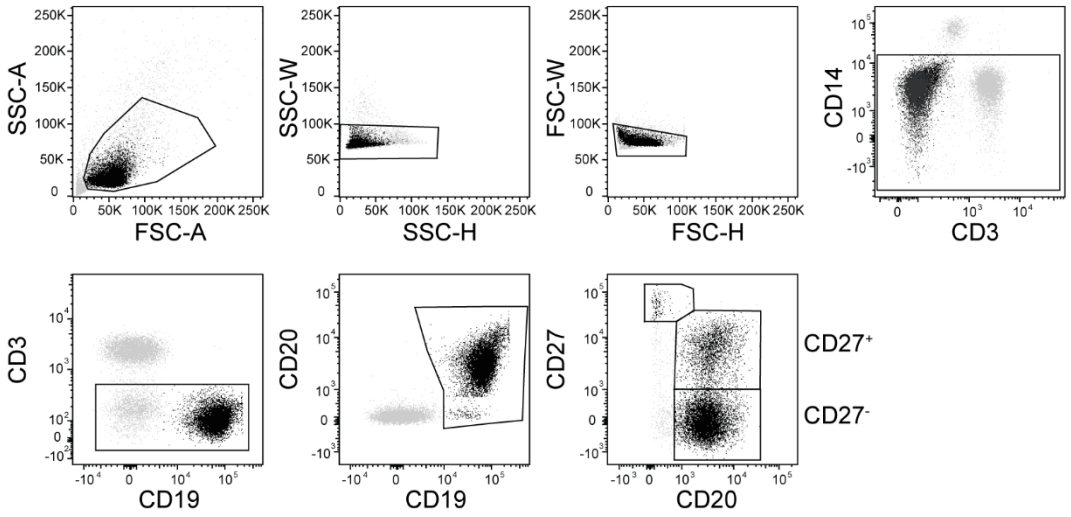


**Figure 3: Analysis of intracellular targets in CD27$^-$ B cells and CD27$^+$ memory B cells.** Lymphocytes and single cells were identified upon their properties in SSC versus FSC scatter (upper left panel). Doublets were excluded (two upper mid panels). CD14$^+$ (upper right panel) and CD3$^+$ (lower left panel) cells were excluded. B cells were identified upon their expression of CD19 (lower mid panel). CD27$^-$ B cells and CD27$^+$ memory B cells were identified upon their characteristic expression of CD20 and CD27 (lower right panel).

## 5.7 Isolation of Peripheral Blood Mononuclear Cells (PBMCs) from Human Blood Samples

PBMCs were isolated from fresh whole blood using density gradient centrifugation. Therefore, whole blood (10 – 25 ml) was diluted with PBS up to a total volume of 30 ml, layered on 15 ml Ficoll reagent and centrifuged (20 min, 840 xg, RT, without brake). The upper layer (plasma) was drawn off and discarded. PBMCs were transferred from the interphase into a new tube and washed with 50 ml MACS buffer (4 °C) for short term stimulation or PBS (RT) for *in vitro* culture and centrifuged (400 xg, 10 min). Cells were filtrated through a 30 µm cell strainer and washed with MACS buffer or PBS accordingly. For short-term anti-IgG/IGM stimulation (phospho-kinetics) and co-stimulation experiments cells were suspended in RPMI. For CFSE staining and subsequent long-term *in vitro* culture cells were suspended with PBS in appropriate concentrations.

## 5.8 Isolation of Mononuclear Cells (MNCs) from Human Spleen, Tonsil and Parotid

MNCs were isolated from human spleen, tonsil and parotid as previously described [249]. Therefore, fresh tissue (spleen, tonsil or parotid) was minced into small pieces with a scalpel, transferred into PBS (RT) and intensely shaken for 1 min. Then, the supernatant was filtered through a cell strainer (70 µm) and the procedure was repeated two more times with fresh PBS. The filtrates were pooled and layered on 15 ml Ficoll reagent. Centrifugation and isolation of MNCs was done as described for PBMC isolation (**Section 5.7**). Cells were washed with MACS buffer (4 °C) and treated with erythrocytes lysis buffer (10 min, on ice), centrifuged (400 xg, 10 min, 4 °C), suspended in MACS buffer and centrifuged again (400 xg, 10 min, 4 °C). Isolated cells were suspended in freezing medium ($2 \cdot 10^7$ cells/ml) and slowly cooled down to -80 °C using a CoolCell freezing container (Biozym). Cells were quickly thawed at the

day of the experiment in 50 ml RPMI (37 °C) and washed two times with RPMI (400 xg, 10 min, RT). Prior to the second washing step, cells were filtrated (30 µm). Finally, cells ($1 \cdot 10^6$) were suspended in 100 µl RPMI for further anti-IgG/IgM short-term stimulation experiments.

## 5.9 Analysis of *Ex Vivo* PTP and PSP Activities within $CD19^+$ B Cell and $CD3^+$ T Cells

Data and method are published [244]. Experiments and analysis were carried out by Franziska Szelinski (PhD student, AG Dörner, Charité – Universitätsmedizin Berlin). Briefly, B and T cell enrichment from PBMCs was performed using human B cell kit II or human Pan T cell kit (Miltenyi Biotec) for magnetic cell sorting according to the manufacturer's protocols. B and T cell purities were checked by flow cytometry and cell suspensions with more than 82 % purity were used for further experiments. Purified cells were lysed using Halt Protease Inhibitor Cocktail (1 % in Pierce IP Lysis Buffer; Thermo Fisher; 30 min on ice) and analyzed using a commercial PTP/PSP activity kit (Promega Corporation, Madison, Wisconsin., United States) as previously described [250]. Phosphatase activity was quantified by the release of free phosphate from the PTP and PSP-specific substrates Tyr PP1/Tyr PP2 and Ser/Thr PP, respectively. Absolute concentrations were assessed from standard dilution series. Assay specificity was ensured by using the inhibitors monovanadate (PTP inhibitor; 10 mM) and sodium fluoride (PSP inhibitor, 10 – 20 mM) (both Sigma-Aldrich). Cell lysates were analyzed at 600 nm using a Spectramax Plus 384 micro plate reader (Molecular Devices, San Jose, CA. USA).

## 5.10 Analysis of CD22/SHP-1 Co-Localization in $CD19^+$ B Cells

Data and method are published [244]. Experiments and analysis were carried out by Dr. Eva Schrezenmeier (MD, AG Dörner, Charité – Universitätsmedizin Berlin). B cells were purified from PBMCs as described in **Section 5.9**. Cells were suspended in 100 µl RPMI ($2 \cdot 10^5$ cells), equilibrated (1 h, 37 °C), stimulated with anti-CD22 $F(ab')_2$ epratuzumab-A488 (10 µg/ml) (UCB Pharma, Slough, United Kingdom) or left unstimulated, fixed and permeabilized as described in **Section 5.5**. Cells were stained with mouse anti-human-SHP-1 (BD Bioscience), goat anti-human-IgG/IgM (Jackson ImmunoResearch) and for unstimulated control with anti-CD22 $F(ab')_2$ epratuzumab-A488. Washed cells were stained with the secondary antibodies donkey anti-mouse-rhodamine red-X (RRX) and donkey anti-goat-A647 (Jackson ImmunoResearch). Finally, cells were centrifuged onto slides and covered with Vectashield HardSet mounting medium containing DAPI (Vector Laboratories, USA) to stain the nucleus. Co-localization/fluorescence overlap of SHP-1/CD22 was evaluated (0 = no co-localization, 1 = all pixels co-localized) using a Nikon A1-Rsi confocal microscope and NIS Elements C imaging software (Nikon, Tokyo, Japan).

## 5.11 Functional Analysis of BCR Associated Signaling Kinases Upon Anti-IgG/IgM Stimulation

The functional analysis of the BCR-associated signaling molecules Syk, Btk and Akt was carried out using freshly isolated PBMCs or thawed MNCs ($1 \cdot 10^6$ cells). Cells were rested for 1 h at 37 °C in 100 µl RPMI and then stimulated with 100 µl anti-IgG/IgM F(ab')$_2$ ($c_{final}$ see **Table 8**) for 2, 5, 8, 15 and 30 min. An additional RPMI control served as control at baseline (0 min). The stimulation was stopped by adding 1 ml pre-warmed (37 °C) Lys/Fix buffer. Lysis, fixation, permeabilization and staining were performed as described above (**Section 5.5**). Cells were stained with anti-CD3-PB, anti-CD14-PB, anti-CD19-PE-Cy7, anti-CD20-PerCp-Cy5.5, anti-CD27-APC and the combinations anti-Syk-FITC/anti-pSyk(Y$^{352}$)-PE, anti-Btk-PE/anti-pBtk(Y$^{223}$)-FITC and anti-Syk/anti-pAkt(S$^{473}$)-PE for analysis of Syk, Btk and Akt, respectively. In some pilot experiments cells were stimulated for 5 min with anti-IgG/IgM F(ab')$_2$ or $H_2O_2$ (3 % in RPMI) as positive staining control and stained with anti-pPI3K p85(Y$^{467}$)/p55(Y$^{199}$)-AF488, anti-PI3CD(Y$^{524}$)-AF488 or anti-pSHP-1(Y$^{564}$)-AF488. Flow cytometry analysis was performed using a FACSCanto II flow cytometer and FACS Diva software. MFIs were used to assess phosphorylation intensity of Akt(S$^{473}$), Btk(Y$^{223}$), PI3CD(Y$^{524}$), PI3K p85(Y$^{467}$)/p55(Y$^{199}$), SHP-1(Y$^{564}$) and Syk(Y$^{352}$) in CD27$^-$ B cells and CD27$^+$ memory B cells (gating strategy is show in **Figure 2**).

## 5.12 Anti-IgG/IgM Induced Syk(Y$^{352}$) Phosphorylation Upon *In Vitro* Pre-Incubation with Cytokines or CpG

Isolated PBMCs ($1 \cdot 10^6$ cells) were incubated with recombinant human IFNα (100 ng/ml), IFNγ (100 ng/ml), IL-21 (20 ng/mL) or combinations of IFNα or IFNγ with IL-21; IL-2 (20 ng/ml), IL-6 (20 ng/ml), IL-10 (20 ng/ml) or CpG (500 ng/ml) with and without IL-4 (20 ng/ml) or IL-21 in a 96-well plate. After incubation (48 h, 37 °C, 5 % $CO_2$) cells were harvested, washed with pre-warmed (37 °C) RPMI and centrifuged (310 xg, RT). BCR stimulation was conducted as described above (**Section 5.11**) for 5 min with anti-IgG/IgM F(ab')$_2$ or RPMI as unstimulated control. Permeabilized cells (Perm II) were stained with anti-CD3-PB, anti-CD14-APC-Cy7, anti-CD19-PE-Cy7, anti-CD20-BV510, anti-CD27-APC, anti-Syk-FITC and anti-pSyk(Y$^{352}$)-PE. Analysis was done using LSR Fortessa flow cytometer and FACS Diva Software. The MFI of pSyk(Y$^{352}$) was analyzed from CD27$^-$ B cells and CD27$^+$ memory B cells (gating strategy in **Figure 3**).

## 5.13 Chronic BCR and TLR9 *In Vitro* Stimulation

For chronic BCR and TLR9 stimulation experiments, cells were pre-incubated with anti-IgG/IgM (2 µg/ml), CpG (500 ng/ml) or RPMI for 24 h, 48 h or 72 h (37 °C, 5 % $CO_2$), washed with pre-warmed (37 °C) RPMI and subsequently stimulated with anti-IgG/IgM or RPMI as a control for 5 min as described above (**Section 5.11**). Permeabilized cells (Perm II) were stained with anti-CD3-PB, anti-CD14-APC-Cy7, anti-CD19-PE-Cy7, anti-CD20-BV510, anti-CD27-APC, anti-Syk-FITC and anti-

pSyk($Y^{352}$)-PE. The MFI of pSyk($Y^{352}$) was analyzed from $CD27^-$ B cells and $CD27^+$ memory B cells using FACS Canto II flow cytometer and FACS Diva Software (gating strategy in **Figure 2**).

## 5.14 CD40 *In Vitro* Co-Stimulation Strategies

The CD40 receptor requires stimulation by CD40L multimers for optimal signaling [251]. Therefore, cross-linking of CD40 is required for optimal stimulation. Stimulation with soluble (s)CD40L might be insufficient. Thus, three different strategies were approached for the optimal stimulation of CD40: (i) an anti-CD40 antibody coated on a micro-well plate, (ii) a co-culturing system with mouse fibroblast cells expressing human (h)CD40L and (iii) a cross-linking kit containing sCD40L and anti-CD40L cross-linking antibody.

### *5.14.1 B Cell Co-Stimulation by Anti-CD40 Coating*

Plate (96-well microplate) coating was performed with 100 µl anti-CD40 antibody (clone G28-5) (0.1, 1, 5, 10 or 100 µg/ml in PBS). PBS only was used as uncoated control. After incubation (2 h, 37 °C) the plate was washed two times with 200 µL PBS and loaded with PBMCs ($1 \cdot 10^6$ cells per well) in 100 µl RPMI. Cells were incubated (48 h, 37 °C, 5 % $CO_2$), harvested, washed with pre-warmed (37 °C) RPMI and centrifuged (310 xg, RT). BCR stimulation was conducted as described above (**Section 5.11**) for 5 min with anti-IgG/IgM $F(ab')_2$ or RPMI as unstimulated control. Permeabilized cells (Perm II) were stained with anti-CD3-PB, anti-CD14-APC-Cy7, anti-CD19-PE-Cy7, anti-CD20-BV510, anti-CD27-APC, anti-Syk-FITC and anti-pSyk($Y^{352}$)-PE. Analyses was performed using an LSR Fortessa flow cytometer and FACS Diva Software. The MFI of pSyk($Y^{352}$) was analyzed from $CD27^-$ B cells and $CD27^+$ memory B cells (gating strategy in **Figure 3**).

### *5.14.2 Co-Culturing System Using hCD40L Expressing Mouse Fibroblast Cell Line*

#### ***5.14.2.1 Thawing, Culturing and Passaging of L Cells***

L cells with and without hCD40L expression were quickly thawed in 50 ml complete medium, washed once with complete medium, centrifuged (350 xg, 10 min, RT) and cultured (37 °C, 5 % $CO_2$). Cells were passaged at approximately 80 % confluence. Therefore, the medium was discarded, and cells were detached using EDTA containing MACS buffer (5 min, 37 °C). Cells were washed with complete medium, centrifuged (350 xg, 10 min, RT) and seeded at a dilution of 1:10. Cells were cultured in 75 $cm^2$ cell culture flasks for maintenance and expansion of the cell line. For the co-culturing experiment, cells were seeded into 24-well flat-bottom cell culture plates and cultured to 80 % confluence.

#### ***5.14.2.2 Attenuation of L Cell Proliferation***

L cell proliferation was attenuated after irradiation using Gammacell® 40 Exactor radiation source. After irradiation the medium was discarded. Attenuation of proliferation was tested using CFSE staining. Therefore, CFSE (37 °C, 5 µM in PBS) was added to the cells and incubated (20 min, 37 °C). Afterwards, the cells were washed twice with complete medium and incubated (10 min) with fresh

complete medium. Medium was exchanged with fresh complete medium and cells were incubated (48 h, 37 °C, 5 % $CO_2$). Medium was removed; cells were washed with PBS and detached using MACS buffer (10 min, 37 °C). Cells were washed and stained with anti-CD40-PE (4 °C, 15 min). Washed cells were analyzed using FACS Canto II flow cytometer and FACS Diva software. Dead cells were excluded using DAPI staining (900 nM).

#### *5.14.2.3 Co-Culturing of Transfectant Cells with PBMCs*

Irradiated L cells with and without hCD40L expression were layered with PBMCs ($5 \cdot 10^6$ cells per well) and incubated with 500 µl RPMI (48 h, 37 °C, 5 % $CO_2$). PBMCs were harvested, washed with pre-warmed (37 °C) RPMI (310 xg, RT) and anti-IgG/IgM stimulation (5 min, 37 °C) was conducted as described previously (**Section 5.11**). Permeabilization, staining and analysis of pSyk($Y^{352}$) were performed as described above (**Section 5.14.1**).

### *5.14.3 Co-Stimulation Using a CD40L Cross-Linking Kit*

CD40L cross-linking kit was prepared according to the manufacture's protocol. Briefly, lyophilized CD40L was suspended in $H_2O$ (0.5 mg/ml). CD40L and the cross-linking antibody were incubated in equivalent volumes with complete medium 30 min prior to use (RT). Finally, isolated PBMCs ($1 \cdot 10^6$ cells) were incubated with cross-linked CD40L (0.5 µg/ml) in a 96-well plate. In some experiments IL-4 (20 ng/ml) or IL-21 (20 ng/ml) were added to the culture. After incubation (48 h, 37 °C, 5 % $CO_2$) cells were harvested and treated as previously described (**Section 5.14.1**).

## 5.15 Analysis of $CD19^+$ B Cell *In Vitro* Proliferation Using CFSE Staining

For cell proliferation analysis upon B cell stimulation, PBMCs ($2 \cdot 10^6$ cells/ml in PBS) were stained with 5 µM CFSE (4 min, 37 °C). After staining, cells were washed once with PBS and incubated in 10 ml RPMI for 30 min at 37 °C. Cells were washed with complete medium before stimulation.

## 5.16 *In Vitro* Differentiation of B Cells into Antibody Secreting Cells (ASCs)

PBMCs with and without previous CFSE staining (**Section 5.15**) were seeded in a 96-well microtiter plate (100 µl, $10^6$ cells), incubated (1 h, 37 °C) and subsequently stimulated with CpG (0.5 µg/ml) or a combination of CpG (0.5 µg/ml) with anti-IgG/IgM antibody (2 µg/ml) for 5 days (37 °C, 5 % $CO_2$) in complete medium. For B cell proliferation IL-2 (20 ng/ml) and IL-10 (20 ng/ml) and for co-stimulation experiments cross-linked CD40L (500 ng/ml), was added to the cells. After stimulation, cells were washed with MACS buffer and stained with anti-CD3-PB, anti-CD14-PB, anti-CD19-PE-Cy7, anti-CD20-BV510, anti-CD27-APC and anti-CD38-APC-Cy7 (15 min, 4 °C). After washing (2 ml MACS buffer, 310 xg, 5 min, 4 °C), counting beads were added to the samples without CFSE staining to assess absolute cell concentrations. Before flow cytometry analysis, DAPI (900 nM) was added to exclude dead cells. Cells were analyzed using a FACSCanto II flow cytometer. The gating was done as shown in **Figure 4**.

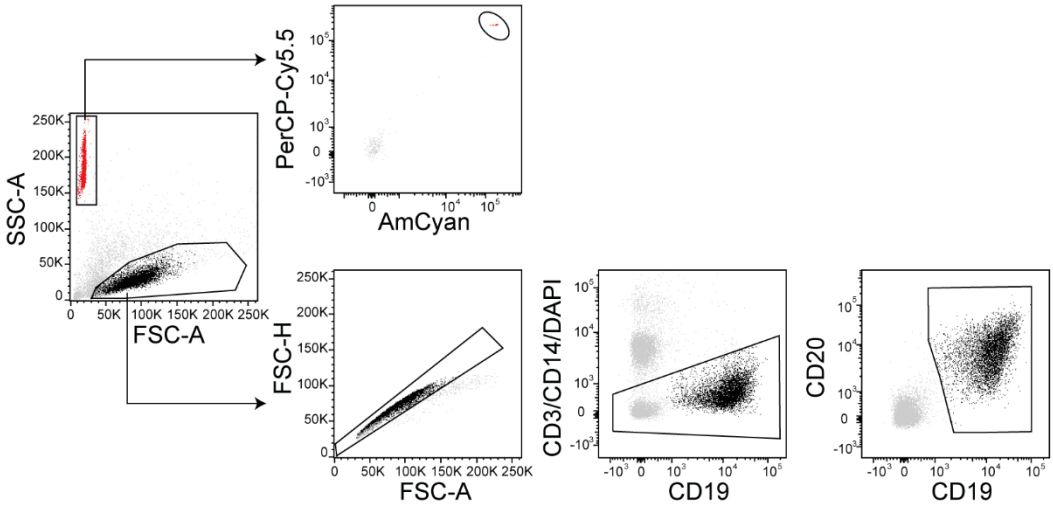


**Figure 4: Analysis of CD19⁺ B cells after *in vitro* stimulation (gating strategy).** Counting beads (red) were identified upon their characteristics in FSC *vs*. SSC scatter (left panel) and their high fluorescence in PerCp-Cy5.5 and AmCyan (upper panel). Lymphocytes and single cells were identified upon SSC versus FSC gating (left panel). Doublets (lower left panel), CD14⁺, CD3⁺ and dead cells (DAPI⁺) cells (lower mid panel) were excluded. B cells (black) were identified upon their CD19 expression (lower right panel).

## 5.17 Cytokine Quantification in Human Sera Using BioPlex Technology

Human serum samples were collected at the day of the respective experiment and stored (-20 °C) until further analysis. Thawed serum samples (450 µl) were transferred into HRP blocking tubes to prevent cross-reactivity of the assay with RF in human samples [252, 253]. Samples were centrifuged (12,000 xg, 10 min, 4 °C) and the supernatants were used for subsequent analysis. The following cytokines were analyzed using the Bio-Plex Pro™ Human Cytokine 27-plex Assay: IL-1b, IL-1Ra, IL-2, IL-4, IL-5, IL-6, IL-7,IL-8,IL-9, IL-10, IL12(p70), IL-13, IL-15, IL-17, eotaxin, fibroblast growth factor 2 (FGF basic), granulocyte colony-stimulating factor (G-CSF), GM-CSF, IFNγ, C-X-C motif chemokine 10 (IP-10), C-C motif chemokine 2 (MCP-1 or MCAF), macrophage inflammatory protein 1-alpha (MIP-1a), MIP-1b, platelet-derived growth factor subunit B (PDGF bb), C-C motif chemokine 5 (RANTES), TNFα and vascular endothelial growth factor A (VEGF). Bio-Plex Pro Human Th17 Cytokine IL-21 was analyzed as single assay. All reagents and buffer were provided with the kit.

Lyophilized standards were dissolved in 250 µL standard diluent and incubated (30 min, on ice). The dissolved standards were split into 3 aliquots (each 70 µL) and frozen for long term storage (-20 °C). At the day of the experiment 64 µL of thawed standard solution was diluted with 136 µl standard diluent. Standard curve was prepared by 8-times 1:40 dilution. 27-plex or IL-21 beads were prepared by 1:40 dilution with assay buffer and incubation prior to use (20 min, RT). The filter plate was moistened with 100 µl assay buffer per well and vacuumed (between -1 to -3 mmHg) using a vacuum station. Then, the plate was prepared with 50 µl diluted beads per well, vacuumed, washed two times with 100 µl wash buffer and vacuumed. Samples, standards and blank (each 50 µl) were pipetted on the plate in technical duplicates and shortly incubated at high rpm (30 sec, 1100 rpm, RT) and then at low rpm (30 min, 300 rpm, RT) in the dark. Detection antibody was prepared at a 1:40 dilution with antibody diluent prior to use (20 min, RT). After incubation, the plate was vacuumed and washed three times

with 100 ml wash buffer. Diluted detection antibody (25 µl) was added to the plate and incubated as described above. Streptavidin-PE was diluted with assay buffer (1:100) and incubated prior to use (10 min, RT). After incubation, the plate was evacuated, washed three times with wash buffer (100 ml), streptavidin-PE (50 µl) was added to the wells and the plate was incubated as described above. After incubation, the plate was washed three times with wash buffer (100 µl). After evacuation, assay buffer (100 µl) was added and then plate was incubated under shaking as described above 10 min before reading. Samples were analyzed using Bio-Plex-Systems. Calibration was performed using BioPlex Calibration Kit prior to the analysis. The running protocol was set to 50 beads per region, 100 regions bead map, sample size 50 µl and DD gates were set to 5,000 (low). Absolute concentrations were assessed according to standard dilution curves (**Supplementary Figure 1**)

## 5.18 Meta-Analysis of Differentially Methylated CpGs in SLE, RA and pSS

This meta-analysis of methylation data from SLE, RA and pSS $CD19^+$ B cells was carried out in cooperation with Prof. Jörn Walter (Department of Genetics and Epigenetics, Saarland University, Saarbrücken, Germany). Data on SLE and RA patients were collected from previously published studies [254-256]. Methylation data of pSS patients were kindly provided by Prof. Lars Rönnblom (Department of Medical Sciences, Rheumatology and Science for Life Laboratory, Uppsala University, Uppsala, Sweden). The data were processed as published [244]. Briefly, Idat files of the Illumina Infinium HumanMethylation450 BeadChip data were processed with RnBeads (v1.6.1) [254-256]. Next, data was aligned to hg19 reference genome, single nucleotide polymorphisms (SNPs) and sex chromosomes were excluded from further processing. A bead count cutoff of ≥ 10 and a greedy cut p-value cutoff of ≤ 0.01 was set to filter the data for high quality. The data was normalized using the Swan method. Finally, demethylated CpGs were defined as CpGs with ≥ 5 % DNA methylation difference and p-value ≤ 0.01.

## 5.19 Differential Gene Expression Analysis of RNA-Sequencing Data

Data analysis was conducted in cooperation with Dr. Peter E. Lipsky (RILITE Research Institute, Charlottesville, Virginia, United States) as published [244] (**Section 5.19.1 and Section 5.19.2**). The experimental procedure of CD40L/IL-4R stimulation was performed by Franziska Szelinski (PhD student, AG Dörner, Charité – Universitätsmedizin Berlin) (**Section 5.19.2**).

### *5.19.1 Analysis of Differential Phosphatase Expression from Publicly Available $CD20^+$, $CD4^+$ and $CD8^+$ SLE Cells and $CD19^+$ Multiple Sclerosis (MS) RNA-Sequencing Data Sets*

Data were derived from publicly available datasets: $CD20^+$ B Cells from SLE patients and HDs (6 SLE, 7 HDs; GSE4588; https://www.ncbi.nlm.nih.gov/geo/query/acc.cgi?acc=GSE4588), $CD19^+$ B cells from MS patients and HDs (10 MS, 10 HDs; GSE117935, https://www.ncbi.nlm.nih.gov/geo/query/acc.cgi), $CD4^+$ T cells from SLE patients and HDs (53 SLE,

41 HDs; E-MTAB-2713, https://www.ebi.ac.uk/arrayexpress/experiments/E-MTAB-2713/) and $CD8^+$ T cells from SLE patients and HDs (22 SLE, 31 HDs; E-MTAB-2713, https://www.ebi.ac.uk/arrayexpress/experiments/E-MTAB-2713/). Differential expression was done for each dataset of SLE patients and HDs. Guanine cytosine robust multi-array analysis (GCRMA) normalized expression values were variance corrected using local empirical Bayesian shrinkage before calculation of differential expression using the ebayes function in the open source package BioConductor LIMMA package (https://www.bioconductor.org/packages/release/bioc/html/limma.html). Resulting p-values were adjusted for multiple hypothesis testing and filtered to retain differentially expressed probes with an false discovery rate (FDR) < 0.2 [257].

### *5.19.2 Analysis of Differential Phosphatase Expression from $CD19^+$ SLE Cells After CD40L/IL-4R Stimulation*

Isolated PBMCs from two SLE and one HD were cultured in the presence of CD40L (0.5 µg/ml) and IL-4 (20 ng/ml) or RPMI as a control as described in **Section 5.14.3** for 48 h. $CD19^+$ B cells were isolated for RNA-sequencing analysis as described in **Section 5.9**. Three technical replicates were included for each cohort and time point; files were obtained from FASTQC. FASTQC, Trimmomatic, STAR, Sambamba, and FeatureCounts were done separately. After careful examination of the principal component analysis (PCA) plots, three technical replicates of each cohort and condition were averaged into one and then used to perform relative gene expression. After FASTQC quality control analysis, Trimmomatic was used to cut adapter sequences, low-quality reads, and the first 14 reads of each sequence due to non-random primer bias. Reads were aligned to the human reference genome hg38 in STAR, and the '.sam' files were converted to sorted '.bam' files using Sambamba. Relative differentially expressed counts were generated in FeatureCounts. FastQC, Trimmomatic, STAR, Sambamba, and the FeatureCounts programs are all free, open source programs (web addresses see **Table 12**). RNA-Sequencing data are available under PRJNA564980 (https://www.ncbi.nlm.nih.gov/bioproject/PRJNA564980).

**Table 12:** Web addresses of open source programs used for RNA-Sequencing analysis

| Open source program | Web address |
|---|---|
| FastQC | https://www.bioinformatics.babraham.ac.uk/projects/fastqc/ |
| Trimmomatic | http://www.usadellab.org/cms/?page=trimmomatic |
| STAR | https://github.com/alexdobin/STAR<br>http://labshare.cshl.edu/shares/gingeraslab/www-data/dobin/STAR/STAR.posix/doc/STARmanual.pdf |
| Sambamba | http://lomereiter.github.io/sambamba/ |
| FeatureCounts | http://subread.sourceforge.net/ |

## 5.20 Data Analysis and Statistics

Flow cytometry data were analyzed with FlowJo 10.4.2. BioPlex raw data were analyzed using BioPlex Manager v4.1.1. Statistical analysis was performed with GraphPad Prism v5.04. For all data sets a

Gaussian distribution was assumed. For the comparison of two groups unpaired t-test and for paired analysis paired t-test was applied. When multiple groups were compared, one-way analysis of variance (ANOVA) with Dunnett's test for multiple comparisons (DMCT) was applied. For the comparison of time-dependent kinetics and multiple groups two-way ANOVA with Bonferroni test for multiple comparisons (BMCT) was used.

# 6 Results

## 6.1 Increased PTP and PSP Activities in SLE and Increased Co-Localization of CD22 with SHP-1 in SLE, RA and pSS CD19$^+$ B Cells

The strength of BCR downstream signaling is transmitted by the activity of signaling kinases such as Syk. Kinase activity is indicated by phosphorylation of specific tyrosine, serine or threonine sites. This phosphorylation is counter balanced by the activity of tyrosine- or serine/threonine-specific phosphatases [95, 112]. SHP-1 recruitment to CD22 provides an essential negative feedback loop to counterbalance Syk tyrosine phosphorylation [95, 105, 106, 112]. Increased global PTP activities in CD19$^+$ B cells, CD22 expression and phosphorylation in CD27$^-$ B cells from SLE patients contribute to reduced Syk phosphorylation in SLE [14]. To analyze whether there are similar signaling abnormalities in other autoimmune diseases, such as RA and pSS, PTP and PSP activities were analyzed in SLE, RA and pSS peripheral CD19$^+$ B cells and compared to HDs (**Figure 5a, b**). Additionally, the localization of the PTP SHP-1 in relation to the negative regulator CD22 with and without anti-CD22 stimulation was analyzed in peripheral CD19$^+$ B cells from SLE, RA, pSS and HDs (**Figure 5c, d**).

PTP activities against both PTP-specific substrates (TyrPP1 and TyrPP2) were statistically significant and specifically increased in SLE CD19$^+$ B cells compared to HDs (median free phosphate in HD *vs.* SLE: 1,030 *vs*. 3,277 pmol for TyrPP1 and 2,257 *vs.* 5,339 ppm for TyrPP2) (**Figure 5a**). Also, PSP activity towards Ser/Thr PP substrate was significantly and particularly increased in SLE CD19$^+$ B cells compared to HDs (median free phosphate in HD *vs.* SLE: 417 *vs.* 1,081 ppm) (**Figure 5b**). Specificity of the assay was validated by adding 10 mM monovanadate for blocking PTP activities and 10 – 20 mM sodium fluoride for blocking PSP activities. The same assay was applied on CD3$^+$ T cells from SLE, RA, pSS and HDs to proof B cell specificity of the results (**Supplementary Figure 2**). Notably, PTP as well as PSP activities in SLE, RA and pSS CD3$^+$ T cells were comparable to HDs.

Of note, baseline co-localization of CD22 receptor and SHP-1 was significantly increased in SLE, RA and pSS CD19$^+$ B cells compared to HDs with co-localization coefficients of 0.80 (SLE), 0.69 (RA) and 0.68 (pSS) compared to 0.55 (HD) (**Figure 5d**). Anti-CD22 stimulation significantly increased CD22/SHP-1 colocalization in RA to 0.84, pSS to 0.79 and HDs to 0.68 compared to unstimulated, but this was not seen for SLE. Noteworthy, CD22/SHP-1 colocalization in SLE CD19$^+$ B cells at baseline was as high as under stimulated conditions (0,80 and 0,81 at baseline and anti-CD22 stimulation, respectively) in all other donors and could not be further increased upon anti-CD22 stimulation.

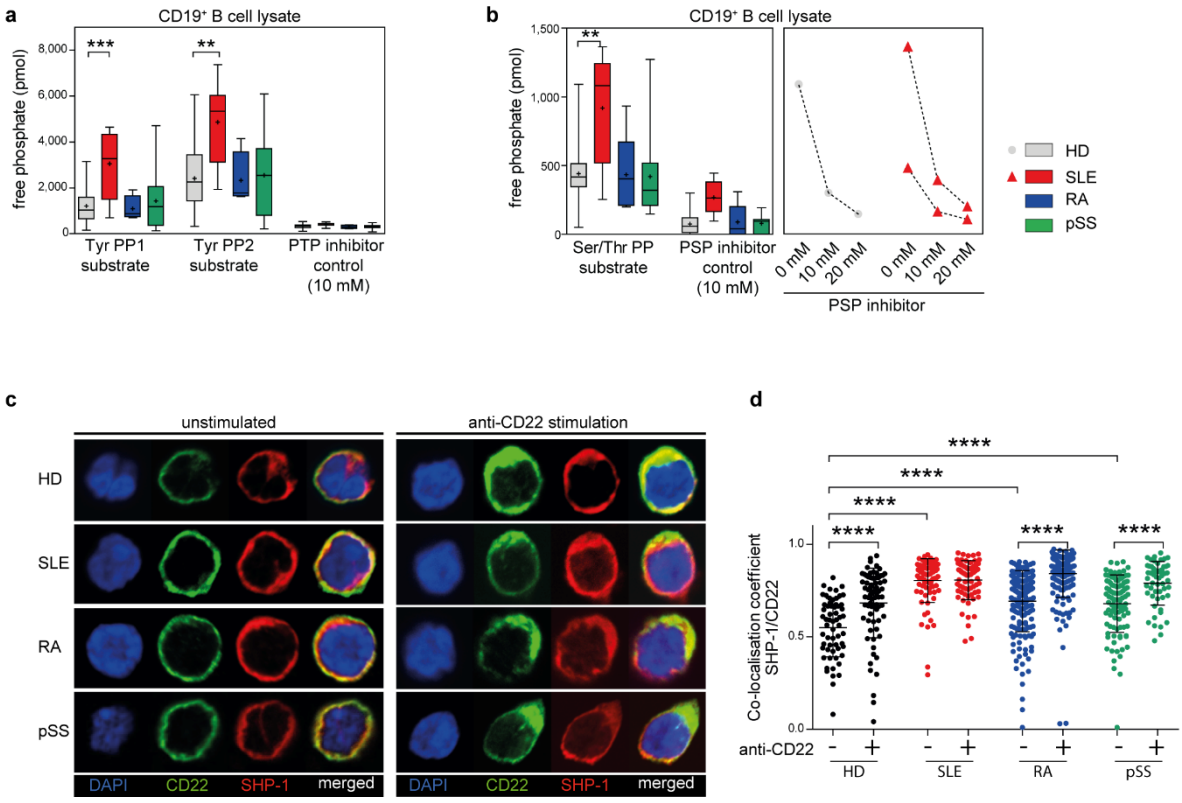


**Figure 5: Enhanced PTP and PSP activities in SLE B cells and enhanced baseline colocalization of SHP-1 with CD22 in B cells from patients with SLE, RA and pSS.** Baseline activities of PTPs and PSPs as well as colocalization of SHP-1 with CD22 was analyzed at baseline and upon anti-CD22 stimulation in SLE, RA, pSS and HD CD19⁺ B cells. (**a**) Activities of PTPs (n(HD/SLE/RA/pSS) = 22/8/4/13) and (**b**) PSPs (n(HD/SLE/RA/pSS) = 19/8/5/10) in HD (grey), SLE (red), RA (blue) and pSS (green) CD19⁺ B cells. Box whisker plots represent median (line), mean (plus) and the range from minimum to maximum. (**c**) Colocalization of SHP-1 (red) with CD22 (green) on HD, SLE, RA and pSS CD19⁺ B cells (representative fluorescence microcopy pictures). The nucleus (blue) was stained with DAPI. (**d**) Scatter dot plot of colocalization coefficients of HD (black), SLE (red), RA (blue) and pSS (green) CD19⁺ B cells (n(HD/SLE/RA/pSS) = 2/2/2/2). Each dot represents a cell and the lines indicate the mean (one-way ANOVA with DMCT; ** $p \leq 0.01$, *** $p \leq 0.001$, **** $p < 0.0001$).

SHP-1/CD22 co-localization at baseline is increased in CD19⁺ B cells from SLE, RA and pSS patients compared to HDs. This co-localization could be increased in HD, RA and pSS CD19⁺ B cells upon anti-CD22-stimulation, but not in SLE CD19⁺ B cells. Thus, CD19⁺ B cells from SLE patients displayed already maximal SHP-1/CD22 co-localization together with increased PTP and PSP activities at baseline.

## 6.2 Comparable Syk, Btk, PLCγ2 and Akt Baseline Expression and Phosphorylation Between SLE, pSS, RA and HDs in CD27⁻ B Cells and CD27⁺ Memory B Cells

Phosphorylation of Syk, Btk, PLCγ2 and Akt at their activation sites Syk($Y^{352}$), Btk($Y^{223}$), PLCγ2($Y^{759}$) and Akt($S^{473}$), respectively, are regulated by PTPs (Syk, Btk and PLCγ2) or PSPs (Akt) [258]. Therefore, Increased PTP and PSP activities and co-localization of CD22 with SHP-1 (**Section 6.1**) may impact the baseline phosphorylation of BCR downstream signaling of those molecules. Hence, protein expression and phosphorylation at their corresponding activation sites were analyzed in SLE, RA, pSS

and HD peripheral B cells. To account for subset-specific signaling properties, $CD19^+$ B cells were subdivided into conventional $CD27^-$ B cells and $CD27^+$ memory B cells [14, 100].

Overall, Syk and pSyk($Y^{352}$) expression was similar among SLE, RA, pSS and HDs for $CD27^-$ B cells and $CD27^+$ memory B cells with the exemption of Syk expression in pSS $CD27^-$ B cells compared to HDs (**Figure 6a**). In pSS, Syk expression in $CD27^-$, but not $CD27^+$ B cells, was significantly higher compared to HDs (mean MFI 3,125 in pSS vs. 2,429 in HD). In general, Syk and pSyk($Y^{352}$) expression were significantly higher in $CD27^+$ memory than in $CD27^-$ B cells for HDs, RA and pSS patients and tend to be higher for pSyk($Y^{352}$) in SLE patients ($p = 0.0762$). As an example, HD $CD27^-$ B cells and $CD27^+$ memory B cells exhibited mean MFIs of 2,492 and 4,181, respectively. Mean MFIs of pSyk($Y^{352}$) were 663 in $CD27^-$ B cells and 932 in $CD27^+$ memory B cells from HDs.

Btk and pBtk($Y^{223}$) MFIs were similar among patients and HDs in $CD27^-$ B cells and $CD27^+$ memory B cells (**Figure 6b**). Exemplarily, mean MFIs of HD $CD27^-$ B cells and $CD27^+$ memory B cells were 1,154 and 1,309 for Btk as well as 2,334 and 3,382 for pBtk($Y^{223}$), respectively. Expression of Btk was comparable between $CD27^-$ B cells and $CD27^+$ memory B cells in SLE, RA and pSS. However, Btk expression in $CD27^+$ B cells from HDs was slightly, but significantly higher compared to $CD27^-$ B cells. Phospho-Btk($Y^{223}$) in $CD27^+$ memory B cells showed a tendency of higher expression in all groups compared to $CD27^-$ B cells, with significantly higher MFIs in HDs and pSS patients.

Similar PLCγ2 and pPLCγ2($Y^{759}$) expressions were found among patients and HDs (**Figure 6c**). HD $CD27^-$ B cells exhibited mean MFIs of 2,222 for PLCγ2 and 375 for pPLCγ2($Y^{759}$), whereas $CD27^+$ memory B cells displayed mean MFIs of 3,230 for PLCγ2 and 595 for pPLCγ2($Y^{759}$). As seen for Syk and pSyk($Y^{352}$), PLCγ2 expression was significantly higher in $CD27^+$ memory B cells than compared to $CD27^-$ B cells from HDs, SLE and pSS patients; there was a trend of somewhat higher expression levels in RA patients (mean MFIs of 2,716 *vs.* 3,262 in $CD27^-$ B cells *vs.* $CD27^+$ memory B cells from RA patients, respectively). Phospho-PLCγ2($Y^{759}$) was significantly increased in HDs and tended to be increased in SLE, RA and pSS $CD27^+$ memory B cells compared to $CD27^-$ B cells. In detail, pPLCγ2($Y^{759}$) mean MFIs were 465 *vs.* 584 (SLE), 434 *vs.* 511 (RA) and 500 *vs.* 629 (pSS) in $CD27^-$ B cells *vs.* $CD27^+$ memory B cells, respectively.

Comparable Akt1 and pAkt($S^{473}$) expression was observed among $CD27^-$ B cells and $CD27^+$ memory B cells from all donor groups with the exemption of pSS (**Figure 6d**). For example, HD mean Akt1 MFIs were 352 *vs.* 410 and mean pAkt($S^{473}$) MFIs were 230 *vs.* 265 in $CD27^-$ B cells *vs*. $CD27^+$ memory B cells, respectively. In pSS patients, Akt1 expression was found to be significantly higher in $CD27^+$ memory B cells (mean MFI 261) compared to $CD27^-$ B cells (mean MFI 232).

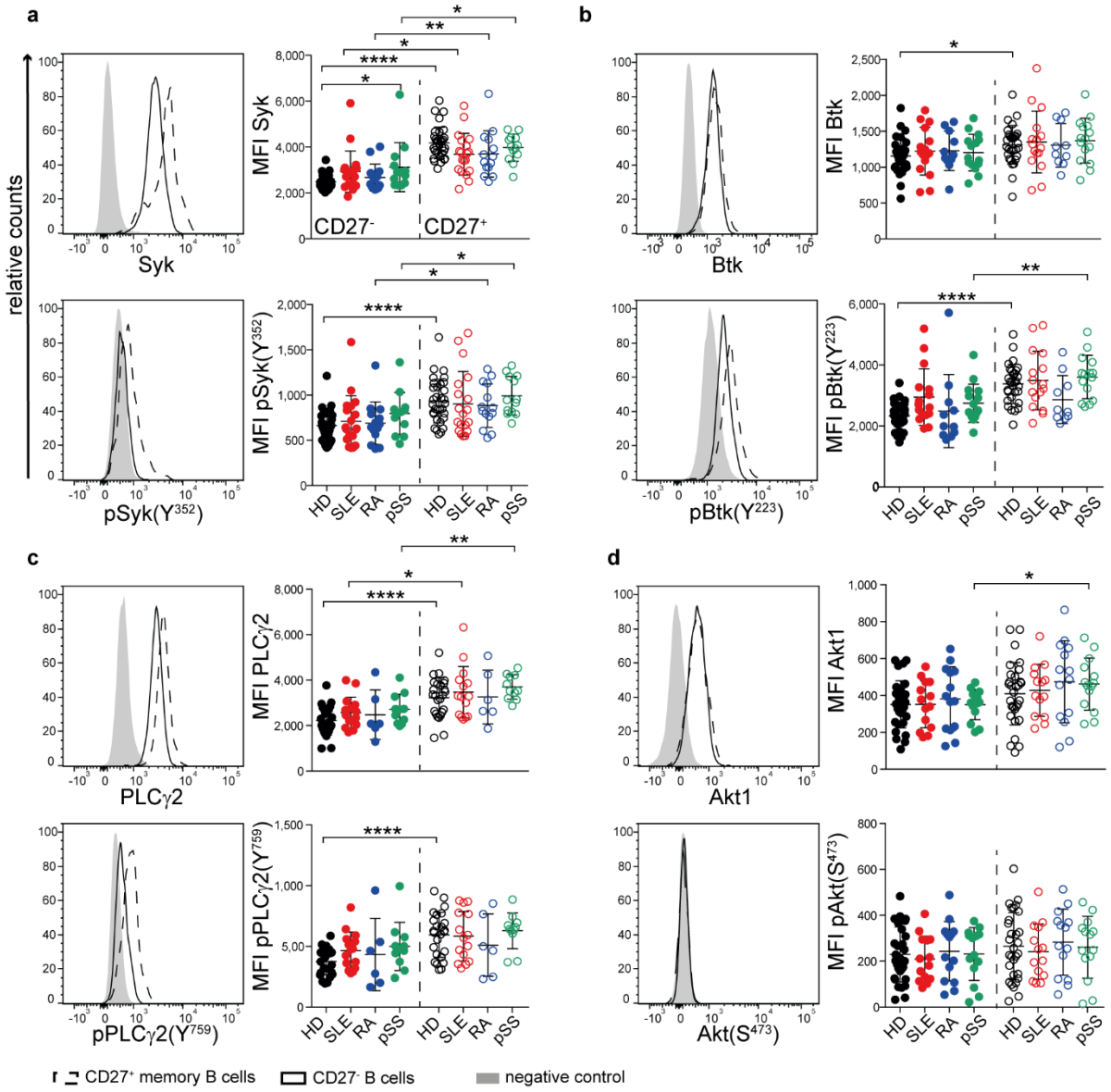


**Figure 6: Comparable baseline expression and phosphorylation of BCR downstream kinases in SLE, RA and pSS patients compared to HDs.** Baseline (**a**) Syk and pSyk($Y^{352}$) (n(HD/SLE/RA/pSS) = 32/19/14/13), (**b**) Btk and pBtk($Y^{223}$) (n(HD/SLE/RA/pSS) = 30/16/11/15), (**c**) PLCγ2 and pPLCγ2($Y^{759}$) (n(HD/SLE/RA/pSS) = 25/15/6/11) and (**d**) Akt and pAkt($S^{473}$) (n(HD/SLE/RA/pSS) = 30/14/14/13) expression and phosphorylation was analyzed in $CD27^-$ B cells (dots) and $CD27^+$ memory (circles) B cells from unstimulated HDs (black), SLE (red), RA (blue) and pSS (green) patients whole blood samples. Representative histograms show the expression of the indicated kinase in $CD27^-$ B cells (solid line) and $CD27^+$ memory B cells (dashed line). Negative controls (grey areas) are defined by (**a, b, c**) $CD3^+$ lymphocytes or (**d**) isotype control. The horizontal line represents the mean ± standard deviation (SD) (one-way ANOVA with DMCT; t-test; * $p \leq 0.05$, ** $p \leq 0.01$, **** $p \leq 0.0001$).

Taken together, baseline expression and phosphorylation of Syk, Btk, PLCγ2 and Akt in SLE, RA and pSS peripheral $CD27^-$ B cells and $CD27^+$ memory B cells are comparable to HDs. Thus, indicating that tonic signaling is not affected by the observed increase in CD22/SHP-1 colocalization in SLE, RA and pSS and increased PTP and PSP activities in SLE (**Section 6.1**). Notably, baseline expression of Syk and PLCγ2 protein and phosphorylation of Syk($Y^{352}$) and PLCγ2($Y^{759}$) was characteristically increased in $CD27^+$ memory versus $CD27^-$ B cells.

## 6.3 Reduced Tyrosine Phosphorylation of Syk($Y^{352}$) and Btk($Y^{223}$) Upon Anti-IgG/IgM Stimulation in B Cells From SLE, RA and pSS Patients

Impaired functional BCR signal due to increased PTP activities was reported in SLE B cells, which is characterized by reduced Syk($Y^{352}$) phosphorylation after BCR stimulation [14]. Increased PTP activities were not observed in RA and pSS, but increased baseline co-localization of CD22 with the PTP SHP-1 (**Section 6.1**). To analyze whether pSS and RA share the same signaling abnormality with SLE, phosphorylation kinetics of Syk($Y^{352}$) were analyzed in peripheral $CD27^-$ B cells and $CD27^+$ memory B cells after IgG/IgM stimulation in autoimmune disease B cells (**Figure 7**). Downstream progression of the signal was analyzed by anti-IgG/IGM induced Btk($Y^{223}$) phosphorylation kinetics in SLE, RA, pSS and HD $CD27^-$ and $CD27^+$ memory B cells (**Figure 8**).

Anti-IgG/IgM induced Syk($Y^{352}$) phosphorylation kinetics of HD $CD27^+$ memory B cells were generally increased for all time points analyzed compared to $CD27^-$ B cells (**Figure 7a, b**). Maximum phosphorylation was reached at 5 min with mean MFIs of 2,906 and 4,273 for HD $CD27^-$ B cells and $CD27^+$ memory B cells, respectively. Syk($Y^{352}$) phosphorylation kinetics were significantly reduced in SLE $CD27^-$ B cells (1,753 mean MFI at 5 min) and $CD27^+$ memory B cells (1,803 mean MFI at 5 min) compared to HDs. Additionally, pSyk($Y^{352}$) kinetics were significantly reduced in RA and pSS $CD27^+$ memory B cells compared to HDs with mean MFIs of 2,855 (RA) and 2,901 (pSS) at 5 min. Phospho-Syk($Y^{352}$) kinetics in RA and pSS $CD27^-$ B cells were comparable to HDs. In SLE, RA and pSS pSyk($Y^{352}$) kinetics completely lack a differentiation between $CD27^-$ B cells and $CD27^+$ memory B cells.

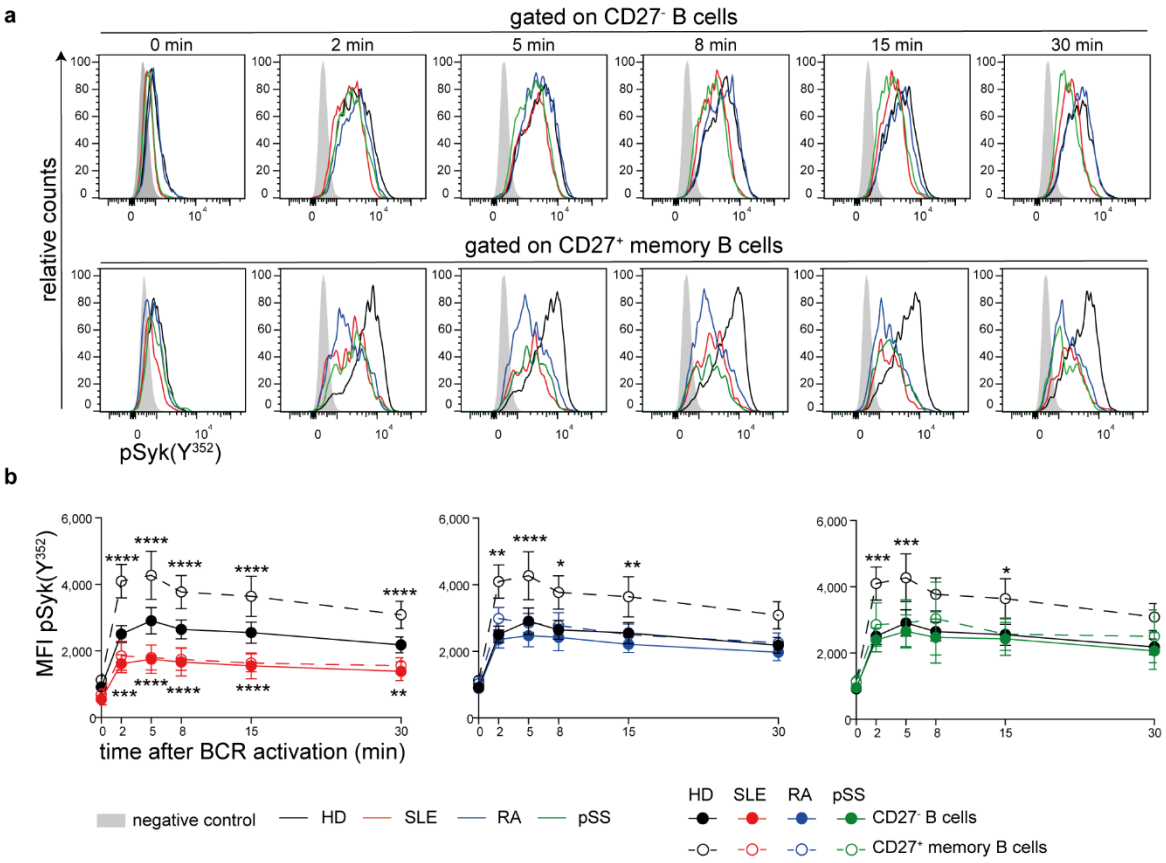


**Figure 7: Reduced anti-IgG/IgM induced Syk($Y^{352}$) phosphorylation kinetics in SLE, RA and pSS $CD27^+$ memory B cells and SLE $CD27^-$ B cells.** PBMCs from HDs, SLE, RA and pSS patients were stimulated with anti-IgG/IgM $F(ab)_2$ fragments for 0 (RPMI control), 2, 5, 8, 15 and 30 min and Syk($Y^{352}$) phosphorylation kinetics were analyzed. (**a**) Representative pSyk($Y^{352}$) histograms of $CD27^-$ B cells (top row) and $CD27^+$ memory B cells (bottom row) were shown for the indicated time points. $CD3^+$ lymphocytes served as negative control (grey areas). (**b**) Phospho-Syk($Y^{352}$) (n(HD/SLE/RA/pSS) = 19/11/11/10) kinetics for HD (black), SLE (red), RA (blue) and pSS (green) $CD27^-$ B cells (solid lines and dots) and $CD27^+$ memory B cells (circles and dashed lines). Data are represented as mean ± 95 % confidence interval (CI) (two-way ANOVA with BMCT; * $p \leq 0.05$, ** $p \leq 0.01$, *** $p \leq 0.001$, **** $p \leq 0.0001$).

Phospho-Btk($Y^{223}$) kinetics were qualitatively comparable to pSyk($Y^{352}$) kinetics: Phosphorylation in HD $CD27^+$ memory B cells was higher than in $CD27^-$ B cells for all time points and maximum phosphorylation was reached at 5 min after anti-IgG/IgM stimulation (**Figure 8a, b**). Mean pBtk($Y^{223}$) MFIs of HD $CD27^-$ B cells and $CD27^+$ memory B cells were 11,036 and 15,613 at 5 min, respectively. In $CD27^+$ memory B cells pBtk($Y^{223}$) kinetics were reduced in SLE (9,271 mean MFI at 5 min), RA (11,320 mean MFI at 5 min) and pSS (11,590 mean MFI at 5 min) compared to HDs (15,613 mean MFI at 5 min). Thus, pBtk($Y^{223}$) kinetics of $CD27^+$ memory B cells of SLE, RA and pSS patients are comparable to $CD27^-$ B cells of HDs. In addition, Btk($Y^{223}$) phosphorylation tend to be reduced in $CD27^-$ B cells from SLE (8,821 mean MFI at 5 min) and RA (9,291 mean MFI at 5 min) patients *vs.* HDs (11,036 mean MFI at 5 min).

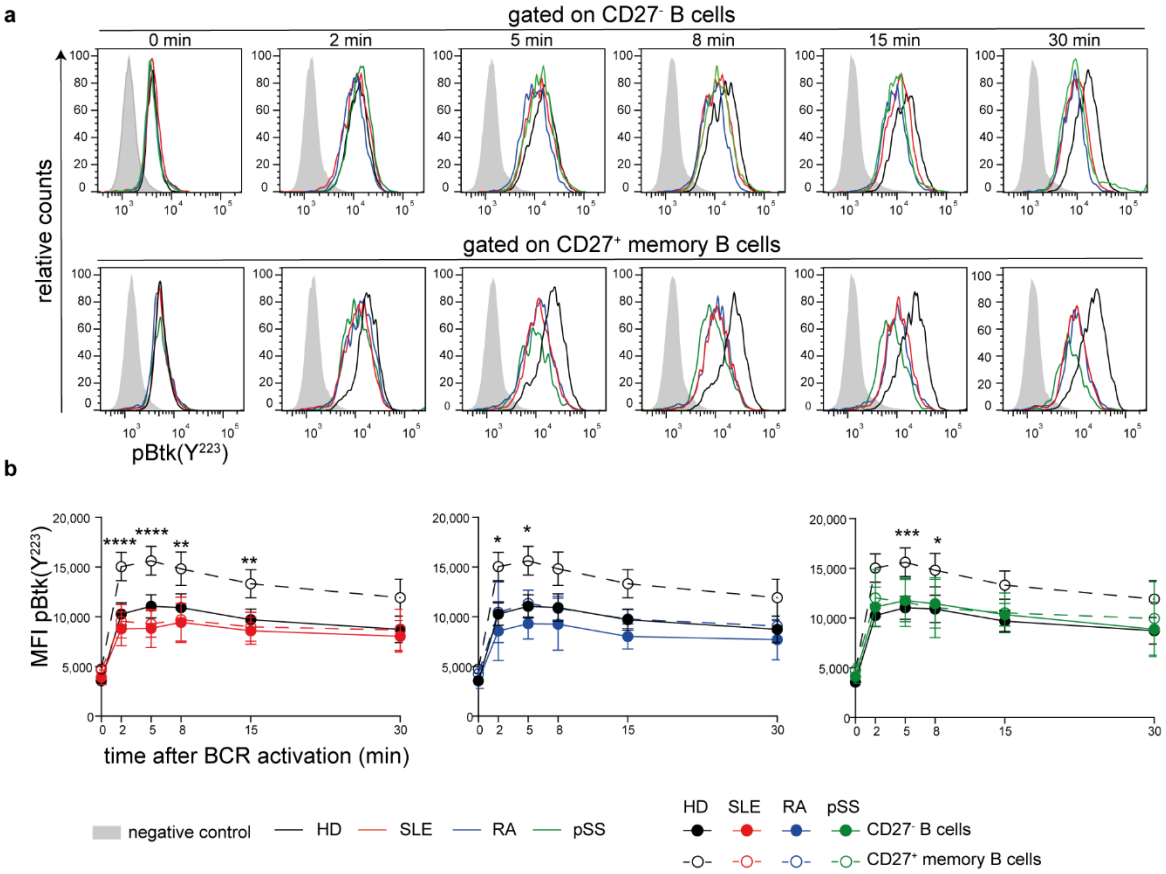


**Figure 8: Reduced anti-IgG/IgM induced Btk($Y^{223}$) phosphorylation kinetics in SLE, RA and pSS $CD27^+$ memory B cells.** PBMCs were stimulated with anti-IgG/IgM $F(ab)_2$ fragments for 0 (RPMI control), 2, 5, 8, 15 and 30 min and Btk($Y^{223}$) phosphorylation kinetics were analyzed. (**a**) Representative histograms of pBtk($Y^{223}$) in $CD27^-$ B cells (top row) and $CD27^+$ (bottom row) memory B cells from HDs (black), SLE (red), RA (blue) and pSS (green) patients upon the indicated stimulation time. $CD3^+$ lymphocytes served as negative control (grey area). (**b**) Phospho-Btk($Y^{223}$) (n(HD/SLE/RA/pSS) = 21/10/6/14) kinetics in $CD27^-$ B cells (solid lines and dots) and $CD27^+$ memory B cells (dashed lines and circles) from HDs (black), SLE (red), RA (blue) and pSS (green) patients. Data are represented as mean ± 95 % CI (two-way ANOVA with BMCT; * $p \leq 0.05$, ** $p \leq 0.01$, *** $p \leq 0.001$, **** $p \leq 0.0001$).

Syk($Y^{352}$) phosphorylation kinetics were reduced in SLE peripheral $CD27^-$ B cells and $CD27^+$ memory B cells compared to HDs which is consistent with the previous reports [14]. As a commonalty SLE, RA and pSS $CD27^+$ memory B cells displayed reduced Syk($Y^{352}$) phosphorylation kinetics. Consistent with this observation, downstream propagation of the BCR signal via Btk($Y^{223}$) phosphorylation was also found to be reduced in SLE, RA and pSS $CD27^+$ memory B cells compared to HDs.

## 6.4 Anti-IgG/IgM Induced Serine Phosphorylation of Akt($S^{473}$) is Increased in SLE and Comparable to HDs in RA and pSS

Next, it was analyzed whether pSS and RA B cells display the same functional BCR signaling unbalance, with increased phosphorylation of Akt($S^{473}$) after anti-IgG/IgM stimulation, as reported for SLE [14]. Anti-IgG/IgM induced Akt($S^{473}$) phosphorylation kinetics were analyzed in peripheral $CD27^-$ B cells and $CD27^+$ memory B cells from SLE, RA and pSS patients in comparison to HDs.

Akt(S$^{473}$) phosphorylation kinetics were distinctive between CD27$^-$ B cells and CD27$^+$ memory B cells with higher phosphorylation in CD27$^+$ memory B cells in all donor groups (**Figure 9a, b**). Maximum phosphorylation was reached after 8 min in CD27$^-$ and CD27$^+$ memory B cells. For example, HD CD27$^-$ B cells and CD27$^+$ memory B cells exhibited mean pAkt(S$^{473}$) MFIs of 1,037 and 1,405 at 8 min, respectively. Phospho-Akt(S$^{473}$) kinetics were increased in SLE CD27$^-$ B cells (1,437 mean MFI at 8 min) and CD27$^+$ memory B cells (1,829 mean MFI at 8 min) compared to HDs (**Figure 9b**). In contrast to SLE, Akt(S$^{473}$) phosphorylation kinetics of CD27$^-$ B cells and CD27$^+$ memory B cells from RA and pSS were comparable to HDs at all the time points after anti-IgG/IgM stimulation.

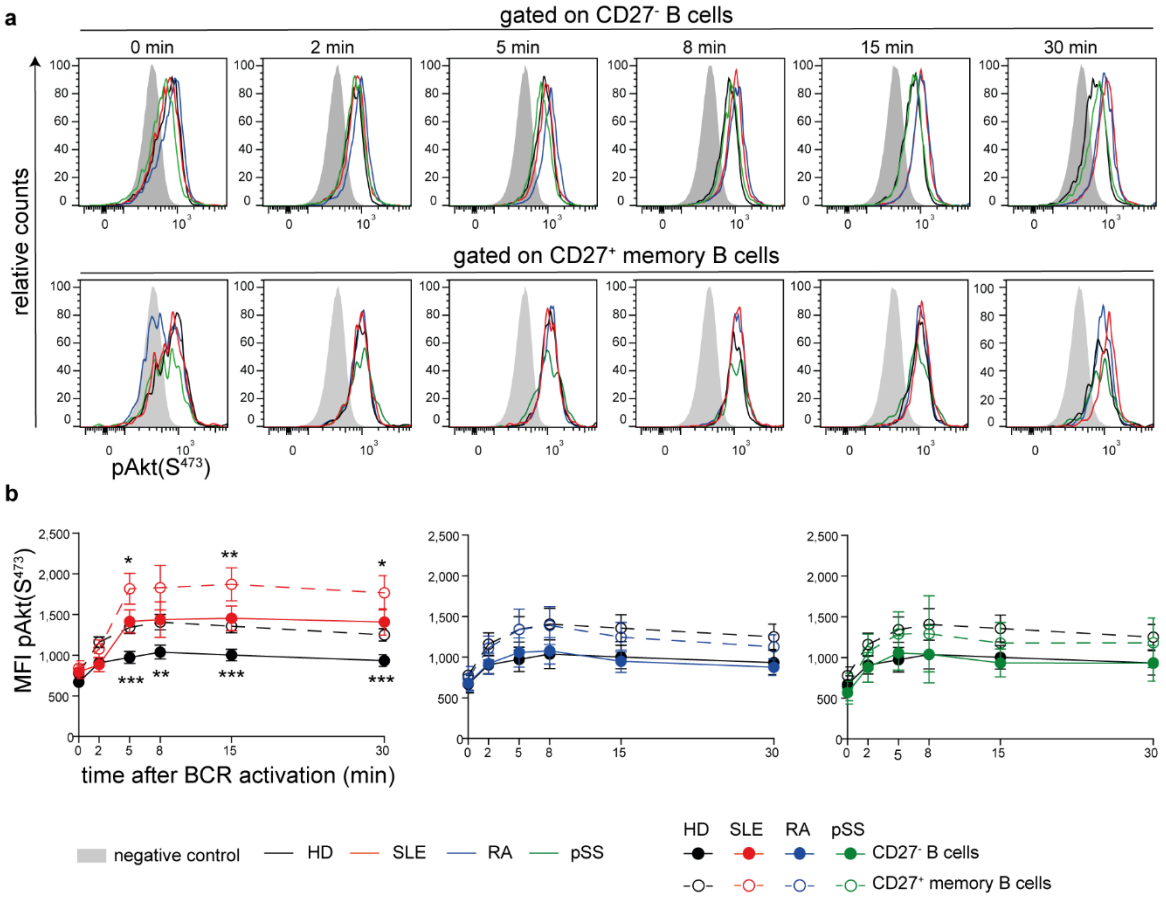


**Figure 9: Increased anti-IgG/IgM induced Akt(S$^{473}$) phosphorylation kinetics in SLE CD27$^-$ and CD27$^+$ memory B cells compared to HDs.** PBMCs from HDs and SLE, RA and pSS patients were stimulated with anti-IgG/IgM for 0 (RPMI control), 2, 5, 8, 15 and 30 min and Akt(S$^{473}$) phosphorylation was analyzed. (**a**) Representative histograms of CD27$^-$ and CD27$^+$ memory B cells from SLE (red), RA (blue) and pSS (green) patients and HDs (black) upon the indicated stimulation time. CD3$^+$ lymphocytes were used as negative control (grey areas). (**b**) Phospho-Akt(S$^{473}$) (n(HD/SLE/RA/pSS) = 29/15/11/10) kinetics for HDs (black), SLE (red), RA (blue) and pSS (green) CD27$^-$ B cells (solid lines and dots) and CD27$^+$ memory B cells (circles and dashed lines). Data are represented as mean ± 95 % CI (two-way ANOVA with BMCT; * p ≤ 0.05, ** p ≤ 0.01, *** p ≤ 0.001).

Reduced Syk(Y$^{352}$) and downstream Btk(Y$^{223}$) phosphorylation kinetics in SLE, RA and pSS (**Section 6.3**) did not directly translate into reduced Akt(S$^{473}$) phosphorylation. Phospho-Akt(S$^{473}$) kinetics of RA and pSS CD27$^-$ B cells and CD27$^+$ memory B cells were comparable to HDs. Phospho-Akt(S$^{473}$) kinetics were increased in SLE CD27$^-$ and CD27$^+$ B cells compared to HDs. In contrast to Syk(Y$^{352}$) and Btk(Y$^{223}$) phosphorylation kinetics (**Section 6.3**), Akt(S$^{473}$) phosphorylation was

distinctive between $CD27^-$ B cells and $CD27^+$ memory B cells with higher phosphorylation in $CD27^+$ memory B cells in autoimmune disease patients compared to HDs.

## 6.5 Reduced Anti-IgG/IgM Induced Syk($Y^{352}$) Phosphorylation in $CD27^+$ Memory B Cells from ITP Spleens

Circulating B cells of autoimmune patients showed reduced Syk($Y^{352}$) phosphorylation upon anti-IgG/IgM treatment (**Section 6.3**). To address the question whether tissue resident B cells from autoimmune patients share the same hyporesponsive phenotype, $CD27^-$ B cells and $CD27^+$ memory B cells from spleens, tonsils and parotid tissue were analyzed for Syk($Y^{352}$) phosphorylation after anti-IgG/IgM stimulation (**Figure 10**). Spleens were obtained from autoimmune patients with ITP and patients without autoimmune disease. Tonsils were obtained from patients with chronic tonsillitis. One parotid was obtained from a pSS patient, and therefore, reflects an actual site of autoimmune inflammation.

In non-ITP splenic B cells, Syk($Y^{352}$) phosphorylation kinetics were qualitatively comparable to Syk($Y^{352}$) phosphorylation kinetics from peripheral blood B cells (**Section 6.3**). Higher phosphorylation in $CD27^+$ memory B cells compared to $CD27^-$ B cells and maximum phosphorylation at 5 min after anti-IgG/IgM stimulation was observed (**Figure 10a**). In detail, mean Syk($Y^{352}$) MFIs were 1,788 and 3,823 in $CD27^-$ B cells and $CD27^+$ memory B cells, respectively. Phospho-Syk($Y^{352}$) kinetics were significantly reduced in ITP $CD27^+$ memory B cells (2,162 mean MFI at 5 min) compared to non-ITP $CD27^+$ memory B cells (3,823 mean MFI at 5 min). ITP samples tend to lack the distinction between $CD27^-$ B cells and $CD27^+$ memory B cells (1,459 *vs.* 2,162 mean MFI at 5 min).

Phospho-Syk($Y^{352}$) kinetics in $CD27^-$ B cells and $CD27^+$ memory B cells from tonsils (917 vs. 1,591 mean MFIs at 5 min) and pSS parotid (1,041 vs. 1,392 mean MFIs at 5 min) were overall lower (**Figure 10b**) compared to non-ITP splenic (1,788 *vs.* 3,823 mean MFIs at 5 min) (**Figure 10a**) and HD peripheral (2,906 *vs.* 4,273 mean MFIs at 5 min) (**Section 6.3**) $CD27^-$ B cells and $CD27^+$ memory B cells. Notably, pSyk($Y^{352}$) phosphorylation kinetics in $CD27^-$ and $CD27^+$ B cells from the pSS parotid was comparable to the kinetics of $CD27^-$ and $CD27^+$ B cells from tonsils.

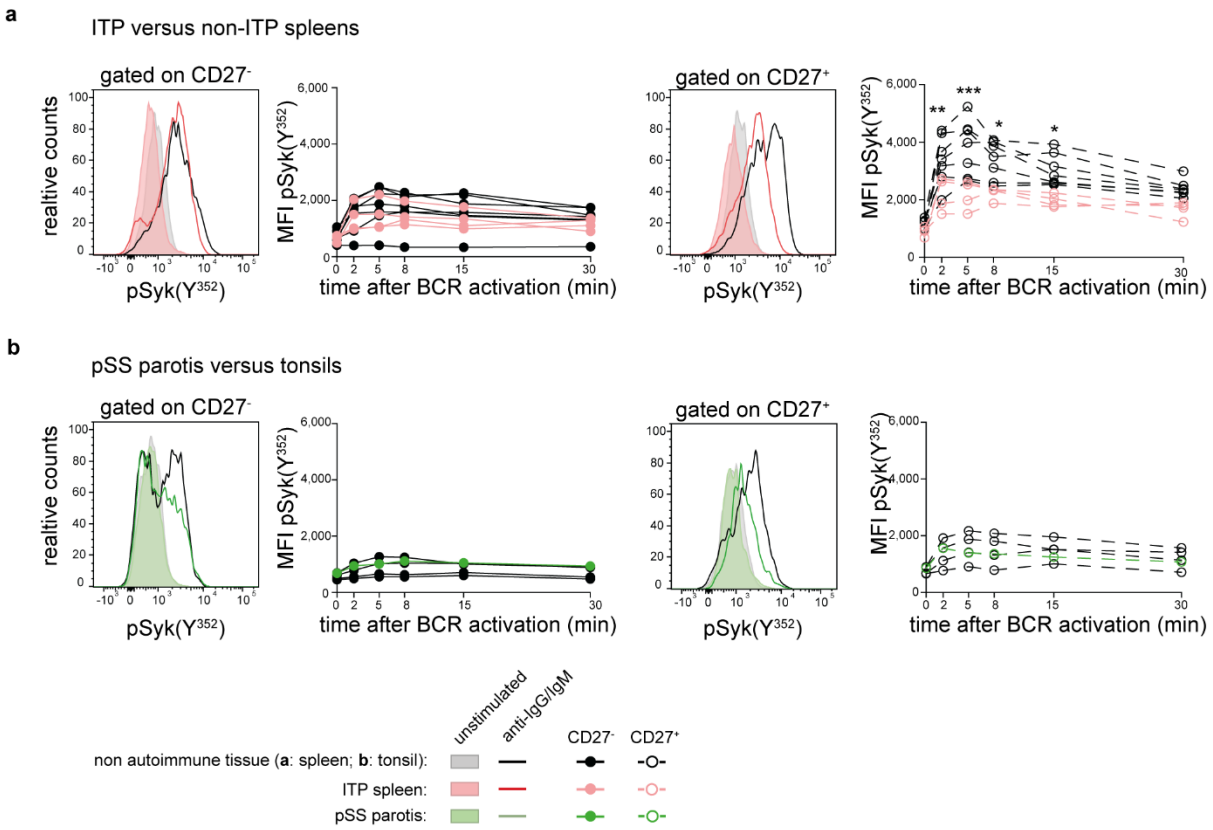


**Figure 10: Reduced anti-IgG/IgM induced Syk(Y$^{352}$) phosphorylation kinetics in splenic B cells from ITP patients compared to non-ITP patients.** MNCs were isolated from spleens, tonsils and one pSS parotid. Cells were stimulated with anti-IgG/IgM F(ab)$_2$ for 0 (RPMI control), 2, 5, 8, 15 and 30 min and analyzed for Syk(Y$^{352}$) phosphorylation. (**a**) Representative pSyk(Y$^{352}$) histograms after 5 min anti-IgG/IgM stimulation (solid line) or unstimulated (filled areas) and Syk(Y$^{352}$) phosphorylation kinetics from ITP (pink) and non-autoimmune (grey/black) CD27$^-$ B cells (left; solid lines and dots) and CD27$^+$ memory B cells (right; dashed lines and circles). Each pSyk(Y$^{352}$) kinetic represents one donor (n(ITP/non-ITP) = 4/7). (**b**) Representative pSyk(Y$^{352}$) histograms and kinetics of CD27$^-$ B cells (left; solid lines and dots) and CD27$^+$ memory B cells (right; dashed lines and circles) from tonsils (grey/black) and pSS parotid (green). Data represent absolute MFIs (two-way ANOVA with BMCT; * p ≤ 0.05, ** p ≤ 0.01, *** p ≤ 0.001).

These functional analysis of tissue resident B cells revealed that pSyk(Y$^{352}$) kinetics in CD27$^-$ B cells and CD27$^+$ memory B cells from spleen are comparable to pSyk(Y$^{352}$) kinetics in peripheral blood B cells. Moreover, ITP CD27$^+$ memory B cells from spleen displayed reduced Syk(Y$^{352}$) phosphorylation kinetics compared to non-ITP CD27$^+$ memory B cells. Overall, B cells from parotid as well as tonsils displayed lower Syk(Y$^{352}$) phosphorylation after anti-IgG/IgM stimulation compared to peripheral blood and splenic B cells. CD27$^+$ memory B cells with reduced Syk(Y$^{352}$) phosphorylation kinetics are also present in autoimmune disease tissues.

## 6.6 Comparable ERK1/2(T$^{202}$/Y$^{204}$) Baseline Phosphorylation in B Cells from HDs, SLE and RA Patients

Reduced BCR responsiveness reflects a functional status of B cells which may be related to B cell anergy. Recently, increased frequencies of pERK1/2(T$^{202}$/Y$^{204}$)$^+$ cells were found among B cells from patients with type #4 mutated chronic lymphatic leukemia (M-CLL) [259-261]. Type #4 M-CLL patients

predominantly express *IGHV4-34/IGKV2-30* Igs whereas the *IGHV4-34* gene encodes for intrinsically autoreactive autoantibodies which are known to be secreted by SLE patients, too. The BCR in type #4 M-CLL is often unresponsive, which may be due to chronic auto-antigen presence. Therefore, increased pERK1/2($T^{202}/Y^{204}$) is thought to be a marker for anergy in type #4 M-CLL. Due to the parallels in terms of *IGHV4-34* expression and unresponsive BCR in SLE (**Section 6.3**), pERK1/2($T^{202}/Y^{204}$) expression was tested in peripheral $CD27^-$ B cells and $CD27^+$ memory B cells as a potential marker for B cell anergy in a pilot experiment.

For comparability to the aforementioned reports, frequencies of pERK1/2($T^{202}/Y^{204}$)$^+$ cells were analyzed to isotype control as a reference (**Figure 11a, b**). Frequencies of pERK1/2($T^{202}/Y^{204}$)$^+$ cells ranged between 3 and 77 % ($CD27^-$ B cells) as well as 9 and 86 % ($CD27^+$ memory B cells). Autoimmune disease groups were comparable to HDs with no significant difference between $CD27^-$ B cells and $CD27^+$ memory B cells (**Figure 11b**).

When MFIs were analyzed, pERK1/2($T^{202}/Y^{204}$) was generally higher expressed in $CD27^+$ memory B cells compared to $CD27^-$ B cells, but this was not significantly different for SLE (**Figure 11c**). In example, mean pERK1/2($T^{202}/Y^{204}$) MFIs of HD $CD27^-$ B cells and $CD27^+$ memory B cells was 431 and 610, respectively. However, no significant difference was observed in the expression of pERK1/2($T^{202}/Y^{204}$) between HDs, SLE and RA patients for $CD27^-$ B cells and $CD27^+$ memory B cells. Nevertheless, there is a tendency of reduced pERK1/2($T^{202}/Y^{204}$) expression in SLE and RA $CD27^-$ B cells as well as $CD27^+$ memory B cells compared to HDs.

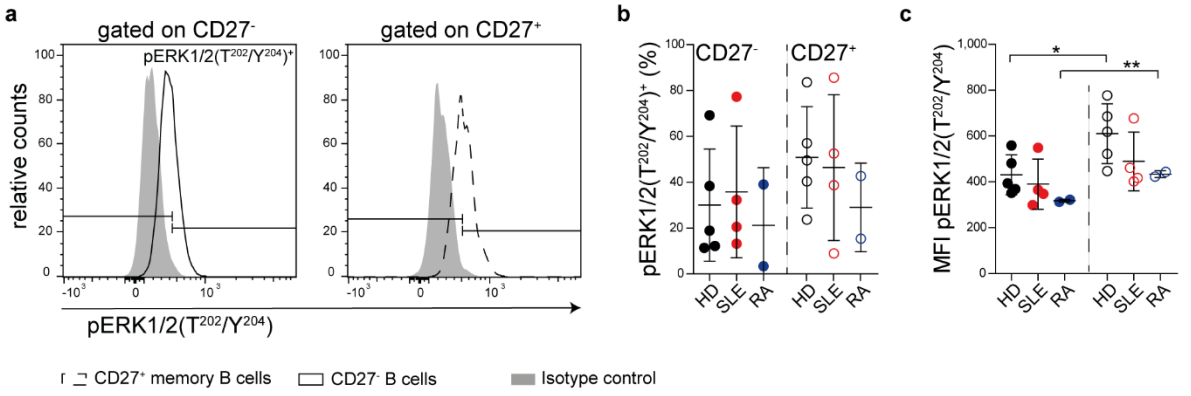


**Figure 11: Comparable baseline phosphorylation of ERK1/2($T^{202}/Y^{204}$) in SLE, RA and HDs.** Baseline ERK($T^{202}/Y^{204}$) phosphorylation was analyzed from unstimulated HD, SLE and RA whole blood samples. (**a**) Representative histograms of pERK($T^{202}/Y^{204}$) in $CD27^-$ B cells (solid line) and $CD27^+$ memory B cells (dashed line) compared to isotype control (grey area). The horizontal lines indicate the gating on pERK1/2($T^{202}/Y^{204}$) positive and negative cells according to isotype control. (**b**) Phospho-ERK1/2($T^{202}/Y^{204}$)$^+$ cells in HD (black), SLE (red) and RA (blue) $CD27^-$ B cells (dots) and $CD27^+$ memory B cells (circles). (**c**) Phospho-ERK1/2($T^{202}/Y^{204}$) MFI from HD (black) SLE, (red) and RA (blue) $CD27^-$ B cells (dots) and $CD27^+$ memory B cells (circles). The horizontal lines indicate means ± SD (test; * $p \leq 0.05$, ** $p \leq 0.01$).

Phospho-ERK1/2($T^{202}/Y^{204}$) does not exhibit any difference in frequencies or the MFI between peripheral $CD27^-$ B cells and $CD27^+$ memory B cells from SLE and RA patients compared to HDs. Moreover, pERK1/2($T^{202}/Y^{204}$) MFI tends to be reduced in SLE and RA $CD27^-$ B cells and $CD27^+$ memory B cells compared to HDs.

## 6.7 Reduced Anti-IgG/IgM Induced pSyk(Y$^{352}$) in SLE, RA and pSS CD27$^{+}$ Memory B Cells Does Not Correlate with Siglec-1 or Cytokine Expression

IFNα signature measured by the expression of Siglec-1 (CD169) on CD14$^{+}$ monocytes is increased in patients with SLE and extraglandular pSS [193, 194]. This IFNα signature might be a commonality between these diseases and a potential inducer of the reduced BCR induced pSyk(Y$^{352}$) signaling observed in SLE, RA and pSS patients (**Section 6.3**). To address this hypothesis Siglec-1 expression was compared between HDs, SLE, RA and pSS patients and correlated with pSyk(Y$^{352}$) MFIs from CD27$^{+}$ memory B cells after 5 min anti-IgG/IgM stimulation (**Figure 12**).

In line with the literature [193, 194], patients with SLE and pSS express more Siglec-1 on CD14$^{+}$ monocytes than HDs (**Figure 12a**). However, on RA CD14$^{+}$ monocytes, the Siglec-1 expression was comparable to HDs. Siglec-1 expression did not correlate with pSyk(Y$^{352}$) in CD27$^{+}$ memory B cells after 5 min anti-IgG/IgM stimulation in HDs, SLE, RA and pSS (**Figure 12b**).

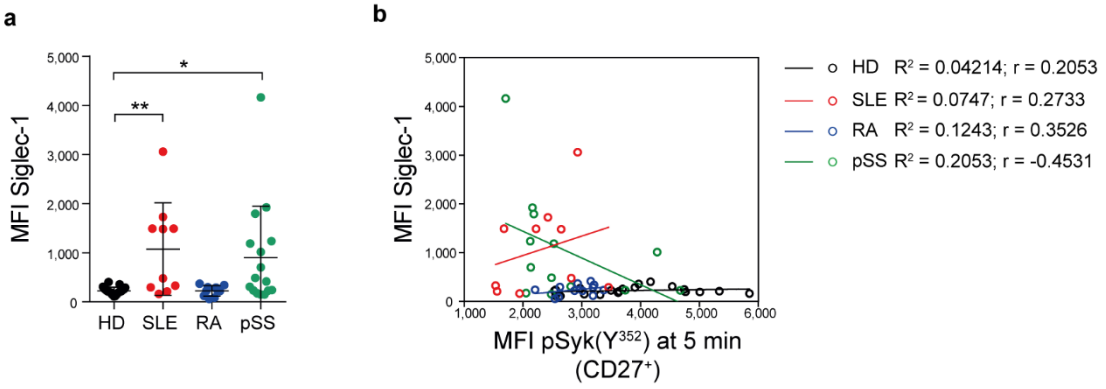


**Figure 12: Increased Siglec-1 expression in SLE and pSS does not correlate with pSyk(Y$^{352}$) phosphorylation at 5 min of anti-IgG/IgM stimulation.** Siglec1 expression was analyzed on CD14$^{+}$ monocytes from unstimulated HD (black), SLE (red), RA (blue) and pSS (green) whole blood samples and correlated with pSyk(Y$^{352}$) in CD27$^{+}$ memory B cells after 5 min anti-IgG/IgM stimulation (n(HD/SLE/RA/pSS) = 12/10/10/16). (**a**) Siglec-1 expression in HDs, SLE, RA and pSS patients. The horizontal lines represent the mean ± SD (one-way ANOVA with DMCT; * $p \leq 0.05$, ** $p \leq 0.01$). (**b**) Linear regression analysis of Siglec-1 expression versus Syk(Y$^{352}$) phosphorylation in CD27$^{+}$ memory B cells after 5 min anti-IgG/IgM stimulation in HDs (black), SLE (red), RA (blue) and pSS (green) patients. Linear regression lines, coefficients of determination ($R^2$) and Pearson's correlation coefficients (r) are indicated in the figure.

Further, there may be serum factors commonly increased or reduced in SLE, RA and pSS patients potentially leading to reduced Syk(Y$^{352}$) phosphorylation in all three diseases. To test this hypothesis, serum samples of 10 HD, 4 SLE, 6 RA and 10 pSS patients were collected at the day of Syk(Y$^{352}$) phosphorylation experiments. Those serum samples were screened for the expression of IL-1β, IL-1Ra, IL-2, IL-4, IL-5, IL-6, IL-7,IL-8,IL-9, IL-10, IL-12(p70), IL-13, IL-15, IL-17, IL-21, eotaxin, FGF basic, G-CSF, GM-CSF, IFNγ, IP-10, MCP-1(MCAF), MIP-1a, MIP-1b, PDGF bb, RANTES, TNFα as well as VEGF and analyzed for differential expression and correlation with pSyk($^{352}$) in CD27$^{+}$ memory B cells after 5 min anti-IgG/IgM stimulation (**Supplementary Figures 2, 3, 4, Supplementary Tables 2, 3**).

Tables with absolute serum concentrations (**Supplementary Tables 2, 3**), a heat map with relative cytokine expression for each donor (**Supplementary Figure 3**) and the correlation analysis

(**Supplementary Figure 4**) are listed in the appendix. Not all parameters were detectable within the range of the standard curves, in particular IL-6, IL-7, IL-15, IL-21 and G-CSF.

IL-1β, IL-1Ra, IL-10, IL-12(p70), IL-17, GM-CSF, RANTES and TNFα serum expression was significantly increased in SLE patients and IP-10 was significantly increased in pSS patients compared to HDs (**Supplementary Figure 4**). However, none of the tested serum factors was found commonly increased among all three autoimmune diseases, neither did the expression of one of the factors correlate with pSyk($Y^{352}$) after 5 min anti-IgG/IgM stimulation in $CD27^+$ memory B cells.

Neither *in vivo* Siglec-1 nor *in vivo* IL-1β, IL-1Ra, IL-2, IL-4, IL-5,IL-8,IL-9, IL-10, IL12(p70), IL-13, IL-17, eotaxin, FGF basic, GM-CSF, IFNγ, IP-10, MCP-1(MCAF), MIP-1a, MIP-1b, PDGF bb, RANTES, TNFα and VEGF expression correlated with the *ex vivo* anti-IgG/IgM induced phosphorylation of Syk($Y^{352}$) in $CD27^+$ memory B cells.

## 6.8 Common CpG Methylation Patterns Among SLE, RA, pSS and HD $CD19^+$ B Cells

T cell hypomethylation is associated with SLE [262]. Therefore, it was hypothesized whether epigenetic factors, such as differential CpG methylation, may control B cell hyperresponsiveness. A meta-analysis of Infinium HumanMethylation450K BeadChip data from individual epigenome-wide association studies (EWAS) was performed by our cooperation partner (**Figure 13**). Differentially methylated regions (DMR) were analyzed from public available data sets of SLE, RA , pSS patients and the respective HD control $CD19^+$ B cells [254-256].

Overall, the global CpG methylation values from autoimmune disease $CD19^+$ B cells correlate with those from HD $CD19^+$ B cells (r =0.99) (**Figure 13a**). Mostly, no substantial differences were found when the methylation status of certain genes, related to CD40 and BCR signaling, B cell activation and the methylation status of kinases and phosphatases, was analyzed (**Figure 13b**). However, some hypomethylation of multiple CpGs at the *interferon-induced transmembrane protein 1* (*IFITM1*) locus, the kinase *eukaryotic translation initiation factor 2 alpha kinase 2* (*EIF2AK2*) (cg14126601) and the kinase modulator *thyroid hormone receptor interactor 6* (*TRIP6*) (cg19279257) were found as a general characteristic in autoimmune disease $CD19^+$ B cells. Genes encoding interferon induced proteins, such as *IFITM1*, *interferon induced protein 44 like* (*IFI44L*) and *myxoma resistance protein 1* (*MX1*) were found to be the most differentially methylated CpGs, mainly in SLE and pSS and to a lesser extent in RA B cells compared to HDs (**Figure 13c, Supplementary Table 4**).

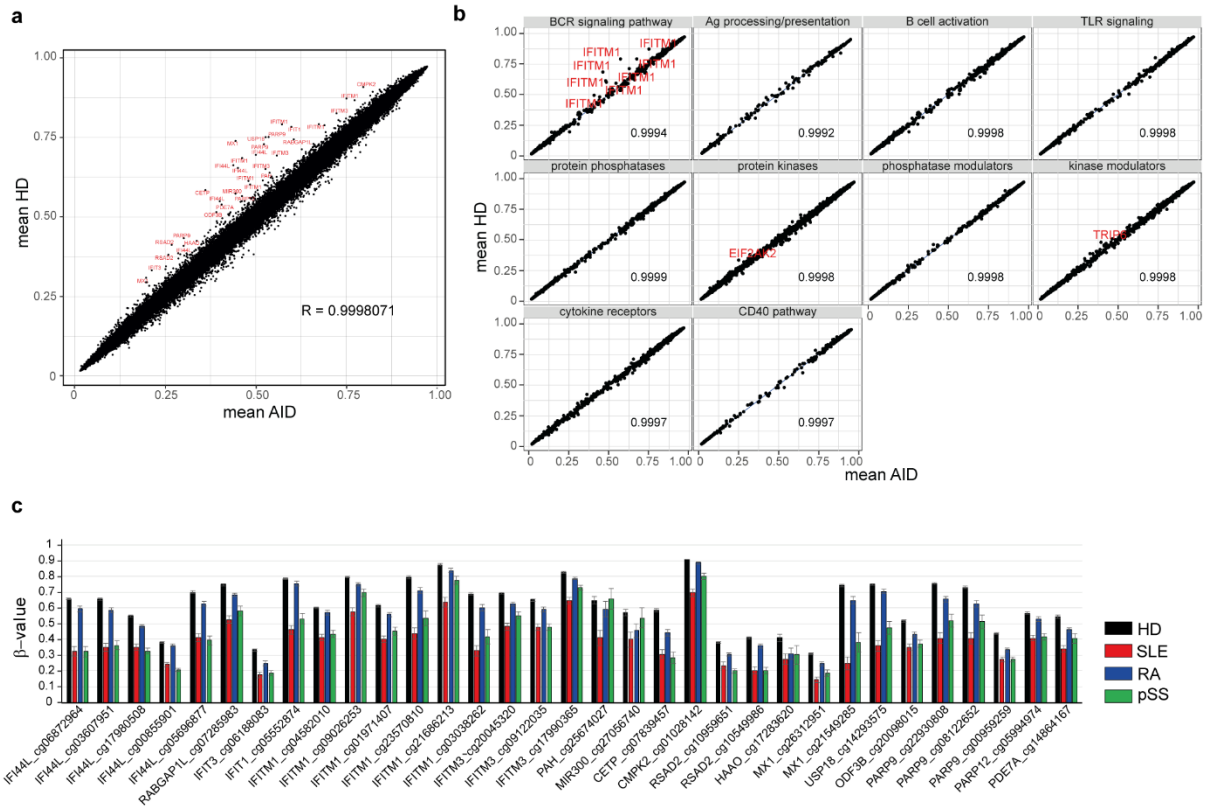


**Figure 13: Comparable methylation pattern of HD, SLE, RA and pSS B cells.** Meta-analysis of publicly available methylome data from HDs (black), SLE (red), RA (blue) and pSS (green) B cells. (**a**) Correlation of mean β-values of total single CpGs in HDs versus autoimmune disease (AID) samples (n(HD/SLE/RA/pSS) = 175/48/49/24). (**b**) Correlation of CpG methylation associated with the indicated categories between HDs and autoimmune disease samples. (**c**) Individual CpGs with 10 % lower DNA methylation in SLE, RA and pSS samples compared to HDs in (**a**). Data shown are represented as mean ± SEM.

## 6.9 Chronic Anti-IgG/IgM Stimulation Prevents Syk(Y$^{352}$) Phosphorylation Upon IgG/IgM Rechallange

A potential underlying mechanism of reduced BCR signaling measured by Syk(Y$^{352}$) phosphorylation may be the induction by external factors such as chronic cytokine, TLR or BCR engagement. Even though there was no solid hint from the tested patient's sera (**Section 6.7**), local environmental differences, for example in autoimmune inflamed tissues, rather than peripheral cytokine levels, might be involved in such events. Thus, a set of cytokines was tested to induces reduced pSyk(Y$^{352}$) upon 48 h *ex vivo* incubation with subsequent anti-IgG/IgM stimulation in HD CD27$^-$ B cells and CD27$^+$ memory B cells.

An increased IFNα signature is typically found in SLE and pSS patients [194, 263], IL-21 may drive autoreactive plasma cell development [264] and, together with IFNγ, t-bet expression in B cells is associated with autoimmunity [265] (**Supplementary Figure 5a, b**). Thus, these cytokines, as well as IL-2, IL-6 and IL-10, which play a role in inflammation and autoimmunity [266-268] were tested to induce reduced pSyk(Y$^{352}$) upon anti-IgG/IgM stimulation (**Supplementary Figure 5c**). However, none of those conditions was able to change the anti-IgG/IgM-induced Syk(Y$^{352}$) phosphorylation in CD27$^-$ B cells or CD27$^+$ memory B cells compared to RPMI control within 48 h of incubation.

TLR9 signaling may govern a checkpoint for DNA-containing antigens [158] and chronic stimulation of the BCR leads to B cell anergy [269]. Therefore, it was tested whether continuous stimulation of the BCR or TLR9 may be able to induce reduced Syk($Y^{352}$) phosphorylation upon re-stimulation with anti-IgG/IgM (**Figure 14**). HD PBMCs were cultured with anti-IgG/IgM or CpG for 24, 48 or 72 h and subsequently stimulated with anti-IgG/IgM for 5 min.

Notably, chronic challenge with anti-IgG/IgM revealed reduced Syk($Y^{352}$) phosphorylation in $CD27^-$ B cells and $CD27^+$ memory B cells after 24, 48 and 72 h (**Figure 14a, b, c**). However, chronic CpG stimulation did not alter anti-IgG/IgM induced pSyk($Y^{352}$) in comparison to unstimulated RPMI control. In detail, chronic anti-IgG/IgM stimulation reduced pSyk($Y^{352}$) MFI from 2,476 (RPMI control) to 1,202 (anti-IgG/IgM) in $CD27^-$ B cells and from 4,593 to 1,316 in $CD27^+$ memory B cells after 24 h of incubation between RPMI control and anti-IgG/IgM stimulation, respectively. Chronic anti-IgG/IgM induced MFIs did not increase after 48 h (1,069 in $CD27^-$ B cells and 1,206 in $CD27^+$ memory B cells) and 72 h (851 and 1,002 in $CD27^-$ B cells and $CD27^+$ memory B cells, respectively). Furthermore, in $CD27^-$ B cells, mean MFI after stimulation with CpG were 3,259, 2,484 and 1,822 for 24, 48 and 72 h, respectively. In $CD27^+$ memory B cells, mean MFI were 5,731, 4,571 and 3,684 after 24, 48 and 72 h stimulation with CpG, respectively. Thus, CpG stimulated cells exhibited comparable MFIs to RPMI control for $CD27^-$ B cells (2,476, 2,079 and 1,762) and $CD27^+$ memory B cells (4,593, 3,675 and 3,459) after 24, 48 and 72 h.

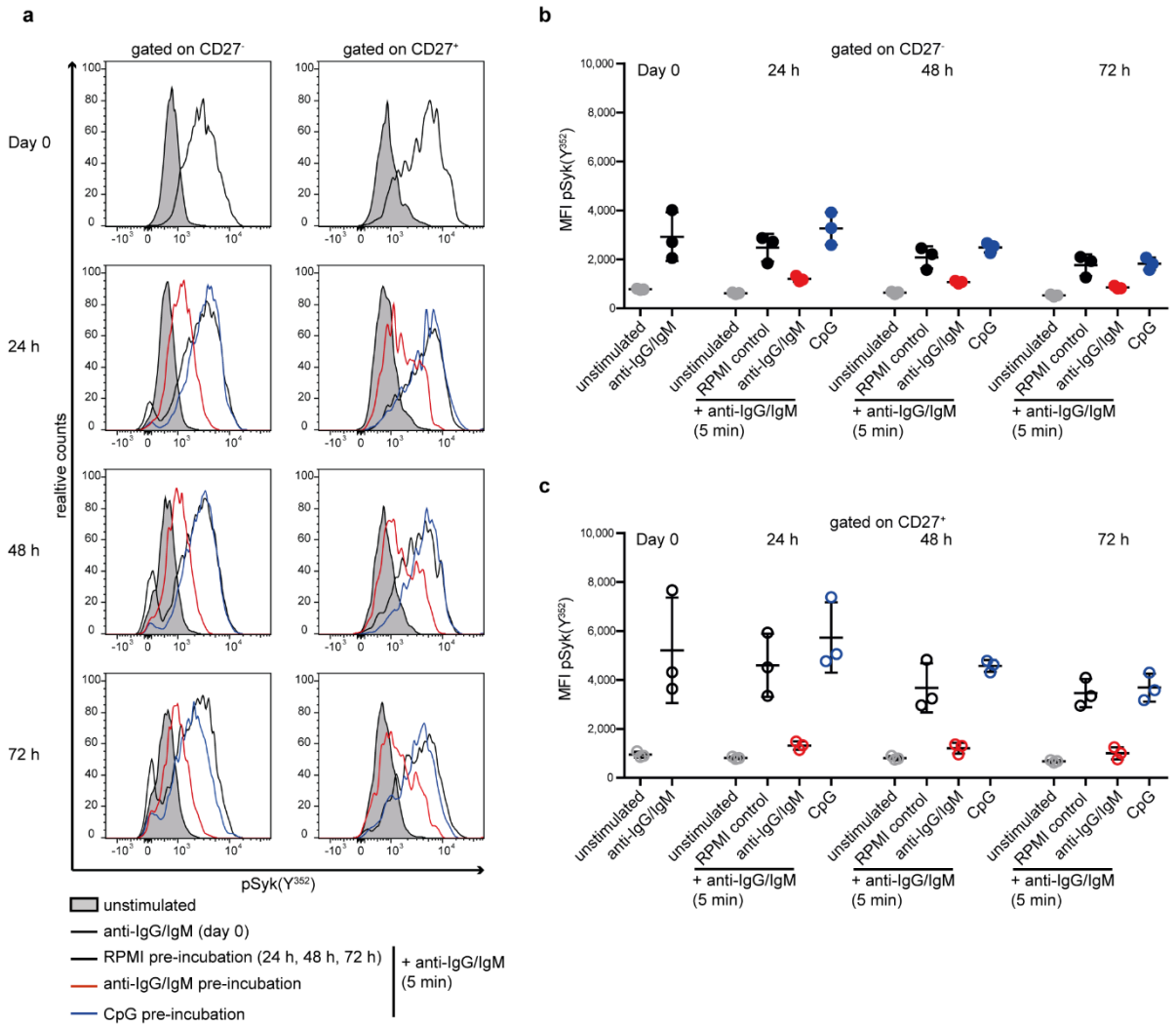


**Figure 14: Reduced pSyk(Y$^{352}$) in CD27$^-$ B cells and CD27$^+$ memory B cells upon chronic IgG/IgM stimulation.** PBMCs were cultured in the presences of anti-IgG/IgM (red), CpG (blue) or RPMI (black) as control for 24, 48 and 72 h. Harvested cells were subsequently re-stimulated with anti-IgG/IgM for 5 min or left unstimulated (grey) and analyzed for pSyk(Y$^{352}$) in CD27$^-$ B cells and CD27$^+$ memory B cells. (**a**) Representative pSyk(Y$^{352}$) histograms of CD27$^-$ B cells (left) and CD27$^+$ memory B cells (right) at day 0 of culture and 24, 48 and 72 h thereafter. Phospho-Syk(Y$^{352}$) MFIs in (**b**) CD27$^-$ B cells and (**c**) CD27$^+$ memory B cells (n(HD) = 3). Horizontal lines indicate the mean ± SD.

*In vitro* pre-incubation of HD B cells with IFNα, IFNγ, IL-21, IL-2, IL-6, IL-10 or CpG could not induce reduced pSyk(Y$^{352}$) MFIs upon re-stimulation with anti-IgG/IgM. However, chronic stimulation of the BCR led to sustained low pSyk(Y$^{352}$) MFIs over 72 h *in vitro*.

## 6.10 CD40 Co-Stimulation Increases Anti-IgG/IgM-Induced Syk(Y$^{352}$) Phosphorylation

Reduced phosphorylation of Syk(Y$^{352}$) and Btk(Y$^{223}$) upon anti-IgG/IgM stimulation appears to be counter-intuitive to the pathogenic involvement of B cells in autoimmunity. Nevertheless, *in vivo* B cell activation in autoimmunity may be linked to abnormal GC activity [2, 181, 270]. Furthermore, cognate T cell help via CD40 signaling is critically involved in GC formation and is further known to augment

BCR signaling via Syk [27]. Therefore, CD40 co-stimulation may be able to enhance the reduction of anti-IgG/IgM induced Syk($Y^{352}$) phosphorylation in SLE, RA and pSS B cells. CD40 requires cross-linking for optimal activation. To reproduce optimal CD40 co-stimulation *in vitro*, three approaches were tested: (i) Anti-CD40 plate coating, (ii) co-culture with an adherent hCD40L expressing cell line and (iii) a CD40L cross-linking kit. Differential expression of pSyk($Y^{352}$) after culturing with a CD40-stimulating reagent for 48 h and subsequent anti-IgG/IgM stimulation for 5 min was analyzed in $CD27^-$ B cells and $CD27^+$ memory B cells. Frequencies of $CD27^-$ and $CD27^+$ memory B cells were monitored to assess negative effects by the respective stimulus on these subsets.

### *6.10.1 Appropriate Activation of CD40 Using the CD40L Cross-Linking Kit*

(i) HD PBMCs were cultured for 48 h on an anti-CD40 coated plate at 0.1, 1, 5, 10, 100 µg $ml^{-1}$ and a PBS control. Frequencies of $CD27^-$ and $CD27^+$ memory B cells did not show any substantial difference up to the highest concentration tested (100 µg/ml) compared to baseline and PBS control (**Figure 15a**). Furthermore, there was no difference on anti-IgG/IgM induced pSyk($Y^{352}$) MFI between PBS control and the antibody at any concentration tested for $CD27^-$ B cells (**Figure 15b**) and $CD27^+$ memory B cells (**Figure 15c**).

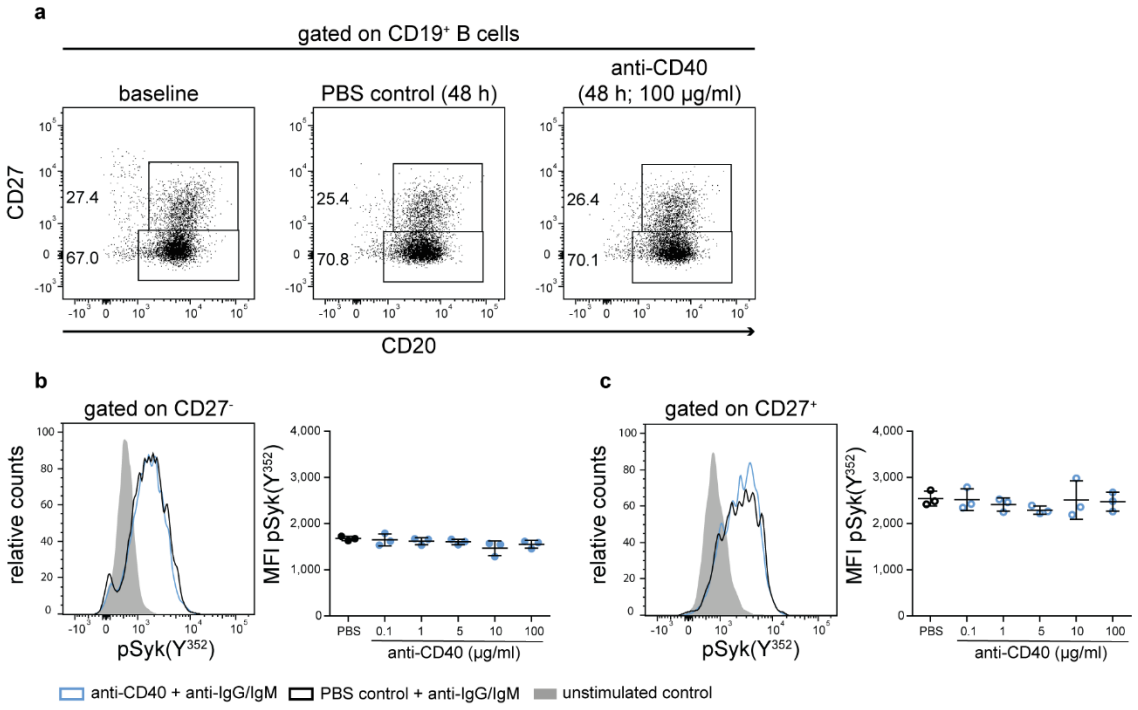


**Figure 15: Comparable Syk($Y^{352}$) phosphorylation with and without anti-CD40 coating.** HD PBMCs were incubated with plate coated anti-CD40 at the concentrations 0 (PBS control), 0.1, 1, 5, 10 and 100 µg/ml, subsequently stimulated with anti-IgG/IgM for 5 min and analyzed for pSyk($Y^{352}$). (**a**) Representative dot plots of $CD27^-$ B cells and $CD27^+$ memory B cell frequencies at baseline (left) and 48 h after culture without (middle) or with anti-CD40 stimulation (right). Representative pSyk($Y^{352}$) histograms and MFIs in (**b**) $CD27^-$ B cells and (**c**) $CD27^+$ memory B cells without (black) and with anti-CD40 co-stimulation at the concentrations 0.1, 1, 5, 10 and 100 µg/ml (blue). Data represent three technical replicates. Horizontal lines represent the mean ± SD.

(ii) A co-culturing system using adherent hCD40L expressing L cells was tested. Proliferation of L cells was stopped using irradiation. The cells became larger upon irradiation compared to non-irradiated cells. This is reflected by their increased SSC *vs*. FSC scatter properties (**Figure 16a, b**). Optimal irradiation dosage was tested using CFSE proliferation staining. The cells did not proliferate upon 5,000, 7,500 and 10,000 rad irradiation dosage (**Figure 16c**). Furthermore, irradiated cells exhibited higher CFSE staining than at baseline. This circumstance can be explained by the increased size of irradiated cells. 5,000 rad was selected and taken forward into the following experiments. In addition, CD40 expression was confirmed on irradiated and non-irradiated hCD40L-transfected versus wild type (WT) L cells (**Figure 16d**). Upon co-culture of hCD40L expressing or WT L cells with PBMCs, $CD27^+$ memory B cell frequencies dropped from 28.7 % at baseline to 7.16 % under CD40L co-stimulation, whereas frequencies under WT conditions remained at 26.8 % (**Figure 168e**). Anti-IgG/IgM induced Syk($Y^{352}$) phosphorylation increased in $CD27^-$ B cells upon CD40L co-stimulation (2,238) compared to the WT condition (1,738) (**Figure 16f**). For the remaining $CD27^+$ memory B cells, no effect was detectable.

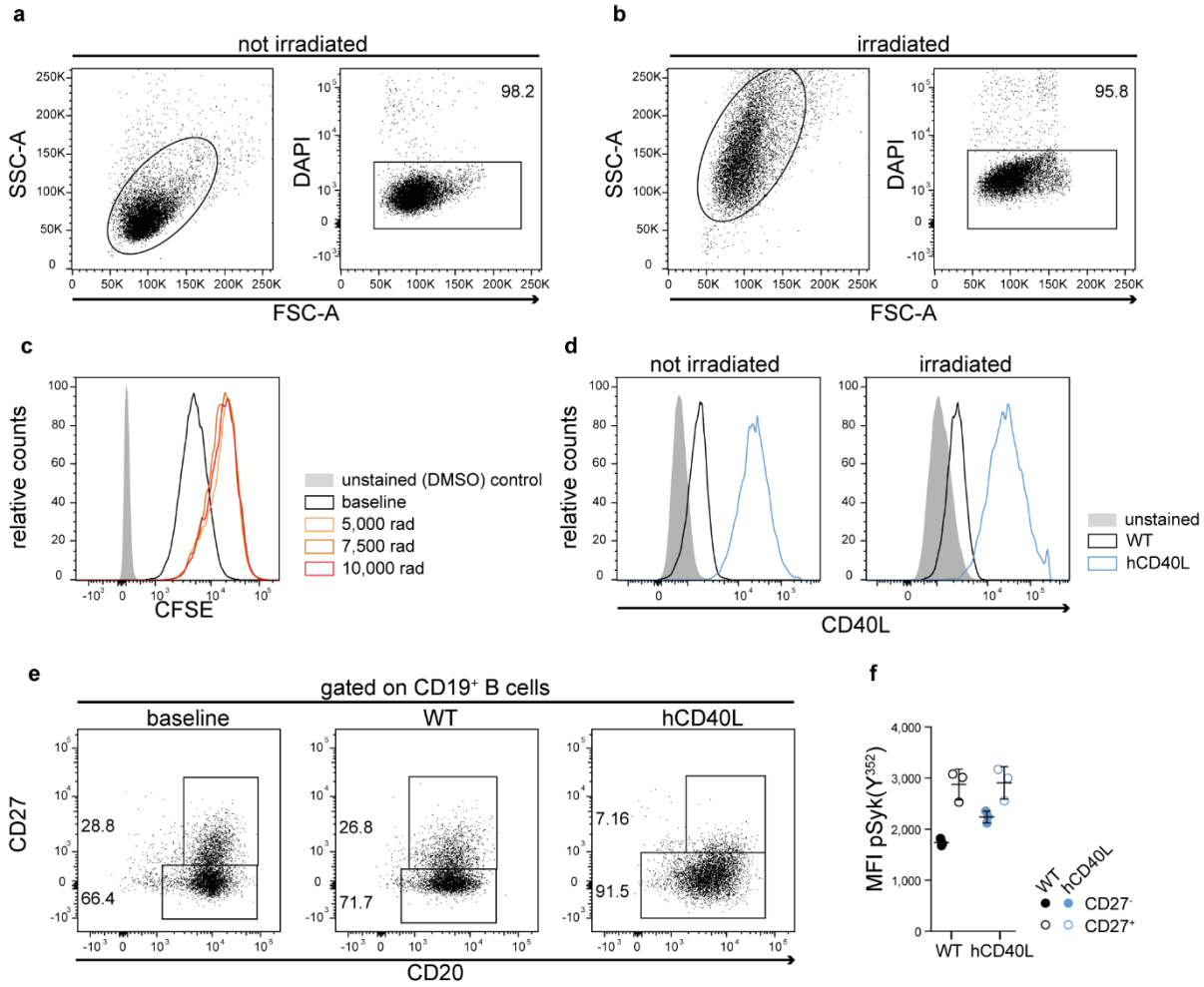


**Figure 16: Reduced frequencies of CD27⁺ memory B cells after co-culture with hCD40L L cells.** HD PBMCs were co-cultured with irradiated murine L cells with and without hCD40L transfection for 48 h. Harvested cells were stimulated with anti-IgG/IgM for 5 min and analyzed for Syk($Y^{352}$) phosphorlyation. Representative dot plots of L cells (**a**) before and (**b**) after irradiation gated on living ($DAPI^-$) cells. (**c**) CFSE staining histograms of L cells at baseline (black line) and after irradiation with 5,000 rad (light orange), 7,500 rad (middle orange) and 10,000 rad (dark orange). Unstained (DMSO) control is shown in grey. (**d**) Human CD40L expression on WT (black line) and transfected (blue line) L cells. The grey area represents the unstained control. (**e**) Dot plots of $CD27^-$ B cells and $CD27^+$ memory B cell frequencies at basline (left) and after co-cultur with WT (middle) and transfected (right) L cells. (**f**) Phospho-Syk($Y^{352}$) MFI in $CD27^-$ B cells (dots) and $CD27^+$ memory B cells (circles) after co-culture with WT (black) or transfected (blue) L cells. Data represent three technical replicates. Horizontal lines indicate the mean ± SD.

(iii) A commercially available cross-linking kit containing sCD40L and a cross-linking antibody was used. Frequencies of $CD27^+$ memory B cells upon co-stimulation were lower (15.9 %) than for RPMI or sCD40L control (19.7 % and 19.8 %, respectively) and compared to baseline (29.8 %) (**Figure 17a**). No effects were observed for sCD40L or the cross-linking antibody alone (**Figure 17b, c, d, e**). However, anti-IgG/IgM induced pSyk($Y^{352}$) MFIs were increased in $CD27^-$ B cells (3,441 *vs*. 2,697), as well as in $CD27^+$ memory B cells (4,290 *vs*. 3,441) using the cross-linked CD40L compare to RPMI control (**Figure 17d, e**).

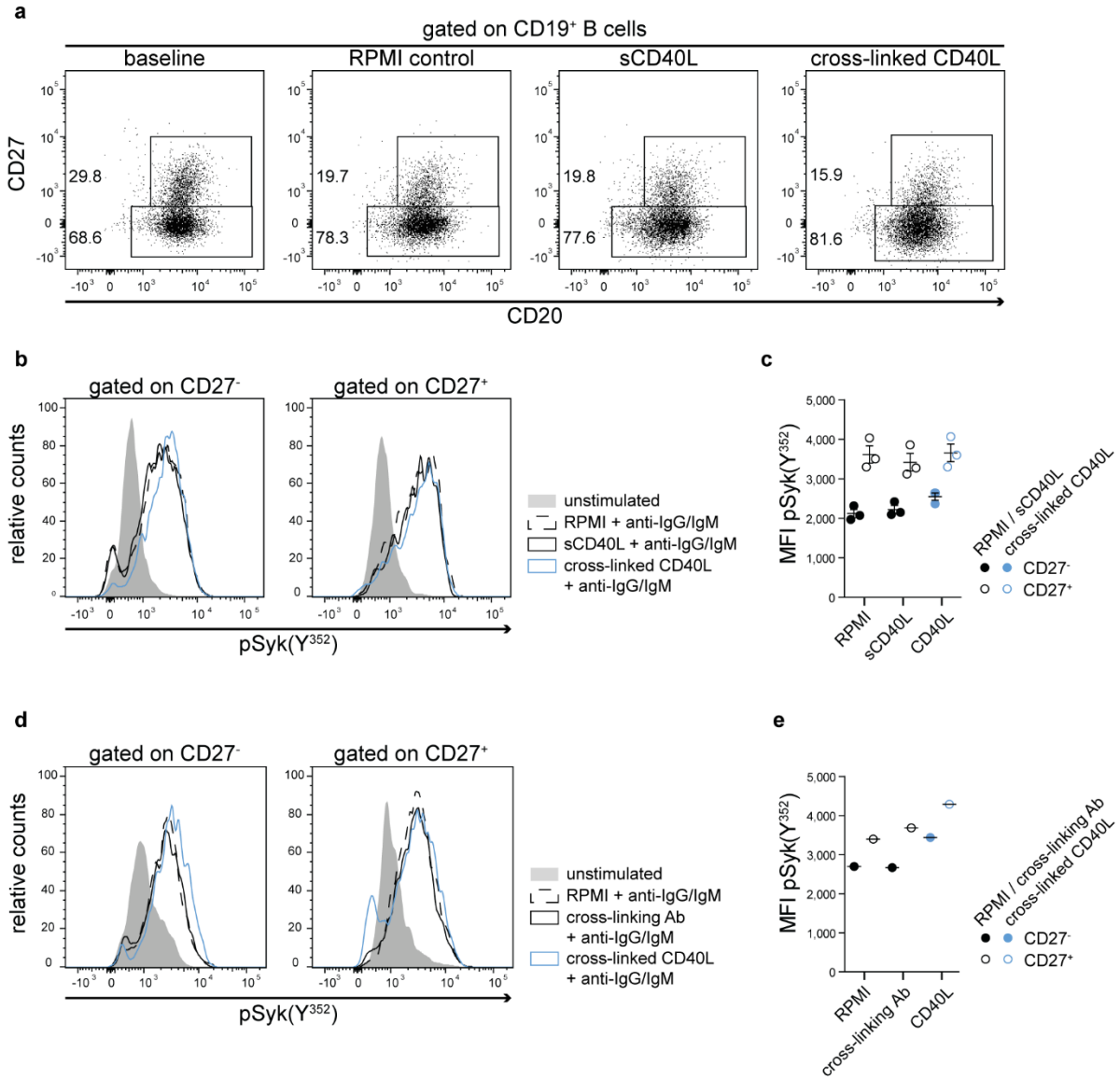


**Figure 17: Increased Syk(Y$^{352}$) phosphorylation upon co-stimulation with CD40L cross-linking kit.** HD PBMCs were incubated with and without the CD40L cross-linking kit for 48 h, subsequently stimulated with anti-IgG/IgM for 5 min and analyzed for pSyk(Y$^{352}$). (**a**) Representative dot plots of CD27$^-$ B cells and CD27$^+$ memory B cell frequencies at baseline (left) and after 48 h culture with RPMI (middle left), sCD40L (middle right) and the CD40L cross-linking kit (right). (**b**) Representative histograms of anti-BCR induced Syk(Y$^{352}$) phosphorylation in CD27$^-$ B cells (left) and CD27$^+$ memory B cells (right) upon co-stimulation with RPMI (dotted line), sCD40 (solid line) and the CD40L cross-linking kit (blue line). Unstimulated control is represented in grey. (**c**) Phospho-Syk(Y$^{352}$) MFI upon co-stimulation with RPMI (black), sCD40L (black) and the CD40L cross-linking kit (blue) in CD27$^-$ B cells (dots) and CD27$^+$ memory B cells (circles). Data represent three technical replicates. Horizontal lines indicate the mean ± SD. (**d**) Representative pSyk(Y$^{352}$) histograms of CD27$^-$ B cells and CD27$^+$ memory B cells upon co-stimulation with RPMI (dashed line), the cross-linking antibody from the kit only (solid line) and cross-linked CD40L (blue). (**e**) Phospho-Syk(Y$^{352}$) MFIs from CD27$^-$ B cells (dots) and CD27$^+$ memory B cells (circles) upon co-stimulation with RPMI (black), the cross-linking antibody (black) and cross-linked CD40L.

Coated anti-CD40L antibody exhibited no efficiency in this experimental setup (**Figure 15**). However, co-culturing with hCD40L expressing cells and co-stimulation with CD40L cross-linking kit increased anti-IgG/IgM induced Syk(Y$^{352}$) phosphorylation mainly in CD27$^-$ B cells (**Figures 16, 17**). Unfortunately, CD40L expressing L cells led to a strong depletion of CD27$^+$ B cells, which makes them

unsuitable for further experiments. Depletion of $CD27^+$ memory B cells was also observed after use of the CD40L cross-linking kit, but to a somewhat lesser extent. Therefore, CD40L cross-linking was chosen for subsequent experiments.

### *6.10.2 Increased Anti-IgG/IgM Induced Syk($Y^{352}$) Phosphorylation Upon CD40-Co-Stimulation in SLE, RA, pSS and HD B cells*

Next, HD, SLE, RA and pSS $CD27^-$ B cells and $CD27^+$ memory B cells were tested for their responsiveness to anti-IgG/IgM stimulation upon CD40 co-stimulation using the CD40L cross-linking kit (**Section 6.10.1**). Anti-IgG/IgM induced pSyk($Y^{352}$) MFIs after stimulation with CD40L increased among $CD27^-$ B cells and $CD27^+$ memory B cells from HDs, SLE, RA and pSS patients compared to anti-IgG/IgM-only stimulation (**Figure 18a, b**). Overall, co-stimulation with CD40L significantly increased mean pSyk($Y^{352}$) MFIs in HD (from 2,101 to 3,333), SLE (from 1,757 to 3,184), RA (from 1,922 to 2,960) and pSS (from 2,036 to 2,698) $CD27^-$ B cells as well as in HD (from 3,688 to 4,769) and pSS (from 2,733 to 3,404) $CD27^+$ memory B cells compared to no co-stimulation (**Figure 18c**). In SLE $CD27^+$ memory B cells, CD40 co-stimulation increased anti-IgG/IgM induced pSyk($Y^{352}$), even though the phosphorylation remained lower compared to HDs. Differences of anti-IgG/IgM induced Syk($Y^{352}$) phosphorylation in RA and pSS $CD27^+$ memory B cells upon CD40 co-stimulation were not significant. Of note, co-stimulation increased anti-IgG/IgM induced Syk($Y^{352}$) phosphorylation in RA and pSS $CD27^+$ memory B cells and SLE $CD27^-$ B cells to almost comparable levels of HDs.

The cytokines IL-4 and IL-21 contribute to $T_{FH}$ helper signals in a GC reaction [62]. Furthermore, CD40L together with IL-4 stimulation is reported of being able to restore reduced BCR signaling in an anergic $IgM^-IgD^+CD45^+$ B cell subset [271] and IL-21 plays a crucial role in the development of autoreactive plasma cells [264]. Therefore, the impact of IL-4, IL-21 and combinations of CD40L with IL-4 or IL-21 were tested on their co-stimulatory capacity to anti-IgG/IgM induced Syk($Y^{352}$) phosphorylation in HDs, SLE, RA and pSS.

IL-4R or IL-21R co-stimulation with the cytokines IL-4 or IL-21 alone had minor effects on Syk($Y^{352}$) phosphorylation in $CD27^-$ B cells and $CD27^+$ memory B cells from all groups (**Figure 18c**). Remarkably, stimulation with CD40L in combination with IL-4 significantly increased anti-IgG/IgM induced Syk($Y^{352}$) phosphorylation in HD, SLE, RA and pSS $CD27^-$ B cells and $CD27^+$ memory B cells in comparison to no co-stimulation. Upon CD40/IL-21R co-stimulation, the effects were moderate with significantly increased Syk($Y^{352}$) phosphorylation in $CD27^-$ B cells from all groups and $CD27^+$ memory B cells from HDs.

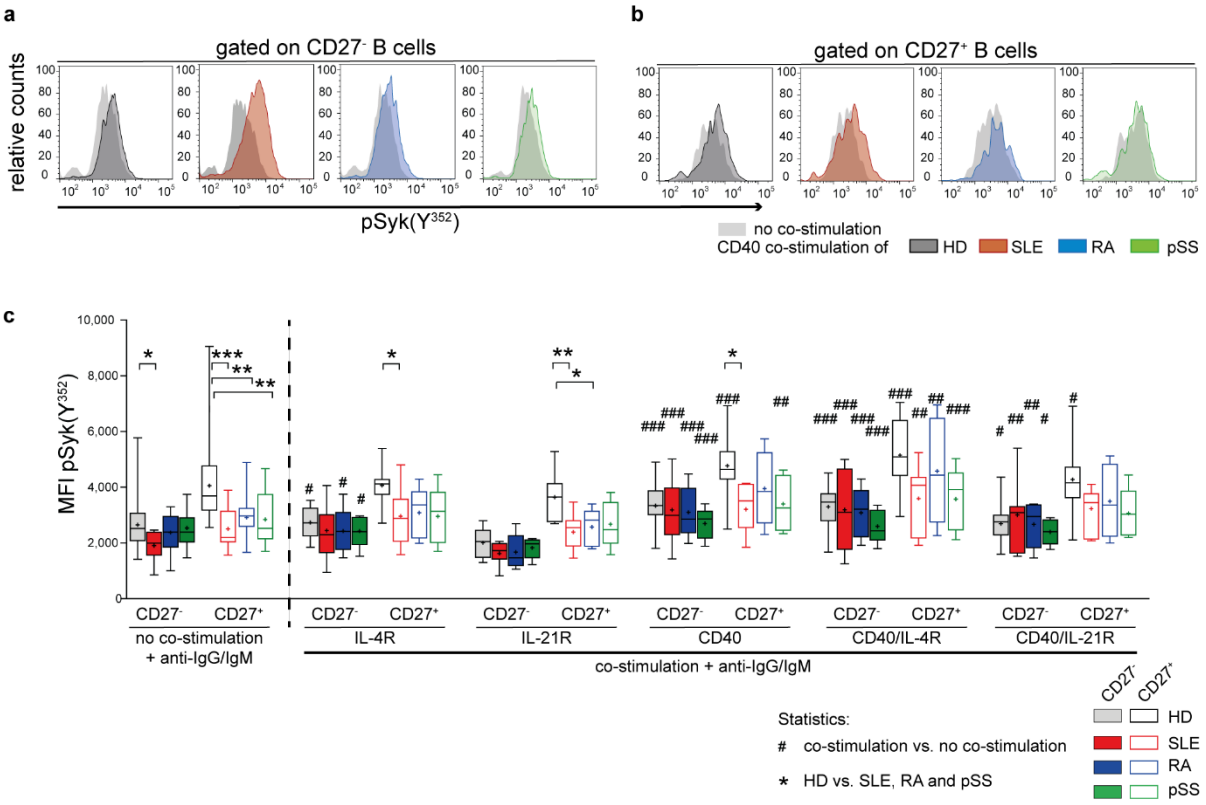


**Figure 18: Increased anti-IgG/IgM induced Syk(Y$^{352}$) phosphorylation after CD40 co-stimulation in HD, SLE, RA and pSS CD27$^-$ and CD27$^+$ memory B cells.** HD (black), SLE (red), RA (blue) and pSS (green) PBMCs were incubated with IL-4, IL-21, CD40L alone or combinations thereof for 48 h, subsequently stimulated with anti-IgG/IgM for 5 min and analyzed for pSyk(Y$^{352}$). Representative pSyk(Y$^{352}$) histograms of (**a**) CD27$^-$ B cells and (**b**) CD27$^+$ memory B cells. Cells without co-stimulation are indicated in grey. (**c**) Phospho-Syk(Y$^{352}$) MFI in CD27$^-$ B cells (filled boxes) and CD27$^+$ memory B cells (blank boxes) with (n(HD/SLE/RA/pSS) = 11/7/5/5) and without co-stimulation (n(HD/SLE/RA/pSS) = 30/18/16/15). Within the Box whisker plots the median (line), mean (plus) and range (whiskers) are represented (one-way ANOVA with DMCT, * $p \leq 0.05$, ** $p \leq 0.01$, *** $p \leq 0.001$; repeated measures ANOVA with DMCT, # $p \leq 0.05$, ## $p \leq 0.01$, ### $p \leq 0.001$).

In this set of experiments, it was also tested whether co-stimulation impacts basal Syk expression and Syk(Y$^{352}$) phosphorylation which may influence signaling capacity of Syk (**Supplementary Figure 6**). A small upregulation of Syk was found upon CD40 and CD40/IL-4R co-stimulation in SLE, RA and HD CD27$^-$ B cells as well as in HD CD27$^+$ memory B cells. Notably, only SLE CD27$^-$ B cells were found to have a significantly increased basal Syk expression upon CD40/IL-21R co-stimulation. Basal pSyk(Y$^{352}$) was overall increased in CD27$^-$ B cells and CD27$^+$ memory B cells from all groups upon CD40L co-stimulation with and without IL-4 or IL-21. However, the extent of the change was modest.

These data show that CD40 co-stimulation with and without IL-4, and to a lesser extend with IL-21, stimulation increases anti-IgG/IgM induced Syk(Y$^{352}$) phosphorylation in SLE, RA, pSS and HD CD27$^-$ B cells as well as CD27$^+$ memory B cells. SLE CD27$^-$ B cells showed remarkable responses upon co-stimulation with CD40L alone or in combination with IL-4 or IL-21.

## 6.11 Reduced TLR9 Induced Differentiation into $CD27^+CD38^+$ ASCs of SLE, RA and pSS B Cells

TLR9 activation and signaling has been linked to the induction of autoantibodies against dsDNA and ribonucleoproteins, indicating a critical role of this receptor in the activation of B cells in autoimmunity [186, 187]. TLR9 engagement mainly activates memory B cells and drives *in vitro* activation, proliferation and differentiation of B cells into ASCs [159, 160, 272]. However, impaired activation of SLE B cells upon TLR9 stimulation has been reported [22-24]. Within this study reduced Syk($Y^{352}$) phosphorylation upon anti-IgG/IgM stimulation was found of being a commonality within SLE, RA and pSS autoimmune disease (**Section 6.3**). Addressing the question whether impaired TLR9 activation is also a shared abnormality in terms of B cell activation among these autoimmune diseases, B cell differentiation into $CD27^+CD38^+$ ASC in HDs, SLE, RA and pSS patients upon *in vitro* stimulation with CpG was analyzed.

As a result, $CD27^+CD38^+$ ASC frequencies and absolute concentrations were approximately 2 to 4-fold higher in HDs (28.5 % with 95.4 cells/ml) compared to SLE (12.2 % with 28.7 cells/ml), RA (13.6 % with 22.3 cells/ml) and pSS (15.0 % with 56.0 cells/ml) patients upon TLR9 stimulation with CpG (**Figure 19a, b, c**). These results were significantly different for SLE, RA and pSS in terms of $CD27^+CD38^+$ frequencies as well as for SLE and RA in terms of $CD27^+CD38^+$ ASC concentrations.

Dual engagement of TLR9 and the BCR is thought of playing a central role in breaking tolerance against nuclear antigens [160, 188, 273] and leads to a stronger activation of naive B cells compared to TLR9 alone [159, 160]. Therefore, dual stimulation of TRL9 and the BCR was tested in HDs, SLE, RA and pSS (**Figure 19a, b, c**). Combined IgG/IgM and TLR9 activation did not substantially alter the frequency of $CD27^+CD38^+$ from HD or pSS B cells compared to TLR9 only stimulation (**Figure 19a, b**). However, mean frequencies of $CD27^+CD38^+$ cells were marginally increased from 12.2 to 19.4 % in SLE and 13.6 to 17.5 % in RA (TLR9 *vs*. TLR9/BCR, respectively) (**Figure 19b**). Absolute $CD27^+CD38^+$ ASC concentrations show a similar pattern with an increase mainly in SLE B cell concentration from 28.7 to 59.0 cells/ml. However, the response of autoimmune disease B cells remained overall lower than for HDs with significantly lower frequencies in pSS (42.9 cells/ml) compared to HDs (70.5 cells/ml) (**Figure 19c**). As a control, $CD27^+CD38^+$ cell frequencies and concentrations after anti-IgG/IgM only stimulation was comparable to IL-2/IL-10 background control in all groups (**Figure 19a, b, c**).

To assess the effects of CD40 co-stimulation, cells were cultured with CD40L only and the combinations of CD40L with CpG or CpG/anti-IgG/IgM (**Figure 19a, b, c**). Overall, frequencies and concentrations of $CD27^+CD38^+$ ASCs upon culture with CD40L alone or in the presence of CpG or CpG/anti-IgG/IgM were comparable with IL-2/IL-10 background control. This is in line with a previous report showing that CD40L stimulation blocks *in vitro* differentiation of B cells [274].

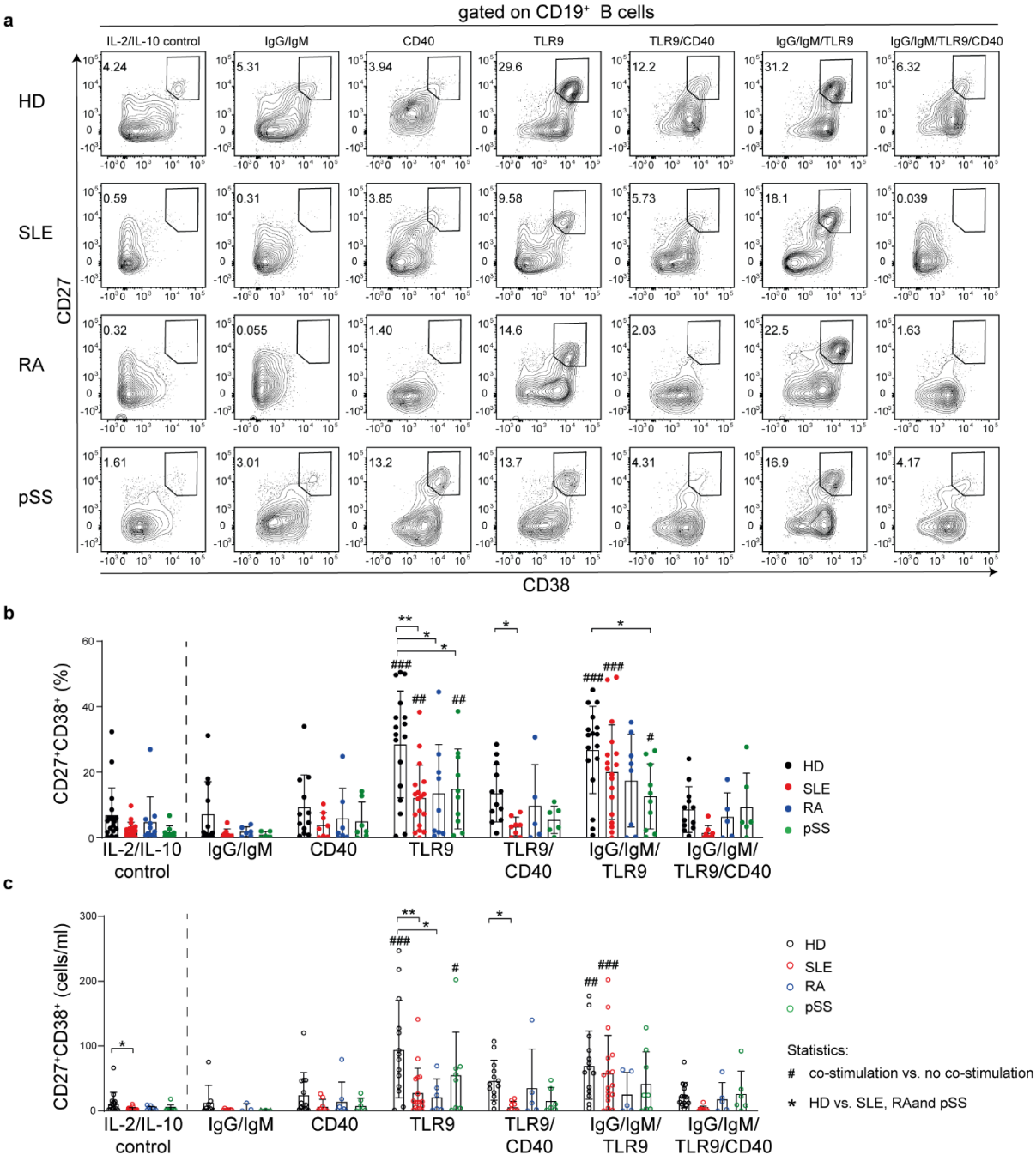


**Figure 19: Less ASC differentiation of SLE, RA and pSS B cells upon TLR9 stimulation.** HD (black), SLE (red), RA (blue) and pSS (green) PBMCs were cultured for 5 days with anti-IgG/IgM, CD40L or CpG and the combinations CD40L/CpG, CpG/anti-IgG/IgM or CD40L/CpG/anti-IgG/IgM in the presence of IL-2 and IL-10. ASCs were analyzed upon their high expression of CD27 and CD38. (**a**) Representative contour plots of $CD19^+$ B cells gated on $CD27^+CD38^+$ ASC from SLE, RA, pSS patients and HDs for the indicated stimulus. (**b**) $CD27^+CD38^+$ frequencies for HD, SLE, RA and pSS samples (n(HD/SLE/RA/pSS) = 18/18/11/10 (IL-2/IL-10 control); 12/8/6/5 (IgG/IgM); 12/8/7/7 (CD40); 17/18/9/10 (TLR9); 12/8/5/6 (TLR9/CD40); 17/18/8/10 (IgG/IgM/TLR9); 12/8/5/6 (IgG/IgM/TLR9/CD40)). (**c**) $CD27^+CD38^+$ concentrations for HD, SLE, RA and pSS samples (n(HD/SLE/RA/pSS) = 15/17/8/8 (IL-2/IL-10 control); 8/7/3/3 (IgG/IgM); 13/8/7/6 (CD40); 14/17/6/8 (TLR9); 12/8/5/6 (TLR9/CD40); 14/17/5/8 (IgG/IgM/TLR9); 12/8/5/6 (IgG/IgM/TLR9/CD40)). Bars indicate the mean ± SD (one-way ANOVA with DMCT; * $p \leq 0.05$, ** $p \leq 0.01$; # $p \leq 0.05$, ## $p \leq 0.01$, ### $p \leq 0.001$).

It has been previously reported that Syk inhibition leads to an impaired *in vitro* B cell activation and differentiation upon TLR9 signaling [162, 163]. Therefore, TLR9 induced B cell differentiation under entospletinib, a specific Syk inhibitor, was tested on HD PBMCs. The effect of entospletinib was concentration-depended with the highest inhibitory capacity at 10 µM (1.14 % $CD27^+CD38^+$ ASCs) compared to DMSO control (16.6 % $CD27^+CD38^+$ ASCs) (**Figure 20a**). *In vitro* inhibition of Syk using 10 µM entospletinib resulted in reduced $CD27^+CD38^+$ frequencies and concentrations upon TLR9 stimulation of HD B cells (**Figure 20b**) mimicking hyporesponsiveness to TLR9 signals observed in SLE, RA and pSS B cells (**Figure 19**).

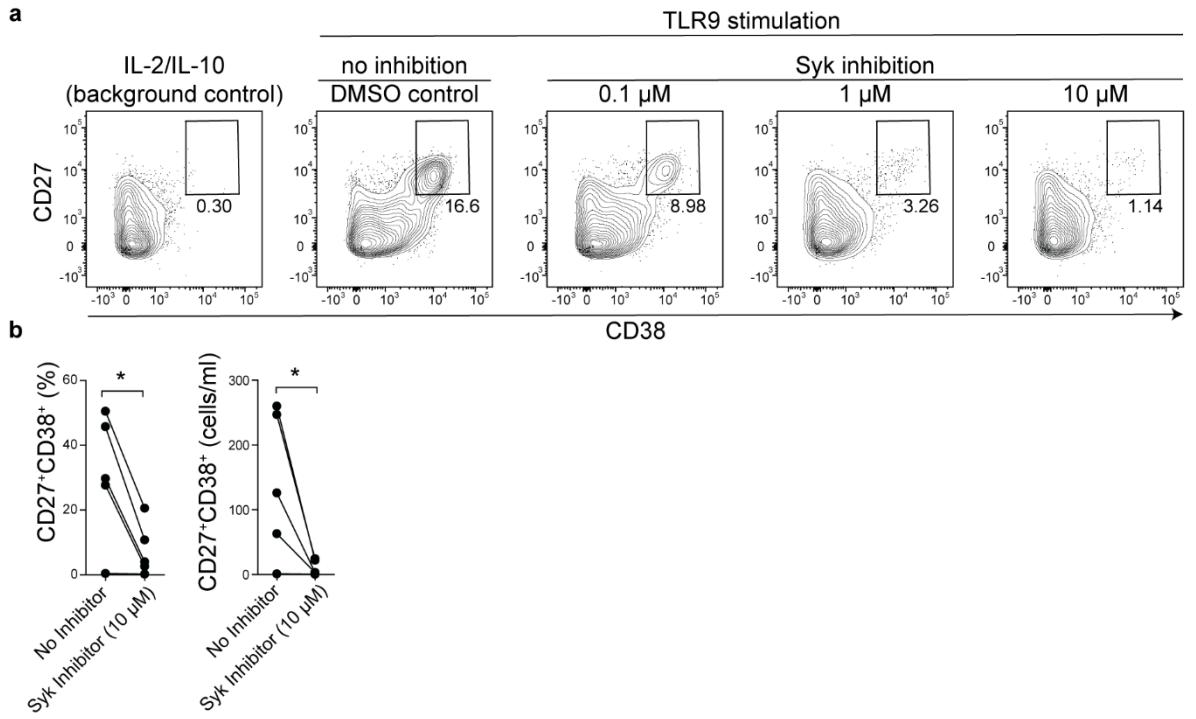


**Figure 20: Less TLR9 induced ASC differentiation upon Syk inhibition.** HD PBMCs were stimulated with CpG for 5 days with or without the presence of entospletinib, a specific Syk inhibitor. $CD19^+$ B cells were analyzed for the differentiation into $CD27^+CD38^+$ ASCs. (**a**) Representative couture plots of $CD27^+CD38^+$ gating for unstimulated (IL-2/IL-10 background control) and stimulated cells with 0.1, 1 and 10 µM entospletinib or DMSO control. (**b**) CpG induced ASC frequencies and concentrations with or without 10 µM Syk inhibitor (n(HD) = 5); (paired t-test; * $p \leq 0.05$).

Differentiation into $CD27^+CD38^+$ ASCs was found to be impaired in SLE, RA and pSS B cells upon TLR9 engagement. Reduced frequencies of $CD27^+CD38^+$ cells upon TLR9 stimulation and Syk inhibition suggested a functional relationship between reduced BCR signaling and reduced responses upon TLR9 stimulation. In line with this, $CD27^+CD38^+$ ASCs were only modestly increased in SLE, RA and pSS upon combined TLR9 and BCR stimulation, but overall were not fully restored to HD responses.

## 6.12 Restored Proliferation of SLE, RA and pSS B Cells Upon Co-Stimulation with CD40L

Besides $CD27^+CD38^+$ B cell differentiation (**Section 6.10**), proliferation was assessed using CFSE staining. In line with reduced TRL9-induced differentiation in SLE, RA and pSS, mean frequencies of proliferated SLE (46.6 %), RA (55.4 %) and pSS (50.0 %) $CD19^+CFSE^{low}$ B cells were reduced compared to HDs (68.2 %) (**Figure 21a, b)**. This was significant for SLE. Combined activation of TLR9 and BCR increased the proliferation of SLE (80.2 %), RA (91.7 %) and pSS (80.6 %) B cells to the levels of HDs (85.4 %). Even though there was low differentiation into $CD27^+CD38^+$ ASCs observed upon CD40 stimulation (**Figure 19a, b, c**), CD40L induced B cell proliferation was comparable between HD, SLE, RA and pSS samples (**Figure 21a, b**). Notably, low TLR9-induced proliferation of SLE, RA and pSS B cells were increased to HD levels upon the addition of CD40L and led to an overall stronger proliferation compared to CD40, TLR9 or anti-IgG/IgM alone.

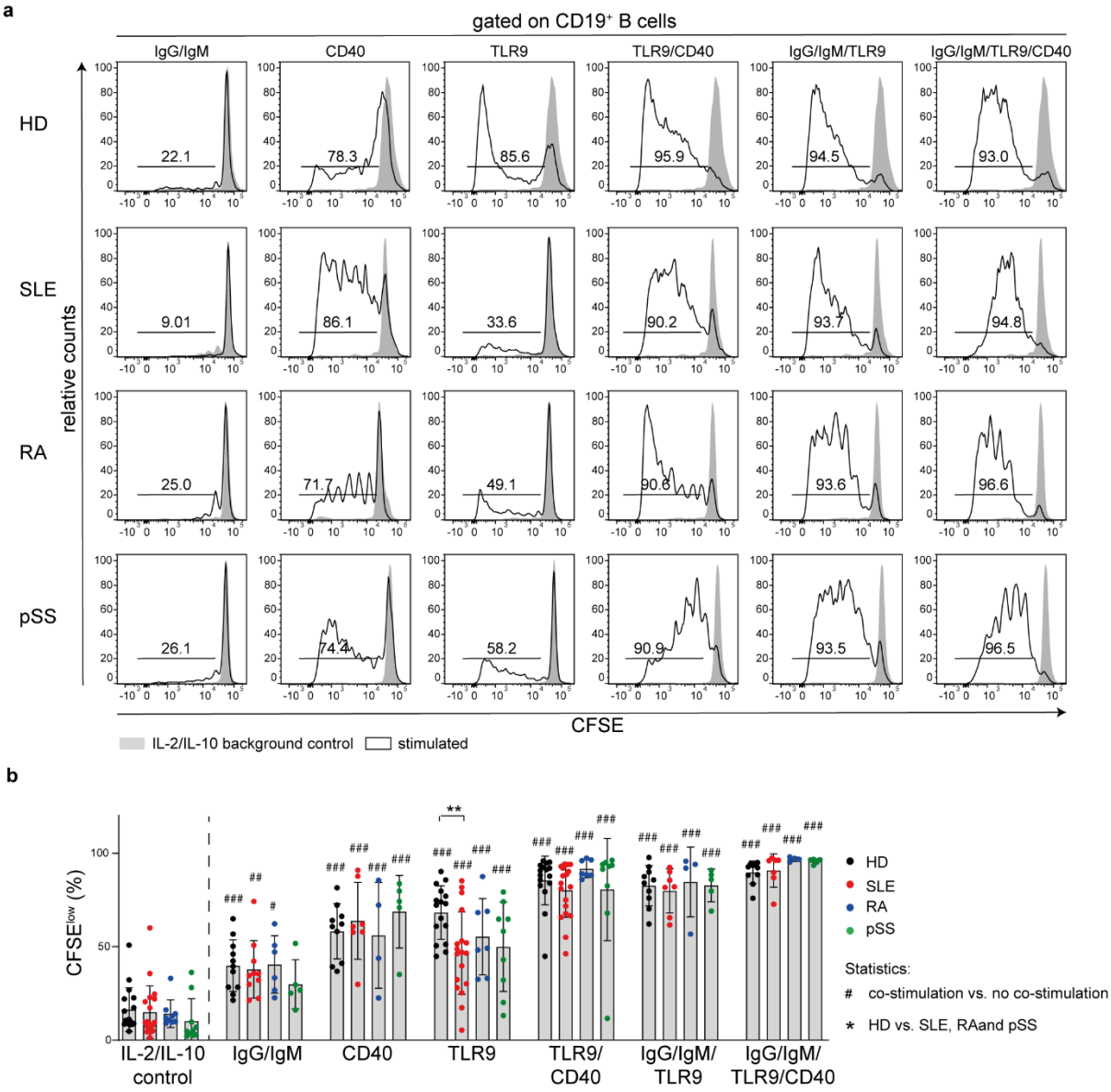


**Figure 21: Decreased proliferation of SLE B cells upon TLR9 stimulation and comparable proliferation of SLE, RA, pSS and HD B cells upon CD40 stimulation or combined IgG/IgM stimulation.** HD (black), SLE (red), RA (blue) and pSS (green) PBMCs were cultured for 5 days and treated to target IgG/IgM, CD40 and/or TLR9. Therefore, anti-IgG/IgM, CD40L or CpG and the combinations CD40L/CpG, CpG/anti-IgG/IgM or CD40L/CpG/anti-IgG/IgM were added in the presence of IL-2 and IL-10. Cultured cells were analyzed for proliferation using CFSE staining (**a**) Representative CFSE histograms of HD, SLE, RA and pSS B cells after stimulation with the indicated stimulus (lines) compared to IL-2/IL-10 background control (grey). (**b**) Frequencies of $CFSE^{low}$ B cells from HD, SLE, RA and pSS samples (n(HD/SLE/RA/pSS) = 17/19/9/10 (IL-2/IL-10 control); 11/10/6/5 (IgG/IgM); 10/7/4/5 (CD40); 16/18/7/9 (TLR9); 10/7/4/5 (TLR9/CD40); 16/19/7/9 (IgG/IgM/TLR9); 10/7/4/5 (IgG/IgM/TLR9/CD40)) (**c**) Resulting frequency of $CD27^{+}CD38^{+}$ B cells upon activation in culture (n(HD/SLE/RA/pSS) = 18/18/11/9 (IL-2/IL-10 control); 12/8/6/5 (IgG/IgM); 12/8/7/7 (CD40); 17/18/9/10 (TLR9); 12/8/5/6 (TLR9/CD40); 17/19/8/10 (IgG/IgM/TLR9); 12/7/5/6 (IgG/IgM/TLR9/CD40)). Bars represent the mean ± SD (one-way ANOVA with DMCT; * $p \leq 0.05$, ** $p \leq 0.01$; # $p \leq 0.05$, ## $p \leq 0.01$, ### $p \leq 0.001$).

These data show that the proliferative capacity of SLE, RA and pSS B cells is limited upon TLR9 stimulation. However, CD40 engagement as co-stimulatory signal induces strong and comparable proliferation in HD, SLE, RA and pSS B cells.

## 6.13 CD40/IL-4R Co-Stimulation Decreases PTP Expression

PTP/PSP activities were found uniquely increased in SLE CD19$^+$ B cells at baseline (**Figure 5**) and CD40/IL-4R co-stimulation was able to increase anti-IgG/IgM induced Syk(Y$^{352}$) phosphorylation (**Figure 18**). This led to the suggestion that CD40/IL-4R signaling may be involved in the modulation of PTP and PSP expression. The Expression of non-receptor and receptor type PTP and PSP genes was analyzed within publicly available gene expression data sets from SLE and HD CD20$^+$ B cells, CD4$^+$ and CD8$^+$ T cells as well as MS and HD CD19$^+$ B cells as controls (**Figure 22**). Furthermore, the impact of CD40/IL-4R co-stimulation on their expression was assessed.

Increased *PTPN2*, *PTPN11*, *PTPN22*, PTP receptor type C (PTPRC) and PTP receptor type O (PTPRO) gene expression was found in SLE CD20$^+$ B cells. However, no differentially expressed PTP was found in MS B cells compared to HDs indicating that differential expression of *PTPN2*, *PTPN11*, *PTPN22*, *PTPRC* and *PTPRO* is specific for SLE. Among the analyzed PTPs, no differentially expressed *RPTP* and only marginal differential expression of the *NRPTPs PTPN1*, *PTPN9* and *PTPN22* among SLE CD4$^+$ T cells and *PTPN1*, *PTPN7*, *PTPN9*, *PTPN11* and *PTPN22* among SLE CD8$^+$ T cells was found when compared to HDs.

*PTPN6* and PTP receptor type N 2 (*PTPRN2*) gene expression was increased in unstimulated SLE CD19$^+$ B cells compared to unstimulated CD19$^+$ B cells from HDs. However, in contrast to the data from the literature gene expression of *PTPRB* was decreased. Of note, CD40L/IL-4 stimulation led to a downregulation of *PTPN2* and *PTPN22* as well as all *RPTP* (except PTP receptor type B (*PTPRB*)) gene expression compared to their overexpression before stimulation.

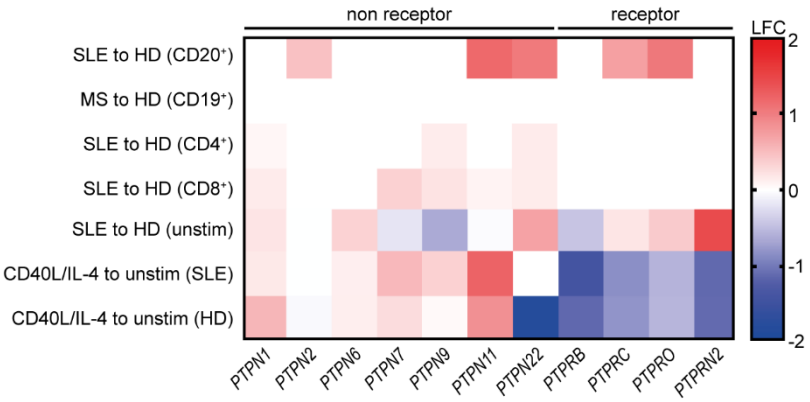


**Figure 22: Receptor-type PTPs show reduced expression upon CD40/IL-4R co-stimulation.** Selcted non-receptor type and receptor type PTPs were differentially analyzed for their gene expression. Data were obtained from publicly available data sets (lines 1 – 4) or collected experimentally upon co-stimulation with CD40L/IL-4 (lines 5 – 8). Lines 1 – 4: SLE *vs.* HD CD20$^+$ B cells (6 SLE, 7 HD), MS *vs.* HD CD19$^+$ B cells (10 MS, 10 HD), SLE *vs.* HD CD4$^+$ (53 SLE, 41 HD) and CD8$^+$ T cells (22 SLE, 31 HD). Lines 5 – 8: Un-stimulated SLE *vs.* HD as well as CD40L/IL-4 stimulated *vs.* un-stimulated SLE or HD CD19$^+$ B cells, respectively (n(HD/SLE) = 1/2). Gene expression is shown as linear fold change (LFC). Red squares indicate induction, white squares indicate no change and blue squares indicate reduction compared to HDs.

As PSP activities were found to be increased in SLE B cells, genes related to serine/threonine-protein phosphatase 2 (PP2) and PP2C family were analyzed (**Supplementary Figure 7**). Analyzing the data from the literature, small differences were found in *PSP* gene expression when SLE B and T cells were

compared to HDs. No differences were found when MS B cells were compared to HDs. In addition, unstimulated B cells displayed small differences in *PP2* and *PP2C* gene expression, whereas CD40/IL-4R co-stimulation led to heterogeneous changes: increased expression of *PP2* family genes except *PP2A subunit B isoform PR48* (*PPP2R3B*) (unaffected) and decreased *PP2A B subunit isoform PR61-delta* (*PPP2R5D*) was detected. However, *PP2C* family members were unaffected.

Taken together, differential baseline expression of the PTPs *PTPN2*, *PTPN11*, *PTPN22*, *PTPRC* and *PTPRO* is specific for SLE B cells compared to HD. Comparable expression of PTPs and PSPs between SLE *vs.* HD in $CD4^+$ and $CD8^+$ T cells correspond to comparable PTP activities in SLE and HD $CD3^+$ T cells (**Section 6.1**, **Supplementary Figure 2**). Provision of T cell help by CD40/IL-4R engagement alters the expression of NRPTPs such as *PTPN22* and different RPTPs in HD and SLE B cells and as such is considered an important modulator of intracellular PTP activity.

## 6.14 Summary of Results

This comparative study of SLE, RA and pSS peripheral B cells shows that autoimmune disease B cells share hyporesponsiveness towards BCR and TLR9 stimulation. This was demonstrated by commonly reduced anti-IgG/IgM induced phosphorylation kinetics of the BCR downstream PTKs Syk and Btk, at their activation sites Syk($Y^{352}$) and Btk($Y^{223}$), in $CD27^+$ memory B cells from SLE, RA and pSS patients (**Section 6.3**). Additionally, Syk($Y^{352}$) phosphorylation kinetics were reduced in SLE $CD27^-$ B cells. Furthermore, reduced proliferation and differentiation of $CD19^+$ B cells upon TLR9 engagement was demonstrated (**Sections 6.11**). Notably, there was no distinction of Syk($Y^{352}$) and Btk($Y^{223}$) phosphorylation kinetics between $CD27^-$ B cells and $CD27^+$ memory B cells in SLE, RA and pSS patients, whereas kinetics in HD $CD27^+$ memory B cells were increased compared to $CD27^-$ B cells. Furthermore, reduced Syk($Y^{352}$) phosphorylation kinetics were observed in tissue resident $CD27^+$ memory B cells from autoimmune disease patients (**Section 6.5**). The increased colocalization of CD22 with SHP-1 in SLE, RA and pSS $CD19^+$ B cells points into the direction of commonly increased negative regulation of BCR downstream signaling (**Section 6.1**). Notably, the strongest phenotype was observed for SLE with reduced kinetics in $CD27^+$ memory as well as $CD27^-$ B cells whereas kinetics of $CD27^-$ B cells in RA and pSS were comparable to HDs. Moreover, increased PTP and PSP activity was only observed in SLE, and CD22/SHP-1 colocalization was at maximum and could not be further increased in SLE. Syk inhibition experiments implicate that impaired TLR9-dependent differentiation of SLE, RA and pSS B cells into $CD27^+CD38^+$ ASCs is Syk-depended. Accordingly, combined engagement of the BCR and TLR9 increased $CD27^+CD38^+$ ASC differentiation only modestly. Reduced Syk activity in SLE, RA and pSS peripheral B cells did not translate into reduced Akt($S^{473}$) phosphorylation (**Section 6.4**). Akt($S^{473}$) phosphorylation kinetics were comparable in RA and pSS and increased in SLE $CD27^-$ B cells and $CD27^+$ memory B cells compared to HDs.

Common differences in baseline expression and phosphorylation of the signaling molecules Syk, Btk, PLCγ2 and Akt, which may account for signaling abnormalities, were not observed (**Section 6.2**). Also, pERK1/2($T^{202}/Y^{204}$), a potential marker for anergy, did not exhibit any differences between HD, SLE, RA and pSS peripheral B cells (**Section 6.6**). Furthermore, no commonality in the expression and

correlation with reduced Syk($Y^{352}$) phosphorylation were observed for Siglec-1, reflecting the characteristic type I IFN signature (incl. IFNα), or any of the 23 tested serum cytokines (**Section 6.7**). In addition, IFNα, IFNγ, IL-2, IL-4, IL-6, IL-10, IL-21 and CpG did not induce reduced anti-IgG/IgM induced Syk($Y^{352}$) phosphorylation in HD B cells. However, chronic engagement of IgG and IgM led to a sustained reduction of Syk($Y^{352}$) phosphorylation upon re-engagement with anti-IgG/IgM in $CD27^-$ B cells and $CD27^+$ memory B cells (**Section 6.9**). Nevertheless, CpG methylation was comparable among autoimmune diseases and HDs, except for some hypomethylation at *IFITM1*, *EIF2AK2* and *TRIP6* locus (**Section 6.8**). CD40 co-stimulation with and without addition of IL-4 or IL-21 increases anti-IgG/IgM induced Syk($Y^{352}$) phosphorylation in SLE, RA, pSS and HD $CD27^-$ B cells as well as in SLE, RA and pSS $CD27^+$ memory B cells (**Section 6.9**). Remarkably, $CD27^-$ B cells from SLE were able to normalize their Syk($Y^{352}$) phosphorylation response to HD level upon CD40 co-stimulation with and without the addition of IL-4 and IL-21. Furthermore, CD40 co-stimulatory induces strong and comparable proliferation of HD, SLE, RA and pSS B cells. (**Section 6.11**). Besides the increase of anti-IgG/IgM induced pSyk($Y^{352}$ ) (**Section 6.9**), CD40/IL-4R co-stimulation reduced gene expression of NRPTPs, for example *PTPN22*, and different RPTPs in HD as well as SLE $CD19^+$ B cells (**Section 6.12**).

# 7 Discussion

## 7.1 Reduced BCR Responsiveness is a Commonality Among Peripheral as Well as Tissue Resident B Cells from Patients with Autoimmune Diseases

Increased B cell activity in autoimmune diseases such as SLE, RA and pSS is characterized by the production of high autoantibody titers and abnormal B cell subset distributions such as increased frequencies of circulating plasma cells and plasmablasts typically found in the peripheral blood of SLE patients [38-40, 44-47, 76, 77, 83-86, 170-174, 275, 276]. Beneficial effects of B cell directed therapies underscore the pathogenic role of B cells in those autoimmune diseases and highlight the importance of B cell directed therapies [3-10]. The intracellular BCR signal as a major driver of B cell activation and cell fate, was thought to be increased and the main driver of B cell activity in autoimmunity [15, 16, 225]. In contrast to this hypothesis, this and other work demonstrated reduced BCR signals measured by Syk($Y^{352}$) phosphorylation in SLE $CD27^-$ B cells and $CD27^+$ memory B cells [14, 244]. Moreover, the presented work demonstrates that phosphorylation of the PTKs Syk and Btk, at their activation sites Syk($Y^{352}$) and Btk($Y^{223}$), is generally reduced in $CD27^+$ memory B cells from SLE, RA and pSS patients. This finding indicates that reduced responsiveness of intracellular BCR signaling is a more general phenomenon of autoimmune diseases. However, reduced Syk($Y^{352}$) phosphorylation upon BCR stimulation is specific for $CD27^-$ B cells from SLE patients. Interestingly, the amplitude of Syk($Y^{352}$) and Btk($Y^{223}$) phosphorylation in SLE, RA and pSS $CD27^+$ memory B cells was comparable to $CD27^-$ B cells of the respective disease indicating $CD27^-$ B cell-like signaling properties. Iwata et al. previously reported increased BCR signaling measured by pSyk($Y^{348}$) expression in SLE $CD19^+$ B cells compared to HDs [277]. However, within that study $CD27^-Syk^{++}$ memory-like B cells, which show higher Syk($^{Y348}$) phosphorylation and increased frequencies in SLE patients can bias the analysis [278]. These cells were not excluded in the study from Iwata et al., 2015, but in the presented study. Thus, the previously reported increase in BCR signaling do not appear contradictory to the data presented in this work. Interestingly, serine phosphorylation of Akt($S^{473}$) was not found to be affected by reduced signaling in SLE, RA and pSS B cells even though it also depends on Syk activation [95]. These results indicate that reduced BCR responsiveness does not globally affect all signaling pathways and point towards alternative regulation pathways of peripheral autoimmune disease B cells. Interestingly, reduced BCR responsiveness of *ex vivo* stimulated SLE, RA and pSS B cells observed in this study may corresponds to the observation of low responsiveness towards vaccination among those patients. Several studies reported unresponsiveness, measured by low antibody titers, mainly analyzed and found in SLE and RA patients, upon pneumococcus or H1N1 vaccination [279-281]. However, an impact of disease-modifying antirheumatic drug (DMARD) treatment on those results cannot be excluded [280, 282]. Furthermore, one study found increased responses after H1N1 influenza vaccination of untreated pSS patients compared to HDs [283]. As the BCR signal is a major driver of B cell fate, it might be possible that these highly reactive B cells, with potentially increased BCR signal in autoimmune disease, migrate to lymphatic or inflamed tissue. However, this work demonstrates that reduced BCR signal is not

restricted to peripheral B cells, it also affects tissue resident B cells. Syk($Y^{352}$) phosphorylation among $CD27^+$ memory B cells from patients with ITP was reduced compared to $CD27^+$ memory B cells from patients without autoimmunity. In addition, the analysis of Syk($Y^{352}$) phosphorylation in $CD27^+$ memory B cells from a pSS parotid was rather decreased compared to peripheral B cells, even though they are located at an actual site of autoimmune inflammation.

## 7.2 Impaired Responsiveness of SLE, RA and pSS Peripheral B Cells to BCR and TLR9 Stimuli is Connected by Syk

Besides BCR signaling, TLR9 signaling is a potential driver of autoimmunity facilitating dsDNA and ribonucleoprotein autoantibody development, drives *in vitro* activation, proliferation and differentiation of B cells into ASCs and is considered to be involved in type I interferon (IFN) production in autoimmunity [159, 160, 186, 187, 284]. Within the presented study, responses towards TLR9 activation were diminished including reduced proliferation and differentiation into $CD27^+CD38^+$ ASCs. This is consistent with previous studies reporting diminished responsiveness of SLE B cells after TRL9 activation [22-24]. Ginsburg *et al*. found that active SLE patients did not generate ASCs in response to pokeweed mitogen *in vitro* [24]. Furthermore, Sieber *et al*. found reduced IL-6, IL-10, vascular endothelial growth factor (VEGF), and IL-1ra production together with reduced expression of the proliferation marker Ki-67 after TLR9 *in vitro* stimulation [22]. Another study reported impaired TLR9 responses in SLE B cells which are characterized by reduced frequencies of $CD69^+CD86^+$ and $TACI^+CD25^+$ B cells [23]. This work, supported by the data from Iwata *et al*. and Kremlitzka *et al*., demonstrates a functional connection between TLR9 and BCR signaling by inhibiting TLR9 induced differentiation upon Syk inhibition [162, 163]. Based on this, a similar regulatory connection between reduced BCR and reduced TLR9 signaling in autoimmune diseases can be assumed. In line with this hypothesis, combined BCR and TLR9 stimulation increased proliferation and differentiation of autoimmune disease $CD19^+$ B cells only modestly.

## 7.3 Reduced BCR Responsiveness is Likely Caused by an Increase in Negative Feedback Regulation Mediated by Protein Phosphatases

GWAS support an association of certain risk mutations within the BCR signaling cascade and the development of autoimmunity [11, 201-210]. Therefore, it might be possible that genetic alterations may play a role in the presented findings of reduced BCR responsiveness in autoimmune diseases. Risk mutations of *LYN*, *BLK*, *BANK1* and *PTPN22* are associated with SLE [11, 201-204] and it is reported that RA and pSS share some of these risk alleles [207-209]. A commonality of all three autoimmune diseases is an association with *PTPN22* 1858C/T risk mutation [211-214], which is reported to be a gain-of-function mutation reducing TCR as well as BCR responses in humans [218-220]. However, Metzler *et al*. reported augmented BCR as well as CD40 responses in mice expressing this risk mutation [221]. Furthermore, the risk mutation of the adapter molecule *BANK1*, which is mainly expressed in $CD19^+$ B cells, leads to a dysbalanced expression of *BANK1* splicing variants, which in turn reduces BCR signaling [204, 223]. However, *PTPN22* as well as *BANK1* risk alleles were reported

to reduce Akt phosphorylation [218, 223], which was not found in the present study. Furthermore, *BANK1* risk mutation appears to be specific for SLE and RA [207-209, 215] or even SLE only [217]. Therefore, an impact of mutation variants on the presented findings of reduced BCR signaling cannot be completely excluded but appears to be less likely.

Within this study, *in vivo* factors, such as the expression of cytokines or Siglec-1 as surrogate marker for type I IFN (IFNα) activity, were excluded as common inducers of reduced pSyk($Y^{352}$) in SLE, RA and pSS patients. Of note, increased Siglec-1 expression was present in SLE and pSS patients, as also previously reported [193, 194], but not in RA compared to HDs. The meta-analysis of common differentially methylated CpGs among SLE, RA and pSS compared to HDs revealed that reduced BCR and TLR9 responsiveness is likely not under epigenetic control. Also, the overall availability of the signaling molecules and the tonic phosphorylation at the distinct sites Syk($Y^{352}$), Btk($Y^{223}$), PLCγ2($Y^{759}$) and Akt($S^{473}$) is not affected and largely comparable to HDs.

Increased co-localization of CD22 and SHP-1 in SLE, RA and pSS $CD19^+$ peripheral B cells compared to HDs favors the idea of a common signaling disbalance in autoimmune disease based on increased negative regulation via PTPs such as SHP-1. Increased PTP and PSP activities and maximal CD22/SHP-1 colocalization indicates a stronger phenotype for SLE. Together with reduced BCR induced Syk($Y^{352}$) phosphorylation after chronic BCR stimulation, chronic *in vivo* stimulation may serve as potential mechanism of reduced BCR signaling observed in SLR, RA and pSS. Of note, baseline expression and phosphorylation of signaling molecules is not different between HDs and autoimmune disease patients indicating that only functionally and not tonic BCR signaling is affected by the negative feedback loop. Furthermore, SLE B cells had maximal colocalization of CD22/SHP-1 which could not be further increased upon anti-CD22 stimulation and increased activities of PTPs in total $CD19^+$ B cells. This might explain the stronger phenotype of reduced Syk($Y^{352}$) phosphorylation in $CD27^+$ memory as well as $CD27^-$ B cells compared to RA and pSS. In this regard, dysregulated recruitment of Syk to the proximal BCR signaling complexes has been recently reported by Vasquez *et al*. The authors hypothesize that this dysregulation is caused by constant activation through the BCR, and thus, strongly supports the hypothesis of the presented work [238].

## 7.4 B Cells from Autoimmune Disease Patients Remain in a 'Post-Activation' State Common to Anergy

Reduced BCR responsiveness is a hallmark of B cell anergy [285], which is a non-reactive state of autoreactive B cells preventing tolerance breach, if cells are not silenced by receptor editing or clonal deletion [143-145]. Between 5 and 7 % of the normal B cell repertoire is anergic [149, 150, 286]. In humans anergic B cells are mainly identified as mature naive $IgD^+/IgM^+$ B cells, which are predominantly autoreactive (2.5 % of peripheral B cells) [149]. Anergy has been previously described with impaired BCR signaling leading to reduced intracellular $Ca^{2+}$ mobilization and phosphorylation of tyrosine residues [125, 144, 269, 287-290]. This is consistent with the presented observations of reduced BCR signal in autoimmune disease $CD27^+$ memory B cells and $CD27^-$ B cells from SLE. Anergic B cells do not proliferate, upregulate activation markers or secret Ig upon BCR stimulation [147,

148]. In line with this, reduced proliferation and differentiation into ASCs by TLR9 and, to a lesser extent, TLR9 and BCR stimulation, both Syk-dependent mechanisms, were observed in this study. Furthermore, it has been reported that reduced signaling of CD19/PI3K suppresses phosphatidylinositol-3,4,5-triphosphate (PIP3) generation by PI3K and is key for B cell anergy [291]. However, in this studies Akt($S^{473}$) phosphorylation, which is downstream of PI3K, was found to be normal in RA and pSS and increased in SLE $CD27^-$ B cells and $CD27^+$ memory B cells. Thus, indicating that there might be other mechanisms for anergy or an anergy-like state independent of CD19/PI3K.

Another characteristic of anergic B cells is elevated basal $Ca^{2+}$ levels [133]. This was not directly assessed within this study. However, our group previously reported no increase of basal $Ca^{2+}$ in $CD19^+$ B cells from SLE patients [14]. In line with the presented data on similar basal phosphorylation between autoimmune disease patients and HDs as well as BCR-activation induced differential signaling, differential $Ca^{2+}$ responses occur after BCR engagement. It is thought that BCR unresponsiveness in anergic cells is due to chronic antigen exposure [269], which has been mimicked *in vitro* within this work. However, B cell anergy is not permanent and can be reversed upon removal of the antigen [269]. It has been reported that reduced BCR signaling of SLE B cells is permanent and cannot be restored upon incubation with medium over 48 h [14]. This is confirmed by the present work in which RPMI control data of CD40 and BCR co-stimulation experiments after 48 h incubation are still reduced in SLE as well as RA and pSS B cells compared to HDs.

Furthermore, it has been reported that continuous signaling via the phosphatases SHIP-1 and SHP-1 is required to maintain anergy [287, 292]. Within this study, we demonstrated enhanced recruitment of SHP-1 to CD22, a negative regulator of BCR downstream signaling, and thus, involved in maintaining low BCR responsiveness, as a commonality among SLE, RA and pSS B cells. Moreover, B cells in GC were found to display reduced BCR signaling, which is maintained by SHP-1 and SHIP-1 activity, as well as increased colocalization of SHP-1 with the BCR after activation [250]. These results indicate that BCR signaling is downmodulated at some point after B cell activation. Following this, post-activation and functional anergy might be characterized by a reduced BCR signaling in peripheral and tissue resident $CD27^+$ memory B cells of autoimmune diseases, such as SLE, RA and pSS. One possible way of inducing this dysfunction in HD B cells is chronic BCR stimulation by self-antigens or immune complexes without an appropriate co-stimulation. However, this study indicates that B cells from patients with SLE, RA and pSS are in a regulated state of low responsiveness. Of note, BCR signaling seems to be crucial for this state of ‘post-activation’, since TLR9 stimulation via CpG alone could not induce low BCR responsiveness in HD B cells. However, decreased TLR9 activation was observed, indicating that also this pathway is controlled during the state of B cell ‘post-activation’.

In addition, B cells expressing *IGVH4-34* gene are suggested to be anergic, because they fail to induce $Ca^{2+}$ upon BCR stimulation [293], which is accompanied by increased pERK1/2($T^{202}/Y^{204}$) expression also observed in autoimmune type #4 M-CLL patient’s B cells [259-261]. However, the analysis of pERK1/2($T^{202}/Y^{204}$) expression in SLE and RA $CD27^-$ B cells and $CD27^+$ memory B cells revealed comparability to HD cells indicating that pERK1/2($T^{202}/Y^{204}$) expression is not a suitable marker for ‘post-activation’.

## 7.5 Lymphocyte Hyporesponsiveness in Autoimmune Diseases is not Restricted to B Cells

Within the presented study global PTP/PSP activities and expression of selected PTPs and PSPs of T cells were investigated as a control to proof B cell specificity of the results. Indeed, PTP and PSP activities of SLE, RA and pSS T cells were found comparable to HD and PTP/PSP genes exhibited only marginal differential expression in SLE indicating normal T cell function. Interestingly, T cell hyporesponsiveness has been reported in SLE, RA and pSS. In detail, responses of SLE $CD8^+$ T cells upon viral antigens are defective due to loss of the protein signaling lymphocytic activation molecule family member 7 (SLAMF7) [294, 295]. McKinney *et al*. found $CD8^+$ T cell exhaustion to be characterized by low IL-7R and enhanced PD-1 expression in virus infections and SLE [296]. Tsokos and colleagues found that T cells from SLE have functional abnormalities including impaired CD3ζ–zeta chain of TCR associated protein kinase 70 (ZAP-70) signaling, as well as transcriptional changes of serine/threonine-protein phosphatase 2A (PP2A) and reduced IL-2 and inversely increased IL-17 expression [297, 298]. T cells in the synovium of inflamed joints of RA patients display severe hyporesponsiveness to antigenic stimulation characterized by impaired phosphorylation of the TCR downstream molecule adaptor protein linker for activation of T cells (LAT) due to oxidative stress [299]. In pSS, reduced $T_{H1}$ and $T_{H2}$ $Ca^{2+}$ responses are reported indicating a state of sustained reactivity possibly due to ongoing immune response [300]. Thus, there might be distinctive mechanisms for dysbalanced functions between B and T cells in these diseases.

## 7.6 Reduced BCR Signaling Can Play a Pathogenic Role in the Development, Maintenance and Progression of Autoimmunity

BCR signaling quality is an essential key point for B cell fate and BCR hypersensitivity or hyperresponsiveness is considered a major driver of tolerance brake and maintenance of autoimmunity [15-17, 301]. This is contrary to the observed BCR hyporesponsiveness within the presented study. However, the development and progression of autoimmunity has been linked to reduced BCR signaling, too [302, 303]. This could be experimentally demonstrated in a diabetes mouse model in which Syk was replaced by the less active Syk-related protein kinase Zap-70 in B cells, leading to disease development. The authors hypothesized that reduced BCR signal transduction allows for positive selection of auto- or polyreactive B cell clones and their survival due to chronic autoantigen stimulation [302]. In this context, Schickel *et al*. demonstrated that inhibition of PTPN22 could reset central B cell tolerance in non-obese diabetic scid gamma (NSG) mice which were engrafted with human hematopoietic stem cells carrying a gain-of-function mutation of *PTPN22* [303]. This indicates that B cell hyporesponsiveness in autoimmune patients may promote persistence of autoreactive cells due to a lower susceptibility to BCR-dependent elimination.

## 7.7 CD40 Co-Stimulation is a Critical Activator of 'Post-Activated B Cells in SLE, RA and pSS

This study demonstrated, that 'post-activated' B cells from SLE, RA and pSS patients are sensitive to T cell help induced co-stimulation. Increase of BCR signaling and B cell proliferation could be induced by CD40 co-stimulation. Furthermore, T cell help by CD40/IL-4R stimulation resulted in a reduced expression of PTPs, like *PTPN22*, in B cells. These results may reflect a more persistent stimulation of B cells by $T_{FH}$ cells. The latter one show enhanced expression in SLE, which positively correlate with SLEDAI, serum IgG, ANA and anti-dsDNA antibody titers [304-307]. Upregulation of CD40 gene expression in *PTPN22* risk gene carriers is also consistent with the idea that this pathway is critical for regulating the overly active immune system in autoimmunity [308]. Consistent with a prior study showing that naive and memory B cell compartments fuel the pool of circulating ASCs in SLE due to abnormal GC reaction [309], our study provides insights that this may be related to an increased susceptibility of 'post-activated' SLE $CD27^-$ naive B cells to T cell help. Xu *et al*. found that *in vitro* blocking of the T/B interaction by anti-CD40L led to decreased antibody production [307]. Furthermore, Rao *et al*. reported an expanded population of non-exhausted 'peripheral helper' T ($T_{PH}$) cells characteristically expressing PD-$1^{hi}CXCR5^-CD4^+$ in RA synovium [310]. Those $T_{PH}$ cells are thought of playing a pathogenic role in promoting B cell responses and antibody production within inflamed tissues and were recently found to correlated with severity of SLE. [310, 311]. The importance of T cell help in autoimmunity is further emphasized by a gene set analysis of naive B cells from RA synovial tissues revealed that CD40L responsive genes are significantly enriched [312]. In addition, it was recently demonstrated that IL-21 promotes $CD11c^{hi}$T-$bet^+$ B cell development, which are enriched for autoreactive cells in SLE [264]. Thus, it is very likely that CD40 is a critical context-dependent co-stimulatory molecule for the regulation of full BCR-dependent B cell activation. Autoreactive B cells (*i.e*. 9G4 B cells) are physiologically eliminated during the early stages of the GC reaction, potentially by anergic responses of the BCR. However, it is hypothesized that cells might escape this anergic stage and progress to memory and plasma cells [293]. In line with this, the data presented in this study as well as the discussed data of increased T cell help in autoimmunity (see above), pointing in the direction that abnormal CD40 stimulation of anergic SLE 9G4 B cells may let these cells pass this checkpoint. The presented result that CD40 co-stimulation can render BCR susceptibility of autoimmune disease 'post-activated' B cells and CD40 co-stimulation of SLE B cells diminished the expression of *e.g.* PTPN22 further support that modulation of the CD40 pathway is of critical importance.

## 7.8 Implications for Therapeutic Approaches

B cell directed therapies such as rituximab and belimumab have been approved and underscore the role of B cells in these diseases [10, 196, 313, 314]. Given that reduced BCR signaling promotes autoimmunity [302, 303], depletion of 'post-activated' B cells appears to be of therapeutic benefit in autoimmune diseases. Belimumab targets the B cell lineage survival factor BAFF and mainly depletes $CD27^-$ naive B cells which includes 'post-activated' $CD27^-$ B cells in SLE [10, 48, 196]. However, memory B cells are not depleted and IgG autoantibody production is not affected by belimumab

treatment [10, 196]. Anti-CD20 Rituximab therapy depletes peripheral B cells [10]. First, immature B cells repopulate the periphery, followed by plasma cells and naive B cells [315]. However, repopulation of $CD27^+$ memory B cells is delayed. This could imply that rituximab successfully depletes 'post-activated' $CD27^+$ memory B cells. In this context, relapse of SLE after autologous stem cell transplantation has been linked to prior recurrence of memory B cells [316]. Of note, targeting CD22 by the therapeutic anti-CD22 antibody epratuzumab was thought to raise the threshold of BCR activation by increasing SHP-1 activity and inhibiting Syk phosphorylation [110]. However, epratuzumab did not show efficacy in phase III clinical trial [317]. This is likely related to B cell 'post-activation' of autoimmune disease B cells. As 'post-activation' is characterized with low BCR induced Syk phosphorylation, autoimmune disease B cells are not further accessible to CD22-induced inhibition.

The current results implicate that CD40 co-stimulation is critical for activation of 'post-activated' B cells in autoimmune diseases such as SLE, RA and pSS. Accordingly, blocking CD40/CD40L interaction could be of therapeutic benefit. Indeed, a therapeutic anti-CD40L antibody was tested and was able to prohibit plasma cell and plasmablasts generation in SLE patients [318]. In addition, anti-CD40L antibody improved SLEDAI score, reduced proteinuria and anti-dsDNA antibodies and increased serum-C3 concentrations. However, clinical trials had to be stopped during phase I/II because of serious Fc-related complications [319] and thrombotic effects [320]. Nevertheless, the therapeutic approach is still under research and a monoclonal antibody with a PEGylated Fc part is currently under clinical development for SLE [321]. Besides positive effects of the anti-CD40L antibody in SLE, data presented and discussed in this work, implicate that beneficial effects of this therapy might also help in other autoimmune diseases like RA and pSS.

## 7.9 Outlook

A deeper understanding of how 'post-activation' is regulated by phosphatases may open new perspectives for the treatment of B cells in autoimmune diseases (**Figure 23**). The dysbalance of BCR downstream kinase phosphorylation in autoimmune diseases is contradictory as Akt phosphorylation depends on Syk activity but does not translate signaling strength. Furthermore, it is reported that Akt feedback mechanisms in GC may negatively regulates BCR responses [322, 323]. Even though PSP activities were found increased in SLE $CD19^+$ B cells, this points into an alternative regulation pathway of Akt signaling. This may be directed by PTEN and SHIP which play a role in anergy maintenance and control of GC B cells responsiveness [287, 292, 322-324]. Increased PTEN expression is associated with low PI(3,4,5)P3 production and may contribute to reduced BCR induced $Ca^{2+}$ signals [292]. Reversely, the depletion of PTEN results in increased $Ca^{2+}$ signals and anergy disruption and tolerance breakdown [291]. SHIP-1 counterbalances PTEN activity by dephosphorylating PTEN generated PI(3,4,5)P3. After BCR engagement it is recruited to the inhibitory co-receptor in a Syk depended manner [325]. Furthermore, PTEN controls GC reaction by regulating the expression of IgD BCR [324] which regulates IgM-induced anergy response in transitional and mature B cells [326]. This and the fact that the composition of $CD27^-$ isotype switched B cells or switched and non-switched $CD27^+$ memory B cells, which were not analyzed in the presented study, can differ among autoimmune patients and

HD underlines the importance of analyzing isotype and subset specific signaling abnormalities in autoimmune diseases [327]. Furthermore, the role of IgA positive B cells is of great interest as around 58 % of plasma blast are $IgA^+$ indicating overactive involvement of the mucosomal immune system [328].

Another field of interest may be checkpoint molecules such as cytotoxic T-lymphocyte-associated protein 4 (CTLA-4), B- and T-lymphocyte attenuator (BTLA) and PD-1. Blockade of CTLA-4 and PD-1 was successful in antitumor therapy [329]. However, side effects such as autoimmune inflammation indicate a molecular switch between developing cancer or autoimmunity [329]. Checkpoint molecules, such as PD-1, can contain ITIM motifs recruiting downstream PTPs such as SHP-1 or SHP-2 to fulfil their negative regulating functions [329] (**Figure 23**). However, no direct interaction of CTLA-4 and SHP-1 was found [330]. Notably, PD-1 has been reported of being increased among SLE B cells and may cause ‘post-activation’ [331]. Furthermore, PD-1 expression and the expression of its ligands, PD-L1 and PD-L2, have been linked to TLR and type I interferon pathways and maybe to aryl hydrocarbon receptor (AhR) pathways [332]. It is reported that PD-1 blockade can recover functionally impaired hepatitis B-specific B cells in chronic hepatitis B infection [333]. Thus, indicating a potential mechanism to release ‘post-activated’ B cells from their reduced functionality.

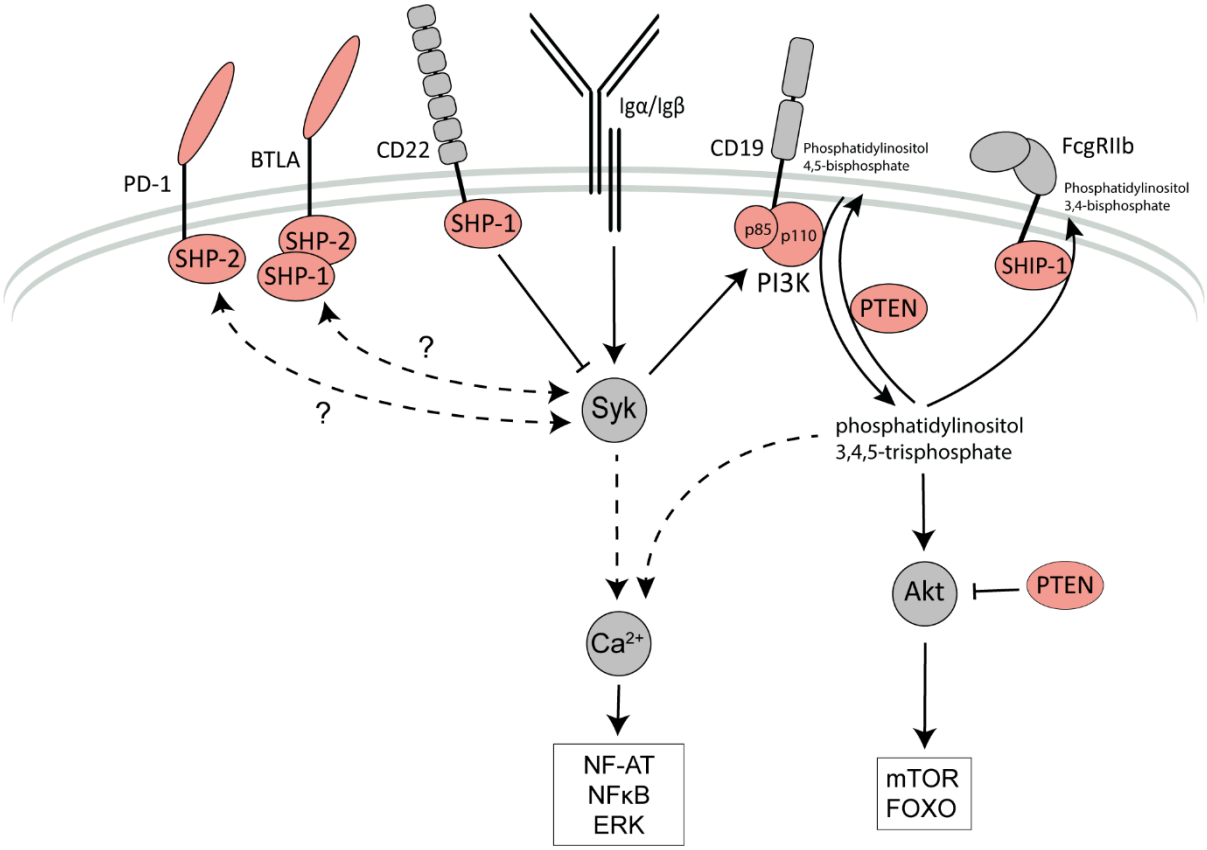


**Figure 23: A complex interplay of phosphatases and kinases regulates BCR signaling.** Syk phosphorylation is counterbalanced by the negative feedback loop of SHP-1 recruitment to the ITIM region of the co-receptor CD22 [105, 106]. Akt phosphorylation is induced after BCR engagement via Syk activity [95, 99]. The activity of Akt is balanced by a complex interplay of PI3K, PTEN and SHIP-1 activity, which regulate the balance of phosphatidylinositol-4,5-biphosphate, phosphatidylinositol-3,4,5-triphosphate and phosphatidylinositol-3,4-biphosphate [291, 292]. Checkpoint molecules such as PD-1 and BTLA recruit the phosphatases SHP-1 and SHP-2 [329] and may play a role in the modulation of BCR downstream signaling. Finally, $Ca^{2+}$- and Akt-dependent transcription factors, such as NF-AT, NFκB, ERK, mechanistic target of rapamycin (mTOR) and forkhead box protein O (FOXO), become active in dependence of the signal strength [100, 101, 139, 140].

A potential target for SHP-1 analysis is tyrosine residue $Y^{564}$, which is indispensable for maximal phosphatase activity and gets phosphorylated by Lyn upon DNA damage [334, 335]. Lyn also translate early BCR signaling events indicating that BCR engagement promotes SHP-1($Y^{564}$) phosphorylation. Indeed, pilot experiments on SHP-1($Y^{564}$) phosphorylation upon anti-IgG/IgM stimulation demonstrated that SHP-1($Y^{564}$) gets phosphorylated in $CD27^-$ B cells and $CD27^+$ memory B cells from HDs. Thus, higher activity in $CD27^+$ memory B cells making this phosphatase interesting as a target for further analysis (**Figure 24**).

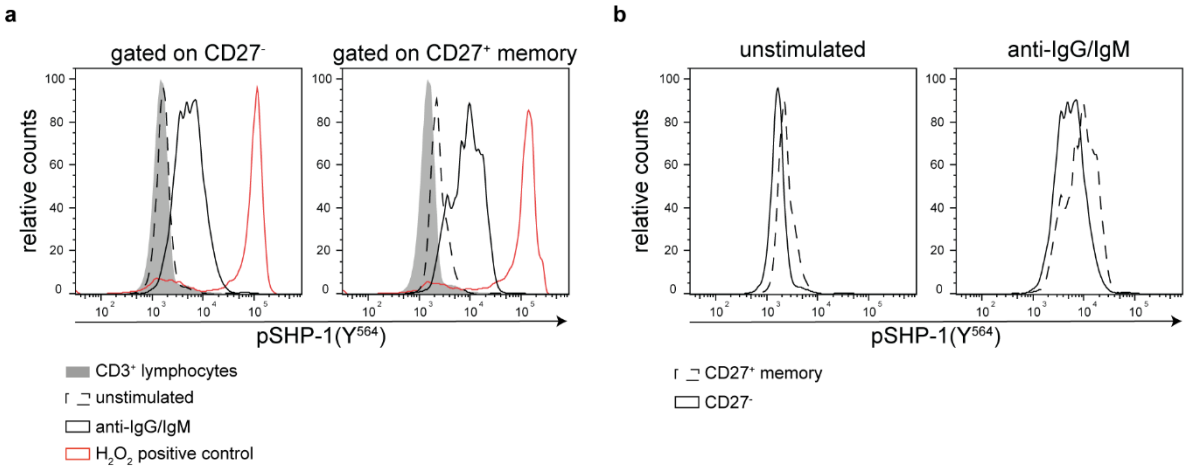


**Figure 24: Enhanced phosphorylation of SHP-1(Y$^{564}$) after BCR stimulation in CD27$^-$ and CD27$^+$ memory B cells.** PBMCs were stimulated with anti-IgG/IgM for 5 min. (**a**) Phospho-SHP-1 in CD27$^-$ (left) and CD27$^+$ memory (right) B cells after anti-IgG/IgM stimulation (solid line) *versus* unstimulated control (dashed line). Unstimulated CD3$^+$ lymphocides (grey area) and $H_2O_2$ (red line) were used as a secondary negative control and a positive control, respectively. (**b**) Baseline phosphorylation (left) and anti-IgG/IgM stimulation (right) in CD27$^-$ B cells (solid line) and CD27$^+$ memory B cells (dashed line).

PI3K consists of a regulatory and a catalytic subunit. PI3CD and PI3K p85 are mainly expressed in lymphoid cells. Phosphorylation of the catalytic PI3CD(Y$^{524}$) as well as regulatory PI3K p85(Y$^{467}$) subunit are connected to enzyme activity. Also, the regulatory subunit p55(Y$^{199}$), which is expressed in lymphoid cells, detects enzyme activity. However, phosphorylation after BCR engagement has not been analyzed in the available literature. Both subunits, PI3CD(Y$^{524}$) and p85(Y$^{467}$)/p55(Y$^{199}$), were found to be phosphorylated after BCR as well as $H_2O_2$ positive control stimulation in CD27$^-$ B cells and CD27$^+$ memory B cells compared to unstimulated control. These preliminary experiments indicate comparable phosphorylation of CD27$^-$ B cells and CD27$^+$ memory B cells (**Figure 25**).

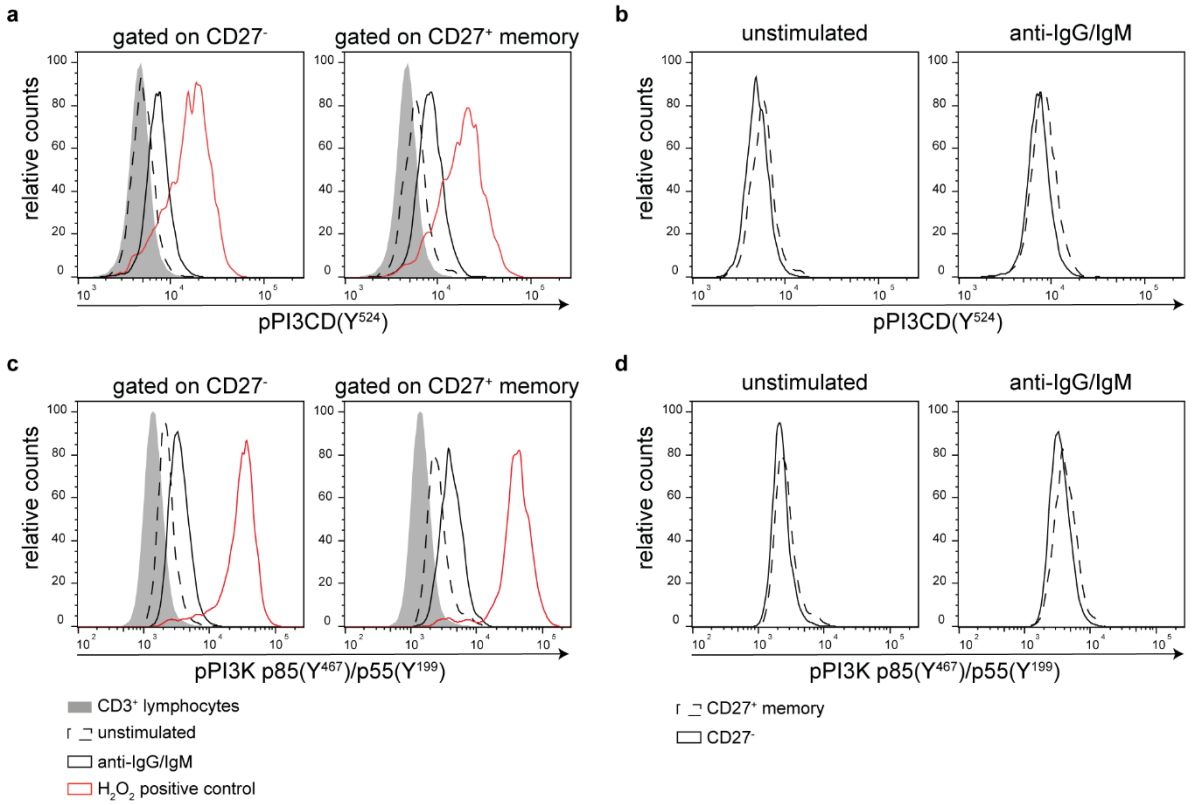


**Figure 25: Enhanced phophorylatio of the PI3K subunits PI3CD(Y$^{524}$) and p85(Y$^{467}$)/p55(Y$^{199}$) in CD27$^-$ B cells and CD27$^+$ memory B cells.** PBMCs were stimulated with anti-IgG/IgM for 5 min. (**a**) Phospho-PI3CD(Y$^{524}$) in CD27$^-$ B cells (left) and CD27$^+$ memory B cells (right) upon stimulation with anti-IgG/IgM (solid line) and unstimulated (dashed line). Grey area represents CD3$^+$ lymphocytes and the red line indicates $H_2O_2$ positive control. (**b**) Phosphorylation of PI3CD(Y$^{524}$) in CD27$^-$ B cells (solid line) and CD27$^+$ memory B cells (dashed line) under unstimulated (left) and stimulated (right) conditions. (**c**) PI3K p85(Y$^{467}$)/p55(Y$^{199}$) phosphorylation was analyzed under the same experimental conditions. Stimulation (solid line) and unstimulated (dashed line) conditions of CD27$^-$ B cells (left) and CD27$^+$ memory B cells (right) as well as CD3$^+$ lymphocytes (grey area) and $H_2O_2$ positive control are shown. (**d**) Comparison of CD27$^-$ B cells (solid line) and CD27$^+$ memory B cells (dashed line) under unstimulated and stimulated conditions.

In these preliminary studies, commercially available SHP-1(Y$^{564}$) and PI3K p85(Y$^{467}$)/p55(Y$^{199}$) antibodies were labeled with AF488. However, a lack of labeling efficiency, and therefore, a lack of functional antibody for flowcytometric analysis makes the development of new tools or antibodies indispensable for detailed analysis.

Furthermore, a deeper understanding of signaling crosstalk between the BCR and CD40 pathway may shed light on how T cell help can activate ‘post-activated’ B cells in autoimmunity. This crosstalk involves MAPK signaling in addition to NFκB signaling. An interesting target would be ERK, as BCR induced ERK phosphorylation is enhanced by CD40 treatment [336]. Further targets of interest involve DOCK8 and TRAF-2 [59]. TRAF-2(Y$^{484}$) phosphorylation is thought to be crucial for BCR and CD40 synergy and enhancement of the CD40 [27, 337]

# 8 Conclusion

In contrast to the generally accepted concept of hyperreactive BCR signaling in autoimmune diseases [15, 16, 225], this study provides evidence on a commonly reduced BCR signal, measured by Syk($Y^{352}$) and Btk($Y^{223}$) phosphorylation, in autoimmune diseases such as SLE, RA and pSS. This signaling abnormality is characteristic of $CD27^+$ memory B cells, but not $CD27^-$ B cells except for SLE. B cells from SLE patients exhibited the strongest phenotype with reduced BCR signaling in $CD27^+$ memory B cells and $CD27^-$ B cells. Interestingly, this signaling abnormality does not extend to Akt signaling, which was found normal in RA and pSS, as well as increased in SLE B cells. These results indicate a complex and differential regulation of BCR downstream signaling pathways. As a potential mechanism, constitutively increased recruitment of SHP-1 to the negative co-receptor CD22 in SLE, RA and pSS B cells may result in increased dephosphorylation of Syk tyrosine residues. The strong phenotype observed in SLE can be explained by maximal SHP-1/CD22 co-localization together with increased PTP activities, which were uniquely found in SLE together with increased PSP activities. Notably, the amplitude of BCR signaling in autoimmune disease $CD27^+$ memory B cells was comparable to $CD27^-$ B cells, indicating naive-like signaling properties. Importantly, reduced BCR signaling of autoimmune disease B cells is not restricted to peripheral B cells but was also found in tissue resident B cells from ITP spleens and pSS parotid gland. Moreover, B cell hyporesponsiveness towards TLR9 signals was also observed in peripheral B cells from SLE, RA and pSS with reduced proliferation and differentiation into ASCs. This abnormality is potentially linked to BCR hyporesponsiveness via Syk activity. Those B cell abnormalities are likely to reflect continuous stimulation through the BCR *in vivo* without appropriate co-stimulation. and therefore, reflect a status of ‘post-activation’ which is functionally comparable but not identical to anergy. CD40 co-stimulation resulted in a gain-of-responsiveness towards BCR stimulation and increased B cell proliferation. The analysis of PTP expression under CD40/IL-4R stimulation and unstimulated conditions was analyzed in two SLE patients and one HD as a proof of concept. This analysis found that co-stimulation reduced gene expression of PTPs such as *PTPN22* in SLE.

Taken together, this study found peripheral as well as tissue resident $CD27^+$ memory B cells in autoimmune diseases remain in ‘post-activation’ with impaired BCR and TLR9 responsiveness. The more extensive ‘post-activation’ status in SLE B cells is possibly related to stronger negative regulation by increased phosphatase activity. This ‘post-activation’ functionally related to anergy likely owing to *in vivo* engagement of the BCR without appropriate T cell-derived co-stimulation. CD40 stimulation of B cells appears to be key for B cell activation in the autoimmune milieu in such a way that it improves BCR responses and is critical to overcome ‘post-activation’. The presented findings support the idea that CD40/CD40L interaction is of clinical relevance and the investigation of therapeutic options interfering with this pathway to foster functional B cell anergy and decreased disease activity.

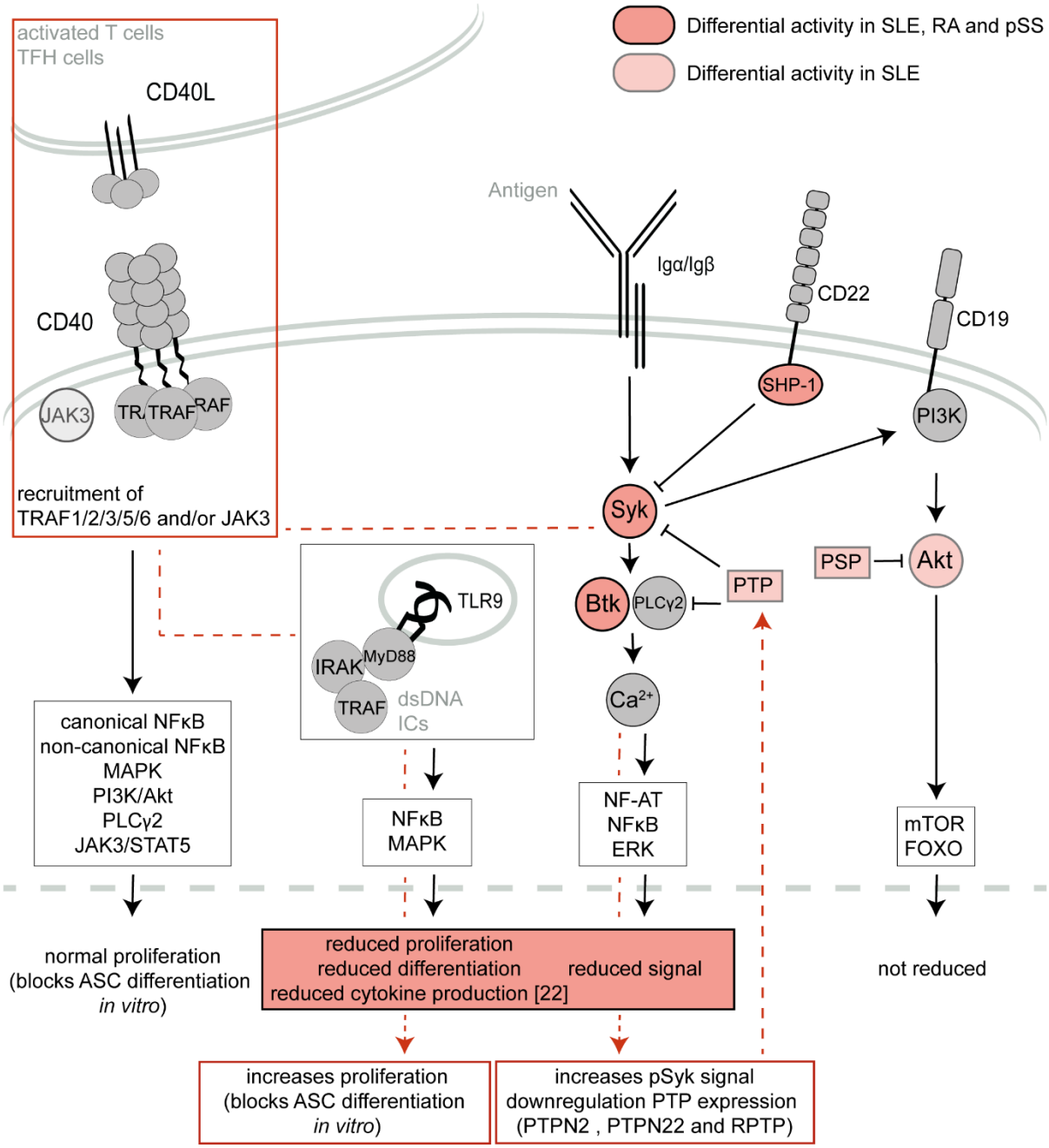


**Figure 26: Reduced BCR and TLR9 responsiveness can be overcome by CD40 co-stimulation.** Overview of the analyzed signaling pathways. Molecules which were found with differential activity in all three autoimmune diseases are highlighted in red. Molecules which were found with differential activity in SLE only are highlighted in light red. BCR engagement in autoimmune diseases leads to reduced phosphorylation of the downstream signaling kinases Syk and Btk potentially leading to reduced $Ca^{2+}$ flux and $Ca^{2+}$-dependent transcription. However, BCR-dependent Akt signaling, which is normal in RA and pSS and increased in SLE, is not affected by reduced Syk phosphorylation. These abnormalities are accompanied by increased PTP/PSP activity in SLE and increased recruitment of SHP-1 to CD22 in SLE, RA and pSS indicating a potential regulatory mechanism. TLR9 induced proliferation, differentiation and cytokine production [22] is reduced in autoimmune diseases, which is potentially connected to a general reduced Syk activity. However, CD40 does not show any abnormality in terms of reduced signaling and is able to overcome or increase the reduced responsiveness by the BCR and TLR9.

# 9 Literature


1. Cervera, R., et al., *Morbidity and mortality in systemic lupus erythematosus during a 10-year period: a comparison of early and late manifestations in a cohort of 1,000 patients.* Medicine (Baltimore), 2003. **82**(5): p. 299-308.
2. Dorner, T., C. Giesecke, and P.E. Lipsky, *Mechanisms of B cell autoimmunity in SLE.* Arthritis Res Ther, 2011. **13**(5): p. 243.
3. Buch, M.H., et al., *Updated consensus statement on the use of rituximab in patients with rheumatoid arthritis.* Ann Rheum Dis, 2011. **70**(6): p. 909-20.
4. Looney, R.J., et al., *B cell depletion as a novel treatment for systemic lupus erythematosus: a phase I/II dose-escalation trial of rituximab.* Arthritis Rheum, 2004. **50**(8): p. 2580-9.
5. Tony, H.P., et al., *Safety and clinical outcomes of rituximab therapy in patients with different autoimmune diseases: experience from a national registry (GRAID).* Arthritis Res Ther, 2011. **13**(3): p. R75.
6. Devauchelle-Pensec, V., et al., *Improvement of Sjogren's syndrome after two infusions of rituximab (anti-CD20).* Arthritis Rheum, 2007. **57**(2): p. 310-7.
7. Devauchelle-Pensec, V., et al., *Effects of rituximab therapy on quality of life in patients with primary Sjogren's syndrome.* Clin Exp Rheumatol, 2011. **29**(1): p. 6-12.
8. Dass, S., et al., *Reduction of fatigue in Sjogren syndrome with rituximab: results of a randomised, double-blind, placebo-controlled pilot study.* Ann Rheum Dis, 2008. **67**(11): p. 1541-4.
9. Meijer, J.M., et al., *Effectiveness of rituximab treatment in primary Sjogren's syndrome: a randomized, double-blind, placebo-controlled trial.* Arthritis Rheum, 2010. **62**(4): p. 960-8.
10. Hofmann, K., A.K. Clauder, and R.A. Manz, *Targeting B Cells and Plasma Cells in Autoimmune Diseases.* Front Immunol, 2018. **9**: p. 835.
11. Vaughn, S.E., et al., *Genetic susceptibility to lupus: the biological basis of genetic risk found in B cell signaling pathways.* J Leukoc Biol, 2012. **92**(3): p. 577-91.
12. Deng, Y. and B.P. Tsao, *Advances in lupus genetics and epigenetics.* Curr Opin Rheumatol, 2014. **26**(5): p. 482-92.
13. Zikherman, J. and A. Weiss, *Antigen receptor signaling in the rheumatic diseases.* Arthritis Res Ther, 2009. **11**(1): p. 202.
14. Fleischer, S.J., et al., *Enhanced Tyrosine Phosphatase Activity Underlies Dysregulated B Cell Receptor Signaling and Promotes Survival of Human Lupus B Cells.* Arthritis Rheumatol, 2016. **68**(5): p. 1210-21.
15. Liossis, S.N., et al., *B cells from patients with systemic lupus erythematosus display abnormal antigen receptor-mediated early signal transduction events.* J Clin Invest, 1996. **98**(11): p. 2549-57.
16. Wu, X.N., et al., *Defective PTEN regulation contributes to B cell hyperresponsiveness in systemic lupus erythematosus.* Sci Transl Med, 2014. **6**(246): p. 246ra99.
17. Casola, S., et al., *B cell receptor signal strength determines B cell fate.* Nat Immunol, 2004. **5**(3): p. 317-27.
18. Paus, D., et al., *Antigen recognition strength regulates the choice between extrafollicular plasma cell and germinal center B cell differentiation.* J Exp Med, 2006. **203**(4): p. 1081-91.
19. Krautler, N.J., et al., *Differentiation of germinal center B cells into plasma cells is initiated by high-affinity antigen and completed by Tfh cells.* J Exp Med, 2017. **214**(5): p. 1259-1267.
20. Shinnakasu, R. and T. Kurosaki, *Regulation of memory B and plasma cell differentiation.* Curr Opin Immunol, 2017. **45**: p. 126-131.
21. Metzler, G., N.S. Kolhatkar, and D.J. Rawlings, *BCR and co-receptor crosstalk facilitate the positive selection of self-reactive transitional B cells.* Curr Opin Immunol, 2015. **37**: p. 46-53.
22. Sieber, J., et al., *Active systemic lupus erythematosus is associated with a reduced cytokine production by B cells in response to TLR9 stimulation.* Arthritis Res Ther, 2014. **16**(6): p. 477.
23. Gies, V., et al., *Impaired TLR9 responses in B cells from patients with systemic lupus erythematosus.* JCI Insight, 2018. **3**(5).
24. Ginsburg, W.W., F.D. Finkelman, and P.E. Lipsky, *Circulating and pokeweed mitogen-induced immunoglobulin-secreting cells in systemic lupus erythematosus.* Clin Exp Immunol, 1979. **35**(1): p. 76-88.
25. Suthers, A.N. and S. Sarantopoulos, *TLR7/TLR9- and B Cell Receptor-Signaling Crosstalk: Promotion of Potentially Dangerous B Cells.* Front Immunol, 2017. **8**: p. 775.

26. Kurosaki, T., K. Kometani, and W. Ise, *Memory B cells.* Nat Rev Immunol, 2015. **15**(3): p. 149-59.
27. Ying, H., et al., *Syk mediates BCR- and CD40-signaling integration during B cell activation.* Immunobiology, 2011. **216**(5): p. 566-70.
28. Parkin, J. and B. Cohen, *An overview of the immune system.* Lancet, 2001. **357**(9270): p. 1777-89.
29. Marshall, J.S., et al., *An introduction to immunology and immunopathology.* Allergy Asthma Clin Immunol, 2018. **14**(Suppl 2): p. 49.
30. Konig, J., et al., *Human Intestinal Barrier Function in Health and Disease.* Clin Transl Gastroenterol, 2016. **7**(10): p. e196.
31. Prescott, S.L., et al., *The skin microbiome: impact of modern environments on skin ecology, barrier integrity, and systemic immune programming.* World Allergy Organ J, 2017. **10**(1): p. 29.
32. Mathieu, E., et al., *Paradigms of Lung Microbiota Functions in Health and Disease, Particularly, in Asthma.* Front Physiol, 2018. **9**: p. 1168.
33. Hoffman, W., F.G. Lakkis, and G. Chalasani, *B Cells, Antibodies, and More.* Clin J Am Soc Nephrol, 2016. **11**(1): p. 137-54.
34. Gao, Y. and A.P. Williams, *Role of Innate T Cells in Anti-Bacterial Immunity.* Front Immunol, 2015. **6**: p. 302.
35. Cerutti, A., M. Cols, and I. Puga, *Marginal zone B cells: virtues of innate-like antibody-producing lymphocytes.* Nat Rev Immunol, 2013. **13**(2): p. 118-32.
36. Krishnan, C. and M.H. Kaplan, *Immunopathologic studies of systemic lupus erythematosus. II. Antinuclear reaction of gamma-globulin eluted from homogenates and isolated glomeruli of kidneys from patients with lupus nephritis.* J Clin Invest, 1967. **46**(4): p. 569-79.
37. Davies, K.A., et al., *Immune complex processing in patients with systemic lupus erythematosus. In vivo imaging and clearance studies.* J Clin Invest, 1992. **90**(5): p. 2075-83.
38. Schellekens, G.A., et al., *Citrulline is an essential constituent of antigenic determinants recognized by rheumatoid arthritis-specific autoantibodies.* J Clin Invest, 1998. **101**(1): p. 273-81.
39. Walker, D.J., et al., *Rheumatoid factor tests in the diagnosis and prediction of rheumatoid arthritis.* Ann Rheum Dis, 1986. **45**(8): p. 684-90.
40. Kraan, M.C., et al., *Asymptomatic synovitis precedes clinically manifest arthritis.* Arthritis Rheum, 1998. **41**(8): p. 1481-8.
41. Cornec, D., et al., *B cells in Sjogren's syndrome: from pathophysiology to diagnosis and treatment.* J Autoimmun, 2012. **39**(3): p. 161-7.
42. Huang, Y.F., et al., *The immune factors involved in the pathogenesis, diagnosis, and treatment of Sjogren's syndrome.* Clin Dev Immunol, 2013. **2013**: p. 160491.
43. Nikolov, N.P. and G.G. Illei, *Pathogenesis of Sjogren's syndrome.* Curr Opin Rheumatol, 2009. **21**(5): p. 465-70.
44. ter Borg, E.J., et al., *Measurement of increases in anti-double-stranded DNA antibody levels as a predictor of disease exacerbation in systemic lupus erythematosus. A long-term, prospective study.* Arthritis Rheum, 1990. **33**(5): p. 634-43.
45. Arbuckle, M.R., et al., *Development of autoantibodies before the clinical onset of systemic lupus erythematosus.* N Engl J Med, 2003. **349**(16): p. 1526-33.
46. Bendaoud, B., et al., *IgA-containing immune complexes in the circulation of patients with primary Sjogren's syndrome.* J Autoimmun, 1991. **4**(1): p. 177-84.
47. Scofield, R.H., et al., *Fine specificity of the autoimmune response to the Ro/SSA and La/SSB ribonucleoproteins.* Arthritis Rheum, 1999. **42**(2): p. 199-209.
48. Wahren-Herlenius, M. and T. Dorner, *Immunopathogenic mechanisms of systemic autoimmune disease.* Lancet, 2013. **382**(9894): p. 819-31.
49. Shen, P. and S. Fillatreau, *Antibody-independent functions of B cells: a focus on cytokines.* Nat Rev Immunol, 2015. **15**(7): p. 441-51.
50. Fillatreau, S., *Regulatory roles of B cells in infectious diseases.* Clin Exp Rheumatol, 2016. **34**(4 Suppl 98): p. 1-5.
51. Rosser, E.C. and C. Mauri, *Regulatory B cells: origin, phenotype, and function.* Immunity, 2015. **42**(4): p. 607-12.
52. Montecino-Rodriguez, E. and K. Dorshkind, *B-1 B cell development in the fetus and adult.* Immunity, 2012. **36**(1): p. 13-21.
53. Baumgarth, N., *The double life of a B-1 cell: self-reactivity selects for protective effector functions.* Nat Rev Immunol, 2011. **11**(1): p. 34-46.

54. Mebius, R.E. and G. Kraal, *Structure and function of the spleen.* Nat Rev Immunol, 2005. **5**(8): p. 606-16.
55. Steiniger, B., E.M. Timphus, and P.J. Barth, *The splenic marginal zone in humans and rodents: an enigmatic compartment and its inhabitants.* Histochem Cell Biol, 2006. **126**(6): p. 641-8.
56. Weller, S., et al., *Human blood IgM "memory" B cells are circulating splenic marginal zone B cells harboring a prediversified immunoglobulin repertoire.* Blood, 2004. **104**(12): p. 3647-54.
57. De Silva, N.S. and U. Klein, *Dynamics of B cells in germinal centres.* Nat Rev Immunol, 2015. **15**(3): p. 137-48.
58. Inoue, T., et al., *Generation of memory B cells and their reactivation.* Immunol Rev, 2018. **283**(1): p. 138-149.
59. Tangye, S.G., et al., *SnapShot: Interactions between B Cells and T Cells.* Cell, 2015. **162**(4): p. 926-6 e1.
60. Elgueta, R., et al., *Molecular mechanism and function of CD40/CD40L engagement in the immune system.* Immunol Rev, 2009. **229**(1): p. 152-72.
61. Crotty, S., *A brief history of T cell help to B cells.* Nat Rev Immunol, 2015. **15**(3): p. 185-9.
62. Belanger, S. and S. Crotty, *Dances with cytokines, featuring TFH cells, IL-21, IL-4 and B cells.* Nat Immunol, 2016. **17**(10): p. 1135-6.
63. Kuchen, S., et al., *Essential role of IL-21 in B cell activation, expansion, and plasma cell generation during CD4+ T cell-B cell collaboration.* J Immunol, 2007. **179**(9): p. 5886-96.
64. Nagumo, H., et al., *The different process of class switching and somatic hypermutation; a novel analysis by CD27(-) naive B cells.* Blood, 2002. **99**(2): p. 567-75.
65. Weisel, F.J., et al., *A Temporal Switch in the Germinal Center Determines Differential Output of Memory B and Plasma Cells.* Immunity, 2016. **44**(1): p. 116-130.
66. Klein, U., K. Rajewsky, and R. Kuppers, *Human immunoglobulin (Ig)M+IgD+ peripheral blood B cells expressing the CD27 cell surface antigen carry somatically mutated variable region genes: CD27 as a general marker for somatically mutated (memory) B cells.* J Exp Med, 1998. **188**(9): p. 1679-89.
67. Agematsu, K., et al., *CD27: a memory B-cell marker.* Immunol Today, 2000. **21**(5): p. 204-6.
68. Tangye, S.G., et al., *Identification of functional human splenic memory B cells by expression of CD148 and CD27.* J Exp Med, 1998. **188**(9): p. 1691-703.
69. Seifert, M., et al., *Functional capacities of human IgM memory B cells in early inflammatory responses and secondary germinal center reactions.* Proc Natl Acad Sci U S A, 2015. **112**(6): p. E546-55.
70. Tangye, S.G. and K.L. Good, *Human IgM+CD27+ B cells: memory B cells or "memory" B cells?* J Immunol, 2007. **179**(1): p. 13-9.
71. Fecteau, J.F., G. Cote, and S. Neron, *A new memory CD27-IgG+ B cell population in peripheral blood expressing VH genes with low frequency of somatic mutation.* J Immunol, 2006. **177**(6): p. 3728-36.
72. Weston-Bell, N., et al., *Defining origins of malignant B cells: a new circulating normal human IgM(+)D(+) B-cell subset lacking CD27 expression and displaying somatically mutated IGHV genes as a relevant memory population.* Leukemia, 2009. **23**(11): p. 2075-80.
73. Seifert, M. and R. Kuppers, *Molecular footprints of a germinal center derivation of human IgM+(IgD+)CD27+ B cells and the dynamics of memory B cell generation.* J Exp Med, 2009. **206**(12): p. 2659-69.
74. Sanz, I., et al., *Phenotypic and functional heterogeneity of human memory B cells.* Semin Immunol, 2008. **20**(1): p. 67-82.
75. Wehr, C., et al., *A new CD21low B cell population in the peripheral blood of patients with SLE.* Clin Immunol, 2004. **113**(2): p. 161-71.
76. Wei, C., et al., *A new population of cells lacking expression of CD27 represents a notable component of the B cell memory compartment in systemic lupus erythematosus.* J Immunol, 2007. **178**(10): p. 6624-33.
77. Jacobi, A.M., et al., *Activated memory B cell subsets correlate with disease activity in systemic lupus erythematosus: delineation by expression of CD27, IgD, and CD95.* Arthritis Rheum, 2008. **58**(6): p. 1762-73.
78. Rodriguez-Bayona, B., et al., *Decreased frequency and activated phenotype of blood CD27 IgD IgM B lymphocytes is a permanent abnormality in systemic lupus erythematosus patients.* Arthritis Res Ther, 2010. **12**(3): p. R108.
79. Tuaillon, E., et al., *Human milk-derived B cells: a highly activated switched memory cell population primed to secrete antibodies.* J Immunol, 2009. **182**(11): p. 7155-62.

80. McHeyzer-Williams, L.J., et al., *Class-switched memory B cells remodel BCRs within secondary germinal centers.* Nat Immunol, 2015. **16**(3): p. 296-305.
81. Giesecke, C., et al., *Simultaneous Presence of Non- and Highly Mutated Keyhole Limpet Hemocyanin (KLH)-Specific Plasmablasts Early after Primary KLH Immunization Suggests Cross-Reactive Memory B Cell Activation.* J Immunol, 2018.
82. Mei, H.E., et al., *A unique population of IgG-expressing plasma cells lacking CD19 is enriched in human bone marrow.* Blood, 2015.
83. Jacobi, A.M., et al., *Correlation between circulating CD27high plasma cells and disease activity in patients with systemic lupus erythematosus.* Arthritis Rheum, 2003. **48**(5): p. 1332-42.
84. Jacobi, A.M., et al., *HLA-DRhigh/CD27high plasmablasts indicate active disease in patients with systemic lupus erythematosus.* Ann Rheum Dis, 2010. **69**(1): p. 305-8.
85. Odendahl, M., et al., *Perturbations of peripheral B lymphocyte homoeostasis in children with systemic lupus erythematosus.* Ann Rheum Dis, 2003. **62**(9): p. 851-8.
86. Odendahl, M., et al., *Disturbed peripheral B lymphocyte homeostasis in systemic lupus erythematosus.* J Immunol, 2000. **165**(10): p. 5970-9.
87. Imkeller, K. and H. Wardemann, *Assessing human B cell repertoire diversity and convergence.* Immunol Rev, 2018. **284**(1): p. 51-66.
88. Schatz, D.G., *V(D)J recombination.* Immunol Rev, 2004. **200**: p. 5-11.
89. Collins, A.M. and C.T. Watson, *Immunoglobulin Light Chain Gene Rearrangements, Receptor Editing and the Development of a Self-Tolerant Antibody Repertoire.* Front Immunol, 2018. **9**: p. 2249.
90. Winkler, T.H. and I.L. Martensson, *The Role of the Pre-B Cell Receptor in B Cell Development, Repertoire Selection, and Tolerance.* Front Immunol, 2018. **9**: p. 2423.
91. Vieira, P. and K. Rajewsky, *The half-lives of serum immunoglobulins in adult mice.* Eur J Immunol, 1988. **18**(2): p. 313-6.
92. Amanna, I.J., N.E. Carlson, and M.K. Slifka, *Duration of humoral immunity to common viral and vaccine antigens.* N Engl J Med, 2007. **357**(19): p. 1903-15.
93. Manz, R.A., et al., *Survival of long-lived plasma cells is independent of antigen.* Int Immunol, 1998. **10**(11): p. 1703-11.
94. Manz, R.A., A. Thiel, and A. Radbruch, *Lifetime of plasma cells in the bone marrow.* Nature, 1997. **388**(6638): p. 133-4.
95. Rolli, V., et al., *Amplification of B cell antigen receptor signaling by a Syk/ITAM positive feedback loop.* Mol Cell, 2002. **10**(5): p. 1057-69.
96. Yang, J. and M. Reth, *Oligomeric organization of the B-cell antigen receptor on resting cells.* Nature, 2010. **467**(7314): p. 465-9.
97. Yang, J. and M. Reth, *The dissociation activation model of B cell antigen receptor triggering.* FEBS Lett, 2010. **584**(24): p. 4872-7.
98. Gold, M.R. and M.G. Reth, *Antigen Receptor Function in the Context of the Nanoscale Organization of the B Cell Membrane.* Annu Rev Immunol, 2019. **37**: p. 97-123.
99. Pogue, S.L., et al., *B cell antigen receptor-induced activation of Akt promotes B cell survival and is dependent on Syk kinase.* J Immunol, 2000. **165**(3): p. 1300-6.
100. Toapanta, F.R., P.J. Bernal, and M.B. Sztein, *Diverse phosphorylation patterns of B cell receptor-associated signaling in naive and memory human B cells revealed by phosphoflow, a powerful technique to study signaling at the single cell level.* Front Cell Infect Microbiol, 2012. **2**: p. 128.
101. Scharenberg, A.M., L.A. Humphries, and D.J. Rawlings, *Calcium signalling and cell-fate choice in B cells.* Nat Rev Immunol, 2007. **7**(10): p. 778-89.
102. Tedder, T.F., K.M. Haas, and J.C. Poe, *CD19-CD21 complex regulates an intrinsic Src family kinase amplification loop that links innate immunity with B-lymphocyte intracellular calcium responses.* Biochem Soc Trans, 2002. **30**(4): p. 807-11.
103. Walsh, C.M., et al., *Role of phosphoinositides in STIM1 dynamics and store-operated calcium entry.* Biochem J, 2009. **425**(1): p. 159-68.
104. Tsubata, T., *Ligand Recognition Determines the Role of Inhibitory B Cell Co-receptors in the Regulation of B Cell Homeostasis and Autoimmunity.* Front Immunol, 2018. **9**: p. 2276.
105. Nitschke, L., *The role of CD22 and other inhibitory co-receptors in B-cell activation.* Curr Opin Immunol, 2005. **17**(3): p. 290-7.
106. Nitschke, L., et al., *CD22 is a negative regulator of B-cell receptor signalling.* Curr Biol, 1997. **7**(2): p. 133-43.
107. Adachi, T., et al., *The B cell surface protein CD72 recruits the tyrosine phosphatase SHP-1 upon tyrosine phosphorylation.* J Immunol, 1998. **160**(10): p. 4662-5.

108. Parnes, J.R. and C. Pan, *CD72, a negative regulator of B-cell responsiveness.* Immunol Rev, 2000. **176**: p. 75-85.
109. Muller, J., et al., *CD22 ligand-binding and signaling domains reciprocally regulate B-cell Ca2+ signaling.* Proc Natl Acad Sci U S A, 2013. **110**(30): p. 12402-7.
110. Sieger, N., et al., *CD22 ligation inhibits downstream B cell receptor signaling and Ca(2+) flux upon activation.* Arthritis Rheum, 2013. **65**(3): p. 770-9.
111. Poe, J.C., et al., *CD22 regulates B lymphocyte function in vivo through both ligand-dependent and ligand-independent mechanisms.* Nat Immunol, 2004. **5**(10): p. 1078-87.
112. Alsadeq, A., et al., *The role of the Syk/Shp-1 kinase-phosphatase equilibrium in B cell development and signaling.* J Immunol, 2014. **193**(1): p. 268-76.
113. Baba, Y. and T. Kurosaki, *Impact of Ca2+ signaling on B cell function.* Trends Immunol, 2011. **32**(12): p. 589-94.
114. Baba, Y. and T. Kurosaki, *Physiological function and molecular basis of STIM1-mediated calcium entry in immune cells.* Immunol Rev, 2009. **231**(1): p. 174-88.
115. Healy, J.I. and C.C. Goodnow, *Positive versus negative signaling by lymphocyte antigen receptors.* Annu Rev Immunol, 1998. **16**: p. 645-70.
116. Goodnow, C.C., et al., *Self-tolerance checkpoints in B lymphocyte development.* Adv Immunol, 1995. **59**: p. 279-368.
117. Wardemann, H., et al., *Predominant autoantibody production by early human B cell precursors.* Science, 2003. **301**(5638): p. 1374-7.
118. Gay, D., et al., *Receptor editing: an approach by autoreactive B cells to escape tolerance. The Journal of Experimental Medicine. 1993. 177: 999-1008.* J Immunol, 2011. **186**(3): p. 1303-12.
119. Gay, D., et al., *Receptor editing: an approach by autoreactive B cells to escape tolerance.* J Exp Med, 1993. **177**(4): p. 999-1008.
120. Tiegs, S.L., D.M. Russell, and D. Nemazee, *Receptor editing in self-reactive bone marrow B cells.* J Exp Med, 1993. **177**(4): p. 1009-20.
121. Melamed, D., et al., *Developmental regulation of B lymphocyte immune tolerance compartmentalizes clonal selection from receptor selection.* Cell, 1998. **92**(2): p. 173-82.
122. Nemazee, D. and K. Buerki, *Clonal deletion of autoreactive B lymphocytes in bone marrow chimeras.* Proc Natl Acad Sci U S A, 1989. **86**(20): p. 8039-43.
123. Nemazee, D.A. and K. Burki, *Clonal deletion of B lymphocytes in a transgenic mouse bearing anti-MHC class I antibody genes.* Nature, 1989. **337**(6207): p. 562-6.
124. Wen, L., et al., *Evidence of marginal-zone B cell-positive selection in spleen.* Immunity, 2005. **23**(3): p. 297-308.
125. Benschop, R.J., et al., *Unique signaling properties of B cell antigen receptor in mature and immature B cells: implications for tolerance and activation.* J Immunol, 2001. **167**(8): p. 4172-9.
126. Gross, A.J., et al., *Developmental acquisition of the Lyn-CD22-SHP-1 inhibitory pathway promotes B cell tolerance.* J Immunol, 2009. **182**(9): p. 5382-92.
127. Yellen, A.J., et al., *Signaling through surface IgM in tolerance-susceptible immature murine B lymphocytes. Developmentally regulated differences in transmembrane signaling in splenic B cells from adult and neonatal mice.* J Immunol, 1991. **146**(5): p. 1446-54.
128. Hillion, S., et al., *Signaling pathways regulating RAG expression in B lymphocytes.* Autoimmun Rev, 2009. **8**(7): p. 599-604.
129. Benschop, R.J., et al., *Distinct signal thresholds for the unique antigen receptor-linked gene expression programs in mature and immature B cells.* J Exp Med, 1999. **190**(6): p. 749-56.
130. Bai, L., et al., *Phospholipase Cgamma2 contributes to light-chain gene activation and receptor editing.* Mol Cell Biol, 2007. **27**(17): p. 5957-67.
131. Hayashi, K., et al., *Impaired receptor editing in the primary B cell repertoire of BASH-deficient mice.* J Immunol, 2004. **173**(10): p. 5980-8.
132. Hillion, S., et al., *Interleukin-6 is responsible for aberrant B-cell receptor-mediated regulation of RAG expression in systemic lupus erythematosus.* Immunology, 2007. **122**(3): p. 371-80.
133. Hemon, P., et al., *Calcium Signaling: From Normal B Cell Development to Tolerance Breakdown and Autoimmunity.* Clin Rev Allergy Immunol, 2017. **53**(2): p. 141-165.
134. Sater, R.A., P.C. Sandel, and J.G. Monroe, *B cell receptor-induced apoptosis in primary transitional murine B cells: signaling requirements and modulation by T cell help.* Int Immunol, 1998. **10**(11): p. 1673-82.
135. King, L.B. and J.G. Monroe, *Immunobiology of the immature B cell: plasticity in the B-cell antigen receptor-induced response fine tunes negative selection.* Immunol Rev, 2000. **176**: p. 86-104.

136. Cyster, J.G., et al., *Regulation of B-lymphocyte negative and positive selection by tyrosine phosphatase CD45.* Nature, 1996. **381**(6580): p. 325-8.
137. Cornall, R.J., et al., *Polygenic autoimmune traits: Lyn, CD22, and SHP-1 are limiting elements of a biochemical pathway regulating BCR signaling and selection.* Immunity, 1998. **8**(4): p. 497-508.
138. Su, T.T., et al., *Signaling in transitional type 2 B cells is critical for peripheral B-cell development.* Immunol Rev, 2004. **197**: p. 161-78.
139. Healy, J.I., et al., *Different nuclear signals are activated by the B cell receptor during positive versus negative signaling.* Immunity, 1997. **6**(4): p. 419-28.
140. Dolmetsch, R.E., et al., *Differential activation of transcription factors induced by Ca2+ response amplitude and duration.* Nature, 1997. **386**(6627): p. 855-8.
141. Cantaert, T., et al., *Decreased somatic hypermutation induces an impaired peripheral B cell tolerance checkpoint.* J Clin Invest, 2016. **126**(11): p. 4289-4302.
142. Reed, J.H., et al., *Clonal redemption of autoantibodies by somatic hypermutation away from self-reactivity during human immunization.* J Exp Med, 2016. **213**(7): p. 1255-65.
143. Nossal, G.J. and B.L. Pike, *Evidence for the clonal abortion theory of B-lymphocyte tolerance.* J Exp Med, 1975. **141**(4): p. 904-17.
144. Yarkoni, Y., A. Getahun, and J.C. Cambier, *Molecular underpinning of B-cell anergy.* Immunol Rev, 2010. **237**(1): p. 249-63.
145. Conrad, F.J., J.S. Rice, and J.C. Cambier, *Multiple paths to loss of anergy and gain of autoimmunity.* Autoimmunity, 2007. **40**(6): p. 418-24.
146. Cooke, M.P., et al., *Immunoglobulin signal transduction guides the specificity of B cell-T cell interactions and is blocked in tolerant self-reactive B cells.* J Exp Med, 1994. **179**(2): p. 425-38.
147. Liubchenko, G.A., et al., *Potentially autoreactive naturally occurring transitional T3 B lymphocytes exhibit a unique signaling profile.* J Autoimmun, 2012. **38**(4): p. 293-303.
148. Allman, D., et al., *Resolution of three nonproliferative immature splenic B cell subsets reveals multiple selection points during peripheral B cell maturation.* J Immunol, 2001. **167**(12): p. 6834-40.
149. Duty, J.A., et al., *Functional anergy in a subpopulation of naive B cells from healthy humans that express autoreactive immunoglobulin receptors.* J Exp Med, 2009. **206**(1): p. 139-51.
150. Merrell, K.T., et al., *Identification of anergic B cells within a wild-type repertoire.* Immunity, 2006. **25**(6): p. 953-62.
151. Teague, B.N., et al., *Cutting edge: Transitional T3 B cells do not give rise to mature B cells, have undergone selection, and are reduced in murine lupus.* J Immunol, 2007. **178**(12): p. 7511-5.
152. Palanichamy, A., et al., *Novel human transitional B cell populations revealed by B cell depletion therapy.* J Immunol, 2009. **182**(10): p. 5982-93.
153. Cambier, J.C., et al., *B-cell anergy: from transgenic models to naturally occurring anergic B cells?* Nat Rev Immunol, 2007. **7**(8): p. 633-43.
154. Peters, A.L., L.L. Stunz, and G.A. Bishop, *CD40 and autoimmunity: the dark side of a great activator.* Semin Immunol, 2009. **21**(5): p. 293-300.
155. Herve, M., et al., *CD40 ligand and MHC class II expression are essential for human peripheral B cell tolerance.* J Exp Med, 2007. **204**(7): p. 1583-93.
156. Nickerson, K.M., et al., *TLR9 promotes tolerance by restricting survival of anergic anti-DNA B cells, yet is also required for their activation.* J Immunol, 2013. **190**(4): p. 1447-56.
157. Luo, W., F. Weisel, and M.J. Shlomchik, *B Cell Receptor and CD40 Signaling Are Rewired for Synergistic Induction of the c-Myc Transcription Factor in Germinal Center B Cells.* Immunity, 2018. **48**(2): p. 313-326 e5.
158. Sindhava, V.J., et al., *A TLR9-dependent checkpoint governs B cell responses to DNA-containing antigens.* J Clin Invest, 2017. **127**(5): p. 1651-1663.
159. Viglianti, G.A., et al., *Activation of autoreactive B cells by CpG dsDNA.* Immunity, 2003. **19**(6): p. 837-47.
160. Bernasconi, N.L., N. Onai, and A. Lanzavecchia, *A role for Toll-like receptors in acquired immunity: up-regulation of TLR9 by BCR triggering in naive B cells and constitutive expression in memory B cells.* Blood, 2003. **101**(11): p. 4500-4.
161. Morbach, H., et al., *CD19 controls Toll-like receptor 9 responses in human B cells.* J Allergy Clin Immunol, 2015.
162. Iwata, S., et al., *Amplification of Toll-like receptor-mediated signaling through spleen tyrosine kinase in human B-cell activation.* J Allergy Clin Immunol, 2012. **129**(6): p. 1594-601 e2.

163. Kremlitzka, M., B. Macsik-Valent, and A. Erdei, *Syk is indispensable for CpG-induced activation and differentiation of human B cells.* Cell Mol Life Sci, 2015. **72**(11): p. 2223-36.
164. Tsokos, G.C., *Systemic lupus erythematosus.* N Engl J Med, 2011. **365**(22): p. 2110-21.
165. Rees, F., et al., *The worldwide incidence and prevalence of systemic lupus erythematosus: a systematic review of epidemiological studies.* Rheumatology (Oxford), 2017. **56**(11): p. 1945-1961.
166. Gaubitz, M., *Epidemiology of connective tissue disorders.* Rheumatology (Oxford), 2006. **45 Suppl 3**: p. iii3-4.
167. Ludwig, R.J., et al., *Mechanisms of Autoantibody-Induced Pathology*. Front Immunol, 2017. **8**: p. 603.
168. Hansen, A., P.E. Lipsky, and T. Dorner, *B cells in Sjogren's syndrome: indications for disturbed selection and differentiation in ectopic lymphoid tissue.* Arthritis Res Ther, 2007. **9**(4): p. 218.
169. Slight-Webb, S., et al., *Autoantibody-Positive Healthy Individuals Display Unique Immune Profiles That May Regulate Autoimmunity.* Arthritis Rheumatol, 2016. **68**(10): p. 2492-502.
170. Yeo, L., et al., *Expression of FcRL4 defines a pro-inflammatory, RANKL-producing B cell subset in rheumatoid arthritis.* Ann Rheum Dis, 2015. **74**(5): p. 928-35.
171. Hansen, A., et al., *Diminished peripheral blood memory B cells and accumulation of memory B cells in the salivary glands of patients with Sjogren's syndrome.* Arthritis Rheum, 2002. **46**(8): p. 2160-71.
172. Bohnhorst, J.O., et al., *Bm1-Bm5 classification of peripheral blood B cells reveals circulating germinal center founder cells in healthy individuals and disturbance in the B cell subpopulations in patients with primary Sjogren's syndrome.* J Immunol, 2001. **167**(7): p. 3610-8.
173. Bohnhorst, J.O., et al., *Significantly depressed percentage of CD27+ (memory) B cells among peripheral blood B cells in patients with primary Sjogren's syndrome.* Scand J Immunol, 2001. **54**(4): p. 421-7.
174. Bohnhorst, J.O., et al., *Abnormal B cell differentiation in primary Sjogren's syndrome results in a depressed percentage of circulating memory B cells and elevated levels of soluble CD27 that correlate with Serum IgG concentration.* Clin Immunol, 2002. **103**(1): p. 79-88.
175. Hansen, A., et al., *Dysregulation of chemokine receptor expression and function by B cells of patients with primary Sjogren's syndrome.* Arthritis Rheum, 2005. **52**(7): p. 2109-19.
176. Scheid, J.F., et al., *Differential regulation of self-reactivity discriminates between IgG+ human circulating memory B cells and bone marrow plasma cells.* Proc Natl Acad Sci U S A, 2011. **108**(44): p. 18044-8.
177. Mietzner, B., et al., *Autoreactive IgG memory antibodies in patients with systemic lupus erythematosus arise from nonreactive and polyreactive precursors.* Proc Natl Acad Sci U S A, 2008. **105**(28): p. 9727-32.
178. Yurasov, S., et al., *Persistent expression of autoantibodies in SLE patients in remission.* J Exp Med, 2006. **203**(10): p. 2255-61.
179. Yurasov, S., et al., *Defective B cell tolerance checkpoints in systemic lupus erythematosus.* J Exp Med, 2005. **201**(5): p. 703-11.
180. Tiller, T., et al., *Autoreactivity in human IgG+ memory B cells.* Immunity, 2007. **26**(2): p. 205-13.
181. Meffre, E. and H. Wardemann, *B-cell tolerance checkpoints in health and autoimmunity.* Curr Opin Immunol, 2008. **20**(6): p. 632-8.
182. Zhang, J., et al., *Pathogenic autoantibodies in systemic lupus erythematosus are derived from both self-reactive and non-self-reactive B cells.* Mol Med, 2008. **14**(11-12): p. 675-81.
183. Shlomchik, M.J., *Sites and stages of autoreactive B cell activation and regulation.* Immunity, 2008. **28**(1): p. 18-28.
184. Rawlings, D.J., et al., *Altered B cell signalling in autoimmunity.* Nat Rev Immunol, 2017. **17**(7): p. 421-436.
185. Suurmond, J. and B. Diamond, *Autoantibodies in systemic autoimmune diseases: specificity and pathogenicity.* J Clin Invest, 2015. **125**(6): p. 2194-202.
186. Christensen, S.R., et al., *Toll-like receptor 9 controls anti-DNA autoantibody production in murine lupus.* J Exp Med, 2005. **202**(2): p. 321-31.
187. Lartigue, A., et al., *Role of TLR9 in anti-nucleosome and anti-DNA antibody production in lpr mutation-induced murine lupus.* J Immunol, 2006. **177**(2): p. 1349-54.
188. Busconi, L., et al., *Functional outcome of B cell activation by chromatin immune complex engagement of the B cell receptor and TLR9.* J Immunol, 2007. **179**(11): p. 7397-405.
189. Krieg, A.M., *A role for Toll in autoimmunity.* Nat Immunol, 2002. **3**(5): p. 423-4.

190. Bengtsson, A.A. and L. Ronnblom, *Role of interferons in SLE.* Best Pract Res Clin Rheumatol, 2017. **31**(3): p. 415-428.
191. Giordani, L., et al., *IFN-alpha amplifies human naive B cell TLR-9-mediated activation and Ig production.* J Leukoc Biol, 2009. **86**(2): p. 261-71.
192. Henault, J., et al., *Self-reactive IgE exacerbates interferon responses associated with autoimmunity.* Nat Immunol, 2016. **17**(2): p. 196-203.
193. Rose, T., et al., *IFNalpha and its response proteins, IP-10 and SIGLEC-1, are biomarkers of disease activity in systemic lupus erythematosus.* Ann Rheum Dis, 2013. **72**(10): p. 1639-45.
194. Rose, T., et al., *SIGLEC1 is a biomarker of disease activity and indicates extraglandular manifestation in primary Sjogren's syndrome.* RMD Open, 2016. **2**(2): p. e000292.
195. Schroeder, K., M. Herrmann, and T.H. Winkler, *The role of somatic hypermutation in the generation of pathogenic antibodies in SLE.* Autoimmunity, 2013. **46**(2): p. 121-7.
196. Schrezenmeier, E., D. Jayne, and T. Dorner, *Targeting B Cells and Plasma Cells in Glomerular Diseases: Translational Perspectives.* J Am Soc Nephrol, 2018. **29**(3): p. 741-758.
197. Tipton, C.M., et al., *Diversity, cellular origin and autoreactivity of antibody-secreting cell population expansions in acute systemic lupus erythematosus.* Nat Immunol, 2015. **16**(7): p. 755-65.
198. Suurmond, J., et al., *Patterns of ANA+ B cells for SLE patient stratification.* JCI Insight, 2019. **4**(9).
199. Pal Singh, S., F. Dammeijer, and R.W. Hendriks, *Role of Bruton's tyrosine kinase in B cells and malignancies.* Mol Cancer, 2018. **17**(1): p. 57.
200. Karrar, S. and D.S. Cunninghame Graham, *Abnormal B Cell Development in Systemic Lupus Erythematosus: What the Genetics Tell Us.* Arthritis Rheumatol, 2018. **70**(4): p. 496-507.
201. Lu, R., et al., *Genetic associations of LYN with systemic lupus erythematosus.* Genes Immun, 2009. **10**(5): p. 397-403.
202. Manjarrez-Orduno, N., et al., *CSK regulatory polymorphism is associated with systemic lupus erythematosus and influences B-cell signaling and activation.* Nat Genet, 2012. **44**(11): p. 1227-30.
203. Jarvinen, T.M., et al., *Replication of GWAS-identified systemic lupus erythematosus susceptibility genes affirms B-cell receptor pathway signalling and strengthens the role of IRF5 in disease susceptibility in a Northern European population.* Rheumatology (Oxford), 2012. **51**(1): p. 87-92.
204. Kozyrev, S.V., et al., *Functional variants in the B-cell gene BANK1 are associated with systemic lupus erythematosus.* Nat Genet, 2008. **40**(2): p. 211-6.
205. International Consortium for Systemic Lupus Erythematosus, G., et al., *Genome-wide association scan in women with systemic lupus erythematosus identifies susceptibility variants in ITGAM, PXK, KIAA1542 and other loci.* Nat Genet, 2008. **40**(2): p. 204-10.
206. Hom, G., et al., *Association of systemic lupus erythematosus with C8orf13-BLK and ITGAM-ITGAX.* N Engl J Med, 2008. **358**(9): p. 900-9.
207. Orozco, G., et al., *Study of the common genetic background for rheumatoid arthritis and systemic lupus erythematosus.* Ann Rheum Dis, 2011. **70**(3): p. 463-8.
208. Sun, F., et al., *Polymorphisms in the FAM167A-BLK, but not BANK1, are associated with primary Sjogren's syndrome in a Han Chinese population.* Clin Exp Rheumatol, 2013. **31**(5): p. 704-10.
209. Burbelo, P.D., K. Ambatipudi, and I. Alevizos, *Genome-wide association studies in Sjogren's syndrome: What do the genes tell us about disease pathogenesis?* Autoimmun Rev, 2014. **13**(7): p. 756-61.
210. Sanchez, E., et al., *Identification of novel genetic susceptibility loci in African American lupus patients in a candidate gene association study.* Arthritis Rheum, 2011. **63**(11): p. 3493-501.
211. Begovich, A.B., et al., *A missense single-nucleotide polymorphism in a gene encoding a protein tyrosine phosphatase (PTPN22) is associated with rheumatoid arthritis.* Am J Hum Genet, 2004. **75**(2): p. 330-7.
212. Gomez, L.M., et al., *PTPN22 C1858T polymorphism in Colombian patients with autoimmune diseases.* Genes Immun, 2005. **6**(7): p. 628-31.
213. Reddy, M.V., et al., *The R620W C/T polymorphism of the gene PTPN22 is associated with SLE independently of the association of PDCD1.* Genes Immun, 2005. **6**(8): p. 658-62.
214. Martin, J.E., et al., *Evidence for PTPN22 R620W polymorphism as the sole common risk variant for rheumatoid arthritis in the 1p13.2 region.* J Rheumatol, 2011. **38**(11): p. 2290-6.
215. Orozco, G., et al., *Study of functional variants of the BANK1 gene in rheumatoid arthritis.* Arthritis Rheum, 2009. **60**(2): p. 372-9.

216. Genin, E., et al., *Epistatic interaction between BANK1 and BLK in rheumatoid arthritis: results from a large trans-ethnic meta-analysis.* PLoS One, 2013. **8**(4): p. e61044.
217. Suarez-Gestal, M., et al., *Rheumatoid arthritis does not share most of the newly identified systemic lupus erythematosus genetic factors.* Arthritis Rheum, 2009. **60**(9): p. 2558-64.
218. Arechiga, A.F., et al., *Cutting edge: the PTPN22 allelic variant associated with autoimmunity impairs B cell signaling.* J Immunol, 2009. **182**(6): p. 3343-7.
219. Vang, T., et al., *Autoimmune-associated lymphoid tyrosine phosphatase is a gain-of-function variant.* Nat Genet, 2005. **37**(12): p. 1317-9.
220. Rieck, M., et al., *Genetic variation in PTPN22 corresponds to altered function of T and B lymphocytes.* J Immunol, 2007. **179**(7): p. 4704-10.
221. Metzler, G., et al., *The Autoimmune Risk Variant PTPN22 C1858T Alters B Cell Tolerance at Discrete Checkpoints and Differentially Shapes the Naive Repertoire.* J Immunol, 2017. **199**(7): p. 2249-2260.
222. Kariuki, S.N., M.K. Crow, and T.B. Niewold, *The PTPN22 C1858T polymorphism is associated with skewing of cytokine profiles toward high interferon-alpha activity and low tumor necrosis factor alpha levels in patients with lupus.* Arthritis Rheum, 2008. **58**(9): p. 2818-23.
223. Dam, E.M., et al., *The BANK1 SLE-risk variants are associated with alterations in peripheral B cell signaling and development in humans.* Clin Immunol, 2016.
224. Liubchenko, G.A., et al., *Rheumatoid arthritis is associated with signaling alterations in naturally occurring autoreactive B-lymphocytes.* J Autoimmun, 2013. **40**: p. 111-21.
225. Galligan, C.L., et al., *Multiparameter phospho-flow analysis of lymphocytes in early rheumatoid arthritis: implications for diagnosis and monitoring drug therapy.* PLoS One, 2009. **4**(8): p. e6703.
226. Kong, W., et al., *Increased expression of Bruton's tyrosine kinase in peripheral blood is associated with lupus nephritis.* Clin Rheumatol, 2018. **37**(1): p. 43-49.
227. O'Keefe, T.L., et al., *Deficiency in CD22, a B cell-specific inhibitory receptor, is sufficient to predispose to development of high affinity autoantibodies.* J Exp Med, 1999. **189**(8): p. 1307-13.
228. Bolland, S. and J.V. Ravetch, *Spontaneous autoimmune disease in Fc(gamma)RIIB-deficient mice results from strain-specific epistasis.* Immunity, 2000. **13**(2): p. 277-85.
229. Pao, L.I., et al., *B cell-specific deletion of protein-tyrosine phosphatase Shp1 promotes B-1a cell development and causes systemic autoimmunity.* Immunity, 2007. **27**(1): p. 35-48.
230. Yu, P., et al., *Autoimmunity and inflammation due to a gain-of-function mutation in phospholipase C gamma 2 that specifically increases external Ca2+ entry.* Immunity, 2005. **22**(4): p. 451-65.
231. Kil, L.P., et al., *Btk levels set the threshold for B-cell activation and negative selection of autoreactive B cells in mice.* Blood, 2012. **119**(16): p. 3744-56.
232. Liossis, S.N., et al., *B-cell kinase lyn deficiency in patients with systemic lupus erythematosus.* J Investig Med, 2001. **49**(2): p. 157-65.
233. Su, K., et al., *Expression profile of FcgammaRIIb on leukocytes and its dysregulation in systemic lupus erythematosus.* J Immunol, 2007. **178**(5): p. 3272-80.
234. Mackay, M., et al., *Selective dysregulation of the FcgammaIIB receptor on memory B cells in SLE.* J Exp Med, 2006. **203**(9): p. 2157-64.
235. Enyedy, E.J., et al., *Defective FcgammaRIIb1 signaling contributes to enhanced calcium response in B cells from patients with systemic lupus erythematosus.* Clin Immunol, 2001. **101**(2): p. 130-5.
236. Anzelon, A.N., H. Wu, and R.C. Rickert, *Pten inactivation alters peripheral B lymphocyte fate and reconstitutes CD19 function.* Nat Immunol, 2003. **4**(3): p. 287-94.
237. Flores-Borja, F., et al., *Decreased Lyn expression and translocation to lipid raft signaling domains in B lymphocytes from patients with systemic lupus erythematosus.* Arthritis Rheum, 2005. **52**(12): p. 3955-65.
238. Vasquez, A., et al., *Altered recruitment of Lyn, Syk and ZAP-70 into lipid rafts of activated B cells in Systemic Lupus Erythematosus.* Cell Signal, 2019. **58**: p. 9-19.
239. Ng, K.P., et al., *B cell depletion therapy in systemic lupus erythematosus: long-term follow-up and predictors of response.* Ann Rheum Dis, 2007. **66**(9): p. 1259-62.
240. Hoyer, B.F., et al., *Long-lived plasma cells and their contribution to autoimmunity.* Ann N Y Acad Sci, 2005. **1050**: p. 124-33.
241. Taddeo, A., et al., *Long-lived plasma cells are early and constantly generated in New Zealand Black/New Zealand White F1 mice and their therapeutic depletion requires a combined targeting of autoreactive plasma cells and their precursors.* Arthritis Res Ther, 2015. **17**: p. 39.

242. Dorner, T., et al., *The mechanistic impact of CD22 engagement with epratuzumab on B cell function: Implications for the treatment of systemic lupus erythematosus.* Autoimmun Rev, 2015. **14**(12): p. 1079-86.
243. Kirou, K.A. and E. Gkrouzman, *Anti-interferon alpha treatment in SLE.* Clin Immunol, 2013. **148**(3): p. 303-12.
244. Weissenberg, S.Y., et al., *Identification and Characterization of Post-activated B Cells in Systemic Autoimmune Diseases.* Front Immunol, 2019. **10**: p. 2136.
245. Aletaha, D., et al., *2010 Rheumatoid arthritis classification criteria: an American College of Rheumatology/European League Against Rheumatism collaborative initiative.* Arthritis Rheum, 2010. **62**(9): p. 2569-81.
246. Petri, M., et al., *Derivation and validation of the Systemic Lupus International Collaborating Clinics classification criteria for systemic lupus erythematosus.* Arthritis Rheum, 2012. **64**(8): p. 2677-86.
247. Vitali, C., et al., *Classification criteria for Sjogren's syndrome: a revised version of the European criteria proposed by the American-European Consensus Group.* Ann Rheum Dis, 2002. **61**(6): p. 554-8.
248. Kalina, T., et al., *EuroFlow standardization of flow cytometer instrument settings and immunophenotyping protocols.* Leukemia, 2012. **26**(9): p. 1986-2010.
249. Giesecke, C., et al., *Tissue distribution and dependence of responsiveness of human antigen-specific memory B cells.* J Immunol, 2014. **192**(7): p. 3091-100.
250. Khalil, A.M., J.C. Cambier, and M.J. Shlomchik, *B cell receptor signal transduction in the GC is short-circuited by high phosphatase activity.* Science, 2012. **336**(6085): p. 1178-81.
251. Neron, S., et al., *Tuning of CD40-CD154 interactions in human B-lymphocyte activation: a broad array of in vitro models for a complex in vivo situation.* Arch Immunol Ther Exp (Warsz), 2011. **59**(1): p. 25-40.
252. Olsson, P., et al., *Multiplex cytokine analyses in patients with rheumatoid arthritis require use of agents blocking heterophilic antibody activity.* Scand J Rheumatol, 2017. **46**(1): p. 1-10.
253. Holm, B.E., et al., *Species cross-reactivity of rheumatoid factors and implications for immunoassays.* Scand J Clin Lab Invest, 2015. **75**(1): p. 51-63.
254. Absher, D.M., et al., *Genome-wide DNA methylation analysis of systemic lupus erythematosus reveals persistent hypomethylation of interferon genes and compositional changes to CD4+ T-cell populations.* PLoS Genet, 2013. **9**(8): p. e1003678.
255. Julia, A., et al., *Epigenome-wide association study of rheumatoid arthritis identifies differentially methylated loci in B cells.* Hum Mol Genet, 2017. **26**(14): p. 2803-2811.
256. Imgenberg-Kreuz, J., et al., *Genome-wide DNA methylation analysis in multiple tissues in primary Sjogren's syndrome reveals regulatory effects at interferon-induced genes.* Ann Rheum Dis, 2016. **75**(11): p. 2029-2036.
257. Benjamini, Y. and Y. Hochberg, *Controlling the false discovery rate: a practical and powerful approach to multiple testing.* J. Royal Stat. Soc. , 1995. **57**: p. 289–300.
258. Wahl, M.I., et al., *Phosphorylation of two regulatory tyrosine residues in the activation of Bruton's tyrosine kinase via alternative receptors.* Proc Natl Acad Sci U S A, 1997. **94**(21): p. 11526-33.
259. Ntoufa, S., et al., *B Cell Anergy Modulated by TLR1/2 and the miR-17 approximately 92 Cluster Underlies the Indolent Clinical Course of Chronic Lymphocytic Leukemia Stereotyped Subset #4.* J Immunol, 2016. **196**(10): p. 4410-7.
260. Muzio, M., et al., *Constitutive activation of distinct BCR-signaling pathways in a subset of CLL patients: a molecular signature of anergy.* Blood, 2008. **112**(1): p. 188-95.
261. Apollonio, B., et al., *Targeting B-cell anergy in chronic lymphocytic leukemia.* Blood, 2013. **121**(19): p. 3879-88, S1-8.
262. Ballestar, E., M. Esteller, and B.C. Richardson, *The epigenetic face of systemic lupus erythematosus.* J Immunol, 2006. **176**(12): p. 7143-7.
263. Rose, T., et al., *Are interferon-related biomarkers advantageous for monitoring disease activity in systemic lupus erythematosus? A longitudinal benchmark study.* Rheumatology (Oxford), 2017. **56**(9): p. 1618-1626.
264. Wang, S., et al., *IL-21 drives expansion and plasma cell differentiation of autoreactive CD11c(hi)T-bet(+) B cells in SLE.* Nat Commun, 2018. **9**(1): p. 1758.
265. Naradikian, M.S., et al., *Cutting Edge: IL-4, IL-21, and IFN-gamma Interact To Govern T-bet and CD11c Expression in TLR-Activated B Cells.* J Immunol, 2016. **197**(4): p. 1023-8.
266. von Spee-Mayer, C., et al., *Low-dose interleukin-2 selectively corrects regulatory T cell defects in patients with systemic lupus erythematosus.* Ann Rheum Dis, 2016. **75**(7): p. 1407-15.

267. Jones, S.A. and B.J. Jenkins, *Recent insights into targeting the IL-6 cytokine family in inflammatory diseases and cancer.* Nat Rev Immunol, 2018. **18**(12): p. 773-789.
268. Floudas, A., S. Amu, and P.G. Fallon, *New Insights into IL-10 Dependent and IL-10 Independent Mechanisms of Regulatory B Cell Immune Suppression.* J Clin Immunol, 2016. **36 Suppl 1**: p. 25-33.
269. Gauld, S.B., et al., *Maintenance of B cell anergy requires constant antigen receptor occupancy and signaling.* Nat Immunol, 2005. **6**(11): p. 1160-7.
270. Vinuesa, C.G., I. Sanz, and M.C. Cook, *Dysregulation of germinal centres in autoimmune disease.* Nat Rev Immunol, 2009. **9**(12): p. 845-57.
271. Szodoray, P., et al., *T-helper signals restore B-cell receptor signaling in autoreactive anergic B cells by upregulating CD45 phosphatase activity.* J Allergy Clin Immunol, 2016. **138**(3): p. 839-851 e8.
272. Jiang, W., et al., *TLR9 stimulation drives naive B cells to proliferate and to attain enhanced antigen presenting function.* Eur J Immunol, 2007. **37**(8): p. 2205-13.
273. Huggins, J., et al., *CpG DNA activation and plasma-cell differentiation of CD27- naive human B cells.* Blood, 2007. **109**(4): p. 1611-9.
274. Marasco, E., et al., *B-cell activation with CD40L or CpG measures the function of B-cell subsets and identifies specific defects in immunodeficient patients.* Eur J Immunol, 2017. **47**(1): p. 131-143.
275. Roberts, M.E., et al., *Primary Sjogren's syndrome is characterized by distinct phenotypic and transcriptional profiles of IgD+ unswitched memory B cells.* Arthritis Rheumatol, 2014. **66**(9): p. 2558-69.
276. Dorner, T. and P.E. Lipsky, *Correlation of circulating CD27high plasma cells and disease activity in systemic lupus erythematosus.* Lupus, 2004. **13**(5): p. 283-9.
277. Iwata, S., et al., *Increased Syk phosphorylation leads to overexpression of TRAF6 in peripheral B cells of patients with systemic lupus erythematosus.* Lupus, 2015. **24**(7): p. 695-704.
278. Fleischer, S.J., et al., *Increased frequency of a unique spleen tyrosine kinase bright memory B cell population in systemic lupus erythematosus.* Arthritis Rheumatol, 2014. **66**(12): p. 3424-35.
279. Elkayam, O., et al., *Immunogenicity and safety of pneumococcal vaccination in patients with rheumatoid arthritis or systemic lupus erythematosus.* Clin Infect Dis, 2002. **34**(2): p. 147-53.
280. Gabay, C., et al., *Impact of synthetic and biologic disease-modifying antirheumatic drugs on antibody responses to the AS03-adjuvanted pandemic influenza vaccine: a prospective, open-label, parallel-cohort, single-center study.* Arthritis Rheum, 2011. **63**(6): p. 1486-96.
281. Saad, C.G., et al., *Immunogenicity and safety of the 2009 non-adjuvanted influenza A/H1N1 vaccine in a large cohort of autoimmune rheumatic diseases.* Ann Rheum Dis, 2011. **70**(6): p. 1068-73.
282. Battafarano, D.F., et al., *Antigen-specific antibody responses in lupus patients following immunization.* Arthritis Rheum, 1998. **41**(10): p. 1828-34.
283. Brauner, S., et al., *H1N1 vaccination in Sjogren's syndrome triggers polyclonal B cell activation and promotes autoantibody production.* Ann Rheum Dis, 2017. **76**(10): p. 1755-1763.
284. Jacquemin, C., et al., *OX40 Ligand Contributes to Human Lupus Pathogenesis by Promoting T Follicular Helper Response.* Immunity, 2015. **42**(6): p. 1159-70.
285. Goodnow, C.C., et al., *Altered immunoglobulin expression and functional silencing of self-reactive B lymphocytes in transgenic mice.* Nature, 1988. **334**(6184): p. 676-82.
286. Quach, T.D., et al., *Anergic responses characterize a large fraction of human autoreactive naive B cells expressing low levels of surface IgM.* J Immunol, 2011. **186**(8): p. 4640-8.
287. Franks, S.E. and J.C. Cambier, *Putting on the Brakes: Regulatory Kinases and Phosphatases Maintaining B Cell Anergy.* Front Immunol, 2018. **9**: p. 665.
288. Khoder, A., et al., *Evidence for B Cell Exhaustion in Chronic Graft-versus-Host Disease.* Front Immunol, 2017. **8**: p. 1937.
289. Benschop, R.J., et al., *Activation and anergy in bone marrow B cells of a novel immunoglobulin transgenic mouse that is both hapten specific and autoreactive.* Immunity, 2001. **14**(1): p. 33-43.
290. Gauld, S.B., K.T. Merrell, and J.C. Cambier, *Silencing of autoreactive B cells by anergy: a fresh perspective.* Curr Opin Immunol, 2006. **18**(3): p. 292-7.
291. Browne, C.D., et al., *Suppression of phosphatidylinositol 3,4,5-trisphosphate production is a key determinant of B cell anergy.* Immunity, 2009. **31**(5): p. 749-60.
292. Getahun, A., et al., *Continuous inhibitory signaling by both SHP-1 and SHIP-1 pathways is required to maintain unresponsiveness of anergic B cells.* J Exp Med, 2016. **213**(5): p. 751-69.

293. Cappione, A., 3rd, et al., *Germinal center exclusion of autoreactive B cells is defective in human systemic lupus erythematosus.* J Clin Invest, 2005. **115**(11): p. 3205-16.
294. Comte, D., et al., *Signaling Lymphocytic Activation Molecule Family Member 7 Engagement Restores Defective Effector CD8+ T Cell Function in Systemic Lupus Erythematosus.* Arthritis Rheumatol, 2017. **69**(5): p. 1035-1044.
295. Kis-Toth, K., et al., *Selective Loss of Signaling Lymphocytic Activation Molecule Family Member 4-Positive CD8+ T Cells Contributes to the Decreased Cytotoxic Cell Activity in Systemic Lupus Erythematosus.* Arthritis Rheumatol, 2016. **68**(1): p. 164-73.
296. McKinney, E.F., et al., *T-cell exhaustion, co-stimulation and clinical outcome in autoimmunity and infection.* Nature, 2015. **523**(7562): p. 612-6.
297. Sharabi, A., I.R. Kasper, and G.C. Tsokos, *The serine/threonine protein phosphatase 2A controls autoimmunity.* Clin Immunol, 2018. **186**: p. 38-42.
298. Katsuyama, T., G.C. Tsokos, and V.R. Moulton, *Aberrant T Cell Signaling and Subsets in Systemic Lupus Erythematosus.* Front Immunol, 2018. **9**: p. 1088.
299. Gringhuis, S.I., et al., *Displacement of linker for activation of T cells from the plasma membrane due to redox balance alterations results in hyporesponsiveness of synovial fluid T lymphocytes in rheumatoid arthritis.* J Immunol, 2000. **164**(4): p. 2170-9.
300. Legany, N., et al., *Calcium influx kinetics, and the features of potassium channels of peripheral lymphocytes in primary Sjogren's syndrome.* Immunobiology, 2016. **221**(11): p. 1266-72.
301. Lechouane, F., et al., *B-cell receptor signal strength influences terminal differentiation.* Eur J Immunol, 2013. **43**(3): p. 619-28.
302. Konigsberger, S., et al., *Altered BCR signalling quality predisposes to autoimmune disease and a pre-diabetic state.* EMBO J, 2012. **31**(15): p. 3363-74.
303. Schickel, J.N., et al., *PTPN22 inhibition resets defective human central B cell tolerance.* Sci Immunol, 2016. **1**(1).
304. Gensous, N., et al., *T Follicular Helper Cells in Autoimmune Disorders.* Front Immunol, 2018. **9**: p. 1637.
305. Choi, J.Y., et al., *Circulating follicular helper-like T cells in systemic lupus erythematosus: association with disease activity.* Arthritis Rheumatol, 2015. **67**(4): p. 988-99.
306. Le Coz, C., et al., *Circulating TFH subset distribution is strongly affected in lupus patients with an active disease.* PLoS One, 2013. **8**(9): p. e75319.
307. Xu, H., et al., *Increased frequency of circulating follicular helper T cells in lupus patients is associated with autoantibody production in a CD40L-dependent manner.* Cell Immunol, 2015. **295**(1): p. 46-51.
308. Menard, L., et al., *The PTPN22 allele encoding an R620W variant interferes with the removal of developing autoreactive B cells in humans.* J Clin Invest, 2011. **121**(9): p. 3635-44.
309. Tipton, C.M., et al., *Understanding B-cell activation and autoantibody repertoire selection in systemic lupus erythematosus: A B-cell immunomics approach.* Immunol Rev, 2018. **284**(1): p. 120-131.
310. Rao, D.A., et al., *Pathologically expanded peripheral T helper cell subset drives B cells in rheumatoid arthritis.* Nature, 2017. **542**(7639): p. 110-114.
311. Lin, J., et al., *PD-1+CXCR5-CD4+T cells are correlated with the severity of systemic lupus erythematosus.* Rheumatology (Oxford), 2019.
312. Guo, Y., et al., *CD40L-Dependent Pathway Is Active at Various Stages of Rheumatoid Arthritis Disease Progression.* J Immunol, 2017. **198**(11): p. 4490-4501.
313. Burmester, G.R., E. Feist, and T. Dorner, *Emerging cell and cytokine targets in rheumatoid arthritis.* Nat Rev Rheumatol, 2014. **10**(2): p. 77-88.
314. Dorner, T. and P.E. Lipsky, *Beyond pan-B-cell-directed therapy - new avenues and insights into the pathogenesis of SLE.* Nat Rev Rheumatol, 2016. **12**(11): p. 645-657.
315. Roll, P., et al., *Regeneration of B cell subsets after transient B cell depletion using anti-CD20 antibodies in rheumatoid arthritis.* Arthritis Rheum, 2006. **54**(8): p. 2377-86.
316. Rosen, O., et al., *Relapse of systemic lupus erythematosus.* Lancet, 2001. **357**(9258): p. 807-8.
317. Clowse, M.E., et al., *Efficacy and Safety of Epratuzumab in Moderately to Severely Active Systemic Lupus Erythematosus: Results From Two Phase III Randomized, Double-Blind, Placebo-Controlled Trials.* Arthritis Rheumatol, 2017. **69**(2): p. 362-375.
318. Grammer, A.C., et al., *Abnormal germinal center reactions in systemic lupus erythematosus demonstrated by blockade of CD154-CD40 interactions.* J Clin Invest, 2003. **112**(10): p. 1506-20.

319. Boumpas, D.T., et al., *A short course of BG9588 (anti-CD40 ligand antibody) improves serologic activity and decreases hematuria in patients with proliferative lupus glomerulonephritis.* Arthritis Rheum, 2003. **48**(3): p. 719-27.
320. Sidiropoulos, P.I. and D.T. Boumpas, *Lessons learned from anti-CD40L treatment in systemic lupus erythematosus patients.* Lupus, 2004. **13**(5): p. 391-7.
321. Chamberlain, C., et al., *Repeated administration of dapirolizumab pegol in a randomised phase I study is well tolerated and accompanied by improvements in several composite measures of systemic lupus erythematosus disease activity and changes in whole blood transcriptomic profiles.* Ann Rheum Dis, 2017. **76**(11): p. 1837-1844.
322. Zikherman, J., *GC B cells 'AKT' to blunt BCR signaling.* Nat Immunol, 2019. **20**(6): p. 671-674.
323. Luo, W., et al., *The AKT kinase signaling network is rewired by PTEN to control proximal BCR signaling in germinal center B cells.* Nat Immunol, 2019. **20**(6): p. 736-746.
324. Setz, C.S., et al., *Pten controls B-cell responsiveness and germinal center reaction by regulating the expression of IgD BCR.* EMBO J, 2019. **38**(11).
325. Pauls, S.D., et al., *FcgammaRIIB-Independent Mechanisms Controlling Membrane Localization of the Inhibitory Phosphatase SHIP in Human B Cells.* J Immunol, 2016.
326. Sabouri, Z., et al., *IgD attenuates the IgM-induced anergy response in transitional and mature B cells.* Nat Commun, 2016. **7**: p. 13381.
327. Wei, C., S. Jenks, and I. Sanz, *Polychromatic flow cytometry in evaluating rheumatic disease patients.* Arthritis Res Ther, 2015. **17**: p. 46.
328. Mei, H.E., et al., *Plasmablasts With a Mucosal Phenotype Contribute to Plasmacytosis in Systemic Lupus Erythematosus.* Arthritis Rheumatol, 2017. **69**(10): p. 2018-2028.
329. van der Vlist, M., et al., *Immune checkpoints and rheumatic diseases: what can cancer immunotherapy teach us?* Nat Rev Rheumatol, 2016. **12**(10): p. 593-604.
330. Yokosuka, T., et al., *Spatiotemporal basis of CTLA-4 costimulatory molecule-mediated negative regulation of T cell activation.* Immunity, 2010. **33**(3): p. 326-39.
331. Stefanski, A.L., et al., *Enhanced PD-1 and diminished PD-L1 upregulation capacity mark post-activated lupus B cells.* Arthritis Rheumatol, 2019.
332. Curran, C.S., et al., *PD-1 immunobiology in systemic lupus erythematosus.* J Autoimmun, 2019. **97**: p. 1-9.
333. Salimzadeh, L., et al., *PD-1 blockade partially recovers dysfunctional virus-specific B cells in chronic hepatitis B infection.* J Clin Invest, 2018. **128**(10): p. 4573-4587.
334. Yoshida, K., S. Kharbanda, and D. Kufe, *Functional interaction between SHPTP1 and the Lyn tyrosine kinase in the apoptotic response to DNA damage.* J Biol Chem, 1999. **274**(49): p. 34663-8.
335. Xiao, W., et al., *Lyn- and PLC-beta3-dependent regulation of SHP-1 phosphorylation controls Stat5 activity and myelomonocytic leukemia-like disease.* Blood, 2010. **116**(26): p. 6003-13.
336. Mizuno, T. and T.L. Rothstein, *B cell receptor (BCR) cross-talk: CD40 engagement creates an alternate pathway for BCR signaling that activates I kappa B kinase/I kappa B alpha/NF-kappa B without the need for PI3K and phospholipase C gamma.* J Immunol, 2005. **174**(10): p. 6062-70.
337. Haxhinasto, S.A. and G.A. Bishop, *Synergistic B cell activation by CD40 and the B cell antigen receptor: role of B lymphocyte antigen receptor-mediated kinase activation and tumor necrosis factor receptor-associated factor regulation.* J Biol Chem, 2004. **279**(4): p. 2575-82.

# 10 Tables and Figures

## 10.1 Table of Main Figures

## 10.2 Table of Supplementary Figures



## 10.3 Table of Tables



## 10.4 Table of Supplementary Tables

# 11 Appendix

**Supplementary Table 1:** Supplier information

| **Supplier** | **Location** |
|---|---|
| BD Bioscience | Franklin Lakes, New Jersey. United States |
| BioLegend | San Diego, California, United States |
| Bioss Antibodies | Woburn, MA, United States |
| Bio-Rad Laboratories | Hercules, California, United States |
| Biozym Scientific GmbH | Hessisch Oldendorf, Germany |
| Corning Inc. | Corning, New York, United States |
| eBioscience/Thermo Fisher | Carlsbad, California, United States |
| Eppendorf AG | Hamburg, Germany |
| Fisher scientific/Thermo Fisher | Carlsbad, California, United States |
| GE Healthcare | Chalfont St Giles, Great Britain |
| gibco by life technologies/Thermo Fisher | Carlsbad, California, United States |
| GraphPad Software | La Jolla, California, United States |
| Greiner Bio-One International GmbH | Kremsmünster, Austria |
| Invitrogen/Thermo Fisher | Carlsbad, California, United States |
| Jackson ImmunoResearch | West Grove, Florida, United States |
| MDS Nordion | Ottawa, Canada |
| Merck KGaA | Darmstadt, Germany |
| Miltenyi Biotec GmbH | Bergisch Gladbach, Germany |
| Molecular Probes/Thermo Fisher | Carlsbad, California, United States |
| PeproTech | Rocky Hill, New Jersey, United States |
| Qiagen | Venlo, Netherlands |
| Sarstedt AG & Co. KG | Nümbrecht, Germany |
| Scantibodies Laboratory | Santa fee, California, United States |
| Selleck Chemicals | Houston, Texas, United States |
| Sigma-Aldrich | St. Louis, Missouri, United States |
| TreeStar | Ashland, Oregon, United States |
| VWR International GmbH | Darmstadt, Germany |

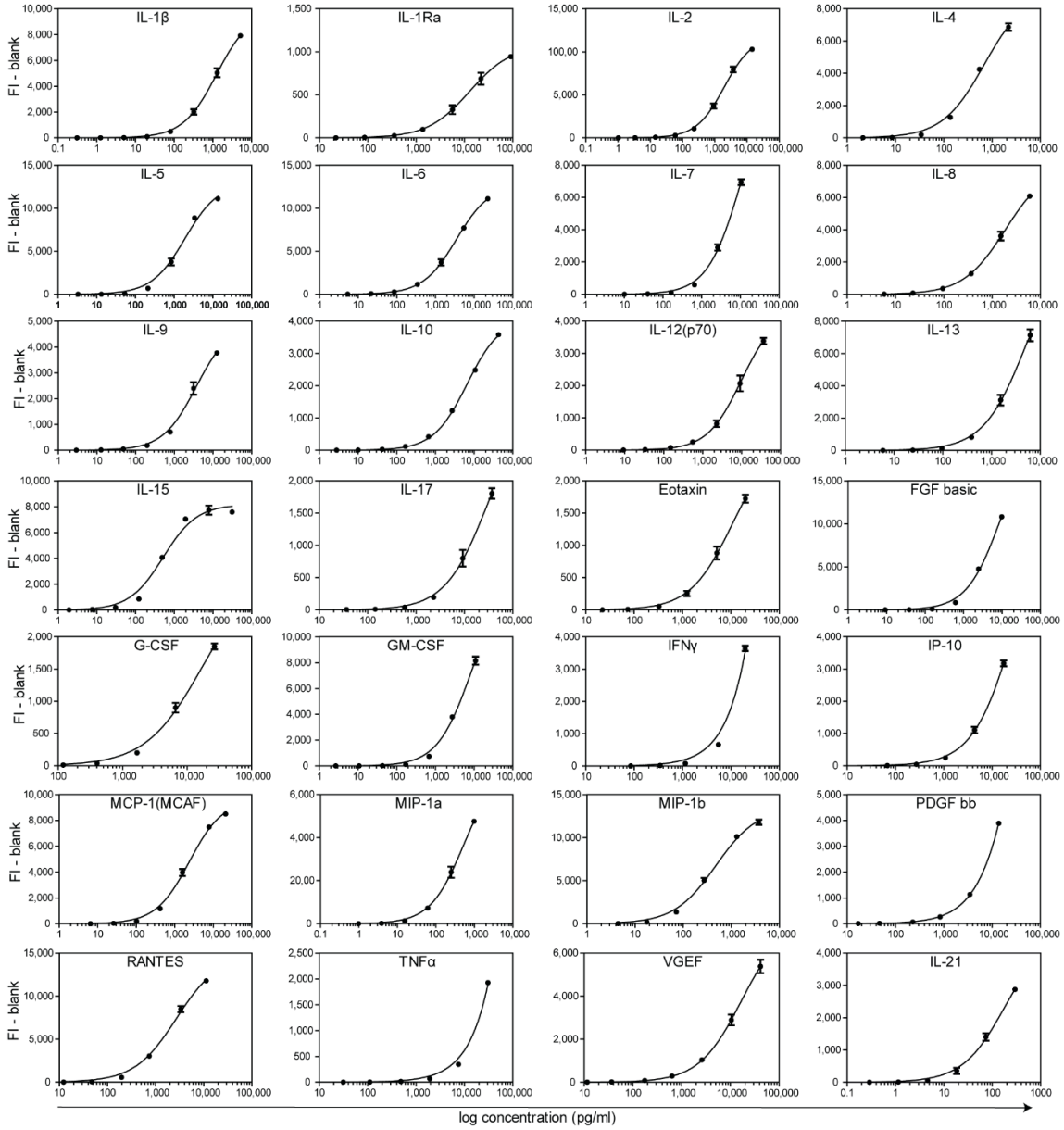


**Supplementary Figure 1: Standard curves for 27plex and IL-21 serum concentration analysis.** For the analysis of cytokine concentrations in human serum samples standard curves for IL-1β, IL-1Ra, IL-2, IL-4, IL-5, IL-6, IL-7 IL-8, IL-9, IL-10, IL-12(p70), IL-13, IL-15, IL-17, Eotaxin, FGF basic, G-CSF, GM-CSF, IFNγ, IP-10, MCP-1(MCAF), MIP-1a, MIP-1b, PDGF bb, RANTES, TNFα, VGEF and IL-21 were calculated. Graphs show blank subtracted fluorescence intensities (FIs) versus diluted standard concentrations (Michales-Menten fit, bars indicate SD).

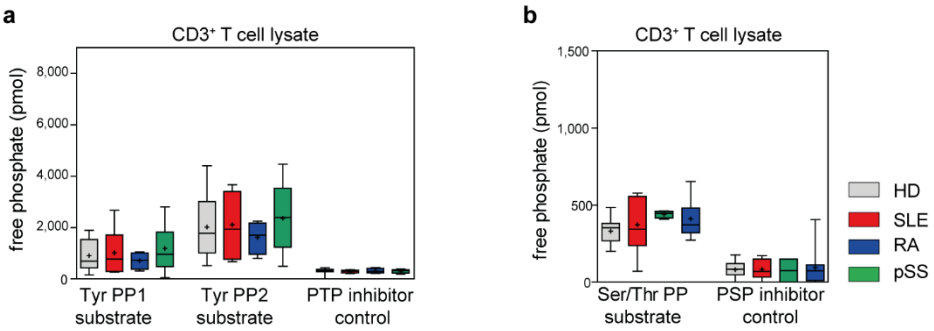


**Supplementary Figure 2: Comparable PTP and PSP activities between SLE, RA, pSS and HD in CD3⁺ T cells.** CD3⁺ T cells from HDs (grey), SLE (red), RA (blue) and pSS (green) were analyzed for their (**a**) PTP (n(HD/SLE/RA/pSS) = 14/10/4/10)) and (**b**) PSP activities (n(HD/SLE/RA/pSS) = 13/9/4/9)) Box whisker plots represent the median (line), mean (plus) and the range (whiskers).

**Supplementary Table 2:** Serum cytokine concentrations (pg/ml) in HD and SLE serum samples

| Cytokines (pg/ml) | Donors | | | | | | | | | | | | | |
|---|---|---|---|---|---|---|---|---|---|---|---|---|---|---|
| | HD | | | | | | | | | | SLE | | | |
| | 1 | 2 | 3 | 4 | 5 | 6 | 7 | 8 | 9 | 10 | 1 | 2 | 3 | 4 |
| **IL-1β** | 2 | ↓ | 3 | 2 | 2 | 2 | 2 | 2 | 2 | 2 | 2 | 3 | 3 | 6 |
| **IL-1Ra** | 93 | 37 | 76 | 76 | 79 | 65 | 100 | 72 | 100 | 90 | 72 | 93 | 148 | 315 |
| **IL-2** | ↓ | ↓ | ↓ | ↓ | 1 | ↓ | ↓ | 1 | 1 | 1 | 2 | 1 | 2 | 4 |
| **IL-4** | 3 | ↓ | 3 | 3 | 4 | ↓ | 3 | 2 | 3 | 3 | 3 | 2 | 5 | 8 |
| **IL-5** | ↓ | ↓ | ↓ | 5 | 5 | ↓ | 6 | 5 | 5 | 3 | ↓ | 6 | 5 | 11 |
| **IL-6** | ↓ | ↓ | ↓ | ↓ | ↓ | ↓ | ↓ | ↓ | ↓ | ↓ | ↓ | ↓ | 5 | 9 |
| **IL-7** | ↓ | ↓ | ↓ | ↓ | ↓ | ↓ | 11 | ↓ | ↓ | 20 | ↓ | 10 | ↓ | 20 |
| **IL-8** | 6 | ↓ | 6 | ↓ | 18 | 7 | 7 | ↓ | 6 | 8 | 7 | 10 | 9 | 20 |
| **IL-9** | 21 | 10 | 21 | 10 | 24 | 15 | 24 | 16 | 14 | 27 | 20 | 33 | 19 | 28 |
| **IL-10** | 6 | ↓ | 6 | ↓ | 3 | 4 | 5 | 4 | 9 | 6 | ↓ | 12 | 18 | 41 |
| **IL-12(p70)** | 20 | ↓ | 20 | ↓ | 12 | 15 | 16 | 14 | 23 | 19 | ↓ | 44 | 29 | 80 |
| **IL-13** | ↓ | ↓ | 15 | 9 | 22 | 24 | 17 | 8 | 8 | 15 | ↓ | 10 | 12 | 21 |
| **IL-15** | ↓ | ↓ | ↓ | ↓ | ↓ | ↓ | ↓ | ↓ | ↓ | ↓ | ↓ | ↓ | ↓ | ↓ |
| **IL-17** | ↓ | ↓ | 75 | 99 | ↓ | ↓ | 89 | ↓ | 113 | 195 | 99 | 166 | 588 | 1613 |
| **IL-21** | ↓ | ↓ | ↓ | ↓ | ↓ | ↓ | ↓ | ↓ | ↓ | ↓ | ↓ | ↓ | ↓ | ↓ |
| **Eotaxin** | 102 | 143 | 137 | 176 | 172 | 141 | 326 | 288 | 437 | 215 | 46 | 88 | 537 | 260 |
| **FGF basic** | ↓ | ↓ | ↓ | 18 | ↓ | ↓ | 9 | 11 | 22 | 42 | 27 | 42 | 18 | 143 |
| **G-CSF** | ↓ | ↓ | ↓ | ↓ | ↓ | ↓ | ↓ | ↓ | ↓ | ↓ | ↓ | 133 | 151 | 368 |
| **GM-CSF** | 18 | 9 | 14 | 19 | 17 | 18 | 21 | 18 | 25 | 41 | 18 | 37 | 47 | 147 |
| **IFN-γ** | 109 | ↓ | 109 | ↓ | 132 | ↓ | 142 | 97 | 103 | 121 | 85 | 121 | 153 | 348 |
| **IP-10** | 861 | 1415 | 868 | 556 | 844 | 1531 | 2187 | 1387 | 1261 | 1321 | 2458 | ↑ | 972 | 2312 |
| **MCP-1(MCAF)** | 19 | 24 | ↓ | 34 | 60 | 36 | 54 | 88 | 94 | 120 | 75 | 28 | 21 | 44 |
| **MIP-1a** | ↓ | 1 | 2 | 2 | 4 | 1 | 2 | 2 | 4 | 2 | 8 | 4 | 3 | 6 |
| **MIP-1b** | 15 | 29 | 25 | 15 | 17 | 16 | 27 | 24 | 13 | 65 | 27 | 54 | 23 | 26 |
| **PDGF bb** | 1281 | 1010 | 1129 | 1218 | 1516 | 619 | 2017 | 267 | 1221 | 7829 | 2282 | 4286 | 1557 | 922 |
| **RANTES** | 379 | 570 | 850 | 835 | 385 | 469 | 1035 | 1387 | 652 | ↑ | 2163 | ↑ | 1031 | 1208 |
| **TNF-α** | 221 | 157 | 112 | 179 | 168 | 200 | 200 | 200 | 231 | 241 | 168 | 280 | 355 | 682 |
| **VEGF** | 74 | 13 | 86 | ↓ | 42 | 90 | 35 | 55 | 162 | 105 | 12 | 332 | 143 | 178 |

↓ below standard curve; ↑ above standard curve

**Supplementary Table 3:** Serum cytokine concentrations (pg/ml) in RA and pSS serum samples

| Cytokines (pg/ml) | Donors | | | | | | | | | | | | | | | |
|---|---|---|---|---|---|---|---|---|---|---|---|---|---|---|---|---|
| | RA | | | | | | pSS | | | | | | | | | |
| | 1 | 2 | 3 | 4 | 5 | 6 | 1 | 2 | 3 | 4 | 5 | 6 | 7 | 8 | 9 | 10 |
| **IL-1β** | 2 | 2 | 3 | 2 | 3 | 4 | 2 | 2 | 2 | 2 | 2 | 3 | 3 | 2 | 4 | 3 |
| **IL-1Ra** | 79 | 100 | 104 | 79 | 114 | 104 | 62 | 58 | 65 | ↓ | 86 | 124 | 128 | 90 | 104 | 100 |
| **IL-2** | 1 | ↓ | 2 | 1 | 1 | 1 | ↓ | ↓ | 1 | ↓ | ↓ | 2 | 2 | ↓ | 2 | 1 |
| **IL-4** | 3 | 3 | 4 | 3 | 4 | 4 | 3 | 2 | 3 | 3 | 3 | 4 | 5 | 2 | 5 | 4 |
| **IL-5** | 3 | 5 | 5 | ↓ | 7 | 7 | ↓ | ↓ | 5 | 4 | ↓ | 5 | 9 | 5 | 10 | 9 |
| **IL-6** | ↓ | 16 | 12 | 7 | ↓ | 9 | ↓ | ↓ | 10 | ↓ | ↓ | ↓ | ↓ | 6 | 6 | 6 |
| **IL-7** | ↓ | ↓ | ↓ | ↓ | 13 | 19 | ↓ | ↓ | ↓ | ↓ | ↓ | ↓ | 10 | ↓ | ↓ | ↓ |
| **IL-8** | ↓ | 7 | 7 | 19 | 7 | 11 | ↓ | ↓ | 7 | ↓ | 9 | 33 | 19 | 29 | 8 | 16 |
| **IL-9** | 18 | 22 | 44 | 17 | 17 | 29 | 12 | 12 | 17 | 15 | 17 | 23 | 33 | 13 | 31 | 37 |
| **IL-10** | 6 | 6 | 9 | 7 | 8 | 6 | 4 | 3 | 3 | 3 | 5 | 5 | 12 | 10 | 15 | 8 |
| **IL-12(p70)** | 19 | 30 | 36 | 29 | 19 | 20 | 22 | 12 | 15 | 15 | 20 | 23 | 26 | 33 | 43 | 32 |
| **IL-13** | 8 | 8 | 11 | 6 | 14 | 9 | 7 | 11 | 10 | 6 | 11 | 11 | 12 | 10 | 38 | 27 |
| **IL-15** | ↓ | ↓ | ↓ | ↓ | ↓ | ↓ | ↓ | ↓ | ↓ | ↓ | ↓ | ↓ | ↓ | ↓ | ↓ | ↓ |
| **IL-17** | 80 | 59 | 99 | 75 | 37 | 140 | 89 | ↓ | 70 | 70 | 64 | 80 | 174 | 131 | 278 | 227 |
| **IL-21** | ↓ | ↓ | ↓ | ↓ | ↓ | ↓ | ↓ | ↓ | ↓ | ↓ | ↓ | ↓ | ↓ | ↓ | ↓ | ↓ |
| **Eotaxin** | 98 | 205 | 234 | 461 | 443 | 443 | 27 | 251 | 253 | 358 | 438 | 373 | 497 | 345 | 193 | 233 |
| **FGF basic** | 20 | 27 | ↓ | ↓ | 24 | 27 | ↓ | ↓ | 17 | 12 | 9 | 15 | 14 | 18 | 42 | 24 |
| **G-CSF** | ↓ | ↓ | ↓ | ↓ | ↓ | 139 | ↓ | ↓ | ↓ | ↓ | ↓ | ↓ | 151 | ê | 160 | 123 |
| **GM-CSF** | 24 | 14 | 21 | 15 | 21 | 30 | 15 | 10 | 18 | 3 | 15 | 22 | 24 | 16 | 52 | 32 |
| **IFN-γ** | 109 | 91 | 85 | 109 | 153 | 153 | ↓ | ↓ | 109 | ↓ | 109 | 153 | 193 | 85 | 221 | 163 |
| **IP-10** | 1192 | 4779 | 2197 | 1232 | 1628 | 3587 | 1991 | 921 | 1464 | 2080 | 1763 | 1947 | 4539 | 9079 | 2887 | 8473 |
| **MCP-1(MCAF)** | ↓ | 82 | 70 | 86 | 115 | 41 | 76 | 54 | 32 | 47 | 93 | 65 | 40 | 211 | 52 | 59 |
| **MIP-1a** | 3 | 1 | 2 | 5 | 3 | 6 | 2 | 2 | 4 | 2 | 4 | 16 | 6 | 3 | 1 | 3 |
| **MIP-1b** | 22 | 18 | 21 | 19 | ↓ | 34 | 14 | 15 | 14 | 13 | 20 | 36 | 71 | 46 | 38 | 52 |
| **PDGF bb** | 1770 | 2098 | 1281 | 1470 | 570 | 2856 | 1293 | 373 | 1248 | 2366 | 1091 | 2332 | 7368 | 1175 | 3019 | 3214 |
| **RANTES** | 672 | 582 | 477 | 686 | 329 | 938 | 680 | 283 | 676 | 649 | 333 | 781 | 898 | 1121 | ↑ | 1898 |
| **TNF-α** | 157 | 221 | ↓ | 231 | 318 | 318 | 157 | 135 | 112 | 200 | 280 | 290 | 241 | 135 | 299 | 261 |
| **VEGF** | 93 | 101 | 88 | 95 | 44 | 59 | 77 | 30 | 32 | 51 | 61 | 110 | 122 | 178 | 283 | 139 |

↓ below standard curve; ↑ above standard curve

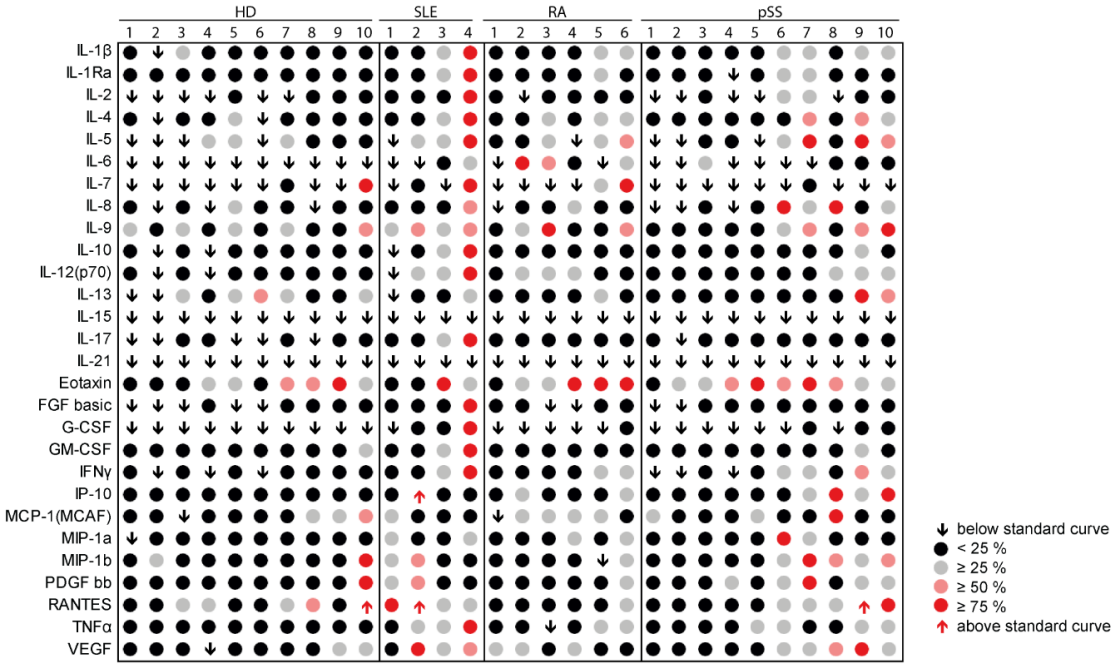


**Supplementary Figure 3: Cytokine expression profile of human serum from HDs, SLE, RA and pSS patients.** Concentrations of the cytokines IL-1β, IL-1Ra, IL-2, IL-4, IL-5, IL-6, IL-7,IL-8,IL-9, IL-10, IL12(p70), IL-13, IL-15, IL-17, Eotaxin, FGF basic, G-CSF, GM-CSF, IFNγ, IP-10, MCP-1(MCAF), MIP-1a, MIP-1b, PDGF bb, RANTES, TNFα and VEGF were analyzed from SLE, RA, pSS and HD serum samples (n(HD/SLE/RA/pSS) = 10/4/6/10). Values ranging in the upper (≥ 75 %), upper middle (≥ 50 %), lower middle (≥ 25 %) and lower (< 25 %) quartile are represented in dark red, light red, light grey and black, respectively. Values below (black arrows down) or above (red arrows up) the detection limit are indicated.

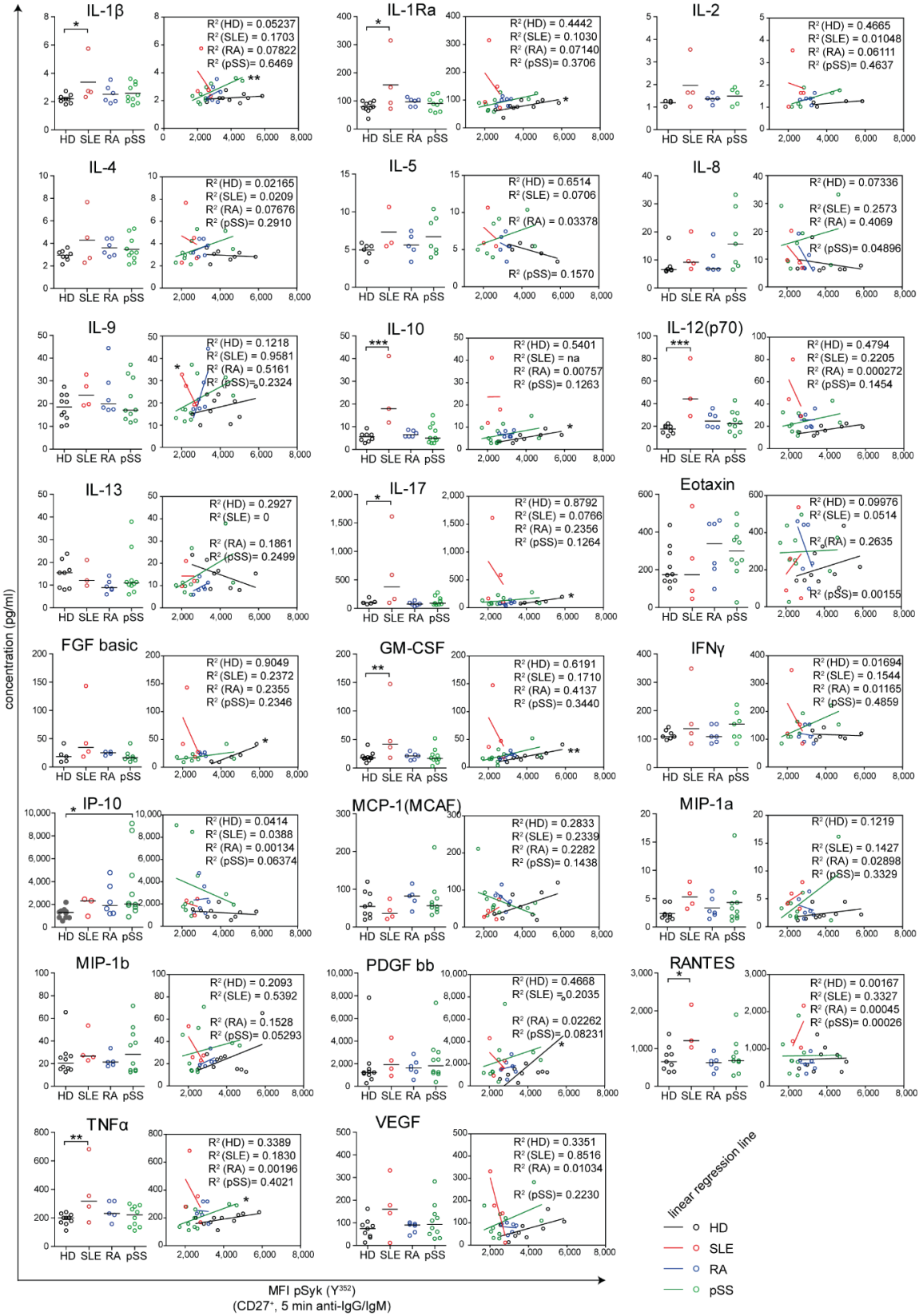
IL-1β
R² (HD) = 0.05237
R² (SLE) = 0.1703
R² (RA) = 0.07822
R² (pSS)= 0.6469
IL-1Ra
R² (HD) = 0.4442
R² (SLE) = 0.1030
R² (RA) = 0.07140
R² (pSS)= 0.3706
IL-2
R² (HD) = 0.4665
R² (SLE) = 0.01048
R² (RA) = 0.06111
R² (pSS)= 0.4637
IL-4
R² (HD) = 0.02165
R² (SLE) = 0.0209
R² (RA) = 0.07676
R² (pSS)= 0.2910
IL-5
R² (HD) = 0.6514
R² (SLE) = 0.0706
R² (RA) = 0.03378
R² (pSS)= 0.1570
IL-8
R² (HD) = 0.07336
R² (SLE) = 0.2573
R² (RA) = 0.4069
R² (pSS)= 0.04896
IL-9
R² (HD) = 0.1218
R² (SLE) = 0.9581
R² (RA) = 0.5161
R² (pSS)= 0.2324
IL-10
R² (HD) = 0.5401
R² (SLE) = na
R² (RA) = 0.00757
R² (pSS)= 0.1263
IL-12(p70)
R² (HD) = 0.4794
R² (SLE) = 0.2205
R² (RA) = 0.000272
R² (pSS)= 0.1454
IL-13
R² (HD) = 0.2927
R² (SLE) = 0
R² (RA) = 0.1861
R² (pSS)= 0.2499
IL-17
R² (HD) = 0.8792
R² (SLE) = 0.0766
R² (RA) = 0.2356
R² (pSS)= 0.1264
Eotaxin
R² (HD) = 0.09976
R² (SLE) = 0.0514
R² (RA) = 0.2635
R² (pSS)= 0.00155
FGF basic
R² (HD) = 0.9049
R² (SLE) = 0.2372
R² (RA) = 0.2355
R² (pSS)= 0.2346
GM-CSF
R² (HD) = 0.6191
R² (SLE) = 0.1710
R² (RA) = 0.4137
R² (pSS)= 0.3440
IFNγ
R² (HD) = 0.01694
R² (SLE) = 0.1544
R² (RA) = 0.01165
R² (pSS)= 0.4859
IP-10
R² (HD) = 0.0414
R² (SLE) = 0.0388
R² (RA) = 0.00134
R² (pSS)= 0.06374
MCP-1(MCAF)
R² (HD) = 0.2833
R² (SLE) = 0.2339
R² (RA) = 0.2282
R² (pSS)= 0.1438
MIP-1a
R² (HD) = 0.1219
R² (SLE) = 0.1427
R² (RA) = 0.02898
R² (pSS)= 0.3329
MIP-1b
R² (HD) = 0.2093
R² (SLE) = 0.5392
R² (RA) = 0.1528
R² (pSS)= 0.05293
PDGF bb
R² (HD) = 0.4668
R² (SLE) = 0.2035
R² (RA) = 0.02262
R² (pSS)= 0.08231
RANTES
R² (HD) = 0.00167
R² (SLE) = 0.3327
R² (RA) = 0.00045
R² (pSS)= 0.00026
TNFα
R² (HD) = 0.3389
R² (SLE) = 0.1830
R² (RA) = 0.00196
R² (pSS)= 0.4021
VEGF
R² (HD) = 0.3351
R² (SLE) = 0.8516
R² (RA) = 0.01034
R² (pSS)= 0.2230
HD SLE RA pSS
concentration (pg/ml)
MFI pSyk (Y352)
(CD27+, 5 min anti-IgG/IgM)
linear regression line
HD
SLE
RA
pSS

**Supplementary Figure 4: Reduced pSyk($Y^{352}$) in $CD27^+$ memory B cells after 5 min anti-IgG/IgM stimulation does not correlate with serum cytokine expression.** Cytokine expression was quantified in human serum from SLE (red), RA (blue) and pSS (green) patients and compared to HDs (black). Cytokine concentrations were correlated with pSyk($Y^{352}$) in $CD27^+$ memory B cells after 5 min of anti-IgG/IgM stimulation. Only data within the range of standard curves are shown and analyzed. Horizontal lines indicate the mean. Linear regression lines, coefficients of determination ($R^2$) and Pearson's correlation coefficients (r) are indicated in the figure (one-way ANOVA with DMCT; linear regression; Person's correlation; * $p \leq 0.05$, ** p  0.01).

**Supplementary Table 4:** List of differentially methylated CpG sides

| Cg ID | Gene ID | Region Annotation | Chromosome | Start | Stop |
|---|---|---|---|---|---|
| cg06872964 | *IFI44L* | TSS1500 | chr1 | 79085250 | 79085251 |
| cg03607951 | *IFI44L* | TSS1500 | chr1 | 79085586 | 79085587 |
| cg17980508 | *IFI44L* | TSS1500 | chr1 | 79085713 | 79085714 |
| cg00855901 | *IFI44L* | TSS1500 | chr1 | 79085765 | 79085766 |
| cg05696877 | *IFI44L* | 5'UTR | chr1 | 79088769 | 79088770 |
| cg07285983 | *RABGAP1L* | body; TSS200 | chr1 | 174844490 | 174844491 |
| cg06188083 | *IFIT3* | body; body | chr10 | 91093005 | 91093006 |
| cg05552874 | *IFIT1* | body | chr10 | 91153143 | 91153144 |
| cg04582010 | *IFITM1* | TSS1500 | chr11 | 313120 | 313121 |
| cg09026253 | *IFITM1* | TSS1500 | chr11 | 313267 | 313268 |
| cg01971407 | *IFITM1* | TSS1500 | chr11 | 313624 | 313625 |
| cg23570810 | *IFITM1* | body | chr11 | 315102 | 315103 |
| cg21686213 | *IFITM1* | 3'UTR | chr11 | 315118 | 315119 |
| cg03038262 | *IFITM1* | 3'UTR | chr11 | 315262 | 315263 |
| cg20045320 | *IFITM3* | downstream | chr11 | 319555 | 319556 |
| cg09122035 | *IFITM3* | downstream | chr11 | 319667 | 319668 |
| cg17990365 | *IFITM3* | 2nd exon | chr11 | 319718 | 319719 |
| cg25674027 | *PAH* | upstream | chr12 | 103325781 | 103325782 |
| cg27056740 | *MIR300* | body | chr14 | 101507727 | 101507728 |
| cg07839457 | *CETP* | TSS1500 | chr16 | 57023022 | 57023023 |
| cg01028142 | *CMPK2* | body | chr2 | 7004578 | 7004579 |
| cg10959651 | *RSAD2* | 1st exon | chr2 | 7018020 | 7018021 |
| cg10549986 | *RSAD2* | 1st exon | chr2 | 7018153 | 7018154 |
| cg17283620 | *HAAO* | body | chr2 | 43013772 | 43013773 |
| cg26312951 | *MX1* | TSS200; 5'UTR | chr21 | 42797847 | 42797848 |
| cg21549285 | *MX1* | 5'UTR | chr21 | 42799141 | 42799142 |
| cg14293575 | *USP18* | 5'UTR | chr22 | 18635460 | 18635461 |
| cg20098015 | *ODF3B* | TSS200 | chr22 | 50971140 | 50971141 |
| cg22930808 | *PARP9* | 5'UTR | chr3 | 122281881 | 122281882 |
| cg08122652 | *PARP9* | 5'UTR | chr3 | 122281939 | 122281940 |
| cg00959259 | *PARP9* | 5'UTR | chr3 | 122281975 | 122281976 |
| cg05994974 | *PARP12* | body | chr7 | 139761087 | 139761088 |
| cg14864167 | *PDE7A* | body | chr8 | 66751182 | 66751183 |

Interferon-induced protein 44-like (*IFI44L*), Rab GTPase-activating protein 1-like (*RABGAP1L*), interferon-induced protein with tetratricopeptide repeats (*IFIT*), interferon-induced transmembrane protein (*IFITM*), phenylalanine-4-hydroxylase (*PAH*), microRNA (*MIR*), cholesteryl ester transfer protein (*CETP*), UMP-CMP kinase 2, mitochondrial (*CMPK2*), radical S-adenosyl methionine domain-containing protein 2 (*RSAD2*), 3-hydroxyanthranilate 3,4-dioxygenase (*HAAO*), interferon-induced GTP-binding protein Mx1 (*MX1*), Ubl carboxyl-terminal hydrolase 18 (*USP18*), outer dense fiber protein 3B (*ODF3B*), poly [ADP-ribose] polymerase (*PARP*), high affinity cAMP-specific 3',5'-cyclic phosphodiesterase 7A (*PDE7A*), transcription start site (*TSS*)

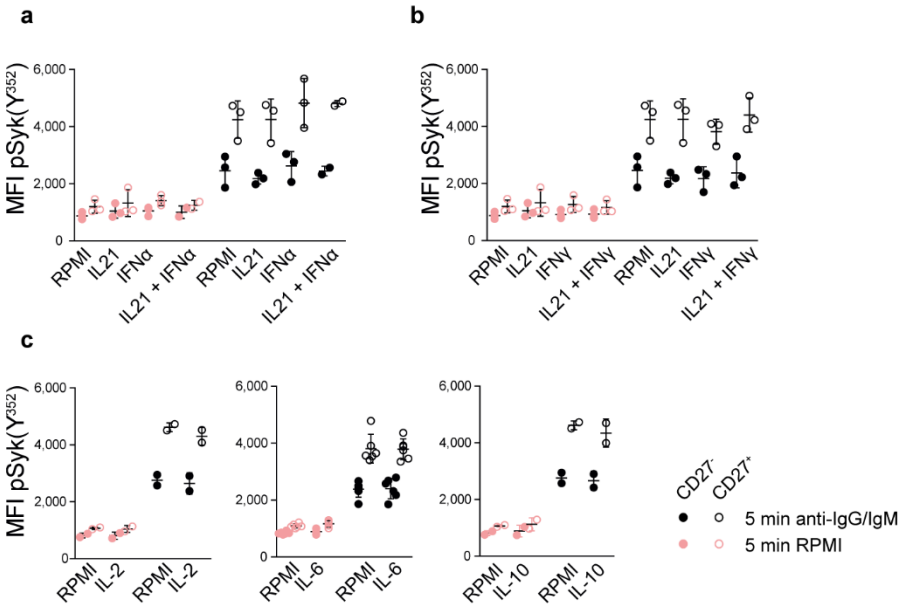


**Supplementary Figure 5: Syk(Y$^{352}$) phosphorylation in HD CD27$^-$ B cells and CD27$^+$ memory B cells remains stable upon co-stimulation with IFNα, IFNγ, IL-2, IL-6 and IL-10.** HD PBMCs were incubated for 48 h with RPMI as unstimulated control or (**a**) IFNα, IL-21, IFNα together with IL-21, (**b**) IFNγ, IL-21, IFNγ together with IL-21 and (**c**) IL-2, IL-6, IL-10 and subsequently stimulated with anti-IgG/IgM (black) or RPMI (pink) for 5 min. Phoso-Syk(Y$^{352}$) was analyzed in CD27$^-$ (dots) and CD27$^+$ memory (circles) B cells. Horizontal lines represent the mean ± SD.

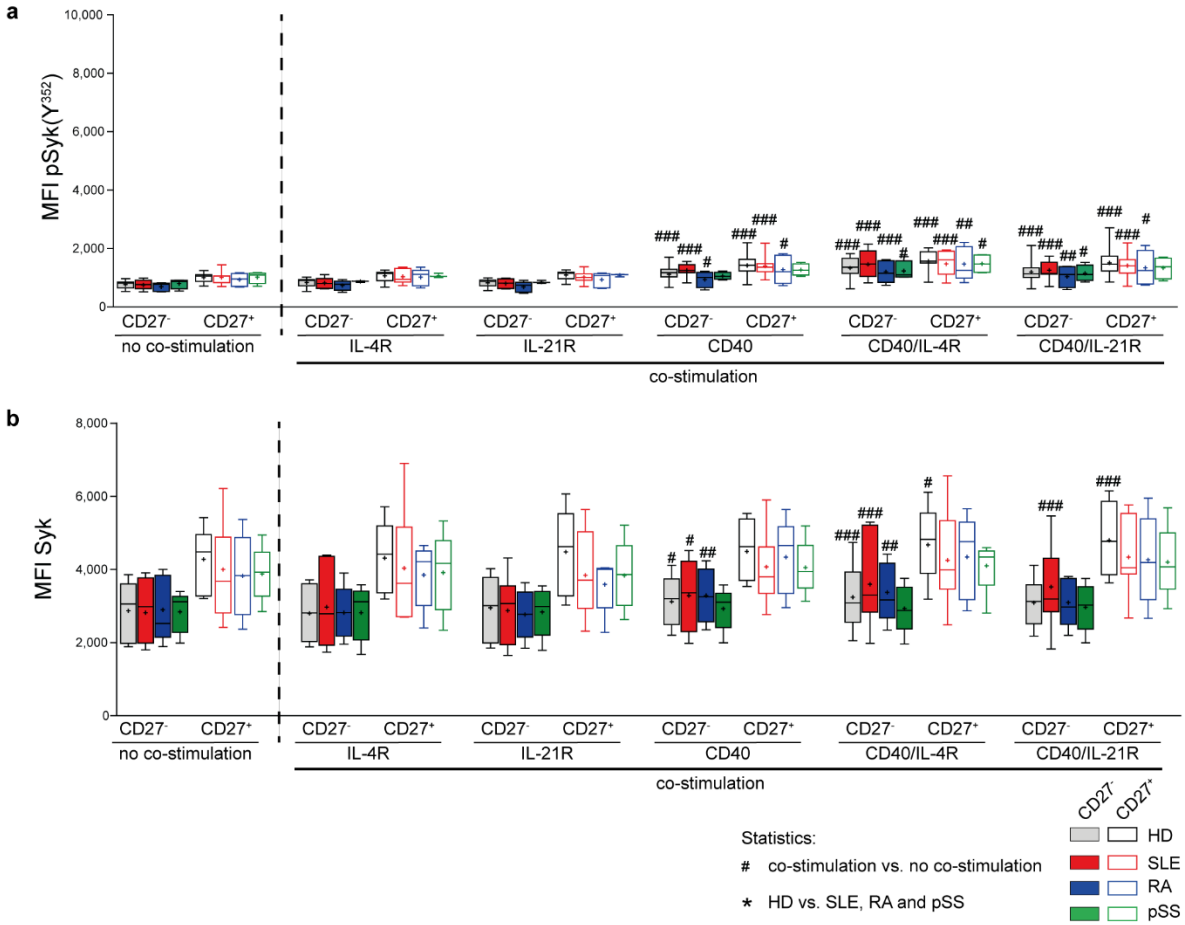


**Supplementary Figure 6: Syk and Syk($Y^{352}$) expression upon co-stimulation with CD40L, IL-4 and IL-21 and combinations thereof in HD, SLE, RA and pSS cells without anti-IgG/IgM stimulation.** HD (black), SlE (red), RA (blue) and pSS (green) PBMCs were incubated with IL-4, IL-21, CD40L alone or combinations thereof for 48 h and analyzed for Syk and pSyk($Y^{352}$) expression. (**a**) Phospho-Syk($Y^{352}$) and (**b**) Syk MFI in $CD27^-$ B cells (filled boxes) and $CD27^+$ memory B cells (blank boxes) with (n(HD/SLE/RA/pSS) = 11/7/5/5) and without co-stimulation (n(HD/SLE/RA/pSS) = 30/18/16/15). Within the Box whisker plots the median (line), mean (plus) and range (whiskers) are represented (repeated measures ANOVA with DMCT, # $p \leq 0.05$, ## $p \leq 0.01$, ### $p \leq 0.001$).

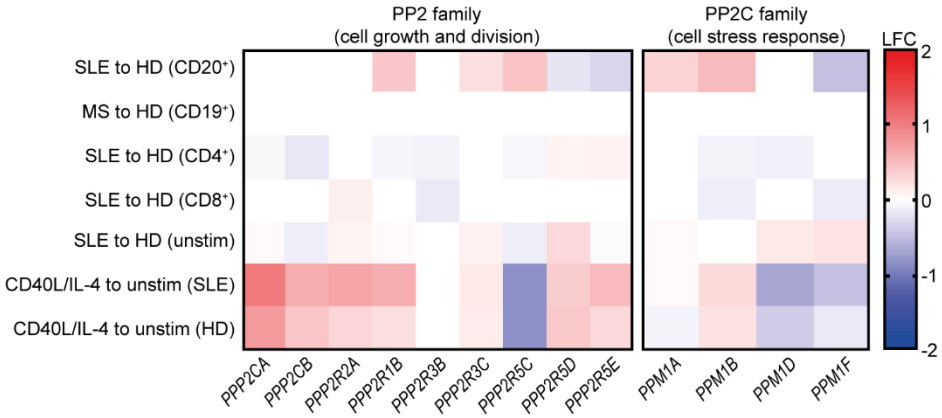


**Supplementary Figure 7: Common expression of PP2 and PP2C family genes upon CD40L/IL-4 co-stimulation in SLE and HD CD19$^+$ B cells.** Differential expression of selcted PSP PP2 and PP2C family genes was analyzed from publicly available data (lines 1-4) and upon co-stimulation with CD40L/IL-4 (lines 4-7). Data show SLE *vs*. HD CD20$^+$ B cells (6 SLE, 7 HD), MS *vs*. HD CD19$^+$ B cells (10 MS, 10 HD), SLE *vs*. HD CD4$^+$ (53 SLE, 41 HD) and CD8$^+$ T cells (22 SLE, 31 HD) and differential gene expression from un-stimulated SLE *vs*. HD and CD40L/IL-4 stimulated for SLE *vs.* un-stimulated SLE or HD CD19$^+$ B cells, respectively (n(HD/SLE) = 1/2).

# 12 Publications, Presentations and Poster

**2020**

Article: Aue, A., Szelinski, F., **Weißenberg S. Y.**, Wiedemann, A., Rose T., Lino A. C., Dörner T. 2020. “Elevated STAT1 expression but not phosphorylation in lupus B cells correlates with disease activity and increased plasmablast susceptibility”. *Rheumatology (Oxford)*.

**2019**

Article: **Weißenberg, S. Y.**, Szelinski, F., Schrezenmeier, E., Stefanski, A. L., Wiedemann, A., Rincon-Arevalo, H., Welle, A., Jungmann, A., Nordstrom, K., Walter, J., Imgenberg-Kreuz, J., Nordmark, G., Ronnblom, L. Bachali, P., Catalina, M. D., Grammer, A. C., Lipsky, P. E., Lino, A. C. & Dörner, T. 2019. „Identification and Characterization of Post-activated B Cells in Systemic Autoimmune Diseases”. *Front Immunol,* 10, 2136.

Article: Schrezenmeier, E., **Weißenberg, S. Y.**, Stefanski, A. L., Szelinski, F., Wiedemann, A., Lino, A. C., Dorner, T. 2019. „Postactivated B cells in systemic lupus erythematosus: update on translational aspects and therapeutic considerations”. *Curr Opin Rheumatol*, 31, 175-184.

**2017**

Poster: **Weißenberg, S. Y.**, Szelinski F., Dörner, T. “Altered B Cell Receptor Signaling in Patients with Systemic Lupus Erythematosus and Primary Sjögren‘s Syndrome”, 6th DGfI Translational Immunology School, 2017, Potsdam.

**2016**

Poster: **Weißenberg, S. Y.**, Fleischer, S. J., Dörner, T. „B Cell Receptor Signaling is Imbalanced in Patients with Systemic Lupus Erythematosus and Primary Sjögren‘s Syndrome“, 8th DGfI Autumn School, 2016, Merseburg.

Poster: Wiedemann, A., **Weißenberg, S. Y.**, Kruck, I., Fleischer, S. J., Reiter, K., Dörner, T. & Mei, H. E. “Delineation of Human Plasma Cell Subsets And Their Bone Marrow Niche”, IMMUNOBONE Annual Meeting 2016, Hamburg.

**2015**

Oral presentation about previous work on the project and recent publication: Mei, H. E., Wirries, I., Frölich, D., Brisslert, M., Giesecke, C., Grün, J. R., Alexander, T., Schmidt, S., Luda, K., Kühl, A. A., Engelmann, R., Dürr, M., Scheel, T., Bokarewa, M., Perka, C., Radbruch, A., Dörner, T. “Characteristics of human $CD19^-$ Plasma Cells”, IMMUNOBONE Annual Meeting 2015, Dresden.

# 13 Acknowledgements

First, I thank Prof. Dr. Thomas Dörner for supervising me during my whole PhD time at the Charité-Universitätsmedizin Berlin and DRFZ. Many thanks for providing the topic, the intellectual input, and constructive discussions. Also, I thank Prof. Dr. Roland Lauster for supervision at the TU Berlin. I thank the whole AG Dörner group for their great scientific and personal support during the whole time: Karin Reiter, Dr. Ana-Luisa Stefanski, Dr. Eva Schrezenmeier, Dr. Thomas Rose, Dr. Sarah Fleischer, Annika Wiedemann, Franziska Szelinski, Dr. Andreia Lino, Mariele Gatto, Hector Rincon-Arevalo, Anna Lisney, Nadja Nomovi, Arman Aue, Cindy Schilling, Sylvia, Kirsten Langpap and Lindsay Serene. Thank you for sharing your knowledge, providing help with sample acquisition and being there for all those everyday problems. Thank you for the great time and the wonderful atmosphere in the lab! Special thanks go to Franziska Szelinski for helping me out in the lab when I was handy capped. Also, many thanks to Franziska Szelinski and Dr. Eva Schrezenmeier for sharing your knowledge and data about phosphatases.

Many thanks go to the cooperation partners and co-authors of my first author research paper: The collegues from the department of 'medical sciences' at the 'rheumatology and science for life laboratory' at Uppsala University (Uppsala, Sweden): Prof. Dr. Lars Rönnblom, Dr. Juliana Imgenberg-Kreuz and Dr. Gunnel Nordmark; the department of 'genetics and epigenetics' at Saarland University (Saarbrücken, Germany): Prof. Dr. Jörn Walter, Anna Welle, Annemarie Jungmann and Dr. Karl Nordström; and the 'RILITE research institute' (Charlottesville, VA, USA): Dr. Peter E. Lipsky, Prathyusha Bachali, Dr. Michelle D. Catalina and Dr. Amrie C. Grammer. Thank you for sharing your data and doing the meta-analysis of epigenetic data sets and the analysis of the RNA sequencing data. Everyone did a great job.

I thank Andreas Hutloff from the 'chronic immune reactions' group at the DRFZ (Berlin, Germany), who kindly shared his knowledge and materials about CD40 stimulation on B cells. Also, the lab manager, kitchen team and particularly Tuula Geske who tried everything to label the SHP-1 and PI3K antibodies. Furthermore, I thank all collegues from der Charité clinic including physicians, surgeons, and nurses, who helped with sample acquisition.

**Thank you! It has been a pleasure working with you!**

Last, but not least: I thank all patients and healthy volunteers. Without their kind donations, this work would not have been possible. I thank Dr. Alexander Weißenberg for critical reading of this work. Special thanks go to my family and friends for their great mental support.

# 14 Eidesstattliche Erklärung

Ich versichere, dass die vorliegende Arbeit mit dem Titel "*CD40 Stimulation Activates 'Post-Activated' B cells which are Hyporesponsive to B Cell Receptor and Toll-like Receptor 9 Stimulation in Autoimmunity*", von mir persönlich mittels der angegebenen Methoden, Hilfsmittel und Literatur erstellt wurde. Beteiligungen von Kollegen und Kooperationspartnern sind an geeigneter Stelle erwähnt. Des Weiteren gab es keine unzulässigen Hilfestellungen Dritter.

Ich versichere, dass ich bisher an keiner in- oder ausländischen Fakultät ein Gesuch auf Zulassung zur Promotion, noch die vorliegende oder eine andere Arbeit zu Promotionszwecken eingereicht habe.

Ort, Datum, Unterschrift